

Some pages of this thesis may have been removed for copyright restrictions.

If you have discovered material in AURA which is unlawful e.g. breaches copyright, (either yours or that of a third party) or any other law, including but not limited to those relating to patent, trademark, confidentiality, data protection, obscenity, defamation, libel, then please read our [Takedown Policy](#) and [contact the service](#) immediately

ORAL UPTAKE AND DISTRIBUTION OF MICROSPHERES

JAMES EDWARD EYLES

Doctor of Philosophy

THE UNIVERSITY OF ASTON IN BIRMINGHAM

SEPTEMBER 1995

This copy of the thesis has been supplied on the condition that anyone who consults it is understood to recognise that its copyright rests with its author and that no quotation from the thesis and no information derived from it may be published without proper acknowledgement.

THE UNIVERSITY OF ASTON IN BIRMINGHAM

ORAL UPTAKE AND DISTRIBUTION OF MICROSPHERES

A thesis submitted by James Edward Eyles BSc. for the degree of Doctor of
Philosophy
1995

SUMMARY

Consumer preference ensures that considerable interest is aroused when the possibility of an exploitable opportunity for the oral delivery of vaccines, labile peptidergic compounds or highly potent insoluble drugs is reported. There is a growing body of experimental evidence suggesting that the gastrointestinal tract (GIT) may be penetrated by sub-micron sized polymeric particles which have the capacity to deliver therapeutic compounds. We investigated this, initially with Fluoresbrite™ carboxylate latex microspheres (0.87 μm diameter) which were administered orally to rats. Microsphere numbers within blood samples were then quantified using fluorescence microscopy or FACS technology. These studies were prone to quantitative error, but indicated that increased microsphere translocation occurred if particles were administered in conjunction with large volumes of hypotonic liquid, and that uptake was very rapid. Test particles were detected in blood only a few minutes after dosing. To improve quantification, GPC technology was adopted. 0.22 μm latex particles were found to accumulate in greatest numbers within the Mononuclear phagocyte system tissues after gavage. Again translocation was rapid. The ability of test particles to leave the intestinal lumen and access systemic compartments was found to be highly dependent on their size and hydrophobicity, determined by Hydrophobic interaction chromatography. Considerably lower numbers of 0.97 μm diameter latex microspheres were detectable within extra-intestinal tissue locations after gavage. Histological studies showed that Fluoresbrite™ microspheres accumulate within the liver, spleen, Mesenteric lymph node and vasculature of rats after oral administration. Fluorescent particles were observed in both the Peyer's patches (PPs), and non lymphoid regions of rat intestinal mucosa after gavage, conducive to the acceptance that more than one mechanism of particle absorption may operate. Polystyrene transfer to the circulation occurred within minutes of introducing 0.220 μm latex particles into *in situ* ileal and duodenal artificial loops, although particle transfer from proximal gut regions appeared to be greater. In the presence of cytochalasin B, particle translocation to the blood diminished. Statistically, much more latex was detected per gram of PP tissue excised from ileal loops compared with non-PP gut. 8.4 % of an oral dose of Poly(lactic acid) microencapsulated ^{125}I -interferon- γ was detected in the blood 15 minutes of gavage. Statistically, less free drug was transferred to the blood, liver and spleen 15 minutes after gavage. Mean Thyroid activity at the 15 minute time point was significantly low, in comparison to rats given unencapsulated drug, indicating minimal encapsulated radiolabelled drug breakdown had occurred.

KEY WORDS: Drug delivery; Latex particle; Translocation;
Cytochalasin B; Interferon

In memory of

Dr. David Arthur Lewis BSc MSc PhD DSc

1932-1994

ACKNOWLEDGEMENTS

I would very much like to thank my supervisors Dr. H.O Alpar, Dr. Martin Keswick and the late Dr. D.A Lewis for their expert help, advice and friendship over the past four years. Thanks also to the Wellcome Foundation and SERC for their generous financial support for this project. Thanks to Miss B. Conway for her HIC analysis, zeta potential measurements, manufacturing the interferon loaded microspheres and her help and friendship in general. Thanks also to Dr. Dunnion (Miss Debbie Stag) for her friendship and scientific support. Histological procedures were carried out at Birmingham City Hospital, Dudley Road. Thank you to Mr. C. Smith and everyone at the hospital's pathology department for the use of their laboratory's facilities. Mr. M. Gamble, Mr. B. Burford and Mr. C. Bach must also be commended for their excellent technical assistance. Thanks also to Dr. S.N. Smith for his friendship and support over the last few years.

CONTENTS

	PAGE
Title	1
Thesis summary	2
Dedication	3
Acknowledgements	4
Contents	5
List of figures	
List of tables	
Abbreviations	
1.0 INTRODUCTION	29
1.1 Morphology and physiology of the gastrointestinal tract	29
1.1.2 Layers of the gastrointestinal tract	30
1.1.2.1 The mucosa	30
1.1.2.1.1 Muscularis mucosa	30
1.1.2.1.2 Lamina propria	32
1.1.2.1.3 Epithelium	32
1.1.2.2 The submucosa	35
1.1.2.3 The muscularis	36
1.1.2.4 The mesentery	36
1.1.3 Regions of the gastrointestinal tract	36
1.1.3.1 The stomach	36
1.1.3.2 The small intestine	37
1.1.3.3 The large intestine	37
1.2 Particle uptake from the gastrointestinal tract	40
1.2.1 Physical barriers to particle uptake: mucus	41
1.2.2 Uptake of particles by endocytosis	42
1.2.3 Paracellular transport of particles: persorption	44
1.2.4 Particle uptake <i>via</i> the Peyer's patches (PPs)	47
1.2.5 Macrophage mediated uptake from the GIT lumen	53
1.2.6 Post uptake dissemination of orally administered particulates	55
1.2.6.1 Transportation of orally absorbed particles by the lymphatic system	58
1.2.6.2 Hematogenous transportation of particles after intestinal absorption	63

1.2.7	Post uptake organ distribution of orally administered particulates	72
1.2.8	Excretion of intestinally absorbed microspheres	74
1.2.9	Microspheres as delivery systems for oral administration	76
1.2.9.1	Drug delivery	76
1.2.9.2	Delivery of antigens	78
1.3	Aims and objectives of the present study	80
2.0	EXPERIMENTAL METHODOLOGY	82
2.1	Animals	82
2.2	Anaesthesia	82
2.3	Microspheres	82
2.4	Microscopy and photography	84
2.4.1	Light microscopy	84
2.4.2	Photography	84
2.4.3	Scanning electron microscopy	85
2.5	Hydrophobic interaction chromatography (HIC)	85
2.6	Determination of Zeta potentials	85
2.7	Methods of quantification of polystyrene microsphere numbers in body fluids and tissues	86
2.7.1	Quantification of Fluoresbrite™ microsphere numbers within blood samples using fluorescence microscopy.	86
2.7.2	Quantification of fluorescent microsphere numbers within blood samples using flow cytometry	87
2.7.3	Quantification of latex microsphere numbers in body fluids and tissues by radiolabelling	88
2.7.4	Detection of polystyrene microspheres in body fluids and tissues by gel permeation chromatography (GPC)	91
2.7.4.1	GPC apparatus	95
2.7.4.2	Molecular weight calibration of the GPC apparatus	96
2.7.4.3	Treatment of tissue samples for assessment of polystyrene microsphere content	98
2.7.4.4	Calibration and sensitivity studies	99

2.7.5	Histological examination of tissues	99
2.7.5.1	Tissue collection and fixation	99
2.7.5.2	Tissue treatment	100
2.7.5.3	Plastic embedding	100
2.7.5.4	Cutting plastic embedded tissues	100
2.7.5.5	Staining sections	100
2.8	Surgical procedures	101
2.8.1	Systemic blood sampling techniques	101
2.8.2	Portal blood collection	101
2.8.3	Preparation of isolated small intestinal loops	102
3.0	EFFECT OF VARIABLES ON THE ORAL UPTAKE OF COLLOIDAL PARTICLES FROM THE GASTROINTESTINAL TRACT	103
3.1	Introduction	103
3.2	Materials and methods	104
3.2.1	Influence of carrier medium tonicity on circulating fluorescent microsphere numbers after oral administration	104
3.2.2	Influence of carrier medium volume on circulating fluorescent microsphere numbers after oral administration	104
3.2.3	Influence of the administered particle concentration on the translocation of particles from the GIT to the blood	105
3.3	Results	105
3.3.1	Influence of carrier medium tonicity on circulating fluorescent microsphere numbers after oral administration	105
3.3.2	Influence of carrier medium volume on circulating fluorescent microsphere numbers after oral administration	106
3.3.3	Influence of the administered particle concentration on the translocation of particles from the GIT to the blood	107
3.4	Discussion	109

4.0	KINETIC ASPECTS OF PARTICLE TRANSLOCATION FROM THE GASTROINTESTINAL TRACT	119
4.1	Introduction	119
4.2	Materials and methods	120
4.2.1	Characterisation of polystyrene test particles	120
4.2.1.1	Hydrophobic interaction chromatography (HIC)	120
4.2.1.2	Zeta potential	120
4.2.1.3	Electron microscopy	121
4.2.2	GPC determined uptake and distribution of polystyrene test particles	121
4.2.2.1	Calibration of GPC system	121
4.2.2.2	Determination of microsphere molecular weight averages	121
4.2.2.3	Calibration and sensitivity studies	121
4.2.2.4	Tissue distribution of 0.22 μm nanospheres after a single oral dose	122
4.2.2.5	Tissue distribution of 1.0 μm microspheres after a single oral dose	124
4.2.3	Preparation and characterisation of ^{125}I labelled microspheres	124
4.2.4	Organ distribution of radiolabelled 0.82 μm microspheres in the rat model	125
4.2.5	Flow cytometric analysis of blood from animals orally dosed with 0.87 μm carboxylated microspheres	126
4.3	Results	127
4.3.1	Characterisation of polystyrene test particles	127
4.3.1.1	Hydrophobic interaction chromatography (HIC)	127
4.3.1.2	Zeta potential	128
4.3.1.3	Electron microscopy	129
4.3.2	GPC determined uptake and distribution of polystyrene test particles	130
4.3.2.1	Calibration of GPC system	130

4.3.2.2	Determination of microsphere molecular weight averages	131
4.3.2.3	Calibration and sensitivity studies	135
4.3.2.4	Tissue distribution of 0.22 μm nanospheres after a single oral dose	136
4.3.2.5	Tissue distribution of 0.97 μm microspheres after a single oral dose	142
4.3.3	Preparation and characterisation of ^{125}I labelled microspheres	146
4.3.4	Organ distribution of radiolabelled 0.82 μm microspheres	146
4.3.5	Flow cytometric analysis of blood from animals orally dosed with 0.87 μm carboxylated microspheres	148
4.4	Discussion	152
4.4.1	Organ distribution of radiolabelled 0.82 μm microspheres in the rat model	152
4.4.2	Flow cytometric analysis of blood from animals orally dosed with 0.87 μm carboxylated microspheres	153
4.4.3	Characterisation of polystyrene test particles	154
4.4.4	GPC determined uptake and distribution of polystyrene test particles	155
4.4.4.1	Latex particle transfer into the vascular compartment after oral administration	156
4.4.4.2	Latex particle uptake by the liver after oral administration	160
4.4.4.3	Latex particle uptake by the spleen after oral administration	163
4.4.4.4	Latex particle uptake by the lung after oral administration	164
4.4.4.5	Latex particle uptake by the kidneys after oral administration	165
4.4.4.6	Latex particle excretion in the urine after oral administration	166

4.4.4.7	Latex particle uptake by the mesentery after oral administration	167
4.4.4.8	Latex particle uptake by the intestines after oral administration	168
4.4.4.9	Latex particle excretion in the faeces after oral administration	171
4.4.5	Conclusion	171
5.0	MECHANISMS OF ABSORPTION OF PARTICULATE MATTER FROM THE GIT	174
5.1	Introduction	174
5.2	Materials and Methods	175
5.2.1	Histological studies investigating microsphere uptake and translocation from the gut after oral administration	175
5.2.2	Investigations into the translocation of 220 nm diameter microspheres from ileal and duodenal gut loops, in the presence and absence of cytochalasin B	175
5.3	Results	177
5.3.1	Histological evidence of microsphere uptake and translocation from the gut after oral administration	177
5.3.2	The translocation of 220 nm diameter microspheres from ileal and duodenal gut loops, in the presence and absence of cytochalasin B	188
5.4	Discussion	190
5.4.1	Histological evidence of microsphere uptake and translocation from the gut after oral administration	190
5.4.2	The translocation of 220 nm diameter microspheres from ileal and duodenal gut loops, in the presence and absence of cytochalasin B	194
5.4.3	Conclusion	205

6.0	UPTAKE AND DISTRIBUTION OF MICROENCAPSULATED INTERFERON AFTER ORAL DELIVERY	207
6.1	Introduction	207
6.2	Materials and Methods	208
6.3	Results	209
6.4	Discussion	216
	6.4.1 Characterisation of IFN- γ loaded PLA microspheres	216
	6.4.2 <i>In vivo</i> distribution after oral administration of microencapsulated and free IFN- γ	217
	6.4.3 Conclusion	226
7.0	CONCLUDING REMARKS	228
8.0	REFERENCES	233
9.0	APPENDICES	247

LIST OF FIGURES

FIGURE		PAGE
1	Diagrammatic representation of the overall histological organisation of the small intestine.	29
2	Diagram illustrating the blood circulation and lymphatic drainage within a typical small intestinal villus.	31
3	Typical enterocyte structure.	33
4	Schematic representation (not to scale) of the different regions within the GIT.	39
5	Proposed mechanisms of particle penetration of the intestinal epithelial barrier: (1) Intracellular uptake and transport via ordinary enterocytes (section 1.22); (2) Lymphatic uptake <i>via</i> M-cells (section 1.24) or macrophages (section 1.25); (3) Uptake by a paracellular pathway (section 1.23). Adapted from Smith <i>et al.</i> , (1994)	42
6	Schematic representation of the different regions of an intestinal lymphoid follicle. Adapted from O'Hagan (1990).	48
7	Vesicular transportation of particles through M-cells. Adapted from O'Hagan (1990)	49
8	Size restrictions imposed on particulate uptake into capillary and lymphatic vessels.	57
9	Lymph node structure. Adapted from Roitt <i>et al.</i> ,	61
10	Schematic view of a liver lobule, the structural unit of the liver. Adapted from Weiss (1988)	64

11	Circulatory pathway for intestinally absorbed, or intravenously injected microspheres within the vascular system. Blood vessels are represented as: A (aorta); HA (hepatic artery); MA (mesenteric artery); HPV (hepatic portal vein); HV (hepatic vein) and VC (vena cava).	65
12	Radioiodination of tyrosine using the chloramine-T method.	89
13	Proposed reaction for the radioiodination of polystyrene using the Chloramine-T method. The pendant aromatic rings would be expected to react in a similar way to toluene molecules.	90
14	Schematic representation of size exclusion chromatography. Adapted from Yau <i>et al.</i> , (1979)	93
15	Components of a modular GPC system: 1. mobile phase reservoir; 2. sintered metal frit; 3. adjustable flow rate pump; 4. pulse damper; 5. sample injector valve; 6. 100 μ l sample loop; 7. guard column; 8. column; 9. U.V detector; 10 chart recorder and integrator; 11. solvent waste bottle.	97
16	The mean percentage (\pm standard deviation) of an initial dose of 2.5 mg latex (in the form of 6.9×10^9 0.87 μ m diameter Fluoresbrite™ carboxylate microspheres) in the blood at various times after gavage. Microspheres were administered in conjunction with either water, 0.9 % w/v Na Cl or 2M Na Cl (n=3).	106

- 17 The percentage (mean values \pm standard deviation) of an orally administered dose of 2.5 mg latex (in the form of 6.91×10^9 0.87 μm Fluoresbrite™ carboxylate microspheres) that was present within the vascular compartment at various times after dosing. Microspheres were suspended in either 0.1, 0.3 or 0.5 ml of water prior to administration (n=3). 107
- 18 The percentage of 0.87 μm latex microspheres dosed (mean values \pm standard deviation) in the blood after oral administration over a range of particle concentrations from 1.4×10^{10} to 7.0×10^{10} spheres / ml (n=3). 108
- 19 The mean number ($\times 10^8$) of 0.87 μm fluorescent carboxylated polystyrene microspheres in the vascular compartment (\pm standard deviation) after oral gavage using a range of microsphere concentrations, from 1.4×10^{10} (equivalent to 5.0 mg / ml) to 7.0×10^{10} microspheres / ml (equivalent to 25 mg / ml) (n=3). 108
- 20 Mean cumulative % eluted (\pm standard deviation) after HIC analysis of 0.22 μm diameter latex Polybeads® (n=3). 127
- 21 Mean cumulative % eluted (\pm standard deviation) after HIC analysis of 0.97 μm diameter latex Polybeads® (n=3). 127
- 22 Mean cumulative % eluted (\pm standard deviation) after HIC analysis of 1.10 μm diameter carboxylated latex microspheres (n=3). 128
- 23 Scanning electron photomicrograph of 0.22 μm Polystyrene microspheres. 129

24	Scanning electron photomicrograph of 0.97 μm Polystyrene microspheres.	129
25	GPC chromatogram produced after injection of EasiCal [®] polymer calibration mixture 1-5. Peaks represent Mw values of 640, 9375, 66000, 321000 and 3066000.	130
26	Semi logarithmic plot showing the relationship between molecular weight and retention time of the molecular weight standards after GPC analysis.	131
27	Manually digitised chromatogram produced after GPC analysis of 3 μg of 0.22 μm diameter latex particles in 100 μl of THF.	132
28	Manually digitised chromatogram produced after GPC analysis of 3 μg of 0.97 μm diameter latex particles in 100 μl of THF.	133
29	Mean peak integration area (\pm SEM) produced by GPC analysis of 0.22 μm polystyrene latex microsphere spiked samples of blood, liver and THF (n = 7).	136
30	A typical chromatogram produced by GPC analysis of a spleen sample removed from a rat 240 minutes after oral administration of 21.7 mg, 0.22 μm diameter, polystyrene nanospheres.	137
31	A typical chromatogram produced by GPC analysis of a spleen sample removed from a rat 45 minutes after oral administration of 1 ml of distilled water.	137
32	Mean (\pm SEM) mass of latex nanospheres within the entire vascular compartment (systemic (S) and portal (P)) of rats after oral administration of 21.7 mg 0.22 μm diameter polystyrene nanospheres (n=4).	138

- 33 Whole organ accumulation of polystyrene (\pm SEM) after oral administration of 21.7 mg polystyrene nanospheres (diameter 0.22 μ m) (n=8). 138
- 34 Mean (\pm SEM) urinary excretion (n=4) and mesenteric accumulation (n=4) in rats after oral administration of 21.7 mg 0.22 μ m diameter nanospheres. Whole liver and spleen accumulation data (n=8) from figure 33 is also shown for comparison. 139
- 35 Whole organ accumulation of polystyrene (\pm SEM) in the small and large intestines and mesenteries of rats that received an oral dose of 21.7 mg polystyrene nanospheres (diameter 0.22 μ m) (n=4). 139
- 36 Mean mass of polystyrene (\pm SEM) recovered from whole intestines (SI/LI) complete intestinal washes (SIW/LIW) and faeces of rodents that received 21.7 mg latex nanospheres (0.22 μ m diameter) orally (n=4). 140
- 37 Polystyrene concentration *per* gram (\pm SEM) of portal / systemic blood after oral administration of 21.7 mg polystyrene nanospheres of diameter 0.22 μ m (n=4). No significant difference exists between the two sample sites at 45 minutes (*). At all other time points a significant difference exist between the two sets of data ($P \leq 0.01$ for 2 tail). 140
- 38 Organ accumulation of polystyrene *per* gram of tissue (\pm SEM) after oral administration of 21.7 mg polystyrene nanospheres of 0.22 μ m diameter (n=8) 141
- 39 Gut and mesenteric accumulation of polystyrene *per* gram of tissue (\pm SEM) after oral administration of 21.7 mg polystyrene nanospheres of 0.22 μ m diameter (n=4). 141

- 40 Mean (\pm SEM) mass of latex microspheres within the entire vascular compartment (systemic (S) and portal (P)) of rats after oral administration of 21.7 mg microspheres (diameter 0.97 μm) (n=4). 142
- 41 Whole organ accumulation of polystyrene (\pm SEM) after oral administration of 21.7 mg polystyrene microspheres (diameter 0.97 μm) (n=4). 142
- 42 Mean (\pm SEM) urinary excretion (n=4) and mesenteric accumulation (n=4) in rats after oral administration of 21.7 mg 0.970 μm diameter microspheres. Whole liver and spleen accumulation data (n=4) from figure 41 is also shown for comparison. 143
- 43 Whole organ accumulation of polystyrene (\pm SEM) in the small and large intestines and mesenteries of rats that received an oral dose of 21.7 mg polystyrene microspheres (diameter 0.970 μm) (n=4). 143
- 44 Whole organ accumulation of polystyrene (\pm SEM) in the small and large intestines and mesenteries of rats that received an oral dose of 21.7 mg polystyrene microspheres (diameter 0.970 μm) (n=4). 144
- 45 Polystyrene concentration *per* gram (\pm SEM) of portal / systemic blood after oral administration of 21.7 mg polystyrene microspheres (diameter 0.97 μm) (n=4). 144
- 46 Organ accumulation of polystyrene *per* gram of tissue (\pm SEM) after oral administration of 21.7 mg polystyrene microspheres (diameter 0.97 μm) (n=4). 145

- 47 Small / large intestinal and mesenteric accumulation of polystyrene *per* gram of tissue (\pm SEM) after oral administration of 21.7 mg polystyrene microspheres (diameter 0.97 μm) (n=4). 145
- 48 Mean relative activities (\pm SEM) from various tissue samples removed from rats which received 1.42×10^{11} microspheres (with a batch diameter of 0.82 μm and an overall activity of 0.614 MBq) by the oral route of administration (n=4). 146
- 49 Mean relative activities (\pm SEM) from blood and thyroid samples removed from rats which received 1.42×10^{11} microspheres (with a batch diameter of 0.82 μm and an overall activity of 0.614 MBq) by the oral route of administration (n=4). 147
- 50 FACS analysis of 0.87 μm diameter Fluoresbrite™ carboxylated polystyrene latex microspheres suspended in distilled water. Running this sample enabled us to instruct the computer to identify microspheres within blood samples by virtue of their high fluorescent activity. Graph 1 shows the window within which microspheres are counted on the basis of their high FITC content (zone 1). The narrow size distribution of the particles is obvious in graph 2 representing forward scattering (FS). The fluorescence activity of all particulate matter in the suspension is shown in graph 3. Graphs 4 and 5 show FS and fluorescent activity of zone 1 particulates respectively. Gates w1 and w2 are defined in graph 5. 149

- 51 FACS analysis of diluted blood from a rat 45 minutes after oral delivery of 4.40×10^9 0.87 μm diameter Fluoresbrite™ carboxylated polystyrene latex microspheres. The diverse range of particle sizes within the suspension is obvious in graph 2 representing forward scattering (FS). The fluorescence activity of all particulate matter in the suspension is shown in graph 3. Cells and cell debris (C) exhibit a much lower level of fluorescence than the microspheres (w1), enabling the microspheres to be distinguished from other particulate matter and quantified. Microspheres are counted within gate w1. There is a wide distribution of particle sizes (graph 4) and FITC intensity (graph 5) within gate w1 compared to Figure 50. This suggests that a proportion of microspheres within this blood sample are associated with cells (internally or externally) or cell debris. 150
- 52 FACS analysis of diluted blood from a rat 4 hours after oral delivery of 4.40×10^9 0.87 μm diameter Fluoresbrite™ carboxylated polystyrene latex microspheres. The high fluorescent intensity of the microspheres compared with other particles is clear in graphs 3 and 5. Again microsphere numbers are quantified within gate w1. Data represented in graph 5 suggests that large numbers of translocated microspheres within the blood are present in multiple groupings. A secondary (doublet) peak can be clearly seen. 151
- 53 Cumulative uptake of polystyrene particles into extra-intestinal (X INTESTINAL) and intestinal tissues at time points after oral delivery of 21.7 mg 0.97 μm or 0.22 μm diameter latex particles in the rat model. 172

- 54 Plastic embedded jejunal / duodenal biopsy taken 15 minutes after oral administration of 2.5 mg 0.87 μm Fluoresbrite™ carboxylate microspheres. The majority of test particles are associated with mucus within the intestinal lumen (L). A proportion of the microsphere (M) dose appears to have entered the intestinal mucosa. These particles are arranged linearly within the villus, suggesting they may be contained within vascular or lymphatic vessels (x100 Total magnification; Longitudinal section; UV light source; Bar= 200 μm). 177
- 55 Plastic embedded jejunal / duodenal biopsy taken 15 minutes after oral administration of 2.5 mg 0.87 μm Fluoresbrite™ carboxylate microspheres. As in figure 54, the spatial distribution of microspheres within the intestinal mucosa does not follow a random pattern, but suggests that particles are conveyed from uptake sites at the villus tips within defined anatomical structures (x100 Total magnification; Transverse section; UV light source, Bar=200 μm). 178
- 56 Plastic embedded ileal biopsy taken 45 minutes after oral administration of 2.5 mg 0.87 μm Fluoresbrite™ carboxylate microspheres. Microspheres (m) are visualised in the process of absorption into a lymphatic follicle (F). (x160 Total magnification; UV light source, Bar=175 μm). 179
- 57 Plastic embedded ileal biopsy taken 45 minutes after oral administration of 2.5 mg 0.87 μm Fluoresbrite™ carboxylate microspheres. Similar photomicrograph to figure 55, only microspheres (M) are located below the follicle associated epithelium (x160 Total magnification; UV light source; Bar=175 μm). 180

- 58 Plastic embedded ileal biopsy taken 45 minutes after oral administration of 2.5 mg 0.87 μm Fluoresbrite™ carboxylate microspheres. This is the same section as shown in figure 56 under higher magnification. Microspheres (M) appear to be in very close association with sub epithelial macrophages (mac) which infiltrate M-cell basolateral membranes (x1000 Total magnification; UV and transmitting light source; Bar=35 μm). 181
- 59 Plastic embedded ileal biopsy taken 240 minutes after oral administration of 2.5 mg 0.87 μm Fluoresbrite™ carboxylate microspheres. Microspheres (M) were frequently visualised deep within the follicle dome of Peyer's patches, often in multiple groupings (x1000 Total magnification; UV and transmitting light source; Bar=35 μm). 182
- 60 Plastic embedded liver biopsy taken 240 minutes after oral administration of 2.5 mg 0.87 μm Fluoresbrite™ carboxylate microspheres. Microspheres appear to be randomly scattered throughout the hepatic tissue, possibly sequestered within Kupffer cells. A central vein (CV) can be seen in the bottom left hand corner of the photomicrograph (x160 Total magnification; UV light source; Bar=175 μm). 183
- 61 Plastic embedded spleen biopsy taken 240 minutes after oral administration of 2.5 mg 0.87 μm Fluoresbrite™ carboxylate microspheres. Entrapped microsphere(s) are denoted (M) (x160 Total magnification; UV light source; Bar=175 μm). 184
62. Plastic embedded Mesenteric lymph node biopsy taken 240 minutes after oral administration of 2.5 mg 0.87 μm Fluoresbrite™ carboxylate microspheres. Entrapped microspheres are denoted (M) (x160 Total magnification; UV light source; Bar=175 μm). 185

- 63 Plastic embedded section of a mesenteric blood vessel taken 240 minutes after oral administration of 2.5 mg 0.87 μm Fluoresbrite™ carboxylate microspheres. Within the arteriole (identified by its internal elastic lamina) microspheres (M) appear internalised within a phagocytic cell. Erythrocytes (E) are also present. (x1000 Total magnification; UV and transmitting light sources; Bar=35 μm). 186
- 64 Photomicrograph of blood, diluted with heparinised glycerol, taken 15 minutes after oral administration of 2.5 mg 0.87 μm Fluoresbrite™ carboxylate microspheres. Amongst the erythrocytes, there is a microsphere containing leukocyte (L) (x100 Total magnification; UV and transmitting light sources; Bar=200 μm). 187
- 65 Mean latex nanosphere concentration within the vascular compartment of rats (\pm SEM) at time points after introduction of 21.7 mg of the particles into isolated duodenal loops in the presence and absence of cytochalasin B (n=4). 188
- 66 Mean latex nanosphere concentration (\pm SEM) within the vascular compartment of rats at time points after introduction of 21.7 mg of the particles into isolated ileal loops in the presence and absence of cytochalasin B (n=4). 189
- 67 Polystyrene accumulation (\pm SEM) *per* gram of dry Peyer's patch tissue or Peyer's patch absent tissue excised from ileal loops after 2 hours incubation of 21.7 mg of 0.22 μm diameter latex nanospheres, in the presence (*) and absence of cytochalasin B at a concentration of 21 μM (n=4). 189

68	Mean polystyrene content (\pm SEM) of combined spleens and livers and MLN removed from rats 120 minutes after introduction of 21.7 mg of latex nanospheres (0.22 μ m diameter) into isolated ileal loops in the presence (*) and absence of cytochalasin B at a concentration of 21 μ M (n=4).	190
69	Schematic representation of particle translocation after intestinal absorption.	201
70	Mean (\pm standard deviation) 125 I concentration within the portal (P) and systemic (S) vascular compartments at monitored time points after oral administration of microencapsulated 125 I-IFN- γ or free 125 I-IFN- γ in conjunction with empty Poly-L-Lactide microspheres (*) (n=3).	213
71	Whole organ distribution of 125 I at various time points after oral administration of Poly-L-Lactide microsphere encapsulated 125 I-IFN- γ . Uptake is represented as a mean percentage (\pm standard deviation) of the initial oral dose (n=3).	213
72	Intestinal accumulation of 125 I at various time points after oral administration of Poly-L-Lactide microsphere encapsulated 125 I-IFN- γ . Uptake is represented as a mean percentage (\pm standard deviation) of the initial oral dose (n=3).	214
73	125 I levels within gut washes taken throughout the experimental period after oral administration of microsphere encapsulated 125 I-IFN- γ . Values are represented as a mean percentage (\pm standard deviation) of the administered 125 I-IFN- γ dose (n=3).	214

74	Mean percentage accumulation (\pm standard deviation) of ^{125}I <i>per</i> gram of dry intestine after oral delivery of microencapsulated ^{125}I -IFN- γ (n=3).	215
75	Mean uptake (\pm standard deviation) of ^{125}I into mesenteric tissue at time points after oral delivery of microencapsulated ^{125}I -IFN- γ (n=3).	215
76	Cumulative uptake of ^{125}I into all monitored tissues, both intestinal and extra-intestinal after oral administration of microencapsulated ^{125}I -IFN- γ (n=3).	216
77	Semilogarithmic plot of blood microsphere uptake at time points after oral administration of 7.5 mg Fluoresbrite™ microspheres in 0.5 ml of water (n=3).	248
78	Semilogarithmic plot of residual values after oral administration of 7.5 mg Fluoresbrite™ microspheres in 0.5 ml of water ($t_{\frac{1}{2}}$ represents the absorption half life)(n=3).	248

LIST OF TABLES

TABLE		PAGE
1	Specifications and methods of detection of latex microspheres employed throughout experimental investigations.	83
2	Zeta potentials of latex microspheres suspended in 10 mM phosphate / citrate buffer pH 7.07 (n=5).	128
3	Peak retention times of monodisperse polystyrene standards of known molecular weight (EasiCal©) (n=4).	131
4	Digitisation of chromatographic data obtained from GPC analysis of 3 µg of 0.97 µm latex microspheres.	134
5	FACS determined transfer of 0.87 µm diameter carboxylated Fluroesbrite™ microspheres into the vascular compartment after a single oral dose of 4.40×10^9 particles suspended in 1 ml of water (n=4).	152
6	Release of trace loaded ^{125}I -IFN- γ from 0.79 ± 0.48 µm diameter PLA microspheres into 20 mM phosphate buffer pH 7.5 (n=3).	210
7	Body distribution, represented as a percentage of the initial dose within each organ (whole) or site, of ^{125}I 15 minutes after oral administration of trace amounts of ^{125}I -IFN- γ encapsulated within Poly-L-Lactide microspheres with a mean diameter of 0.79 ± 0.48 µm (n=3).	211

- 8 Body distribution, represented as a percentage of the initial dose within each organ (whole) or site, of ^{125}I 15 minutes after oral administration of trace amounts of free ^{125}I -IFN- γ in conjunction with empty Poly-L-Lactide microspheres with a mean diameter of $0.79 \pm 0.48 \mu\text{m}$ (n=3). 211
- 9 Body distribution, represented as a percentage of the initial dose within each organ (whole) or site, of ^{125}I 240 minutes after oral administration of trace amounts of ^{125}I -IFN- γ encapsulated within Poly-L-Lactide microspheres with a mean diameter of $0.79 \pm 0.48 \mu\text{m}$ (n=3). 212
- 10 Body distribution, represented as a percentage of the initial dose within each organ (whole) or site, of ^{125}I 240 minutes after oral administration of trace amounts of free ^{125}I -IFN- γ in conjunction with empty Poly-L-Lactide microspheres with a mean diameter of $0.79 \pm 0.48 \mu\text{m}$ (n=3). 212

LIST OF ABBREVIATIONS

ANOVA	Analysis of variance
ATP	Adenosine triphosphate
AUC	Area under the curve
Bq	Becquerel
C	Carbon
Cl	Chlorine
ELISA	Enzyme-linked immunosorbent assay
FACS	Fluorescence activated cell sorter
FAE	Follicle-associated epithelium
FITC	Fluorescein isothiocyanate
FS	Forward scattering
GALT	Gut associated lymphoid tissue
GIT	Gastrointestinal tract
GPC	Gel permeation chromatography
H & E	Haematoxylin and Eosin
HIC	Hydrophobic interaction chromatography
HPLC	High-performance liquid chromatography
I	Iodine
Ig	Immunoglobulin
IL	Interleukin
i.m.	Intramuscular
IFN	Interferon
i.p.	Intraperitoneal
i.v.	Intravenous
K	Potassium
K_a	Absorption rate constant
M	Molar
MBq	Megabecquerels
M-cell	Microfold cell
MLN	Mesenteric lymph node
M_n	Number-average molecular weight
MPS	Mononuclear phagocyte system
M_w	Weight-average molecular weight
MWD	Molecular weight distribution
Na	Sodium
OD	Optical density
P	Probability

PLA	Poly (lactic acid)
PP	Peyer's patch
PPs	Peyer's patches
SEM	Standard error of the mean
SLFs	Small, solitary lymphatic follicles
THF	Tetrahydrofuran
UV	Ultra-violet
VR	Retention volume
w/v	Weight per volume
w/w	Weight per weight

1.0 INTRODUCTION

Factors related to the uptake of inert particulate matter from the intestinal lumen are discussed in the second half of this chapter, after revision of the relevant morphological and physiological aspects of the gastrointestinal tract (GIT).

1.1 MORPHOLOGY AND PHYSIOLOGY OF THE GASTROINTESTINAL TRACT (GIT)

The structure of the digestive tract reflects the sequential functional changes that occur as food is propelled from the mouth toward the anus by peristalsis, although histologically, the entire GIT is made up of four concentric layers: mucosa, submucosa, muscularis and mesentery (see figure 1 below).

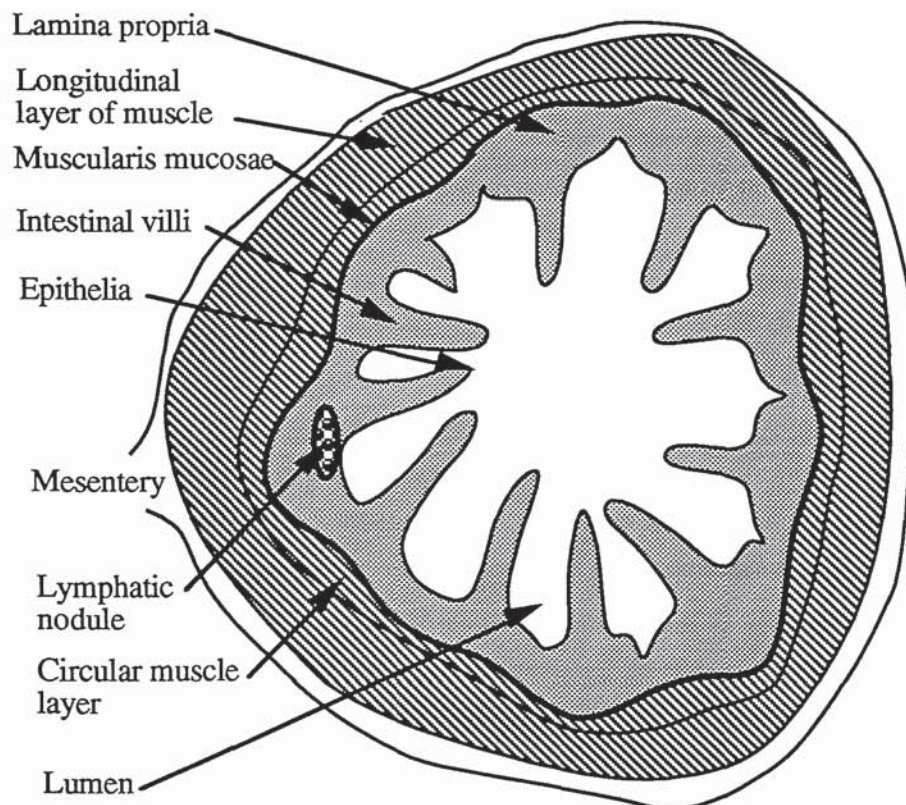


Figure 1. Diagrammatic representation of the overall histological organisation of the small intestine.

After the oral cavity, the hollow digestive tube is differentiated into four major organs: oesophagus, stomach, small intestine, and large intestine. At

the interface of these organs the nature of the mucus membrane changes abruptly as regards epithelial histology, folding, mucosal drainage, the presence of crypts, processes, glands and secretion of various digestive enzymes (Neutra, 1988).

1.1.2 LAYERS OF THE GASTROINTESTINAL TRACT

1.1.2.1 THE MUCOSA

The mucosa, or mucous membrane, can be conveniently divided into three components: a superficial epithelium comprising of a single layer of columnar cells; an underlying stroma composed of vascularised, loose connective tissue rich in immunocompetent cells in an aqueous ground substance (lamina propria); and a three to ten cell thick layer of smooth muscle (muscularis mucosae). Dramatic changes in the micro and macroscopic appearance and function of the mucous membrane occur from segment to segment of the alimentary canal. The luminal surface of the small intestine is so organised that the surface area available for contact with the intestinal contents is greatly amplified. In some mammals, but not in commonly studied laboratory rodents, the entire lining, including mucosa and submucosa may be thrown into large folds (pinnace and rugae). In addition to this, the surface of the small intestine is studded with innumerable villi, 23 *per* mm² in rat jejunum (Carr *et al.*, 1984), which amplify the absorptive surface area seven to 14 fold and are unique to this region of the GIT (figure 2). The villi are essentially finger like evaginations of the mucosa. Each villus contains an arteriole, a capillary network, a vein and a central lymphatic vessel or lacteal (section 1.2.6.1 and 1.2.6.2). At the bases of the villi are simple tubular invaginations or pits, called the crypts of Liberkuhn, that extend to the muscularis mucosae but do not penetrate it. Large intestinal mucosa is almost entirely devoid of villi but is heavily populated with mucus secreting glands, reflecting the need for lubrication and protection of the tissues from the dry luminal contents.

1.1.2.1.1 MUSCULARIS MUCOSA

The deepest layer of small intestinal mucosa is the muscularis mucosa, a continuous thin sheet of smooth muscle, 3 - 10 cells thick, that separates the mucosa from the submucosa. The contractile potential of this layer suggest

it may contribute to the movement of villi, and thus modulate the unstirred layer adjacent to the absorptive epithelium. Also, contraction of the muscularis mucosa may facilitate emptying of crypt luminal contents by causing luminal compression (Neutra, 1988).

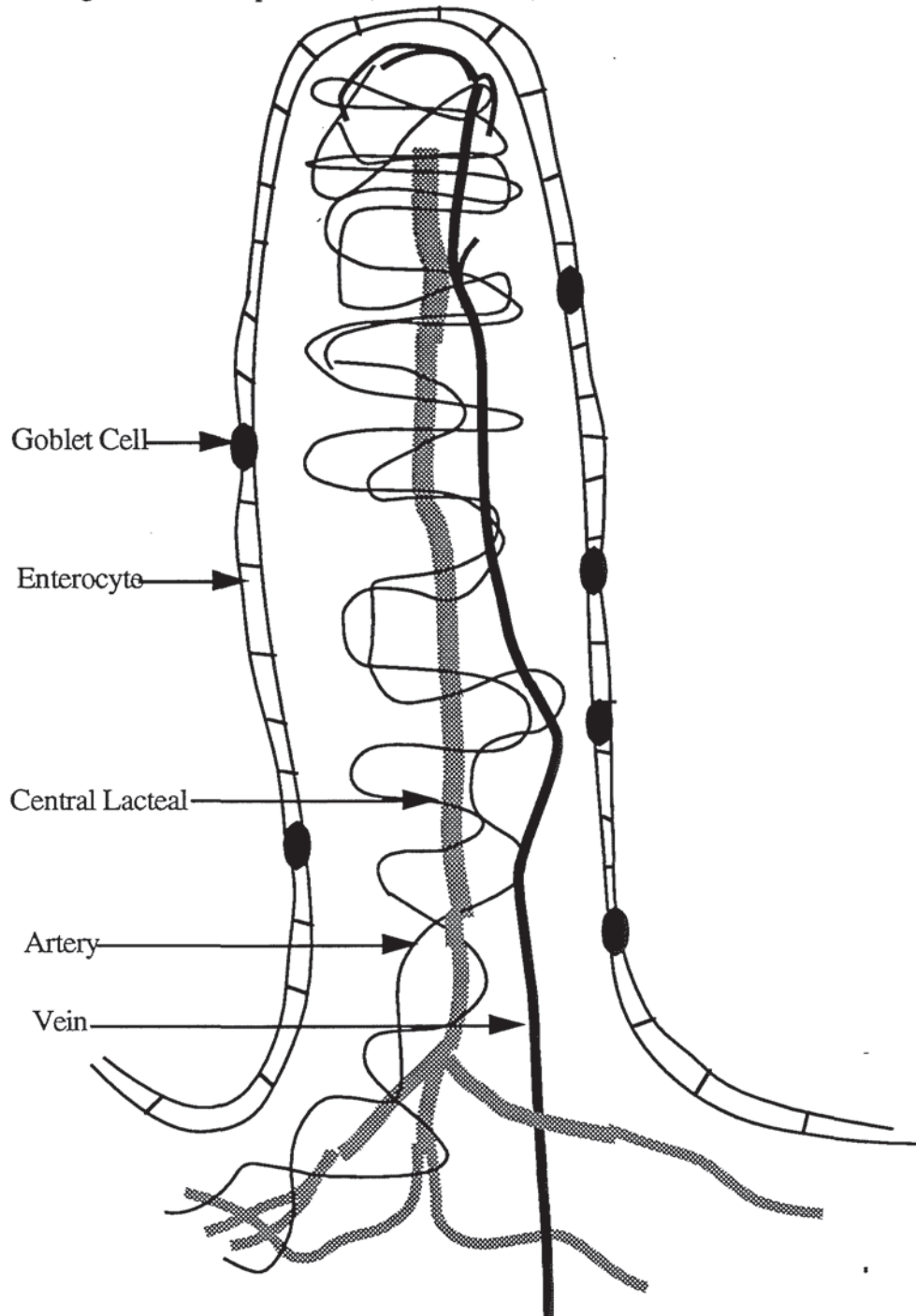


Figure 2. Diagram illustrating the blood circulation and lymphatic drainage within a typical small intestinal villus.

1.1.2.1.2 LAMINA PROPRIA

The middle mucosal layer is the continuous connective tissue space, the lamina propria, which is bounded above by the epithelium and below by the muscularis mucosa. In the small intestine, it forms the connective tissue core of villi and surrounds crypt epithelium. In normal mammals, the most abundant cell types in the lamina propria are mononuclear cells of great immunological importance: plasma cells, lymphocytes and macrophages. In addition, the lamina normally contains a few eosinophils, mast cells, fibroblasts, small unmyelinated nerve fibres, blood and lymph vessels, and smooth muscle cells. Extracellular connective tissue elements including collagen and elastic fibres are also present. The lamina propria provides an important support on which the intestinal epithelial cells rest and contains the blood vessels that nourish the epithelium. Additionally, the blood and lymphatic vascular channels in the lamina propria provide the means for transport to distant sites of material absorbed by the epithelium (section 1.2.6.1 and 1.2.6.2) (Neutra, 1988).

1.1.2.1.3 EPITHELIUM

The intestinal epithelial layer is an interface between the body and the external environment. It has both absorptive and secretory functions. During absorption many nutrients are modified by synthetic and degenerative processes as they cross the intestinal epithelium. In addition, many of the secretions delivered into the intestinal lumen are actually synthesised and assembled within epithelial cells.

Large and small intestinal epithelium is a continuous sheet of single layered, non-keratinised, cuboidal or columnar cells that is constantly being renewed due to a zone of intense mitotic activity located in the lower half of the crypts. This site is rich in undifferentiated stem cells. Also present are; mucus secreting goblet cells, a variety of different endocrine epithelial cells and in most mammals the Paneth cells with large secretory granules. In the small intestine, new cells migrate upward and are eventually extruded from the villus tip. This process takes two days in the rat. Similarly, in the large intestine undifferentiated cells give rise to daughter cells committed to differentiation into columnar, goblet and enteroendocrine cells as well as rarer cell types of unknown function. These cells migrate up the crypt wall and onto the flat mucosal surface. They are sloughed from the luminal

surface at extrusion zones located approximately midway between crypt openings, after a lifetime of about 6 days (Neutra, 1988).

Small intestinal epithelium is mostly composed of absorptive cells (enterocytes) with smaller numbers of mucus secreting goblet cells and other rarer cell types (M-cells) sometimes present. The main function of small intestinal epithelium is the absorption of nutrients (Madara *et al.*, 1987). Enterocytes possess an apical brush border (0.5 - 1.5 μm wide) consisting of microvilli arranged in a parallel array. It is estimated that the microvilli increase the apical surface area 14 - 40 fold (Brown, 1962). Within the microvillus membrane itself, there are high concentrations of enzymes including disaccharidases and peptidases which play a crucial role in the terminal digestion of dietary carbohydrate and peptides prior to their absorption. Proteins responsible for the transport of Na^+ and D-glucose, Na^+ and amino acids, and perhaps fatty acids (Hopfer, 1977) are also associated with the microvillus membrane.



Figure 3. Typical enterocyte structure.

The apical-lateral surfaces of intestinal epithelial cells are bound together by junctional complexes consisting of three parts: the zona occludens, or 'tight junction'; the zona adherens; and the most basally located spot desmosome (figure 3). The tight junctions are closest to the lumen and form a barrier to the movement of integral membrane proteins, thus preserving membrane polarity and the unique composition of the apical plasma membrane as opposed to the basolateral plasma membranes. The tight junction also prevents the passage of macromolecules from the lumen into the intercellular

spaces and lamina propria. It consists of a circumferential band (0.1 - 0.6 μm in depth) in which the lateral membranes of adjacent cells are closely opposed. Electron microscopy of thin sections cut perpendicular to this zone reveals a series of punctate fusion's of the outer membrane leaflets of adjacent cells (Madara *et al.*, 1987).

The zona adherens lies directly below the zona occludens. At this site the plasma membranes are separated by a 20 nm zone rich in fine fibrils thought to consist of cell-adhesion protein. The cytoplasmic side of the plasma membrane at the zona adherens has a transversely oriented mesh of 7 nm microfilaments which splay into the terminal web region (a horizontal ring of actin and myosin filaments which are thought to be involved in the movement of microvilli) (Madara *et al.*, 1987, Neutra, 1988).

Spot desmosomes do not form a continuous belt around the cell as do the occluding and adherent junctions. Instead they serve as spot welds between epithelial cells and as sites of attachment for stabilising cytoskeletal cables. The lateral membranes of adjacent cells in the region of a spot desmosome run parallel to each other and are separated by a 30-50 nm space with glycoprotein like fibrils running in-between. The fibrils from both cells appear to be connected in the middle of the 30-50 nm space. In the region of a spot desmosome, the cytoplasm of adjacent cells contains an electron dense 15 - 20 nm thick disk like plaque, which is separated from the lateral membrane by about 8 nm. Embedded within these plaques are numerous filaments which loop through the terminal web and attach to other spot desmosomes (Madara *et al.*, 1987).

The enterocyte basolateral cell membrane (plasma) has no digestive enzymes but is rich in Na / K-dependent ATPase, a membrane-intercalated enzyme that pumps sodium into the lateral intercellular space. Subsequently, sodium moves into the epithelial cell from the lumen down a concentration gradient. The accumulation of sodium in the intercellular space creates an osmotic gradient. Water is induced to enter the lateral intercellular space either from across the cell walls or in a paracellular manner from the intestinal lumen through the tight junctions. The consequential increase of hydrostatic pressure produces fluid flow into the lamina propria (Diamond *et al.*, 1967 and Loeschke *et al.*, 1970). The enterocyte basolateral membrane, like most other mammalian plasma membranes, is approximately 7 nm wide. In the absence of substantial water and

electrolyte absorption the lateral plasma membranes are closely opposed to one another (15 - 30 nm apart) along their entire length (DiBona *et al.*, 1974). In contrast, during net fluid absorption, the intracellular space is widened, often to 2 to 3 μm , between cells lining the upper third to half of the villi (DiBona *et al.*, 1974). This expansion of the lateral intercellular space is most pronounced along the basal half of cells, but may extend towards the apex to the tight junction, especially between cells on or near the villus tip. The appearance of these spaces during net water and electrolyte absorption and their absence during net fluid and electrolyte secretion suggest that the size of the intercellular spaces is controlled at least in part by solute flow and osmotic gradients (Madara *et al.*, 1987).

The portion of the basolateral membrane that encloses the basal surface of enterocytes is devoid of intercellular junctions and is applied closely to the basal lamina (basement membrane) interposed between epithelium and lamina propria. The basal lamina appears under the electron microscope as a continuous sheet of amorphous or fine fibrillar material of intermediate electron density. It is approximately 30 nm wide but has numerous oval shape defects (McClugage *et al.*, 1984). These gaps are large enough (0.5-5 μm) to permit the migration of chylomicrons and other lipoproteins from the epithelial space to the lamina propria (Tytgat *et al.*, 1971), and lamina propria cells such as lymphocytes into the lateral intercellular space between epithelial cells (intraepithelial lymphocytes). Additionally, small foot like extensions of enterocyte cell basal cytoplasm occasionally project into the lamina propria through gaps in the basement membrane. The exact function of the epithelial cell basement membrane is unknown. It may serve as a barrier with a regulatory role in the exchange of material between the lamina propria and enterocyte, together with its intercellular spaces. Whether the components of the basal lamina are stable or rapidly renewed is unknown. It is also unclear if the basal lamina migrates from crypt to villus tip in concert with its overlying epithelium or remains in place as epithelial cells glide over its surface (Madara *et al.*, 1987).

1.1.2.2 THE SUBMUCOSA

The submucosa is a collagenous connective tissue layer, often containing lymphatic cells, separated from the mucosa by the muscularis mucosa. It is extremely vascularised with large blood vessels, as well as lymphatic vessels and nerves that send finer branches into the mucosa and muscularis.

1.1.2.3 THE MUSCULARIS

The muscularis contains two layers of muscle, which are smooth, except in the case of the upper oesophagus and anal sphincter, where the fibres are skeletal in nature. The inner layer of muscle fibres are arranged in a circular manner around the tube (circular layer), whilst those of the outer layer are disposed lengthwise along the tube (longitudinal layer). Contractions of the circular layer constrict the lumen; contractions of the longitudinal layer shorten the tube. There are various sphincters and valves along the GIT at which the layer of circular muscle is much thicker (Neutra, 1988).

1.1.2.4 THE MESENTERY

The stomach and intestines are supported by suspensory folds from the peritoneal wall known as the omenta and mesenteries, through which the lymphatic vessels, blood vessels, and nerves that supply the GIT extend. The peritoneum is a closed sac lined by a moist slippery membrane that allows the suspended abdominal organs to slide freely over one another during peristaltic movements. The mesentery contains interwoven, elastic networks of collagen fibres, which harbour mononuclear phagocytes, lymphocytes and adipose cells. Dense aggregates of lymphocytes, monocytes, and macrophages are visible to the naked eye as 'milky spots', especially common in the omenta and in the peritoneal lining of the diaphragm. These leukocyte cells are also found free in the peritoneal fluid (Neutra, 1988). The mesentery also contains the mesenteric lymph nodes (MLN) which are part of the mucosal immune system even though they are situated outside the intestine. MLN receive lymph from the small and large intestine *via* lymphatics running along the mesenteric arteries (Laissue *et al* ., 1993).

1.1.3 REGIONS OF THE GASTROINTESTINAL TRACT

1.1.3.1 THE STOMACH

The cardiac sphincter denotes the end of the oesophagus and entrance to the stomach. The more powerful pyloric sphincter joins the small intestine with the stomach (figure 4). The stomach is flattened anteroposteriorly and is J shaped with upper (right) concave and lower (left) convex borders called the lesser and greater curvatures. Above and to the left of the cardiac sphincter

is a bulge called the *fundus*, with the main body of the stomach below it and passing into a region called the pyloric antrum. This in turn, is continuous with the pyloric canal, which narrows to the pylorus, the opening into the duodenum (Neutra, 1988).

1.1.3.2 THE SMALL INTESTINE

The small intestine is a thin walled tube extending from the pylorus of the stomach to the colon (figure 4) At the pylorus, the smooth-surfaced gastric mucosa changes abruptly to a rough-surfaced intestinal mucosa with numerous villi. The small intestine consists of three portions: the duodenum, jejunum, and ileum. The duodenal-jejunal junction is marked externally by a thickening of the mesentery. Otherwise, no definite structures distinguish the three segments, although certain histological features characterise their mucosae (Neutra, 1988).

Macromolecular nutrients in food are digested extracellularly in the small intestine, largely by the action of pancreatic enzymes. The terminal digestion of proteins and carbohydrates occurs at the mucosal surface by enzymes of intestinal origin. The resultant amino acids, monosaccharides, fatty acids, and monoglycerides are absorbed along a vast intestinal absorptive surface. Water and electrolytes from salivary, gastric, pancreatic and hepatic secretions are also re absorbed (Section 1.1.2.1.3).

1.1.3.3 THE LARGE INTESTINE

The large intestine begins at the ileocecal valve and ends at the anus. It includes: an initial blind pouch, the cecum; the ascending, transverse, descending and sigmoid colon; and the rectum, ending at the external orifice or anus. The histological organisation of the colon reflects its principal functions: reabsorption of water and elimination of undigested material, i.e. faeces. Hence the mucosa of the large intestine lacks villi, but its flat surface is punctuated by the openings of numerous crypts or glands concerned with lubrication of the mucosa, thus protecting it from the solid dehydrated luminal contents. Lymphatic nodules are also abundant within the lamina propria, alongside macrophages, lymphocytes and plasma cells. Certain bacteria are associated closely with the surface epithelium of the colon, in which they abound, without causing ill effects. They digest residual organic matter whose breakdown products may then be absorbed.

Trace nutrients synthesised by bacteria are also absorbed. The submucosa is identical to that in the small intestine, except it contains large accumulations of fat cells (Neutra, 1988).

A principal function of surface cells throughout the colon is the final absorption of water and salt from the faeces; thus their basolateral membranes are rich in Na/ K-dependant ATPase. Sodium and chloride are absorbed with water following passively, whereas potassium and bicarbonate are released into the lumen (Neutra, 1988).

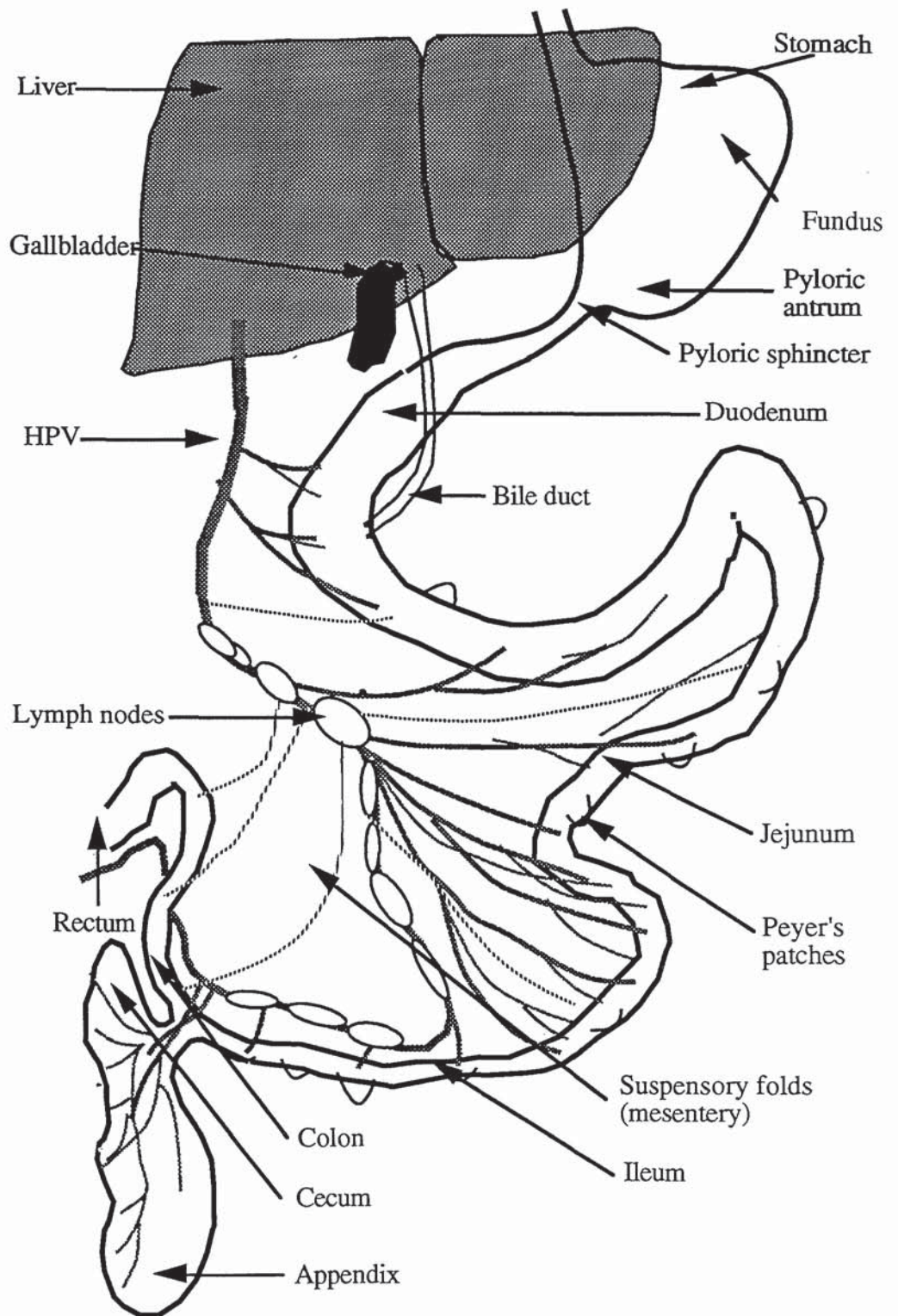


Figure 4. Schematic representation (not to scale) of the different regions within the GIT.

The cecum is a blind pouch at the proximal end of the colon, its terminal thin tip is known as the vermiform appendix. The structure of the cecum resembles that of the rest of the colon, and the vermiform appendix has a similar structure in miniature. The glands of the appendix are simple tubes,

sometimes forked; the epithelium is rich in mucous cells and contains many endocrine cells. The surface epithelium consists of columnar cells with a few mucous cells. Lymphatic nodules are abundant and more or less confluent. The wealth of lymphatic vessels and lymphatic tissues is a distinguishing feature of the appendix (Neutra 1988).

The rectum is divided into two parts, the lower part of which continues to the anus (the anal canal). The lining of the first part is thrown into several large, semi-lunar, circular folds. For most of its length the anal canal has on its inner wall a number of longitudinal folds, the anal columns.

The mucosa in the first part of the rectum is similar to that of the colon, but its glands are longer. Solitary lymphatic nodules are common in the rectum which has no mesentery, and its serosa is replaced by adventitial connective tissue. The epithelium of the lower anal canal changes abruptly from simple columnar to stratified cuboidal cells. The outer layers of the anal canal include a very vascular submucosa that contains blood vessels, numerous valves and veins which form the haemorrhoid plexus. The circular layer of the muscularis becomes thickened at its termination, forming the internal anal sphincter. Beyond this, striated muscle fibres surround the orifice and form the external anal sphincter (Neutra, 1988).

1.2 PARTICLE UPTAKE FROM THE GASTROINTESTINAL TRACT

Healthy gastrointestinal epithelium is generally thought to exclude all macromolecules and particulates. However, for the purposes of immunisation, macromolecular drug delivery, and the study of pathogen entry, the subject is a focus of much research activity. This is not just a recent exercise. German scientists reported the translocation of starch particles from the GIT to the circulation in test animals 140 years ago (Herbst, 1844). 85 years ago Rahel Hirsh noticed starch grains, which had been orally administered, in the blood and urine of patients at her clinic. Her report, delivered to the society of doctors at the University of Berlin, was thought to be implausible and she was ridiculed (Volkheimer, 1993). More recent work has led to the formulation of several models regarding the uptake, transport and the eventual fate of particulate matter after oral administration (reviewed below). Despite these different theories regarding particle translocation, represented graphically in figure 5, it is possible that a combination of mechanisms is responsible for this phenomenon.

1.2.1 PHYSICAL BARRIERS TO PARTICLE UPTAKE: MUCUS

Mucus provides a continuous unstirred layer over the GIT mucosa and is the first layer that interacts with foreign materials, e.g., food, bacteria and microspheres. The thickness of the mucus layer along the GIT varies considerably from 5 μm to 200 μm . It has a mean thickness of 81 μm in the rat duodenum. (Gu *et al.*, 1988). Mucus and its gel-forming polyionic glycoprotein component has the ability to change its physical state from that of a viscous, mobile solution to a relatively impermeable state with fluid rejecting properties ((Florence & Jani, 1993)). It is a water-insoluble viscoelastic gel created by its non covalently, cross linked polymer structure. Mucus viscosity increases when the ionic strength of the hydrating medium is lowered (Gu *et al.*, 1988).

The fluidity of the mucus layer of the GIT may also be altered by surfactants (Gullikso *et al.*, 1977 and Ma *et al.*, 1990). Surfactants will reduce the viscosity of mucus, resulting in increased uptake of dietary protein, in high molecular mass from, and particulate matter, along the lamina propria (Hemmings, 1980) and mucosal surfaces. Experiments with the behaviour of mucus and colloidal microspheres show that mucus can cause aggregation, as can very low pH. If microspheres were administered with an appropriate surfactant, then the extent of aggregation of the particles might be reduced and uptake may be increased (LeFevre *et al.*, 1980, Alpar *et al.*, 1989), but if any additive results in excess mucus and mucin production this may counteract such an effect (Gerhart *et al.*, 1981). It is difficult to define precisely the extent of uptake and the consequences of mucus-microsphere aggregation, but it can be surmised that this must be one vital factor which reduces the overall quantitative uptake of microspheres from the GIT (Florence & Jani, 1993)

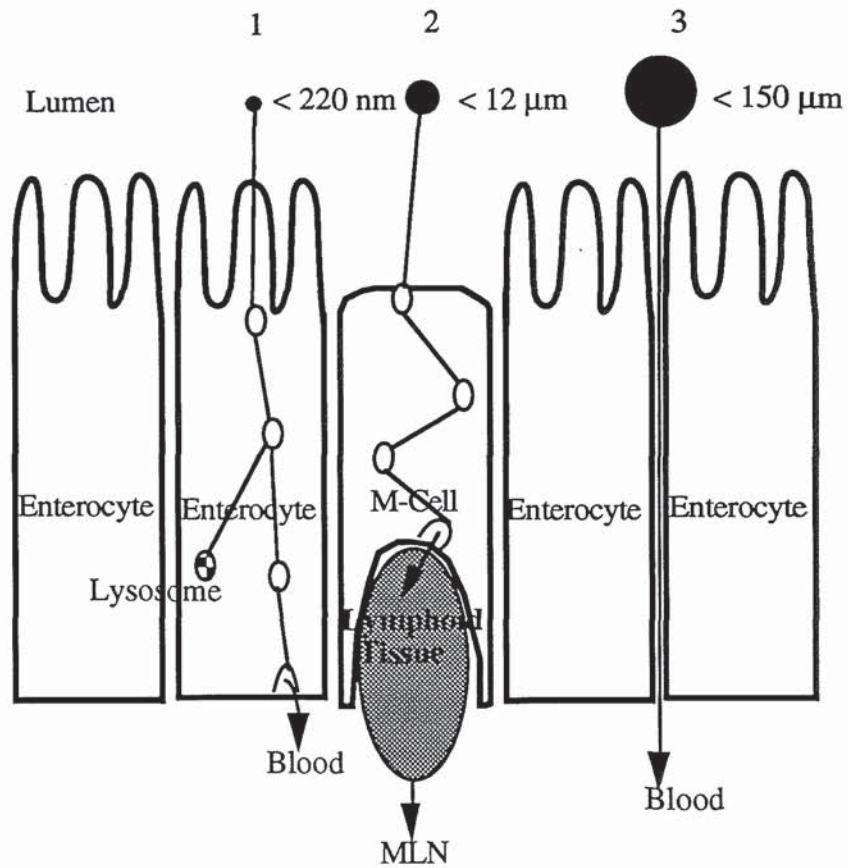


Figure 5. Proposed mechanisms of particle penetration of the intestinal epithelial barrier: (1) Intracellular uptake and transport *via* ordinary enterocytes (section 1.22); (2) Lymphatic uptake *via* M-cells (section 1.24) or macrophages (section 1.25); (3) Uptake by a paracellular pathway (section 1.23). Adapted from Smith *et al.*, (1994).

1.2.2 UPTAKE OF PARTICLES BY ENDOCYTOSIS

Neonatal intestinal epithelium is known to absorb macromolecules as a mechanism of passive immunisation, a decrease in permeability ('closure') is considered a physiological step in maturation (Pang *et al.*, 1983; Udall *et al.*, 1981b; Yammamoto, 1982). As well as the products of food breakdown by enzymes in the gut, it has been established that larger molecules may be taken up by enterocytes in the adult intestine (O'Hagan *et al.*, 1987). The uptake of azo dye particles (20-40 nm) by adult duodenal cells *via* pinocytosis has been established (Barnett, 1959). Pinocytosis is the non-specific uptake of extracellular fluid by incorporation within an invaginated plasma membrane before internalisation in vesicles of up to 200

nm. Transportation of azo dye occurred intracellularly in membrane bound vesicles, with the dye finally appearing in the intercellular spaces of the epithelium. Other workers (Saunders *et al.*, 1961) demonstrated the uptake of latex particles (220 nm) by jejunal absorptive cells within an hour of administration. Vesicular transportation through the cytoplasm was followed by discharge of some of the beads into the lamina propria. 2-4 hours after dosing particles were observed in the interstices of the lamina propria and in the lymphatics of the mucosa. Examination of the liver, 2-4 hours post dosing, revealed circulating particles had accumulated within the space of Disse or in vesicles within hepatic cells. Polystyrene beads were also visualised within the lumen of glomerular capillaries. Despite this significant entry of the microspheres to extra-intestinal sites, transport to enterocyte lysosomes was found to be the most common intracellular fate for absorbed material.

Jani *et al.*, (1989) suggested that endocytosis might be involved as a second pathway for the intestinal uptake of small (100 nm) fluorescent latex particles. Further experimental evidence for transcytotic transport was provided after oral administration of Percoll particles (30 nm) to young mice (Matsumo *et al.*, 1983). After uptake by enterocytes, spheres were demonstrated in the MLN, PPs and the milky spots of the omentum. Minor Percoll aggregates were readily found in Kupffer cells of the liver, indicating hematogenous translocation. The presence of Percoll in perivascular macrophages of the thymic cortex supported this. Kukan *et al.*, (1989) detected ^{14}C in the plasma of rats who had received a 4 ml oral dose of ^{14}C -terpolymer nanoparticles (270 nm). Plasma activity reached a peak (0.002 % dose / ml plasma) 2 hours after administration. Activity in liver, spleen and lung persisted up to 7 days from administration. Uptake of nanospheres from the GIT was said to occur by endocytosis and / or pinocytosis, but by the admission of the authors, it may well have represented low molecular weight fractions of the polymer.

Hussain *et al.*, (1994) found that covalently coupling *Lycopersicon esculentum* (tomato lectin) to carboxylated 500 nm diameter polystyrene microspheres resulted in significant systemic absorption of the particles through intestinal enterocytes. Receptor mediated endocytosis *via* class II receptors on the enterocyte apical membrane was suggested as the mechanism of uptake. Tomato lectin was thought to interact with these receptors and enable the relatively large microspheres to be absorbed.

Considerable systemic accumulation (23.0 % of dose) resulted, with significant numbers of particles detected within the blood, liver, spleen and kidney. The polystyrene content of intestinal segments devoid of Peyer's patches (see below) was found to be far greater than that of identical tissue which contained lymphatic nodules, indicating a re-routing of particle uptake through villus tissue.

In the large intestine, Colonic absorptive and goblet cells were seen to demonstrate endocytotic properties after exposure to cationized ferritin (Barbour *et al.*, 1983). The major pathway for the cationized ferritin was rapid vesicular transport to secondary lysosomes.

Although several reports suggest that very small particles may infrequently be taken up into intestinal absorptive cells by an endocytosis like process, the enterocyte membrane still remains an effective barrier to the overwhelming majority of particulates (O'Hagan, 1990), although studies by Hussain *et al.*, (1994) indicate that it may be possible to up-regulate this mode of particle uptake.

1.2.3 PARACELLULAR TRANSPORT OF PARTICLES: PERSORPTION

In healthy gut the zona occludens (tight junctions) of the epithelial cell membrane is thought to act as an effective barrier against the absorption of all but the smallest of molecules (section 1.2.1.3). However, during the 1960's it was claimed that a wide variety of particles of diverse shapes, sizes, and compositions are transported by this pathway in many species, including humans (Volkheimer, 1968, 1972, 1975, 1977, 1993).

Volkheimer coined the term persorption to describe the absorption of solid particles of up to 150 μm diameter whose nondeformability ruled out transcytotic movement within vesicles. The 'persorbability' of particles was said to be related to their size and hardness, with particles of between 7 and 70 μm diameter and of high rigidity exhibiting the highest rates of absorption (Volkheimer, 1977). The age of the subject and gastrointestinal motility were also implicated as factors affecting the phenomenon.

Volkheimer and his team, using corn starch granules of 3-25 μm diameter, detected particles in the vascular compartment as early as 5 minutes after

oral administration. This was followed by one or two "waves" of absorption in the 5 hours after dosing, possibly indicative of particle translocation *via* different mechanisms of absorption (Kreuter, 1991). Few starch granules were found in the circulation at 12 hours, and none at 24 hours after ingestion. Starch grains were eliminated in the urine within 4 hours of administration. The efficiency of starch particle transport was estimated to be 0.002 % (Volkheimer, 1972, 1977, 1993). In a more recent study, sediments prepared from freshly voided urine of four patients with leucine-sensitive hypoglycaemia, on oral cornstarch therapy contained numerous starch granules. Sediments of 7 controls contained no granules. Urine was examined 2-3 hours after dosing (Gitzelmann *et al.*, 1993).

Polyvinyl chloride particles (10-60 μm) were detected within the vascular compartment shortly (10 minutes) after oral administration to dogs (see section 1.2.6.2). More particles were found in the portal circulation than the systemic, suggesting hematogenous dissemination (see section 1.2.6.2) from uptake sites (Volkheimer, 1975). Persorbed particles were reported to pass through the epithelial layer between the enterocytes in a paracellular fashion. This was particularly exaggerated at extrusion sites of mature enterocytes (section 1.2.1.3) and between villi. A mechanical 'kneading' process, mediated by action of the muscularis mucosae, was reported to be an important factor in the process of persorption. Lee, (1971) noted a similar process in that the villi of isolated dog intestine extrude cells during contraction and take in fluid at the tip during relaxation. Volkheimer, (1975) found that nicotine and caffeine increased the rate of persorption, while atropine significantly reduces the effect. This is consistent with the theory that intestinal motility plays an important role in the process.

Histological examination of tissue, using light microscopy, revealed particles in spaces between epithelial cells, the lamina propria, and in the lumen of blood and lymphatic vessels (Volkheimer, 1975) However, the possibility of artefact due to tissue damage has caused many to view this evidence with scepticism. The mechanism by which very large particles cross epithelial barriers as well as the endothelium of villus capillaries to reach the portal circulation also remains the subject of speculation. Current knowledge suggests that a size restriction of approximately 100 nm would be imposed by the fenestrae of capillary endothelia. Thus the transport of very large particles, such as starch grains, away from the lamina propria would be expected to occur almost exclusively within the lymphatic system

(Barrowman, 1978). In addition, the presence of very large particulates (>7 μm in diameter) in the circulation many hours after dosing is surprising as these would be expected to become entrapped in the capillary beds of the lungs. Smaller particles may be removed from the vascular compartment by hepatic Kupffer cells (see section 1.2.6.2).

Other workers (LeFevre *et al.*, 1980) performed similar experiments to Volkheimer, the results of which failed to confirm the rapid appearance in the blood of particles greater than 10 μm in diameter. Blood taken from groups of 6 mice 20, 60 and 240 minutes after gavage of 3.5×10^6 15.8 μm diameter carbonised microspheres contained no particles. Low numbers of microspheres were seen in cardiac blood taken at similar time intervals after gavage of 5.7 μm diameter latex microspheres. Tissues removed from these test animals, failed to provide conclusive evidence of microsphere translocation. LeFevre *et al.*, (1980) concluded that the intestine provided an effective barrier to the uptake of particles greater than 5-6 μm in diameter. Long term feeding studies with microcrystalline cellulose (>20 μm) in rats also indicated negligible uptake (Steege *et al.*, 1980).

In contrast, two different ^{35}S -labelled polystyrene sulphonate preparations, with grain sizes of 15-35 μm and 80-125 μm , were detected in blood, urine and internal organs 50 hours after oral administration to pigs (Schneider *et al.*, 1983). Unfortunately, the low levels detected were deemed insignificant in light of quantification of the water-soluble radioactivity within the particles prior to dosing. Dedek *et al.*, (1983) conducted experiments with similar sized ^{35}S -labelled preparations of styrene / divinyl benzene copolymer. Extensive analytical precautions were taken to remove water soluble radioactivity. After a single oral dose (5 g) of labelled material to pigs, about 0.002 % of the particles were detected within the urine from animals monitored over 35 days. Digested kidneys and MLN excised from sheep were found to contain opal-phytoliths, large plant particles, which had been ingested by the animals (Nottle, 1977 and Baker *et al.*, 1961).

Aprahamian *et al.*, (1987) described the transmucosal passage of polyalkylcyanoacrylate nanocapsules *via* a paracellular pathway (see also section 1.2.6.2). Nanocapsules (100-200 nm) loaded with an iodinated oil were identified in the intercellular spaces of the proximal jejunal cells, of dogs, by X-ray microprobe analysis using a scanning electron microscope

following cryofixation and freeze-drying of intestinal biopsies. 10-15 minutes after administration, capsules were found at the tips of villi within defects of the mucosa representing areas of desquamation of mature epithelial cells. 15 minutes after administration, nanocapsules were seen in the lamina propria in the vicinity of the basal membrane. They then appeared in the small capillaries near the epithelium and finally in the intravillus capillaries, where the nanocapsules were observed in close contact with red blood cells and the inner wall of endothelial cells. Plasma iodine levels within the mesenteric vein increased rapidly between 15 and 45 minutes after administration. After this time iodemia slowly decreased reaching basal levels 105 minutes after dosing. Between 15 and 30 minutes after administration, a few nanocapsules were also seen within the lacteals.

1.2.4 PARTICLE UPTAKE VIA THE PEYER'S PATCHES (PPs)

Peyer's patches (PPs) are located on the antimesenteric wall of the small intestines, being particularly abundant in the ileum close to the ileocecal junction. They are also present, although less numerous, in the jejunum and lower duodenum (Ritschel, 1991). PPs appear to the naked eye as white oval bodies, although microscopically, they are composed of many lymphatic nodules in close contact, forming a dome-like shape exposed to intestinal lumen. In humans PPs can be detected at 24 weeks' gestation. The average number of patches increases from about 60, at 24-29 weeks of gestation, to about 240 at the age of 14. After 14 years the numbers decline to about 100 patches in persons older than 70 years (Laissue *et al.*, 1993).

The typical Peyer's patch lymphatic follicle (figure 6), situated below the follicle associated epithelium (FAE) contains three zones. The dome region, located immediately beneath the epithelium, contains many lymphocytes, plasma cells, and macrophages. The corona surrounds a large germinal centre and separates the follicle from the interfollicular area. Structure and proliferative activity of the germinal centre in the patch are similar to those in other lymphoid organs. The thymus dependant area contains mainly small T lymphocytes clustered between large follicles, interdigitating cells, and many venules with a high endothelium, important sites for the (in)migration of lymphocytes into PPs (Laissue *et al.*, 1993).

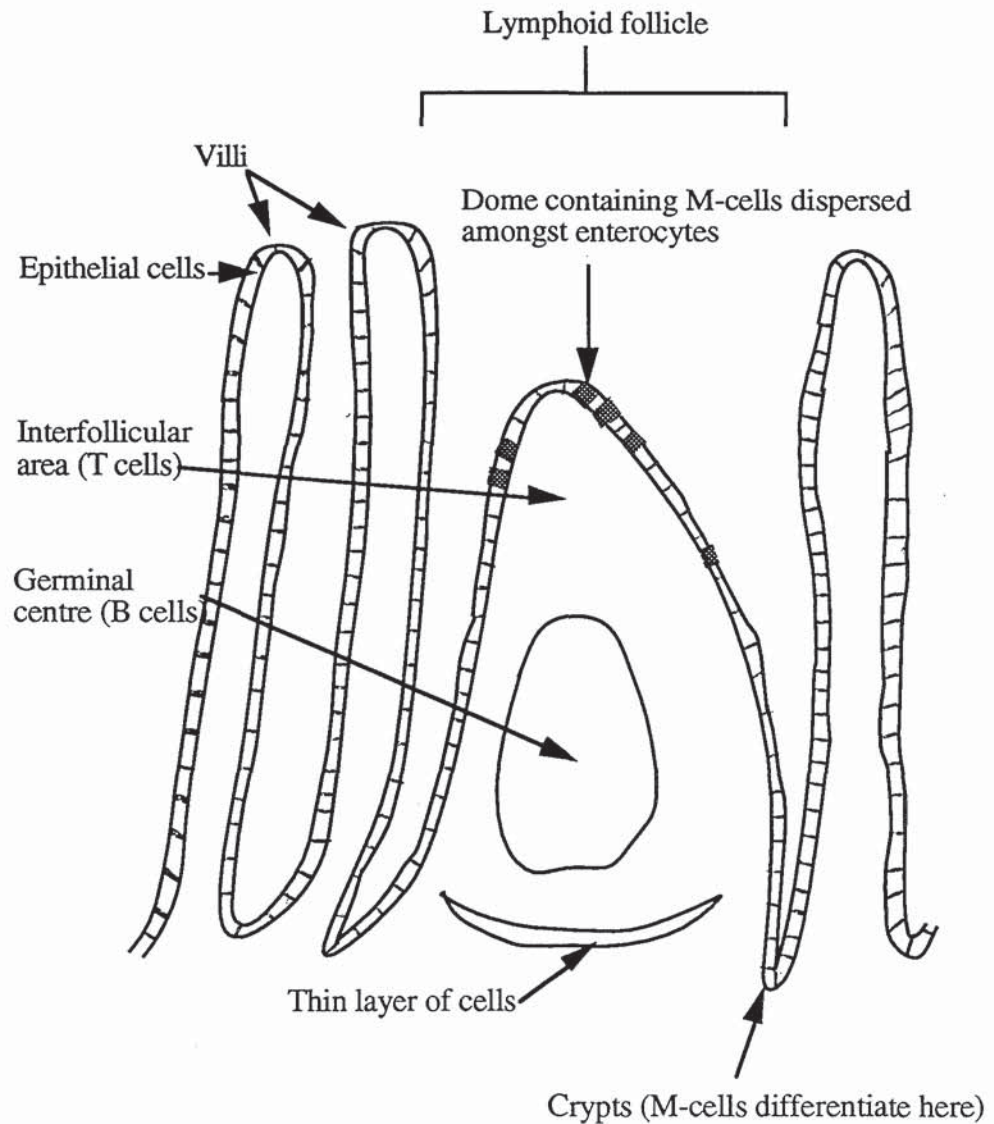


Figure 6. Schematic representation of the different regions of an intestinal lymphoid follicle. Adapted from O'Hagan, (1990).

FAE contains a peculiar type of epithelial cell (M-cell) whose apical surface carries microfolds and no microvilli. FAE contains reduced numbers of goblet cells resulting in lower levels of mucus secretion in the vicinity of M-cells. This factor makes M-cells more accessible to particulate matter than epithelial cells in other regions of the GIT (Kreuter, 1991). M-cells possess a relatively sparse glycocalyx and very few lysosomes. They have the ability to recognise and take up intraluminal antigens (Owen *et al.*, 1974, 1977) (see figure 7) .

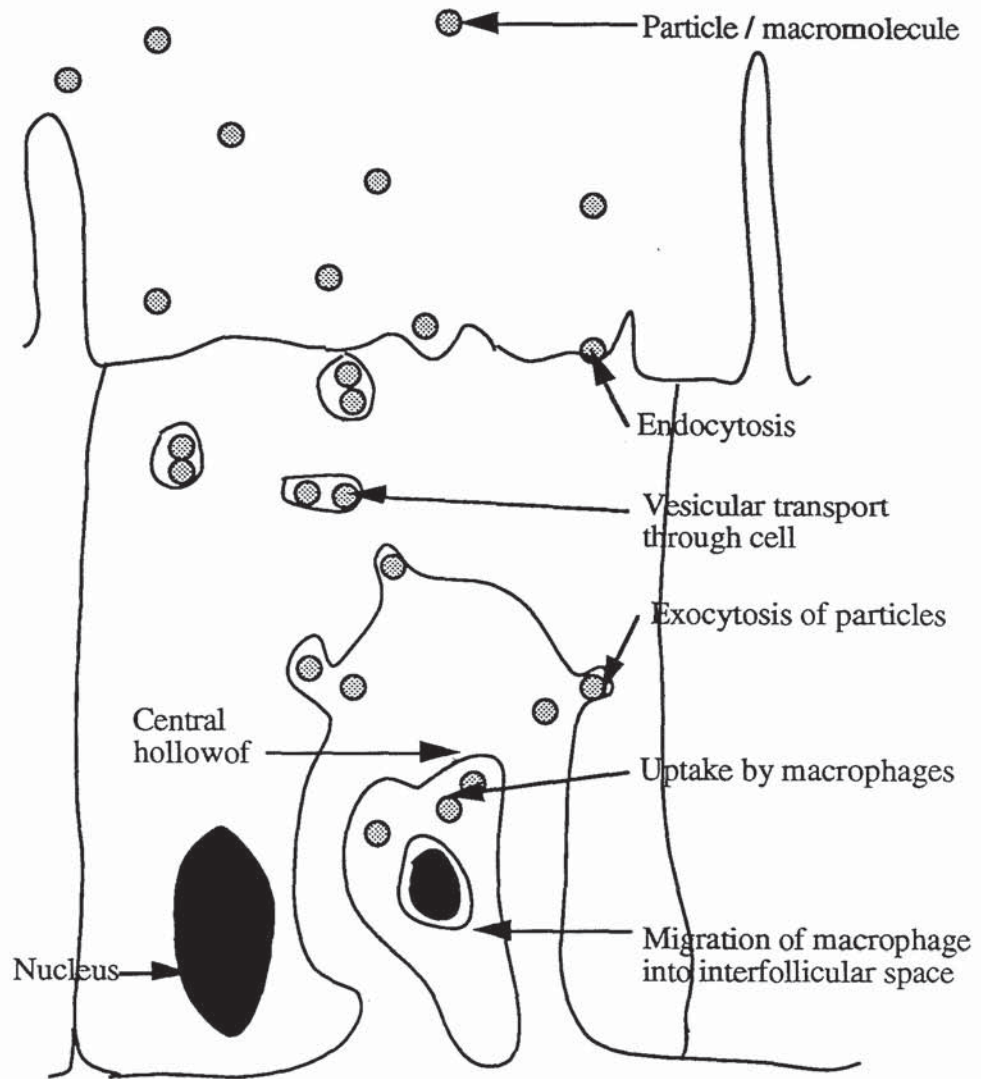


Figure 7. Vesicular transportation of particles through M-cells. Adapted from O'Hagan, (1990).

Binding of macromolecule (e.g. an antigen) to the highly anionic M-cell apical membrane is followed by rapid endocytosis (figure 7). Vesicles then shuttle antigen across the thin apical cytoplasm as a prelude to exocytosis at the basolateral membrane (Bye *et al.*, 1984). M-cell architecture makes them specialised for endocytosis and transcellular transport of intact macromolecules and particles which incur negligible degradation during transit through the cell (LeFevre *et al.*, 1984). The M-cell basolateral surface is infiltrated by lymphocytes and macrophages, forming a pocket subdomain in which these cells are in extremely close proximity ($0.3 \mu\text{m}$) to the intestinal lumen (Pappo *et al.*, 1991). Following exocytosis of antigen, exposed lymphocytes and macrophages migrate out of the epithelium and towards the aggregates of lymphoid cells in the follicle. The passage of

lymphocytes and macrophages through the FAE is facilitated by the porosity of the basement membrane which is considerably more "leaky" than that of adjacent villus cores, with pores of up to 10 μm or larger (McClugage *et al.*, 1986). Within the Peyer's patch follicle, helper T cells may participate in the maturation of B cells into antibody producers after antigen presentation. Phagocytes and lymphocytes are also capable of entering the draining MLN from the PPs. Within the MLN, lymphocytes proliferate and may enter the vascular compartment *via* the thoracic duct. Circulating lymphocytes may then lodge in the lamina propria of the GIT where terminal differentiation into sedentary IgA producing plasma cells occurs under the influence of locally produced cytokines such as IL-5 and IL-6, derived from T cells and mucosal epithelial cells. By this long route lymphocytes eventually "home in" on the mucosal surfaces, conferring local, secretory immunity (Mestecky *et al.*, 1992).

In addition to PPs there is an abundance of small, solitary lymphatic follicles (SLFs) throughout the intestinal tract, particularly in the vermiform appendix, colon and rectum. Like PPs, SLFs contain a germinal centre and their associated epithelium contains M-cells. SLFs are structural and probably functional equivalents of aggregate lymphoid follicles, the PPs (Laissue *et al.*, 1993).

Joel *et al.*, (1978) demonstrated that carbon particles (20-50 nm) became intimately associated with the PPs of mice during administration for a year in their drinking water. The uptake of colloidal carbon was shown to be cumulative, since particles could be found with difficulty after only 2 days gavage, but with ease after 2 months administration in the drinking water. Carbon particles were initially associated, primarily in macrophages, within the subepithelial tissue of the PPs. At longer time periods (2 months) carbon was readily seen within macrophages of the MLN. Small amounts of carbon were also identified in the lamina propria, liver and lung. These observations suggest that sub-epithelial macrophages are responsible, at least in part, for transportation of phagocytosed particles out of the PPs (Jeurissen, 1987). In another chronic feeding study, LeFevre *et al.*, (1977) fed 2 μm latex microspheres to mice for 6 weeks and demonstrated that PP associated latex exhibited a non-linear dependence on the concentrations ingested. It was also clear that although PP tissue comprised only a small fraction of the weight of the intestine, it contained the majority of the latex. Hillery *et al.*, (1994) also highlighted the importance of the PPs as a site of

particle accumulation in the GIT. After 5 days oral dosing of 50 nm polystyrene nanospheres to rats, 60% of the uptake in the small intestine had occurred through PP tissue. Gel permeation chromatography (GPC) was used to determine the polystyrene content of intestinal samples.

LeFevre *et al.*, (1980, 1985a, 1985b and 1989) found that PP accumulation of some particulates, chrysotile asbestos fibres, quartz, carmine particles, and 15.8 μm diameter carbonised styrene divinylbenzene particles, does not occur to any great extent. In contrast, appreciable numbers of less hydrophilic iron oxide particles, 2 μm latex microspheres and 5.7 μm diameter styrene divinylbenzene particles were detected within patch tissue. These findings have led to the suggestion that a correlation between particle hydrophobicity and PP uptake may exist.

Work by Jani *et al.*, (1989), demonstrated that carboxylated polystyrene microspheres were not as efficiently taken up by PPs as, more hydrophobic, non-ionised beads of the same diameter. Eldridge *et al.*, (1990) tried to investigate the relationship between surface charge and uptake by comparing the accumulation of fluorescently labelled particles of different compositions in PP tissue. Polymers with the greatest relative hydrophobicity poly (styrene), poly (methylmethacrylate), poly (hydroxybutyrate) were taken up best, polymers of poly (DL-lactide), poly (L-lactide), and poly (DL-lactide-co-glycolide) were taken up in lower numbers. Jepson *et al.*, (1994), employing optical sectioning of whole PP tissue by confocal microscopy, found fewer poly (DL-lactide-co-glycolide) microspheres on the FAE surface in comparison with polystyrene. The proportion of bound poly (DL-lactide-co-glycolide) microspheres transcytosed was greater, although of smaller overall magnitude, than the latex. Surface modification of the latex microspheres by coating them with anti M-cell monoclonal antibody resulted in a marked increase in transcytosis across, and adherence to the Peyer's patch epithelium (Pappo *et al.*, 1991).

A relationship between particle size and gut associated lymphoid tissue (GALT) uptake may also exist. The difference in observed uptake between 5.7 μm diameter styrene divinylbenzene latex beads and 15.8 μm diameter carbonised styrene divinylbenzene microspheres supports this (LeFevre *et al.*, 1980). Jani *et al.*, (1990) described a size dependent process for the translocation of polystyrene latex particles (0.5-3 μm) into extraintestinal

sites (MLN, spleen and liver). Conversely, initial uptake of microspheres (<3 μm diameter) into PPs was found to be size independent. Eldridge *et al.*, (1989) saw no size dependency of uptake into PPs after administration of poly (DL-lactide-co-glycolide) microspheres with diameters between 1 and 10 μm . In contrast, Damgé *et al.*, (1994) concluded that transmucosal passage by way of PPs occurred only when polymeric microspheres were smaller than 5 μm diameter. Ebel *et al.*, (1990) found more 2.6 μm diameter latex microspheres had accumulated in PPs of mice, after gavage, than 9.13 μm diameter beads using fluorescence activated cell sorting (FACS) technology. There have been no documented reports of accumulation within PPs of microspheres larger than about 10 μm in diameter, which suggests this value represents an upper size limit for this phenomenon.

Experiments investigating the rapidity of microsphere uptake into PP tissue have been reported. Pappo *et al.*, (1989) investigated the uptake and transport of fluorescent latex particles (600-750 nm) by the FAE of rabbit PPs. Intestinal loops were inoculated with microspheres, and incubated for 10, 30 or 90 minutes. The particles were localised sequentially at the FAE cell surface, spanning the entire width of the FAE cells and within the subepithelial dome area of the PPs as a function of time. Particles were internalised by M-cells within 10 minutes of inoculation, and subsequent transport was estimated to occur at an average rate of 2 μm / min. About 5% of the total intraluminal dose was detected within the PPs (2000 particles / mm of PP) indicating that polystyrene particles are taken up and transported more efficiently than bacteria or viruses (O'Hagan *et al.*, 1990). Jepson *et al.*, (1993) using the same model, found similar results to Pappo and Ermak, i.e. 460-670 nm latex beads were intimately associated with the lymphocyte containing pocket of M-cells within 45 minutes of administration. M-cells were identified by vimentin-immunostaining and lack of alkaline phosphatase activity (Jepson *et al.*, 1992). Different concentrations of particles were used to demonstrate a saturation of M-cell binding capacity, suggesting that the overall rate of particle uptake is not limited by binding, but by endocytosis. Sass *et al.*, (1990) used the term 'insorption' to describe the appearance of intra jejunally administered latex microspheres (0.5 and 1 μm) in sub FAE macrophages after 10 minutes. At this time point, and beyond, latex beads were observed within phagocytes at the base of the PP lymphoid follicles, indicating an extremely rapid transfer from the lumen. Again M-cells were identified as the portal for particulate

influx. Kreuter *et al.*, (1992) and Scherer *et al.*, (1993) found that ¹⁴C labelled poly (butylcyanoacrylate) nanoparticles permeated rabbit small intestinal mucosa rapidly *in vitro*. Permeation of labelled material through excised ileal tissue placed between donor and acceptor sides of a diffusion cell was much greater if excised intestine contained PPs. Nanoparticle permeation through porcine ileal mucosa was much lower, and did not occur at all if PPs were absent from intestinal samples.

Jenkins *et al.*, (1994) administered a range of fluorescent polystyrene microspheres (0.15, 0.5, 1.0, 3.0 and 10.0 µm diameter) intraduodenally to groups of 3 rats, and, by cannulating the superior mesenteric lymph duct assessed levels of absorption by flow cytometry. From five minutes after administration all particle sizes could be detected within draining mesenteric lymph in variable numbers (see section 1.2.6.1). Flow cytometric analysis of the PPs and MLN 90 minutes after administration revealed that significantly fewer 0.15 and 1.0, 3.0 and 10.0 µm diameter microspheres were retained within the PPs, in contrast to the 0.5 µm microspheres. Significantly more 3.0 and 10.0 µm particles were detected in PP tissue at 90 minutes than 0.15 or 1.0 µm diameter particulates. The authors proposed that a size dependant mechanism for particle retention within PP tissue may exist.

1.2.5 MACROPHAGE MEDIATED UPTAKE FROM THE GIT LUMEN

If a particle penetrates the epithelial surface of the GIT, it encounters phagocytic cells of the monocyte / macrophage lineage. Phagocytes are derived from bone marrow stem cells and their function is to engulf particles, internalise and destroy them (phagocytosis). The initial event in phagocytosis involves the recognition of a particle as foreign. Macrophages have lectin-like receptors on their surface which allow them to attach non-specifically to particulates, such as uncoated microspheres. They also have receptors for the Fc regions of IgG, for C3b complement component and for glyco-conjugates with terminal mannosyl or fucosyl residues which promote uptake and destruction of micro-organisms and macromolecules. The size and charge of particulates is thought to influence their susceptibility to phagocytosis. Hydrophobicity is a prerequisite for internalisation, water must be excluded from the interface between phagocyte and particle. Polystyrene microspheres with a diameter of 600 nm were found by Seymour *et al.*, (1991) to be most efficiently captured by peritoneal

macrophages compared with beads of other sizes. In the same investigation, modification of the latex microspheres by hydroxymethylation caused an increase in the number of phagocytic events.

During engulfment by macrophages, the plasma membrane is closely applied to the surface of the target, and phagocytosis proceeds by the so called 'zipper' mechanism. This involves the folding of macrophage pseudopodia around a particle, thus enclosing it within a vacuole (phagosome), before the particle is dragged into the cytoplasm. Lysosomes then fuse with the phagosome to form a phagolysosome, towards which several microbicidal mechanisms are activated (Oss, 1978). Generally, biodegradable particulates will be destroyed by these events, albumin microspheres become disrupted by the proteolytic activity of enzymes released (Saunders *et al.*, 1991).

In addition to macrophages being an important vector for the transportation of particulates out of GALT (LeFevre *et al.*, 1985a) (section 1.2.6.1), they are also thought to be capable of particle uptake directly from the intestinal lumen. Macrophage mediated translocation of latex particles from the small intestinal lumen has been demonstrated in dogs and rats (Wells *et al.*, 1988). Fluorescent latex beads of two different colours (fluorescein and rhodamine) were implanted into separate jejunal segments devoid of visible Peyer's patches. Examination of mesenteric lymph node phagocytes after seven days revealed that the cells contained multiple beads of one or the other colour, but rarely both colours. This led to the conclusion that engulfment had occurred at a site where beads of only one colour were present, i.e. in one of the intestinal compartments. This uptake and transport from intestinal loops devoid of grossly visible lymphoid aggregates implies that their presence is not a prerequisite for microsphere translocation.

In another investigation Wells *et al.*, (1987) discovered fluorescent latex particles (1 μ m diameter) were not found within the MLN of macrophage deficient (C3H/HeJ) mice after oral administration, but were present in the immunocompetent control group. Fluorescence was found solely in esterase positive (macrophage) lymph node cell suspensions obtained from immunocompetent control animals.

Small, solitary lymphatic follicles (SLFs) in the gut have been shown to transport particulate matter (Joel *et al.*, 1978). After ingestion of carbon particles for 6 months, SLFs were identified in mice as 150-200 black dots along the entire length of the small intestine. Particulate carbon was initially associated with macrophages in the subepithelial tissue of the SLFs. Two months after administration, carbon particles were readily detected within macrophages of the MLN. Microscopic examination of the follicles revealed that they had a similar epithelial structure to Peyer's patches (section 1.2.4). The presence of SLFs along the length of the small intestine suggest they could be responsible for reports of particle uptake from gut loops lacking PPs, as described by Wells *et al.*, (1988).

Owen *et al.*, (1981) observed the phagocytic uptake of the protozoa *Giardia muris* by macrophages in the mouse lamina propria after examination of the antigen sampling epithelium over PP follicles by electron microscopy. Macrophages beneath the basement membrane in PPs extended pseudopods into the epithelium to trap invading protozoa and enclose them in phagolysosomes. Owen *et al.*, (1981) suggested that this process enables micro-organisms such as *Giardia muris*, which are too big to pass through the M-cell tubulovesicular system, to be sampled by GALT. Uptake of particulates from the lumen by intestinal macrophages in this manner may also be involved in microsphere uptake from SLFs, since it seems likely that macrophages present in SLFs are capable of similar functions to those found in the PPs. Owen *et al.*, (1985) also observed lymphocyte diapedesis into the intestinal lumen from lymphoid follicles. Suggested pathways for lymphocyte entry into the lumen included: extrusion through eroded portions of epithelium, passive escape along with desquamated epithelial cells, and migration between epithelial cells.

1.2.6 POST UPTAKE DISSEMINATION OF ORALLY ADMINISTERED PARTICULATES

Accumulation of microspheres within extra-intestinal organs may occur after their uptake from the intestinal lumen (Jani *et al.*, 1990). In order for this to occur, colloidal particles must be transported away from sites of uptake in the intestine. The blood and lymph are body fluids within which micro-particulates are found after oral administration and may account for their dissemination to anatomically remote sites. In order for this to happen, particulate matter may have to transverse several physiological barriers after

uptake from the intestinal lumen. Figure 8 (below) represents the size restrictions imposed by capillary and lymphatic barriers. Microspheres taken up from the intestinal lumen by endocytosis or paracellular processes would have to negotiate these barriers in order to access the lymphatics (see section 1.2.6.1) or the blood (see section 1.2.6.2).

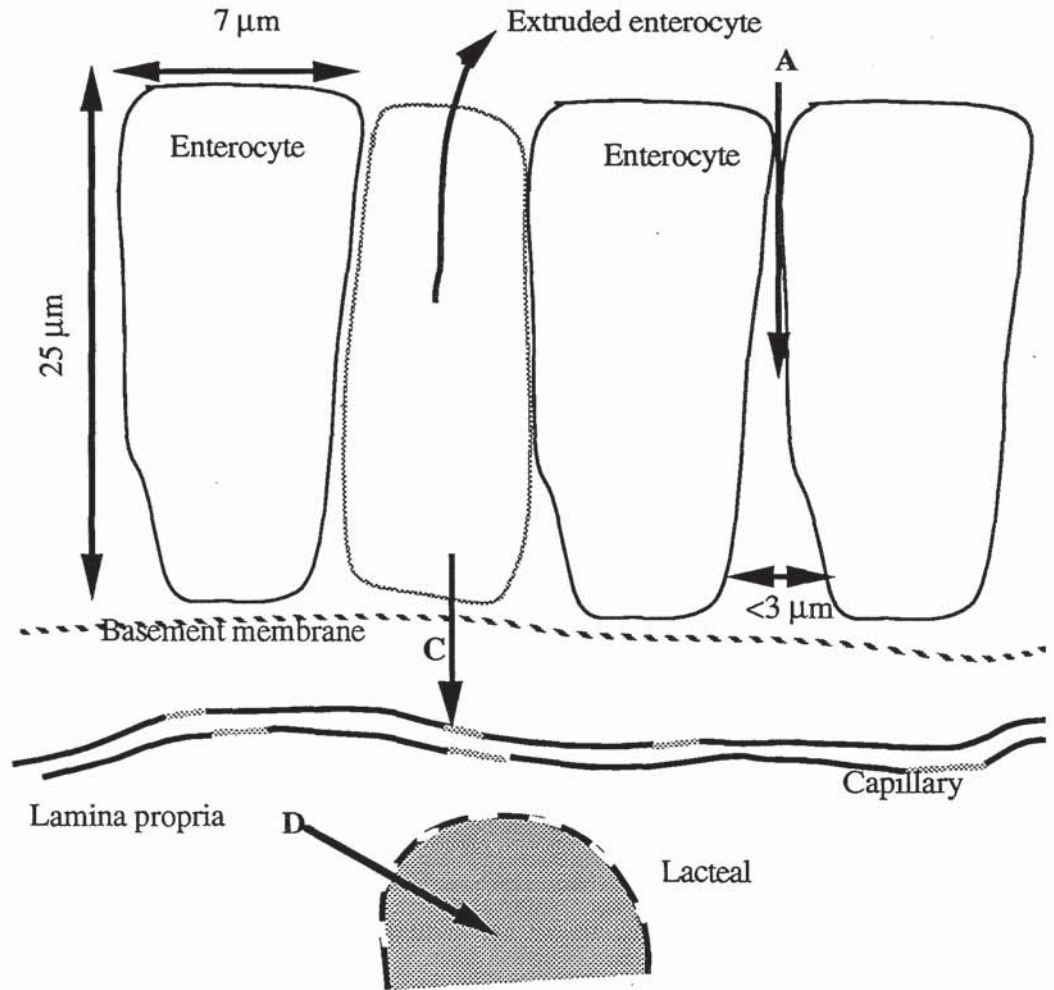


Figure 8. Size restrictions imposed on particulate uptake into capillary and lymphatic vessels. The dimensions of a typical intestinal enterocyte are about 7 by 25 μm . Paracellular transport (A) occurs *via* aqueous channels with an equivalent pore diameter in humans of 0.4 - 0.8 nm and a somewhat larger pore diameter in animals (1-1.5 nm) (Madara, 1990). The basement membrane (B) contains several fenestrations of between 500 and 5000 nm in diameter (Komuro, 1985) which could explain the passage of small particles through this barrier. Nanoparticle passage through capillary walls and into the capillary lumen could occur through fenestral diaphragms (C) which under certain physiological conditions may be over 100 nm wide (Bearer *et al.*, 1985). Lymphatic endothelial junctional complexes (D) are devoid of desmosomes and occasionally lack intercellular tight junctions, resulting in a system that is open to the entry of large molecules and particles such as chylomicra (37-300 nm radius) (Weiss, 1988).

1.2.6.1 TRANSPORTATION OF ORALLY ABSORBED PARTICLES BY THE LYMPHATIC SYSTEM

The lymphatic system comprises of both the vessels for transporting lymph, and the tissues such as PPs and lymph nodes which are connected by these vessels. The lymphatic system plays an important role in the distribution and eventual fate of any particulates that penetrate the intestinal epithelium.

Lymphatic vessels originate in connective tissue spaces as anastomosing capillaries. They are either superficial or visceral, draining the internal organs of the body. The capillaries flow into larger collecting vessels which eventually empty into the thoracic duct. The thoracic duct, the largest lymphatic vessel, eventually drains into the left subclavian vein at the base of the neck (Weiss, 1988). Lymph is the interstitial fluid that fills lymphatic vessels. It is mostly made up of plasma proteins such as albumin and globulins that have leaked out through capillary fenestrations. Other components of lymph include water insoluble fats and foreign antigens from the GIT (Florence & Jani 1993).

The GIT is richly supplied with lymphatic vessels that arise as elongate, blind-ended tubes in the mucosa. In the small intestine, each villus usually contains a single blind ending central lymphatic vessel, a lacteal. Lacteals are approximately 20 μm in diameter and lie about 50 μm beneath the epithelial cell layer. They are constructed of endothelial cells that contain no fenestrae but are widely separated with gaps of up to 100 nm between adjacent cells (Weiss, 1988). Lymphatic endothelial junctional complexes are devoid of desmosomes and occasionally lack intercellular tight junctions, resulting in a system that is open to the entry of large molecules and particles such as chylomicra (37-300 nm radius). Lacteals are connected to a plexus of lymphatic capillaries in the glandular layer of the mucosa, and joined to a submucosal network of collecting lymphatics, in which the larger vessels possess valves. The lymphatics leave the intestine at the mesenteric border and pass out through the mesentery in association with blood vessels. Lymphatics in the mesentery have the ability to propel their contents due to their muscular walls (Granger, 1981).

Dissemination of microspheres absorbed from the intestinal lumen by M-cells is thought to occur principally *via* the lymphatic system, although intestinal absorption of particles by other mechanisms may also result in

their appearance within the lymphatics. Volkheimer (1977) observed large PVC particles within intestinal lymphatic vessels shortly after oral administration. In another study, polyalkylcyanoacrylate nanospheres (100-200 nm) were detected within jejunal lacteals between 15 and 30 minutes after administration (Aprahamian *et al.*, 1987). The presence of only incomplete basement membranes in lacteal endothelial cells means that the entry of particulate matter into the lymphatic system by this route after paracellular absorption seems feasible. Enterocyte uptake by pinocytosis of Percoll (30 nm) microspheres from the intestinal lumen also resulted in particle accumulation within the draining MLN (Matsumo *et al.*, 1983).

PPs and isolated lymphoid follicles are invaginated with numerous lymphatic ducts and vessels, the structure of which suggests they are responsible for transportation of lymphocytes and absorbed particles from these tissues to the draining MLN. Histological evidence provided by Jani *et al.*, (1989, 1990, 1992a, 1992b) has repeatedly demonstrated microspheres within lymphatic vessels in the process of transportation towards draining MLN after oral administration. Particles may be transported inside these vessels either within phagocytic cells or in a free state in the lymph. Studies by Wells *et al.*, (1988) suggest particulate matter such as latex microspheres would be transported to draining MLN almost exclusively inside phagocytic cells rather than simply suspended free in the lymph fluid.

Under certain conditions the time span over which particulates appear in the afferent lymphatics, after oral administration, may be extremely short. Jenkins *et al.*, (1994) administered a range of fluorescent polystyrene microspheres (0.15, 0.5, 1.0, 3.0 and 10.0 μm diameter) intraduodenally to groups of 3 rats, and, by cannulating the superior mesenteric lymph duct assessed levels of microsphere absorption from the intestine into the draining lymph using flow cytometry. From five minutes after administration all particle sizes could be detected within draining mesenteric lymph in variable numbers, with maximum uptake estimated at 0.14% of the dose. The 0.15 μm diameter microspheres showed large absorptive peaks at 5, 35 and 65 minutes. The 0.5 μm microspheres behaved differently with maximal absorptive events occurring between 10 and 30, 60 and 80 minutes. The 0.5 μm diameter latex microspheres were found to be absorbed in significantly greater numbers in comparison to other particles used in the study. The 1.0 μm spheres showed peaks after 20 and 25

minutes and maximally after 65 minutes. Lower numbers of 3.0 and 10.0 μm diameter microspheres were detected in the lymph, with the 3.0 μm particles exhibiting maximal absorption 10 minutes after administration. Flow cytometric analysis of digested PPs and MLN at the 90 minute time point revealed that significantly fewer 0.15, 1.0, 3.0 and 10.0 μm diameter microspheres were retained within the PPs, in contrast to the 0.5 μm size which showed evidence of considerable accumulation in this tissue. The 1.0 and 3.0 μm diameter microspheres were detected in greatest numbers within the MLN suggesting these microsphere sizes represent an optimal size for nodal retention. Very low numbers of the 10 μm diameter test particle were recovered from excised MLN at 90 minutes.

In the studies by Jenkins *et al.*, (1994), although temporally variable, patterns of absorption across the intestinal epithelium into the mesenteric lymph seemed to show an 'early' period of absorption between 5 and 30 minutes followed by a 'later' phase between 60 and 70 minutes after administration. The authors speculated that is could be due to the presence of sinus-like lymphatic cavities below the follicular domes of the PP, that may allow periodic retention and release of delivered particulates (Lowden *et al.*, 1992).

Other studies also suggested that microparticulate absorption into the lymphatic system from the GIT lumen could be rapid. Analysis by light microscopy of tissue preparations 10 minutes after intestinal particle application revealed latex beads not only within the basal areas of PPs, but also within draining lymphatic capillaries (Sass *et al.*, 1990). Jani *et al.*, (1992b) gavaged polystyrene latex particles of diameter 50 nm, 500 nm and 1 μm in a single dose form to Sprague-Dawley rats. Translocation to MLN from GIT lumen was found to be particle-size dependent. At 6 hours after dosing all particle sizes were observed in patch tissue, but only the 50 and 500 nm beads were seen within the MLN. 12 hours after dosing all particle sizes were observable within MLN.

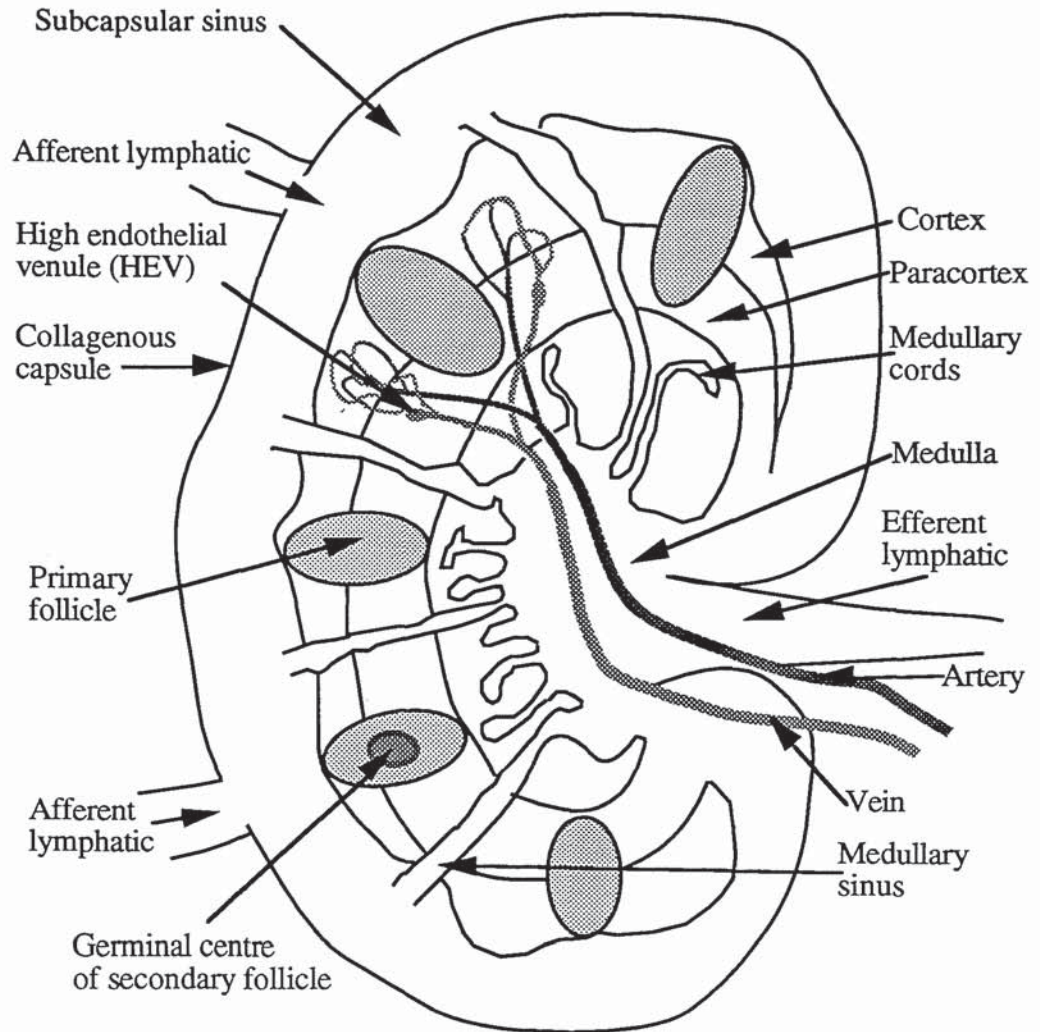


Figure 9. Typical mesenteric lymph node structure. Adapted from Roitt *et al.*, (1987)

In common with other lymph nodes, MLN are composed of a collagenous capsule beneath which there is a subcapsular sinus lined with numerous phagocytes (figure 9). Afferent lymph vessels from the GIT pierce the capsule and empty into the subcapsular sinus. Lymph then flows through medullary sinuses, which pass between medullary cords and converge on the centre of the node where they drain into efferent lymphatics. The lymphatic sinuses are lined with reticular cells which extend cytoplasmic processes across the lumen causing turbulent and retarded lymph flow. Macrophages line the sinuses, and actively engulf particulate matter within the lymph. As they do so, they increase in volume; their bulk further impedes lymph flow and thus enhances phagocytosis (Weiss, 1988). The cortex of the MLN contains aggregates of B cells, while the paracortex is the T cell area. Lymphocytes enter the node from the blood through high

endothelial venules (HEV). Lymphocytes and micoparticulates can only leave the MLN through the efferent lymphatics, which eventually converge on the thoracic duct (Roitt *et al.*, 1987). As the thoracic duct enters the left subclavian vein at the base of the neck, its possible for intestinally absorbed particles within the lymph to access the general circulation.

The extent to which orally absorbed microspheres are retained within the MLN is likely to be related to particle size (Jenkins *et al.*, 1994) and charge (Jani *et al.*, 1989) as well as other physiological conditions. 2, 4 and 11 days after oral administration, latex beads (1 μm) were detected almost exclusively in the macrophage population of cells extracted from excised MLN tissue (Wells *et al.*, 1987). The abundance of macrophages within MLN suggest that nodal retention within these cells is likely to be the destiny for some of the orally absorbed particles conveyed within afferent lymph over the short term. In experiments performed by Jani *et al.*, (1992b) latex microspheres were still readily detectable within the MLN 24 and 36 hours after a single oral dose. 48 hours after the cessation of a 10 day particle administration regime latex microspheres of 1 μm diameter and below were clearly seen in frozen tissue sections of MLN (Jani *et al.*, 1992a). Mice which had received 5.7 μm styrene divinylbenzene latex beads orally for 60 days readily showed evidence of particle retention within the MLN 77 days after the last dose (LeFevre *et al.*, 1980). Jenkins *et al.*, (1994) found maximum nodal retention occurred with particles of diameters between 1 and 3 μm . Sub micron particles were not well retained and were transported away within the efferent lymph.

Intestinally absorbed microspheres not retained within MLN will eventually enter the systemic blood stream *via* the thoracic duct. The time course over which this may occur is not well defined. In experiments by Jani *et al.*, (1992b), 50 and 500 nm latex beads were detected in the liver 18 hours after oral dosing. The 50 nm test particles were detected in hepatic tissue at 12 hours, but not before 6 hours. This suggests that at least 6 hours are required for intestinally absorbed microspheres to make the journey through the mesentery and thoracic duct to the systemic circulation as described. Jenkins *et al.*, (1994), stated that particulate absorption is more rapid and complex than assumed previously. Their results indicated that particulates in the sub micron size bracket did not undergo significant sequestration within MLN and could enter the blood stream, in low numbers, with some rapidity (<90 minutes). Eldridge *et al.*, (1989) found that biodegradable

poly (DL-lactide-co-glycolide) microspheres with mean diameters below 5 μm were disseminated within macrophages to the MLN, blood and spleen. Microspheres were seen within MLN from 24 hours to 35 days after oral administration. However, it was not until 4 days after administration that any test particles appeared within splenic tissue. Peak numbers of microspheres were observed within the spleen at 14 days, indicating the rate of colloid transportation up the thoracic duct from MLN is relatively sluggish.

1.2.6.2 HEMATOGENOUS TRANSPORTATION OF PARTICLES AFTER INTESTINAL ABSORPTION

In some circumstances, intestinally absorbed particulates may appear within the blood stream as a result of direct particle penetration of the mucosal microcirculation (see figure 8). Volkheimer (1975), reached this conclusion after detecting Polyvinyl chloride particles of between 10 and 60 μm diameter in the hepatic portal vein 10 minutes after oral administration. Histological examination of gut tissues from dosed animals revealed particles in spaces between epithelial cells, indicative of paracellular uptake. Polyvinyl chloride particles were also visualised in the lamina propria and within the lumen of mucosal blood and lymphatic vessels. Direct delivery of nanocapsules (100 - 200 nm) loaded within radioactive iodinated oil, from the intestinal wall into jejunal blood capillaries, was observed by Aprahamian *et al.*, (1987). Paracellular uptake through defects in the mucosa representing areas of desquamation of mature epithelial cells was followed by the rapid appearance of particles inside local blood capillaries and efferent mesenteric vasculature. The initial absorptive events took place within 15 minutes of administration, by which time microspheres were clearly seen in the lamina propria in the vicinity of the basement membrane and in the small capillaries near the epithelium and villus core. Nanosphere penetration of the basement membrane occurred *via* the numerous 500 - 5000 nm fenestrations which punctuate the 30 nm wide fibrillar sheet. Nanoparticle passage through capillary walls and into the capillary lumen was thought to have occurred *via* fenestral diaphragms (see figure 8). These holes in capillary endothelial cells, which make up the vessel walls, can be larger than 100 nm depending on the surrounding physiological conditions (Bearer *et al.*, 1985).

Microparticles inside mucosal capillaries would enter the portal circulation in venules that form an extensive network just internal to the muscularis mucosae. Veins pass outward into the submucosa, forming an extensive plexus drained by large calibre vessels passing through the muscularis to the serosa and mesentery (see figures 1 and 2). Within the mesentery, blood vessels converge on the hepatic portal vein. The hepatic portal vein supplies 75 % of the afferent blood flowing into the liver (figure 11). The remaining 25 % is supplied by the hepatic artery, carrying well oxygenated blood. Portal blood is poor in oxygen but rich in nutrients having passed through the capillary beds of the spleen, pancreas and GIT (Jones *et al.*, 1988). In the studies by Aprahamian *et al.*, 1987) plasma iodine levels within the mesenteric vein increased markedly between 15 and 45 minutes after administration, suggesting rapid dissemination of nanospheres after direct penetration of mucosal vasculature, as proposed by the authors. At time points beyond 45 minutes, iodemia declined, reaching basal levels 105 minutes after administration.

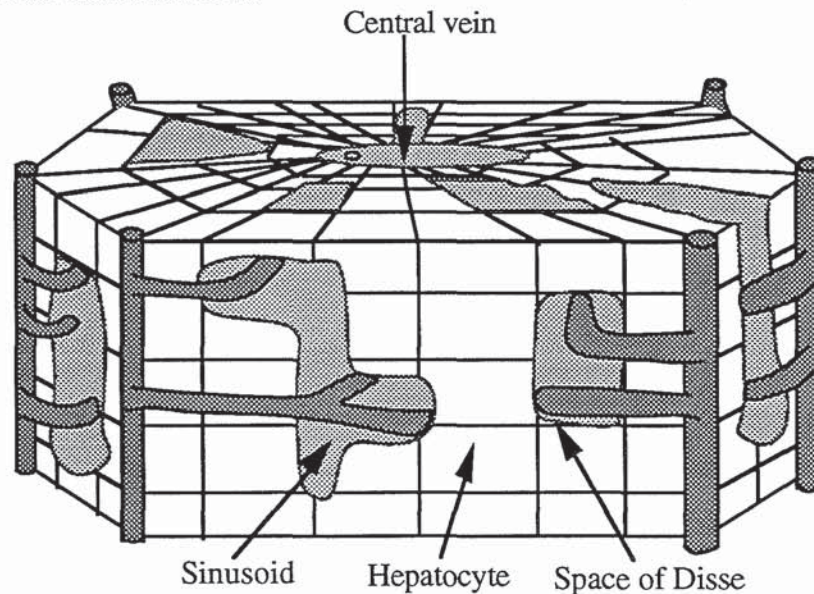


Figure 10. Schematic view of a liver lobule, the structural unit of the liver. Adapted from Weiss, (1988). See text for details.

Considerable accumulation of particles within the liver would be expected if particles are conveyed from the intestine within the portal blood supply. Inside the liver, afferent blood from portal vein and hepatic artery mix and pass into and through hepatic lobules, the structural unit of the liver. Within these polyhedral prisms of tissue, blood flows through complicated vascular

sinusoids which anastomose and unite into a central vein in the middle of the unit (figure 10). The six "triads" around the periphery of the lobule represent branches of the portal vein, hepatic artery and bile duct. Hepatocytes separated on either side by sinusoids, radiate from the central vein forming interconnecting plates one cell thick. The small gap in-between sinusoid and hepatocyte, the space of Disse, is the primary site for the formation of liver lymph, 80% of which drains into the thoracic duct. Bile is produced by hepatocytes. It is secreted into minute bile canaliculi and flows, in the opposite direction to blood, into small ducts at the periphery of each hepatic lobule (figure 10). Hepatic sinusoids are larger and more variable in calibre (9-12 μm wide) than normal capillaries. Basement membranes and fenestral diaphragms are absent from sinusoidal endothelial cells. This means that no significant morphological barrier exists between the fluid phase of the blood and hepatocyte membrane. In addition to endothelial cells, sinusoids are composed of large fixed macrophages called Kupffer cells. Kupffer cells lie across hepatic sinusoids in an ideal position to engulf passing particles, and represent an important component of the mononuclear phagocyte system (MPS). Mononuclear phagocytic cells originate from precursors in the bone marrow, enter the circulation as monocytes, and then pass into various tissues where they differentiate into macrophages, chiefly concerned with particle uptake (Florence & Jani, 1993)

Saunders *et al.*, (1962) noted substantial hepatic accumulation of 220 nm latex particles 2 hours after oral administration to rats. Endocytosis by jejunal absorptive cells resulted in microsphere transfer to the portal circulation in the first hour of the study. Using electron microscopy, latex microspheres were observed in hepatic sinusoids, the space of Disse, and in the process of being taken into liver cells by pinocytotic vesicles. Volkheimer (1975) also observed particulate matter in histological sections of rat liver. Peak numbers of particles were seen in the liver 2-3 and 10 minutes after oesophageal administration of 10 - 60 μm diameter polyvinyl chloride particles. More recently, Le Ray *et al.*, (1994) detected 0.0267 % of an oral dose of [^{14}C]poly(DL-lactide-co-glycolide) nanoparticles within excised hepatic tissue one hour after administration. Circulating particles not entrapped within hepatic tissue would leave the liver through the hepatic vein which empties into the vena cava (figure 11).

The kinetic behaviour of orally administered microspheres within the general circulation has been investigated by Volkheimer (1968, 1977), Le Ray *et al.*, (1994), Alpar *et al.*, (1989) and Lewis *et al.*, (1992). Alpar *et al.*, (1989) found major quantities (24 %) of an oral dose of 1.1 μ m latex microspheres were detectable in the blood 10 minutes after administration. 45 minutes after dosing, about 39% of the original dose was estimated to be circulating within the systemic vascular compartment. Lower microsphere levels were detected 2 and 3 hours after dosing (12% and 2 % respectively). 24 hours into the investigation very low particle numbers were observable within blood samples. Lewis *et al.*, (1992) estimated that up to 15 % of an oral dose of Fluorescein isothiocyanate (FITC) labelled albumin microspheres (3.1 μ m diameter) were circulating as quickly as 5 minutes after gavage. In this investigation, blood microsphere numbers declined to 12%, 10% and 8% of the original dose at times 15, 60 and 120 minutes respectively. As suggested by Kreuter (1991) when reviewing these reports, the short space of time elapsed between particle dosing and appearance in the blood, is indicative of a paracellular route of uptake. After his investigations, Volkheimer observed that the appearance of particles in the blood does not follow a simple first-order process leading to one single blood level maximum. Instead, 2-3 maxima were seen: a first maximum very rapidly after a few minutes, a second after about 100 minutes and often a third 210 minutes after oral dosing. He speculated that these multiple maxima result from the operation of different particle uptake mechanisms (Kreuter, 1991).

Particles may gain indirect access to the circulation through GALT after oral administration. One possible mechanism has been suggested by Wells *et al.*, (1988) which involves lymphatic transportation of particles to the left subclavian vein *via* the thoracic duct (section 1.2.5). This route of particle transportation to the blood is likely to be considerably slower than that in which particles gain direct access to the intestinal microcirculation. However, microsphere uptake from the intestinal lumen into draining mesenteric lymph has been shown to be rapid (5 minutes), as demonstrated by Jenkins *et al.*, (1994). Thus microsphere transfer into the general circulation by this route could conceivably occur over a reasonably short time course, as suggested by the findings of Le Ray *et al.*, (1994) (see below).

Studies by Kreuter *et al.*, (1989) suggest that radiolabelled polycyanoacrylate nanoparticles entered the circulation after oral administration to mice. Jani *et al.*, (1990) detected over 1 % of a dose of 300 nm latex microspheres in heart blood after chronic oral administration. Under the same dosing regime, circulating numbers of smaller beads (50 and 100 nm) were found to be even higher. The small particles were thought to have entered the circulation after PP mediated translocation from the GIT to the mesenteric lymph nodes. Hussain *et al.*, (1994) detected 3.04 % of an oral dose of 0.5 μm carboxylated polystyrene microspheres conjugated to tomato lectin in 2 ml of heart blood taken after a 5 day chronic dosing regime (see section 1.2.2). After his experiments, Eldridge *et al.*, (1989) suggested a more direct route for particle entry to the blood after intestinal absorption. This study indicated that vaccine containing microspheres smaller than 5 μm in diameter could extravasate PPs within macrophage cells to stimulate systemic immunity. When Rhodamine loaded microspheres (1-5 μm) were injected into the ileal lumen of rats, levels of fluorescence within the mesenteric vein peaked after 4 hours (Dange *et al.*, 1994). Microsphere absorption only occurred *via* PPs with an overall efficiency of 12.7 %.

One hour after oral administration of [^{14}C]poly(DL-lactide-co-glycolide) nanoparticles (0.133 μm diameter), 0.0209 % of the total recovered radioactivity was detected in the blood of test rodents (Le Ray *et al.*, 1994). At the 4 hour, 24 hour and 48 hour time points this figure was 0.0241, 0.0159 and 0.0434 % respectively. Interestingly, administration of the nanoparticles in conjunction with concentrated milk resulted in an increase in the apparent level of nanoparticle transfer to the vascular compartment (0.0620 % at 1 hour, 0.0419 % at 2 hours, 0.0438 % at 24 hours and 0.0291 % at 48 hours). This observed increase in nanoparticle uptake, after gavage in conjunction with milk, was attributed to stimulation of gastrointestinal lymphatic absorption pathways (Charman *et al.*, 1986).

Irrespective of the route of entry, the fate of any particle in the blood will be determined by its size and surface characteristics, as indicated by the numerous investigations into the body distribution of colloidal particles after intravenous (i.v.) administration (Singer *et al.*, 1969, Adlersberg *et al.*, 1969, Kreuter *et al.*, 1979, Kreuter 1983, Leu *et al.*, 1984, Illum *et al.*, 1982, Illum *et al.*, 1984, Illum *et al.*, 1987a, Illum *et al.*, 1987b, Davis *et al.*, 1993). Yamaoka *et al.*, (1993) found that large polystyrene microspheres

(>7 μm) are removed from the blood rapidly and efficiently by the filtering propensity of the lung capillaries after i.v. injection. Large orally administered particles within the vascular compartment would be expected to behave in the same way. The half life of small microspheres (< 2 μm) in the circulation was found to decrease with increasing diameter. Most of the smaller spheres were removed by cells of the MPS, exhibiting further size dependency as regards subsequent organ distribution. Intravenous injection of small (<2 μm) microspheres resulted in about 70 % of the dose accumulating in the liver. Of those entrapped, 70 % were located in non hepatocyte cells, particularly the Kupffer cells. The spleen was also found to be an organ with a high capacity for microsphere accumulation after i.v. administration.

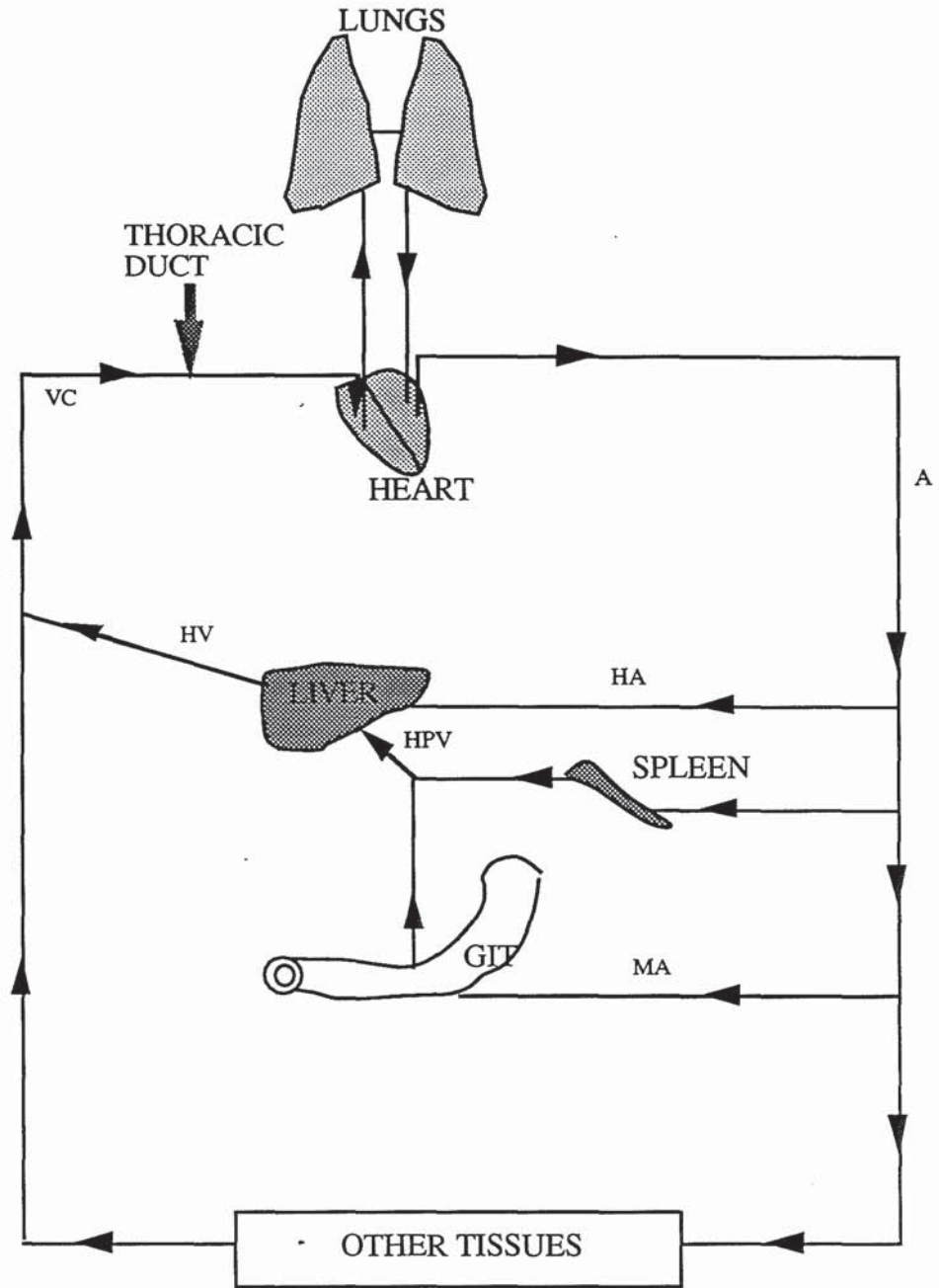


Figure 11. Circulatory pathway for intestinally absorbed, or intravenously injected microspheres within the vascular system. Blood vessels are represented as: A (aorta); HA (hepatic artery); MA (mesenteric artery); HPV (hepatic portal vein); HV (hepatic vein) and VC (vena cava).

Splenic architecture is thought to serve as a sieve or filtration bed to filter physically blood cells, infectious agents and colloidal particles (Weiss, 1988). This mechanism does not operate in the liver since, unlike the spleen, the passage of blood through the liver is not impeded by an

endothelial border and removal of particulates is due solely to Kupffer cell sequestration. The filtration mechanism within the splenic cords of the red pulp is particularly important in the clearance of rigid and less deformable particles such as polystyrene microspheres, aged or plasmodial-parasitised erythrocytes and poorly opsonised encapsulated strains of bacteria which can not squeeze easily through inter endothelial cell-slits and gain access to the venous circulation. The splenic cords are lined by macrophages, part of the MPS, which sequester particulate matter in the same way as hepatic Kupffer cells (Moghimi *et al.*, 1991 and Davis *et al.*, 1993). In experiments performed by Yamaoka *et al.*, (1993) the density of 4 μm diameter latex microspheres in the spleen was the equivalent of 234.1 % of the i.v. dose *per* gram of tissue compared to 37.5 % *per* gram of liver, demonstrating that while lungs, liver, bone marrow and other MPS tissues also clear blood of particulate matter, the spleen's clearance capacity *per* gram of tissue is greatest. Again accumulation was found to be size dependant. Entrapment efficiency for small (<4 μm diameter) latex beads increased with increasing size. Intravenous injection of microspheres larger than 4 μm resulted in lower splenic accumulation, supporting the thesis that capture is due to mechanical filtration as well as uptake by cells of the MPS. Similarly, Moghimi *et al.*, (1991) found that the localisation of latex microspheres in the rat spleen was found to increase with an increase in diameter over the size range 60 to 250 nm, and suggested that 200-300 nm represented an optimal diameter for mechanical capture.

Surface modification of microspheres results in dramatic changes in their circulating half life and organ distribution after i.v. injection. Yamaoka *et al.*, (1993) found that adsorption of Poly(vinyl alcohol) onto the surface of polystyrene microspheres resulted in prolonged circulatory half lives and decreased sequestration by the liver. These are similar findings to those of Illum *et al.*, (1987a) who found that coating latex microspheres (60 nm) with a block co-polymer (poloxamine 908) kept the i.v. injected particles circulating for protracted periods of time compared to un-coated microspheres. Leu *et al.*, (1984) found that blood concentrations of poloxamer coated particles was 70 times higher after 30 minutes, than uncoated polymethyl (2-¹⁴C) methacrylate nanoparticles. The uptake of colloidal particles from the blood and adherence to mononuclear phagocytes is often mediated by the adsorption of specific blood components (opsonins) onto the particles. Opsonic factors include immunoglobulin G, complement C3b and fibronectin. Reduction in opsonisation is achieved by

coating the particles with block co-polymers. This renders the particle surfaces more hydrophilic and introduces a steric barrier which minimises adhesion to macrophage cells.

By coating colloidal microspheres with another type of block co-polymer (poloxamer 407) Illum *et al.*, (1987b) were able to target the bone marrow site after i.v. administration. Again hindrance of mononuclear phagocyte function in the liver and spleen allowed the considerably smaller bone marrow mononuclear phagocyte compartment to achieve considerable uptake. It is believed that subtle chemical differences in poloxamer 407 compared to poloxamine 908 account for selective targeting of the colloids to the bones after i.v. injection. Only the very smallest (60 and 150 nm diameter) poloxamer 407 coated latex particles were taken up into bone marrow to any great extent. This size cut off was attributed to differences in the absorption of poloxamer 407 rather than any anatomical size restriction (Davis *et al.*, 1993).

Biostim, a glycoprotein extract of *Klebsiella pneumoniae*, was found to change the distribution of injected albumin colloids of between 0.02 and 1.0 μm in diameter (Jacobsson, *et al.*, 1993). Apart from being a powerful stimulator of both T- and B- lymphocyte function, Biostim is one of the most potent activators of phagocytes. Intraperitoneal (i.p.) injection of the drug enhanced entrapment in the lung and spleen compartments. Oral administration of Biostim caused a dose dependant decrease in albumin colloid trapping by the lungs. Liver accumulation of albumin microspheres was found to be high after both oral and i.p. administration of Biostim.

1.2.7 POST UPTAKE ORGAN DISTRIBUTION OF ORALLY ADMINISTERED PARTICULATES

Microspheres may accumulate in diverse organs, particularly those of the MPS, if they enter the vascular compartment after oral delivery. The flow of particle traffic between different body compartments after oral delivery is complicated and difficult to quantify, this is because unlike i.v. injection of particles into the blood stream, many more variables exist. Oral administration probably results in a slow trickle of small numbers of microspheres into the circulation several hours, days or weeks after dosing.

The organ distribution of polystyrene microspheres after oral administration was determined by Jani *et al.*, (1990) using GPC. Rats were dosed with microspheres from 50 nm to 3 μm in diameter over 10 consecutive days. A size dependent accumulation of microspheres in some extra-intestinal tissues was observed. All test particles demonstrated association with PPs and GALT, although uptake was considerably greater for the smaller particles. Only microspheres with diameters of 1 μm or less were detected within the liver and spleen. The greatest accumulation within the spleen was found to be 0.92 % of the initial dose of 50 nm particles. Maximal liver accumulation (3.8 %) occurred after oral delivery of 0.1 μm diameter microspheres. No microspheres were detected within lung or heart tissue and only the 50 and 100 nm spheres were detected within any of the kidney and bone marrow samples respectively. The extent of translocation for each size of microsphere was thought to be represented by the cumulative uptake of polystyrene into blood, liver, spleen and bone marrow. Thus translocation occurred to the extent of: 6 % for the 50 nm beads, 3 % for the 0.5 μm beads, 1 % for the 1 μm beads and 0 % for the 3 μm beads. Hussain *et al.*, (1994) found that 23 % of a chronic oral dose of 0.5 μm carboxylated polystyrene microspheres conjugated to tomato lectin could be detected in systemic organs using GPC technology. 18.24 % was detected within the blood, 1.17 % in spleen tissue, 2.64 % in the liver, 0.29 % in the heart and 0.67 % in the kidney. No particles were detected in the heart, blood or kidney in studies by Jani *et al.*, (1990) using plain 0.5 μm diameter latex beads, suggesting that coupling of plant lectins to particulate matter may influence organ distribution as well as uptake pathway (see section 1.2.2).

Radiolabeling of microspheres in order to determine organ distributions after oral administration has been attempted by Jani *et al.*, (1990) and Kukan *et al.*, (1989). In these cases problems have arisen with either stability of the particles or leaching of the radiolabel *in vivo*. Other studies have employed histological procedures to visualise microspheres within extra-intestinal tissues after oral administration. Saunders *et al.*, (1961) observed 220 nm latex beads within hepatic cells 2-4 hours after dosing. Matsumo *et al.*, (1983) found strong evidence of Percol (30 nm) accumulation in extra-intestinal sites after oral dosing (section 2.1). Jani *et al.*, (1989, 1992a) found that rats fed 0.1, 0.5, and 1 μm non-ionic latex beads for 10 days, showed unequivocal evidence of uptake after histological examination of PPs, villi, lymph nodes, spleen and liver. Carboxylated microspheres of similar diameters were found to be translocated to a lesser extent. In another study, Jani *et al.*, (1992b) examined MLN, PPs, liver and spleen in a semi-quantitative manner at various times after a single oral dose of microspheres. 12 hours after gavage, small (50 nm) microspheres were observed in the MLN and hepatic tissue. 18 hours after administration, nearly all microsphere sizes (50, 500 and 1000 nm) could be detected in all monitored organs. No microspheres could be detected in liver and spleen 6 hours after dosing. Histological investigations by Eldridge *et al.*, (1989) using fluorescently labelled poly (DL-lactide-co-glycolide) microspheres, found no size selectivity under 10 μm as regards to uptake into PPs. Microspheres larger than 5 μm were selectively retained within patch tissue, while smaller particles were removed into the circulation to appear sequentially in MLN and spleen: particle numbers peaked at 4 days in GALT, 7 days in MLN and 14 days in the spleen. Microspheres were not observed to penetrate the GI mucosa at any sites other than PPs. FACS analysis of solubilised tissue samples identified the spleen as an organ with a high propensity to accumulate microspheres, after a single oral gavage of 10^8 2.65 μm diameter particles (Ebel, 1990). Accumulation within PPs and MLN was also high.

A recent publication by Jani *et al.*, (1994) documents the organ distribution of Titanium dioxide (0.5 μm diameter) particles after a ten day gavage program in Sprague Dawley rats. Quantification was achieved using inductively coupled plasma atomic emission spectrometry. 0.02 % of the administered dose was detectable *per* ml of cardiac blood, with 2.4 % in the liver, 1.2 % in the lungs, 4 % in the colon and 2.86 % in the PPs and mesenteric network. Total systemic uptake of test material was estimated at

about 6.5 % of the administered dose. No particles were recovered from the kidneys or cardiac tissue.

Le Ray *et al.*, (1994) detected 0.1380 % of total recovered radioactivity in the liver, one hour after oral administration of [¹⁴C]poly(DL-lactide-co-glycolide) nanoparticles with milk. Four hours after gavage, liver accumulation was 0.4239 %, but declined steadily from then on. Splenic accumulation was about 0.0321 % one hour after gavage. Other tissues, such as mesentery, lymph nodes, lungs and kidney also exhibited evidence of nanoparticle accumulation from as early as one hour after administration. Cumulative absorption of radioactivity into extra-intestinal sites was estimated to be 2.4 % at one hour and 1.7 % at the four hour time points.

Despite a substantial number of reports claiming that particulates may accumulate within diverse extra-intestinal sites after oral delivery, many investigations have failed to provide confirmatory evidence. Extensive studies by LeFevre *et al.*, (1977, 1978a, 1978b, 1985a, 1985b, 1980, 1986, 1989) and Joel *et al.*, (1978) suggest insorbed particulates tend to accumulate in the MLN and patch tissue, and only rarely translocate to liver, lung or spleen.

1.2.8 EXCRETION OF INTESTINALLY ABSORBED MICROSPHERES

The fate of the vast majority of orally administered micro-particulates is obvious. Of the small fraction of particles which are absorbed across the intestinal barrier, the eventual fate may also be faecal elimination. Some evidence exists that intestinally absorbed particles may be eliminated by other routes, which are described below.

A quantitative study on the distribution and elimination of perorally administered nanoparticles was conducted by Nefzger *et al.*, (1984). These authors administered ¹⁴C-labelled poly(methyl methacrylate) nanoparticles with a stomach tube in bile duct cannulated rats. It was estimated that between 10 and 15 % of the radioactivity was absorbed from the GIT lumen. 58 % of the absorbed radioactivity was excreted in the bile and 42 % in the urine. 80 and 95 % of the absorbed amount of radioactivity was excreted within 24 and 48 hours of dosing respectively (Kreuter, 1991). Biliary excretion of polystyrene microspheres after oral administration to rats was quantified by Jani *et al.*, (1995). 9 % of a single oral dose of 50

nm FITC labelled microspheres were detected in draining bile 6 hours after gavage. A total of 17 % of the oral dose was excreted in the bile within 24 hours of administration. Excretion of particles in the bile occurs after sequestration of circulating microspheres within Kupffer cells (see section 1.2.6.2). Phagocytosed microspheres may be exocytosed into the space of Disse and thus gain access to the minute hepatic bile canaliculi. Bile canaliculi drain into larger calibre vessels, and the bile duct, which eventually empties into the duodenum (see figures 4 and 10). Thus microspheres excreted *via* this pathway may eventually be re-introduced to absorptive cells in the lower segments of the GIT, possibly gaining re-entry (Jani *et al.*, 1992).

Rapid elimination of intestinally absorbed particles within the urine was reported after investigations by Volkheimer (1977), and Gitzelmann *et al.*, (1993). Stag (1994) detected about 0.2 % of an oral dose consisting of 6.51 mg latex nanospheres (0.220 μm diameter) in urine collected from rats up to 24 hours post dosing. In another study, Stag (1994) found that between 5 and 10 % of an oral dose of ^{125}I labelled albumin microspheres (2.67 μm diameter) could be detected within urine collected from treated rodents. Examination, using a scanning electron microscope, of centrifuged urine samples demonstrated the presence of spherical, non-biodegraded albumin microspheres amongst urate crystals. Jani *et al.*, (1990) also detected high levels of radioactivity in the urine of rats orally dosed with ^{125}I labelled latex particles. Jani *et al.*, (1990) suggested that the high urinary levels may have been the result of undialysed ^{125}I associated with the microspheres before dosing.

Nanoparticles may also be excreted *via* exocytosis directly through the intestinal wall, back into the intestinal lumen (Sjoholm, *et al.*, 1979). In some cases, elimination is thought to occur *via* the lungs, where the particles transverse into the alveoli after being phagocytosed by macrophages (Alderserberg *et al.*, 1969). After travelling up the bronchial tree, they may be swallowed with saliva, excreted within faeces or gastrointestinally re-absorbed (Kreuter, 1991).

1.2.9 MICROSPHERES AS DELIVERY SYSTEMS FOR ORAL ADMINISTRATION

The development of a wide range of proteins, peptides and other molecules with therapeutic applications has led to the search for reliable oral delivery schemes. Such strategies must overcome formidable problems normally associated with size, membrane permeability, stability and solubility of these drugs. While absorption across the GIT is the major barrier to oral delivery, achievement of good absorption may not equate with adequate bioavailability. First pass metabolism, rapid clearance, peptide and protein instability or susceptibility to proteolysis, further complicates matters. Despite this, the enormous market potential and patient compliance offered by the oral route of administration has generated considerable interest into the possibility that microspheres could be used to target therapeutic compounds.

Encapsulating drugs within microspheres may have several important implications for oral drug delivery. In addition to providing a vehicle for drug transportation across the epithelial barrier, they also provide some level of protection against degradation in the GIT. Normal GI transit times for drugs may be prolonged by microencapsulation using materials with mucoadhesive properties. Thus in certain cases, prolonged transit times may facilitate better drug absorption due to increased exposure to gut uptake sites.

1.2.9.1 DRUG DELIVERY

Several research groups have investigated the use of microsphere and nanosphere systems for oral drug delivery, however, documentation of successful systemic therapy is limited to a few reports. Polyisobutylcyanoacrylate nanocapsules (165 nm) have been shown to be capable of promoting the intestinal absorption of an entrapped lipophilic tracer in dogs (Dange *et al.*, 1987). Fasted diabetic rats who received an oral dose of insulin encapsulated within polyisobutylcyanoacrylate nanocapsules displayed pronounced hypoglycaemia. The hypoglycaemic effects were only detected 2 days after dosing, but they lasted for up to 20 days at an initial dose of 20 units / kg. Non-diabetic or fed animals did not respond as well to this therapy. For comparison, equivalent doses of encapsulated insulin were injected subcutaneously. This resulted in the

rapid onset of a 2-3 times stronger hypoglycaemic response which lasted about 32 hours (Couvreur, 1988, Damgé *et al.*, 1990, 1988). Oral administration of nanocapsules with insulin simply adsorbed on to their surface resulted in no hypoglycaemic response, suggesting encapsulation was needed to protect the peptide from degradation in the GIT. In another study, insulin was incorporated into polyacrylic polymer microspheres in conjunction with protease inhibitors. Oral administration of this formulation resulted in a 2-3 fold increase in the efficiency of induction of a hypoglycaemic response in both normal and diabetic rats. Omission of the protease inhibitors from the microspheres abolished any glycaemic response (Morishita *et al.*, 1992). Nanoparticles (diameter 200 nm) prepared directly from insulin have been shown to elicit a hypoglycaemic response following intrajejunal administration in rat and mice (Oppenheim *et al.*, 1982).

Hydrocortisone incorporated into albumin microspheres reduced carrageenan induced inflammation in rats at a much lower dose than free drug after oral administration (Lewis *et al.*, 1992). The FITC labelled bovine serum albumin microspheres used in the study had a mean diameter of 3 μm and were detected within tail vein blood samples (by FACS analysis) as quickly as 5 minutes after gavage. Inflammation was reduced by hydrocortisone released from the particles due to proteolytic breakdown.

Sarubbi *et al.*, (1994) used proteinoid microspheres in an attempt to deliver calcitonin to the systemic circulation in rodent and primate studies. One hour after dosing encapsulated calcitonin and free drug, serum calcium concentrations decreased by 23 $\mu\text{g} / \text{ml}$ in rats which received encapsulated drug compared to a decrease of only 6.5 $\mu\text{g} / \text{ml}$ in control animals. Similar findings resulted from the primate studies. Dramatic decreases in serum calcium levels were observed following intraduodenal administration of encapsulated calcitonin to rats. No effect was seen in rats administered free drug.

A co-polymeric nanoparticle delivery system was used successfully to deliver modest (1.6 %) amounts of the peptide Luteinizing Hormone Releasing Hormone to the blood after oral administration (Hillery *et al.*, 1995). The level of hormone in the blood of rats, after a single gavage, was measured using a double antibody radioimmunoassay. Luteinizing Hormone Releasing Hormone could be detected in the blood as quickly as one hour after administration.

Hexylcyanoacrylate nanoparticles (200 nm) were found to enhance the bioavailability of vincamine relative to an aqueous solution of the drug after oral administration in the rabbit model. Increased bioavailability was attributed to protection of the drug in the GIT combined with increased presentation to uptake sites rather than nanoparticle translocation (Maincent *et al.*, 1986).

1.2.9.2 DELIVERY OF ANTIGENS

Oral immunisation has several distinct advantages over the parenteral route; it would be inexpensive, easy and convenient to administer without the need for highly trained personnel and refrigerated storage, relatively free from side effects and would be acceptable to the majority of patients enabling frequent boosting. Furthermore, because of the presence of a common mucosal immune system, oral administration may induce a vigorous immune response at multiple mucosal surfaces, which are the most common sites of entry of infectious agents (O'Hagan *et al.*, 1989). Systems which deliver antigens to mucosal sites (lymphoid tissues in mucosae and external secretory glands) may initiate some degree of systemic immunity (bone marrow, spleen and lymph nodes). Conversely, peripheral immunisation induces poor mucosal immunity (Mestecky *et al.*, 1992).

Empirical experience with mucosal immunisation has resulted in a generally accepted conclusion that considerably higher doses of antigens are required. This is due to elimination of antigens, existence of effective mechanical (epithelial cells) and chemical (mucus) barriers, and degradation and denaturation of antigens by enzymes and acids. Thus only small quantities of fully potent antigens reach the mucosal lymphoid tissues. In addition, pre-existing secretory antibodies complex with antigens at mucosal surfaces and further reduce antigen uptake (Mestecky *et al.*, 1992 and Walker *et al.*, 1987). Thus the use of colloidal carrier systems for the oral delivery of antigens might be expected to confer a number of potential advantages over alternative approaches. Colloidal systems are known to access GALT *via* PPs and provide some protection against degradation. In addition, several antigens can be delivered simultaneously, in conjunction with immunological adjuvants or cytokines if necessary.

Biodegradable microsphere technology has been employed in several studies to mediate both mucosal and systemic immunity after oral administration. Poly DL-lactide-co-glycolide (DL-PLG) copolymer microspheres (1-10 μm) carrying staphylococcal enterotoxoid have demonstrated their ability to elicit both systemic and mucosal immunity in mice after an oral immunisation protocol (Eldridge *et al.*, 1990, 1993). Santiago *et al.*, (1993) prepared proteinoid microspheres (0.1-5 μm diameter) encapsulating influenza virus antigens (M1 or HA-NA). They examined the efficacy of this preparation to induce specific IgG responses after oral administration in rats. Plasma samples from rats dosed orally with 'empty' microspheres showed no significant antibody titer against either M1 or HA-NA antigens, using ELISA (an enzyme-linked immunosorbent assay). Plasma samples from three of the five rats dosed with M1 microspheres showed a very significant primary response to M1 antigen 14 days post dosing. IgG titers remained elevated up to 42 days after oral administration of the encapsulated M1 antigen. Oral administration of unencapsulated M1 antigen resulted in very slightly elevated serum IgG titers. Significantly high anti HA-NA titers were observed in a proportion (2 of 5) of the animals dosed with encapsulated antibody compared with those who received unencapsulated protein. The authors suggested that PP mediated transportation of the microspheres had occurred, followed by delivery of antigen to the general circulation. The microspheres were said to have played two roles in the delivery of antigen, that of protection and site specific targeting to GALT.

O'Hagan *et al.*, (1989) used non-biodegradable polyacrylamide microspheres (2.55 μm) as adjuvants for oral immunisation of rats with ovalbumin. Microspheres of polyacrylamide were prepared by emulsion polymerisation of a water-in oil emulsion, with the ovalbumin dissolved in the aqueous phase. The resulting microspheres were macroporous beads in which entrapped proteins were partly exposed on the particle surface. The microspheres were administered orally on four consecutive days to rats primed 14 days before by intraperitoneal injection. The levels of IgA in the saliva of rodents who received microparticulate incorporated antigen was significantly higher at 65 days after administration than the control group. Incorporation of ovalbumin into the carrier system was thought to have afforded some level of protection against enzymic degradation in the GIT. Entrapment of ovalbumin in poly (lactide-co-glycolide) microspheres resulted in a significantly greater salivary IgA response after oral

administration than soluble ovalbumin (O'Hagan *et al.*, 1993). Cholera B toxin subunit was also entrapped in microspheres. Following oral immunisation in mice, specific antibody secreting cells were detected both in the MLN and spleen.

1.3 AIMS AND OBJECTIVES OF THE PRESENT STUDY

The development of a system capable of delivering systemically active therapeutic compounds by the oral route of administration was the primary impetus behind this research undertaking. Following nanotechnological advances, considerable interest has been aroused within the field of drug delivery in the use of microparticulate drug carrier systems. We wanted to investigate the possibility that microspheres could be used as an oral drug delivery system. Microspheres were selected in preference to liposomal systems as it is generally accepted that liposomes are unsuited to oral drug delivery applications (Woodley, 1986).

Although very small particles are thought to penetrate the GIT mucosa and accumulate within anatomically remote locations after oral delivery, the literature is fairly incohesive regarding the time course, quantification, and mechanistic aspects of such events. Our ultimate aim was to investigate the feasibility of using microsphere systems to deliver systematically active compounds by the oral route. In order to achieve this it was important for us to try and investigate some of the aforementioned variables which underpin this phenomenon.

Previous work at Aston University by Alpar *et al.*, (1989) using polystyrene microspheres demonstrated a very rapid transport of test particles from the GIT to the blood and inflammatory air-pouches of experimental rats. In a later study at Aston, Lewis *et al.*, (1992) manufactured albumin microspheres which were rapidly (within minutes) translocated to the blood stream of laboratory rodents after oral delivery. One of our primary objectives was to confirm the existence of this rapid uptake mechanism and examine its potential for exploitation for drug delivery purposes. We also wished to ascertain which conditions, if any, favoured particle exit from the GIT lumen into the blood, lymph and other tissues.

Following on from the earlier work at Aston (Alpar *et al.*, 1989) we wanted to find out the extent of microsphere accumulation within organs, such as the spleens and livers, of rodents treated orally with latex particles. This information was required in order for us to ascertain whether oral administration would allow sufficient numbers of microspheres to access important systemic compartments other than the blood. We envisaged that elucidation of the pattern of microsphere traffic between different organs at known time points after oral administration would give valuable insight into the kinetics of particle uptake and translocation from the GIT lumen.

A fundamental objective of this project was to gain more insight into the mechanisms which allow particles to exit the gut lumen. As mentioned earlier in this chapter, the majority of researchers in this area *cite* the PPs as the exclusive portal for microparticulate insorption. The rapidity of microsphere uptake observed by Alpar *et al.*, (1989) and Lewis *et al.*, (1992) did not seem to equate with PP mediated uptake, and we thought that this finding warranted further investigation.

Finally it was hoped that we might test the efficacy of a microsphere system, in terms of its ability to deliver a therapeutically active compound by the oral route of administration.

2.0 EXPERIMENTAL METHODOLOGY

2.1 ANIMALS

All rats were young males of the Wistar strain which weighed between 200 and 300 g (Aston University, Birmingham). Prior to oral dosing procedures they were starved overnight (12 hours) on grids five centimetres above their bedding to prevent coprophagia. At all other times, unless otherwise stated, they were allowed a diet of food and water *ad libitum*.

2.2 ANAESTHESIA

In experiments that required anaesthesia of animals, an inhaled gaseous mixture of 3% halothane (RMB Animal Health Ltd, Dagenham) in oxygen (300 cubic cm / min) and nitrous oxide (1000 cubic cm / min) was used. This was administered using a Boyle's veterinary anaesthetic apparatus (British Oxygen Company, Crawley). Total anaesthesia was maintained for the appropriate length of time using a mixture of 1.5% halothane in oxygen and nitrous oxide.

2.3 MICROSPHERES

The term 'microsphere' is generally employed to describe spherical particles within the size range 50 nm - 2 mm. Particles smaller than 1 μm in diameter may be referred to as 'nanospheres' to emphasise their smaller size. The terms 'microparticles' and 'nanoparticles' are also employed, but without emphasis on the spherical shape of the particles. The word 'particle' implies a variety of relatively rigid and non compressible morphologies, as compared with membranous entities such as artificial cells and liposomes (Arshady, 1993).

Monodispersed polystyrene (2.5 % solids) latex microspheres were purchased from Polysciences, Inc., Northampton, U.K. Seven different batches of polystyrene latex microspheres were used in experimental studies.

Microsphere type	Size (μm)	Catalogue number	Detection method	Experimental section (s)
Fluoresbrite carboxylate	0.87 ± 0.006	15702	FITC	Chapter 3 & Chapter 6
Polybead	0.82 ± 0.010	07309	^{125}I	Chapter 4
Polybead	0.21 ± 0.003	07304	GPC	Chapter 4
Polybead	0.22 ± 0.010	07304	GPC	Chapter 4
Polybead	0.22 ± 0.010	07304	GPC	Chapter 4 & Chapter 5
Polybead	0.97 ± 0.010	07310	GPC	Chapter 4
Polybead	0.97 ± 0.002	07310	GPC	Chapter 4

Table 1. Specifications and methods of detection of latex microspheres employed throughout experimental investigations.

Fluoresbrite™ carboxylate microspheres are labelled with FITC and were used extensively during preliminary studies. FITC dye has an emission maxima of 540 nm, and thus Fluoresbrite™ particles are highly visible in fluorescent light. In experiments where microspheres were radio-labelled, or detected by GPC, monodisperse Polybead® microparticles were employed. Polybead® particles are prepared without surfactant which reduces the need for clean up procedures (Polyscience, 1987). The concentration of latex particles in a given volume of stock solution can be calculated using a formula provided by Polysciences (1987):

$$N = \frac{6W 10^{12}}{\pi p d^3}$$

Where:

N = number of particles / ml

W = % solids

d = diameter (μm)

p = density of bulk polymer (g/ml)

When: W = 2.5 % solids
 d = diameter (μm)
 $\rho = 1.05$ for polystyrene

Prior to any manipulation, microsphere suspensions were vortexed with a WhirliMixer™ (Fisons) for at least 30 seconds. All microspheres were washed thoroughly before oral administration to remove any traces of surfactant residues from the manufacturing process. Microsphere aliquots were centrifuged (MSE, Micro Centaur) in eppendorf tubes before discarding the resulting supernatant. The particles were then re-suspended in distilled water, vortexed, and micro centrifuged. The clean up process was repeated up to 4 times until microspheres were re suspended with the desired volume of carrier solution for dosing. The mass of microspheres in any given volume of suspending medium was determined by freeze drying the particles in a pre - weighed container. As 2.5 % of the volume of any stock solution is represented by latex microspheres, this value can also be used to make a quick estimate the mass of polystyrene in a given volume of stock particles.

2.4 MICROSCOPY AND PHOTOGRAPHY

2.4.1 LIGHT MICROSCOPY

Stained slides or blood samples were examined using a Zeiss universal microscope fitted with an IV FI epi-fluorescence condenser containing a HBO 50W super-pressure mercury light source. Two sets of eyepieces were used (x10 or x12 magnification). The microscope was fitted with 5 objective lenses (x4, x10, x16, x40 and x100). When using the oil immersion objective (x100) it had to be connected to the slide with a drop of immersion oil. The final magnification obtained was calculated by multiplying the eyepiece magnification by the objective magnification.

2.4.2 PHOTOGRAPHY

Photographs were taken using an Olympus PM6-213181 camera and Fuji colour film. Exposure times of up to 100 seconds were used depending on the light intensity measured using an Olympus EMM V light meter. In order to calibrate resulting photomicrographs, an eyepiece graticule with 10 μm graduations was used. A drawing of the camera's field of view was made

and the graticule was used to measure the distance between morphological features. This measurement was then translated onto the photomicrograph, after development, in the form of a size bar.

2.4.3 SCANNING ELECTRON MICROSCOPY

Scanning electron microscopy was used to check the size and appearance of polystyrene microspheres purchased for use *in vivo*. 100 µl (2.5 mg) of stock particles were freeze dried overnight. Dry microspheres were then attached to stubs and a fine gold film was electrolytically deposited (sputtered) onto the sample stubs in a (Emscope SC 500) sputter coater. Mounted microsphere samples were then examined and photographed using a Cambridge Instruments Stereoscan 90 scanning electron microscope with camera attachment. The size distribution of microsphere sample batches was obtained by comparison of large numbers ($n > 100$) of particles and the size bar of the resulting photomicrographs.

2.5 HYDROPHOBICITY INTERACTION CHROMATOGRAPHY (HIC)

HIC was employed to determine the relative hydrophobicities of microsphere suspensions used in uptake studies (see section 4.2.1.1). It involves passing a dilute suspension of microspheres through gels of different relative hydrophobicities, and quantifying the percentage of particles eluted each time the columns are washed. Hexyl-agarose was the most hydrophobic gel employed, followed by pentyl-agarose, propyl agarose and sepharose. The more hydrophilic particles are eluted relatively easily, while hydrophobic entities remain bound to the gels. The number of particles in each eluent sample is determined by comparing the optical density (OD) to that of the original microsphere suspension. The percentage decrease in OD with each washing will give a good indication of the extent of hydrophobic interaction between the microsphere sample suspension and the respective gel.

2.6 DETERMINATION OF ZETA POTENTIALS

The Zeta potential of microsphere systems was determined using a Malvern Zetamaster (Malvern Instruments, U.K).

2.7 METHODS OF QUANTIFICATION OF POLYSTYRENE MICROSPHERE NUMBERS IN BODY FLUIDS AND TISSUES

In order to assess the feasibility of using microspheres as an oral drug delivery system it was important to determine the extent of particle transfer from the GIT lumen to extra - intestinal sites. Several methods of quantification were employed, although some were found to be limited in usefulness. Provisionally, animals were dosed with fluorescent polystyrene microspheres and the number of particles in blood and tissue samples determined by fluorescent light microscopy. FACS was also used in some experiments to count the number of fluorescent latex particles in blood samples. Later on in the project, radioactive polystyrene microspheres were manufactured and used as a model particle. Finally GPC technology was utilised, and became the method of choice, for determination of polystyrene particle uptake into body fluids and tissues after oral administration.

2.7.1 QUANTIFICATION OF FLUORESBRITE™ MICROSPHERE NUMBERS WITHIN BLOOD SAMPLES USING FLUORESCENCE MICROSCOPY.

The number of Fluoresbrite™ carboxylate polystyrene latex microspheres within a given sample of whole blood was determined by using the method described by Alpar *et al.*, (1989).

Immediately after sampling, blood was diluted with a solution of glycerol (Fisons) and heparin (CP Pharmaceuticals, Wrexham) (1000 units / ml) mixture. Diluted blood was then examined within a Neubaur counting chamber using a Zeiss universal microscope fitted with an IV FI epi-fluorescence condenser containing a HBO 50W super-pressure mercury light source. Individual Fluoresbrite™ particles are highly visible under the fluorescent light source and thus their numbers in a given blood sample could be estimated. The small size of the spheres, in conjunction with the surface tension of the sample in the counting chamber, tend to scatter the particles which then reside in the grooves either side of the grid when counting low viscosity liquids. The addition of glycerol increases the viscosity of the blood which tends to ensure that any particles present remain within the counting zone of the haemocytometer. The average number of erythrocytes associated with 200 fluorescent particles was determined using a combination of fluorescent and tungsten light sources.

Different aliquots of each blood sample were counted numerous times, until a representative fluorescent microsphere / erythrocyte ratio was obtained (it was not always possible to find 200 microspheres despite exhaustive searching). Having determined the mean number of fluorescent microspheres *per* erythrocyte, the number of microspheres in whole vascular compartment was estimated using the method of Alpar *et al.*, (1989). As there are 5.25×10^9 erythrocytes *per* ml of blood in a rat, and on average, 14.6 ml of blood in a 200 g rat (Archer, 1965) the total number of erythrocytes (7.665×10^{10} in a 200 g rat) and thus circulating numbers of particles in the whole animal may be calculated. Values for microsphere uptake after oral delivery were represented as a percentage of the dosed particles that were estimated to be circulating within the whole animal's vascular compartment.

2.7.2 QUANTIFICATION OF FLUORESCENT MICROSPHERE NUMBERS WITHIN BLOOD SAMPLES USING FLOW CYTOMETRY.

Determination of particle concentrations in blood and tissue samples after oral dosing was carried out initially following a protocol described by Ebel, (1990) for quantifying particle numbers in lymphatic tissue. The extraction technique, which employed extremely harsh treatment of tissue and blood samples (Triton X-100 (Sigma) and 1% KOH at 60°C) was found to be very destructive, even to polystyrene microspheres. We abandoned the extraction process, modifying the technique for counting microspheres in heparinised blood samples.

A fluorescence activated cell sorter (Becton Dickinson FACS 440) at Birmingham University Medical School, was used to count the number of Fluoresbrite™ carboxylated polystyrene latex microspheres within blood samples from rodents orally administered the particles. In the flow cytometer, diluted blood was passed as a fine jet through a narrow beam of laser light of the excitation wavelength of the fluorescent microspheres. The exact volume of each sample analysed was recorded. The intensity of the fluoresced light that results from the excitation of the particles within the sample stream was detected with a photomultiplier situated at 90° to the angle of incidence. Forward scattering intensity, which was indicative of particle size, shape and refractive index, was also detected. The forward scattering (FS) and green fluorescence signal were used to differentiate between the latex particles and other particulate matter, cell debris etc. The

uniformity in the size and FITC content of the beads resulted in a narrow distribution in the forward scattering and fluorescence signals, around which an electronic window was positioned. Microsphere events registered within the window were defined as representing either single or multiple particles. Unfortunately the software package did not define the number of particles within a multiple microsphere event, which could represent two, three, four or more closely associated microspheres. By examining the forward scattering and fluorescence profiles it was, however, possible to make a rough estimate of the number of doublet, triplet and quadruplet microparticle groupings registered within the multiple particle window.

2.7.3 QUANTIFICATION OF LATEX MICROSPHERE NUMBERS IN BODY FLUIDS AND TISSUES BY RADIOLABELLING

Polybead[®] polystyrene particles were radioiodinated according to Pratten *et al.*, (1984) and Seymour *et al.*, (1991) using Hunter and Greenwood (1963) methodology (see below). This enabled the uptake of the microspheres into blood and tissue sites after oral administration to be monitored by virtue of gamma ray emission.

The oxidising agent chloramine-T, is normally used for iodinating proteins having existing tyrosine residues. Depending on the reaction conditions, iodinations can be performed to produce mono-iodo, di-iodo tyrosine or a mixture of both. Electrophilic substitution of ¹²⁵I atoms from Na¹²⁵I occurs at *ortho* positions on the aromatic ring. The hydroxyl substituent serves to force lone pair electrons onto the aromatic ring encouraging *ortho* position directed electrophilic substitution of the ¹²⁵I atoms into the molecule (see figure 12 below).

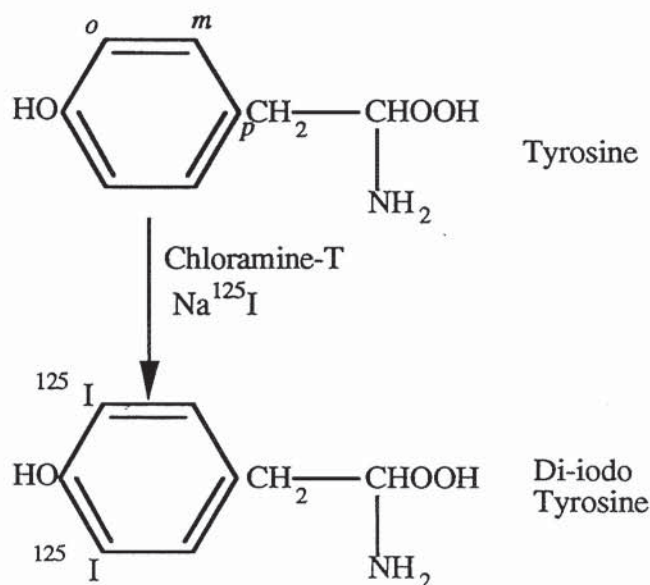


Figure 12. Radiodination of Tyrosine using the chloramine-T method.

Radiodination of polystyrene may result from a similar reaction mechanism to that of tyrosine. Using toluene as a hypothetical model for the reaction, electrophilic substitution would be most likely to occur at the *ortho* and *para* positions of the benzene ring. This is because, in the case of toluene, the *ortho* and *para* carbon atoms become activated by the action of the methyl (CH₃) substituent. Activation of the ring by the methyl group occurs because it, like the hydroxyl in tyrosine, pushes electrons onto the structure. However, this effect is not as pronounced as in the case of tyrosine and thus substitution by an electrophile is slightly less favoured. In the case of polystyrene, the same effect will activate the *ortho* and *para* carbon atoms of the six member ring. However, the long carbon backbone will introduce an element of steric hindrance, shielding the *ortho* carbons. Thus electrophilic substitution is most likely to occur at the *para* positions. This is most likely to result in *para* directed substitutions of the ¹²⁵I atom (see figure 13). Covalent bonding of the halogen will tend to induce a slight electropositive charge onto the carbon which may result in decreased stability of the bound radiolabel. In particular, the structure will become susceptible to attack from nucleophilic elements such as OH⁻. Thus *in vivo* considerable leaching of the weakly bound ¹²⁵I label might not be unexpected. In the case of iodo-tyrosine, the presence of the electron donating hydroxyl group in the *para* position of the aromatic ring confers stability to the molecule, rendering it less susceptible to nucleophilic attack.

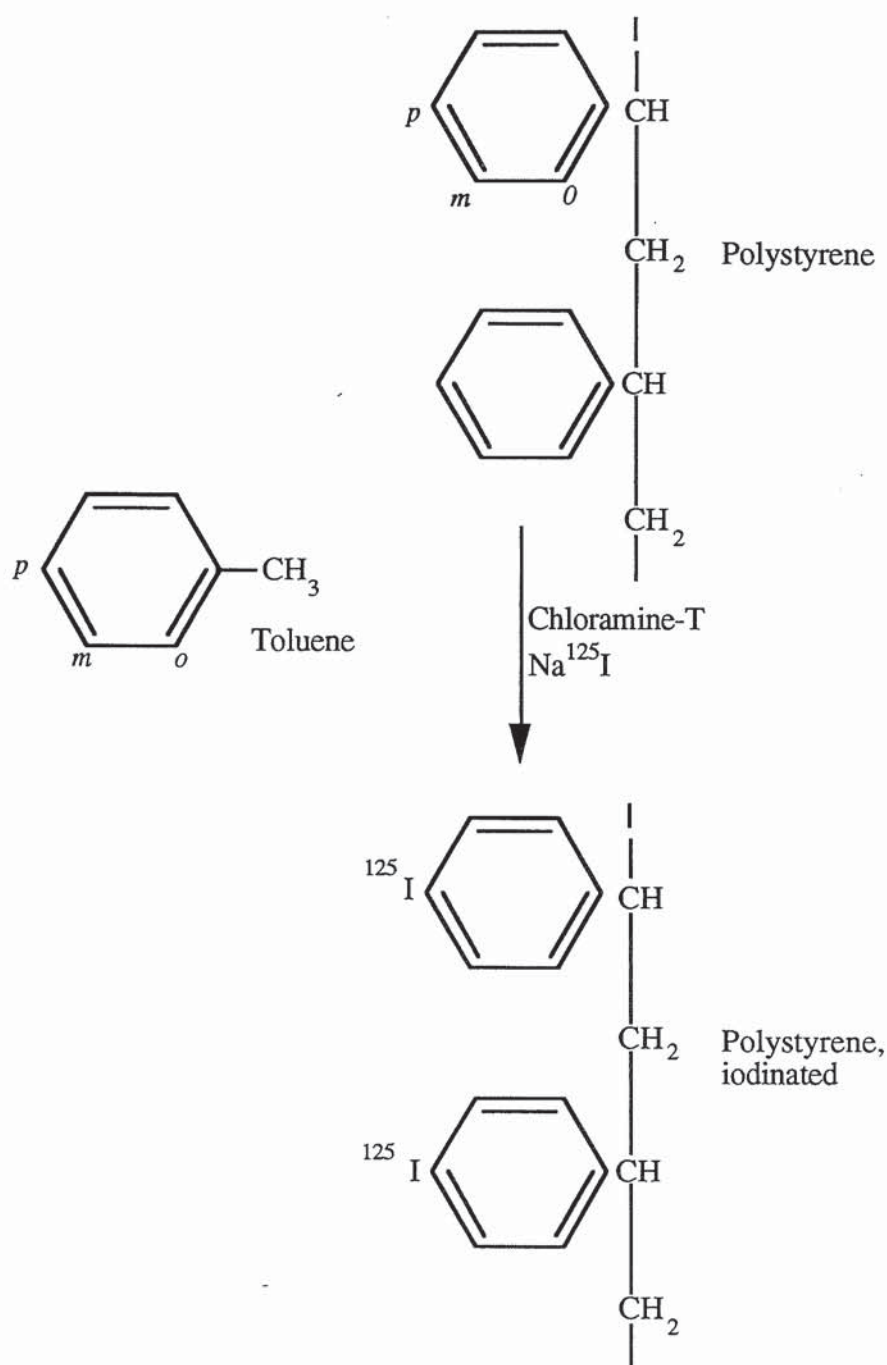


Figure 13. Proposed reaction for the radiodination of polystyrene using the chloramine-T method. The pendant aromatic rings would be expected to react in a similar way to toluene molecules.

10 ml of stock microspheres were centrifuged (MSE) at about 5000 rpm for 10 minutes. 7 ml of the resulting supernatant was discarded in order to reduce the overall reaction volume. The microspheres were then transferred to a scintillation vial which could easily fit inside a shielding lead pot.

Na^{125}I solution (96.2 MBq, ICN) and chloramine-T (100 μg / mg microspheres) were added to the vial which was then sealed and placed inside the lead pot. The reaction vessel was then gently shaken for 10 minutes, after which, 60 mg of sodium metabisulphate ($\text{Na}_2\text{S}_2\text{O}_5$) was added in order to terminate the reaction. The radioactive microspheres were then poured down a clamped funnel into a dialysis sack suspended inside a large bucket with clamps. The dialysis sack consisted of dialysis tubing tied at the end opposite the funnel. The bucket was filled with tap water by means of rubber tubing connected directly to a tap. Adherent microspheres on the funnel and inside the reaction vial were washed into the dialysis sack using tap water. The dialysis bag, bucket and funnel were located inside a fume cupboard behind lead shielding such that water addition could be controlled remotely using a tap external to the cupboard. Dialysate water was removed through plastic tubing, normally used for siphoning solvents, which emptied into another bucket. All aqueous radioactive waste was disposed of using sinks designated for such procedures.

2.7.4 DETECTION OF POLYSTYRENE MICROSPHERES IN BODY FLUIDS AND TISSUES BY GEL PERMEATION CHROMATOGRAPHY (GPC)

Gel permeation chromatography (GPC) is in simplest terms a mechanism of solute separation with molecular size as the discriminating factor. Sample molecules permeate the stationary phase to different degrees and are thus retained within the column for periods of time proportional to their molecular size. Columns are tightly packed with a gel or some other porous material and completely filled with solvent (the mobile phase). The same solvent is used to dissolve the sample before introducing it into the column. Within the column the pore size of the packing particles determines the molecular size range within which separation occurs. Using the appropriate type of packing material it is possible to separate soluble molecules with molecular weights ranging from 100 to several millions. Cross linked polystyrene resulting from the co-polymerisation of styrene and divinylbenzene is frequently used for packing GPC columns. The ratio of divinylbenzene to styrene dictates the amount of cross-linking, and thus pore size, as well as behaviour of the gel on contact with organic solvents. Resins with low concentrations of divinylbenzene are not pressure stable, conversely a high ratio of divinylbenzene to styrene results in highly cross-linked rigid gels. Molecular size sorting takes place by repeated exchange

of solute molecules between the bulk solvent of the mobile phase and the stagnant liquid phase within the pores of the packing. Redistribution of solute molecules between phases in this manner occurs in order to satisfy the thermodynamic equilibrium. Thus unlike other forms of liquid chromatography, like HPLC where enthalpic (chemical) reactions are used to separate solute molecules, GPC relies on entropic interactions based solely on molecular size to attain separation.

Traditionally, GPC has been used for the analysis of molecular weight distributions (MWD) of synthetic polymers. Sample solutions are injected into the column and size sorting takes place in the packing material by the exclusion process, the largest molecules exiting the column first, followed by those of decreasing size (figure 14). The retention volume (VR) is the volume of solvent which has passed through the system from the time of sample introduction to the time of the peak maximum. Subsequent examination of the detector response versus retention volume for a given polymer reveals its molecular size distribution, often taking the form of a Gaussian type peak. Having ascertained the molecular size distribution of a given sample, conversion to a molecular weight distribution is achieved using calibration data from chromatograms of standard solutions analysed under identical experimental conditions. Standard polymer fractions of narrow MWD elute as sharp peaks with their retention volumes varying with differences in molecular weight. Hence comparison of standard retention volumes to unknown retention volumes allows construction of a MWD for an unknown polymer. Once a system is standardised, the retention volume of a peak is directly proportional to the retention time or time elapsed from injection and is usually referred to as such (Yau *et al*.,1979).

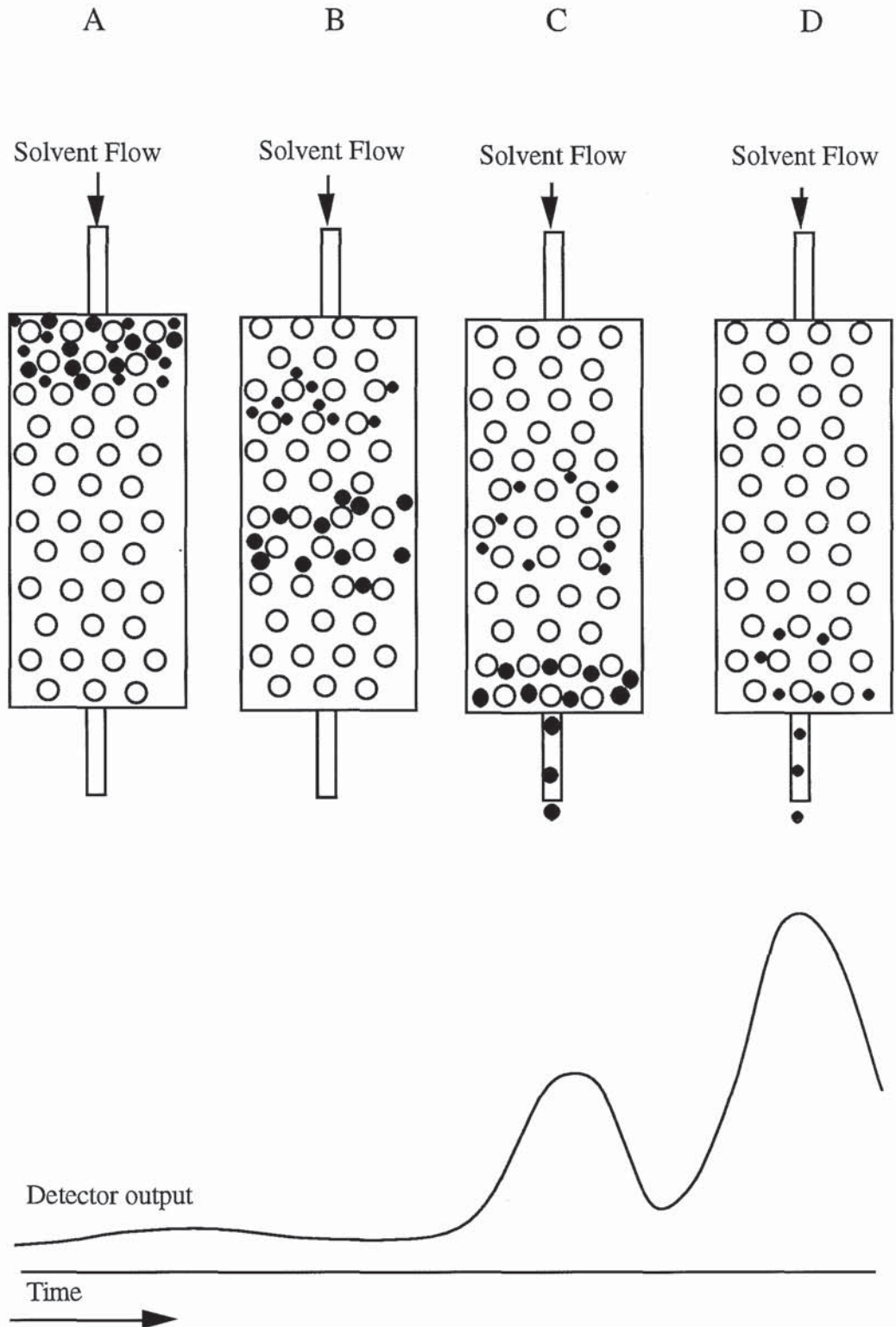


Figure 14. Schematic representation of size exclusion chromatography: A. Sample injected; B. Size separation; C. Large solutes eluted; D. Small solutes eluted. Adapted from Yau *et al.*, (1979).

More elaborate data treatment involves the calculation of molecular weight averages which give information about chain length and the extent of cross linking within a polymer. During the course of a polymerisation reaction, a large quantity of polymer chains are initiated, grow, and are terminated. The molecular weight averages (M_n , M_w) indicate the number and length (or weight) of the polymeric chains formed during manufacture. M_n is the number-average molecular weight, which is the molecular weight of the average chain length in a polymer sample. M_w refers to the molecular weight equal to the modal molecular weight of polymer chains, known as the weight average molecular weight. As M_n represents the molecular weight of the average chain length in a polymer sample, and M_w refers to the molecular weight equal to the modal molecular weight of the polymer chains the value of M_w is always larger than M_n except in the case of a truly monodisperse system where the values are identical. Manual calculation of M_n and M_w is accomplished by digitisation of chromatograms. This involves division of a chromatogram into many vertical strips. Each strip will have an area (h_i), and a molecular weight (M_i) obtained by reference to a molecular weight calibration curve generated separately. The number-average molecular weight (M_n) is calculated by dividing the total area under the curve by the sum of the individual strip area's divided by the same strip's molecular weight:

$$M_n = \frac{\sum h_i}{\sum (h_i / M_i)}$$

The number-average molecular weight can also be related to physical properties (fibre strength, melt fluidity) of an individual polymer and in this case is defined as the mass of the sample in grams ($\sum w_i$ or $\sum N_i M_i$) divided by the total number of chains present $\sum N_i$. W_i and N_i are the weight and number of molecules of molecular weight M_i , respectively. i is simply the incrementing index over all molecular weights present:

$$M_n = \frac{\sum h_i}{\sum (h_i / M_i)} = \frac{\sum W_i}{\sum (W_i / M_i)} = \frac{\sum N_i M_i}{\sum N_i}$$

The weight average molecular weight (M_w) is equal to the molecular weight corresponding to the retention time of the apex of a peak. For digitised chromatograms M_w is represented as:

$$M_w = \frac{\sum (h_i M_i)}{\sum h_i}$$

The ratio M_w / M_n is a measure of the spread of a polymer's molecular weight distribution. Thus the value of M_w/M_n may be extremely large as in the case of highly cross linked polymer species. M_w is greatly influenced by the representation of high molecular weight species within a polymer sample. The opposite is true for the molecular weight average M_n (Yau *et al*.,1979).

Jani *et al.*, (1990) used GPC to determine the MWD of polystyrene microspheres. This enabled them to quantify latex microsphere accumulation within organs after GPC analysis of tissue extracts. Tetrahydrofuran (THF) was used as the versatile mobile phase during these studies. Polystyrene in common with a large number of polymers is soluble in THF, which is ideal for GPC due to its low viscosity and low refractive index. Biological macromolecules are also soluble in THF but in contrast to polystyrene, they are reduced to relatively small compounds by the extraction process and thus can be resolved as separate peaks on a GPC chromatogram. This technique enabled Jani *et al.*, (1990) to successfully quantify the extent of polystyrene microsphere translocation from the gastro-intestinal tract to other organs and tissues.

2.7.4.1 GPC APPARATUS

The components of a modular GPC system is shown in figure 15. Simplistically the set up consists of a 2 litre glass bottle acting as the mobile phase reservoir and filled with GPC grade THF (Aldrich, U.K). An Altex model 110A adjustable flow rate pump preceded by a sintered metal frit was used to pump solvent at 1ml / minute around the system. Sample introduction was achieved by including a Rheodyne injector valve (Waters' CA U.S.A 7125), fitted with a 100 μ l sample loop, in the system. Two 300 x 7.5 mm, 10 μ m mixed pore highly cross linked spherical macro porous polystyrene-divinylbenzene matrix (PLGel) columns (Polymer Laboratories Ltd, Shropshire U.K) were set up in series according to Jani *et al.*, (1990), and were protected by a 50 x 7.5 mm 10 μ m mixed pore guard column (PLGel) (Polymer Laboratories Ltd, Shropshire U.K). A Pye Unicam LC3 UV detector was tuned at a wavelength of 224 nm and was

connected in parallel to a Gallenkamp Euroscribe chart recorder and a Hewlett Packard 3390 A integrator. Detector sensitivity was set at a range value of 0.08 (arbitrary units). Effluent THF from the UV detector was simply directed to a 2 litre waste solvent bottle for safe disposal. All chromatography work was performed at room temperature.

2.7.4.2 MOLECULAR WEIGHT CALIBRATION OF THE GPC APPARATUS

Standardisation of the GPC system was achieved using narrow-MWD standards and the peak position calibration technique (Yau *et al.*, 1979, Jani *et al.*, 1990) (see section 4.2.2.1).

For latex microspheres the molecular weight averages were calculated by freeze drying the particles prior to dissolution in THF. GPC analysis of the microspheres and the molecular weight standards enabled M_n and M_w values for the particles to be estimated (see section 4.2.2.2). GPC analysis of microspheres and tissue samples took place under identical conditions to all analytical work undertaken. In all cases, detector sensitivity was set at an optimal for particle detection.

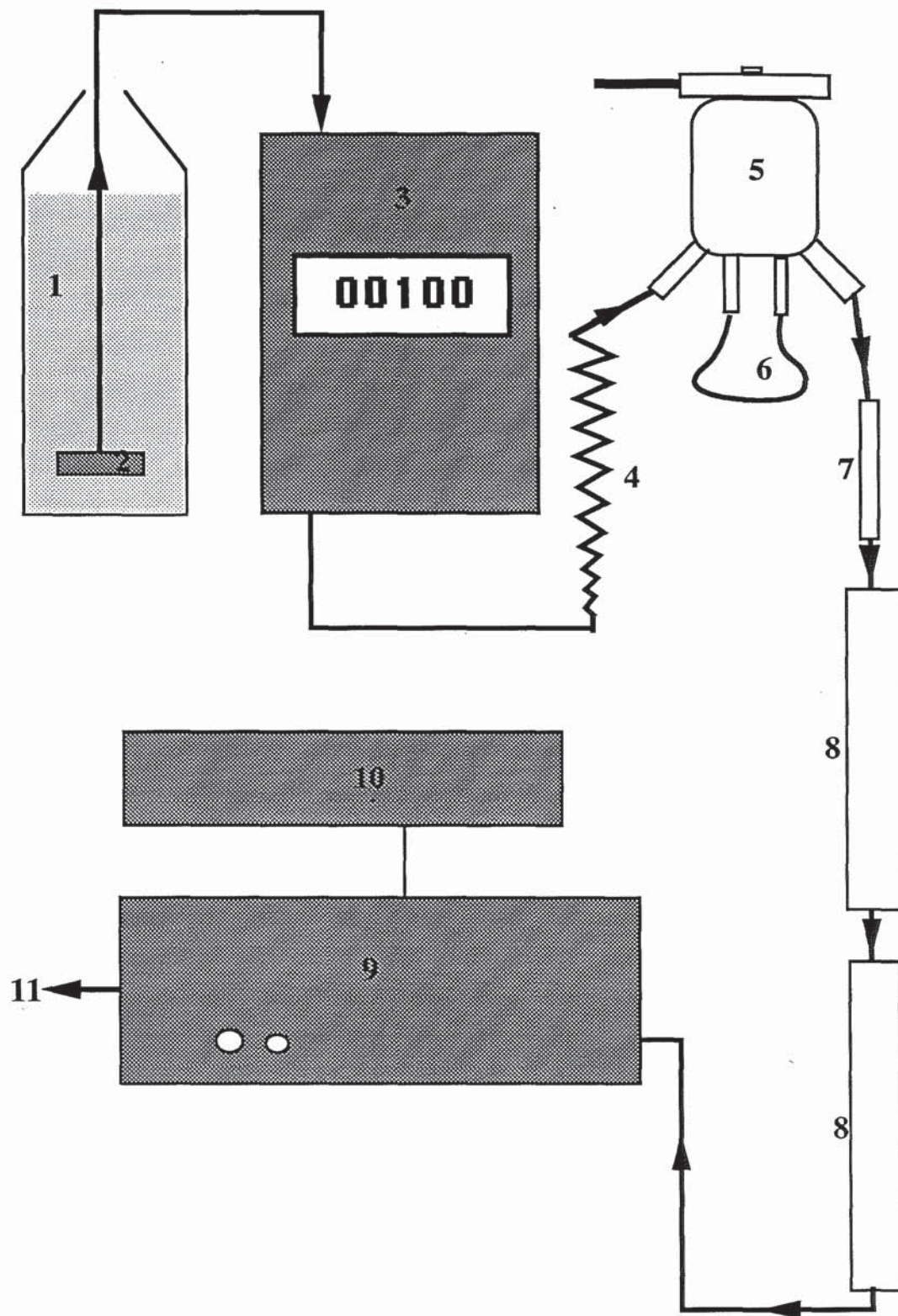


Figure 15. Components of a modular GPC system: 1. mobile phase reservoir; 2. sintered metal frit; 3. adjustable flow rate pump; 4. pulse damper; 5. sample injector valve; 6. 100 µl sample loop; 7. guard column; 8. column; 9. U.V detector; 10. chart recorder and integrator; 11. solvent waste bottle.

2.7.4.3 TREATMENT OF TISSUE SAMPLES FOR ASSESSMENT OF POLYSTYRENE MICROSPHERE CONTENT

Animal tissues and clotted blood samples removed for GPC analysis were placed into pre weighed conical flasks, which had ground glass necks, and weighed. Physiological data from Poole *et al.*, (1987) (shown in the appendices) was used to calculate what proportion of the whole organ mass each blood and tissue sample represented. This enabled us to report the amount of latex within whole organs.

Flasks were frozen at -20°C for 3-4 hours before being placed in the freeze dryer overnight. Gut wash, urine and faecal samples were treated differently. The large volumes of liquid used to wash the intestines was reduced to about 5 ml by placing gut wash containers onto a hot plate set at about 60°C . Urine was treated similarly if it too occupied a large volume. After reducing the volumes of these samples they were frozen at -20°C for 3-4 hours before being placed in the Modulyo freeze dryer (Edwards, Crawley) overnight. Faecal samples from the animals were placed in a drying oven for 6 hours prior to freeze drying procedures.

After the initial freeze drying, the dehydrated tissues were crushed to a powder using a pestle and mortar containing liquid nitrogen. The fine powders were then transferred back to their respective conical flasks and subjected to further period of lyophilization for 60 hours. At the end of the 60 hour period the dry tissue containing glass conical flasks were removed, and about 30 ml of chloroform was poured into each one. The conical flasks were then tightly stoppered and incubated within a shaking water bath at 30°C for 12 hours. The contents of the conical flasks were then filtered through a glass funnel containing glass wool, with further chloroform washes, into round bottomed flasks. In the case of faecal or gut wash samples the volume of chloroform was measured into glass measuring cylinders, and diluted further in a known volume of chloroform. This action avoided extensive dilution of these particular samples, which were known to be heavily contaminated with polymer, prior to GPC analysis. The diluted or un-diluted chloroform extracts were then evaporated to dryness using a rotary evaporator (Rotavapor R-110, Buchi) and water bath at a temperature of 30°C . The dry residue remaining on the insides of the round bottomed flask was then re suspended in GPC grade THF (Aldrich, UK). The exact volume of THF used, between 2 and 10 ml, was recorded.

Each sample was then filtered through a 0.5 µm disposable solvent resistant filter (Millex-SR, Millipore SLSR025NS) and injected into the GPC system for polystyrene analysis (Jani *et al.*, 1990).

2.7.4.4 CALIBRATION AND SENSITIVITY STUDIES.

The amount of polystyrene in a given tissue sample was determined by generating a standard curve. GPC analysis of known amounts of latex particles dissolved in THF was performed. The area under the polystyrene (Gaussian) type peak for each known mass of latex microspheres was recorded, and a relationship between the two variables calculated (see section 4.2.2.3).

The efficiency of the tissue extraction process and subsequent GPC determination of latex was quantified by spiking animal tissues and fluids with known amounts of latex microspheres before extraction and analysis (see section 4.2.2.3)

2.7.5 HISTOLOGICAL EXAMINATION OF TISSUES

Qualitative and semi-quantitative information about microsphere uptake into tissues after oral administration was gained by histological examination of samples removed from treated animals. Latex particles are soluble in most solvents ordinarily employed in thin sectioning processes. Sims (1974) glycol methacrylate embedding protocol enabled very thin sections (<1µm) to be cut without destroying the fluorescent microspheres. The work was carried out in collaboration with Birmingham City Hospital Trust's Histology Department who kindly provided the facilities and equipment for cutting plastic embedded tissue sections.

2.7.5.1 TISSUE COLLECTION AND FIXATION

Tissues were collected post-mortem, and placed in a 10% formal saline (10% formaldehyde 40% w / v diluted in 90% physiological saline) solution for a minimum of 48 hours for fixation.

2.7.5.2 TISSUE TREATMENT

All procedures were carried out in a fume cupboard. Fixed specimens were trimmed to an optimum thickness of 1 mm using a razor blade. The tissues were then dehydrated in at least three changes of absolute alcohol (Fisons) over a period of 24 hours.

2.7.5.3 PLASTIC EMBEDDING

The plastic resin used to embed tissues is composed of two solutions which are mixed at the time of embedding. The protocol is depicted below:

Solution A:	hydroxyethyl methacrylate (Sigma)	90 ml
	butoxyethanol (Sigma)	10 ml
	polyethylene glycol 400 (Sigma)	2 ml
	benzoyl peroxide (Sigma)	1.5g

Solution B: dimethyl aniline (Sigma)

One drop of dimethyl aniline was added to 10 ml of solution A in a glass beaker and then quickly poured over tissues placed in the moulds (Agar Scientific, Stansted). Stubs (Agar Scientific, Stansted) are then carefully lowered into the rapidly polymerising solution and left to set for 12 hours or more. The hardness of the resin is dependent on the concentration of Polyethylene glycol and butoxy ethanol. Softer blocks may also be obtained by adding two drops of dimethyl aniline.

2.7.5.4 CUTTING PLASTIC EMBEDDED TISSUES

Sections were cut at Birmingham City Hospital using a Reichert-Jung Ultramicrotome, enabling sections as thin as 500 nm to be cut. Glass knives were made using a Reichert-Jung Histoknife maker. Freshly cut sections were 'floated' in a cold water bath, transferred to clean microscope slides (Blue Star, Warley) and air dried.

2.7.5.5 STAINING SECTIONS

The freshly prepared plastic sections were stained with Haematoxylin and Eosin (H&E). Using a Pasteur pipette, Ehrlich's aqueous Haematoxylin

(Sigma) was dropped onto the slides and left for 45 minutes. Excess Haematoxylin was removed using a Pasteur pipette and the sections were 'blued' with cold tap water, again dispensed from a pipette. The slides were then air-dried and counter stained with 1% eosin (Sigma) for 15 minutes. Finally, the slides were washed carefully with tap water and air-dried.

2.8 SURGICAL PROCEDURES

Blood samples were withdrawn from the hepatic portal vein, tail vein and cardiac sites of microsphere dosed animals. In other experiments artificial gut loops were isolated, by ligation, and exposed to known concentrations of particles or metabolic inhibitor in order to study the mechanics of particle translocation.

2.8.1 SYSTEMIC BLOOD SAMPLING TECHNIQUES

Blood was sampled from dosed animals at either tail vein or cardiac sites. In order to collect tail vein blood, the very tip of the rats tail was sliced off using a razor blade. Blood was then 'milked' into heparinised eppendorf tubes by gently squeezing from the top of the tail to the site of haemorrhage. Heart blood was sampled using a 25 G hypodermic needle (Becton Dickinson, Dublin) and syringe. The animals were terminally anaesthetised whilst this technique was performed.

2.8.2 PORTAL BLOOD COLLECTION

In order to sample blood from the hepatic portal vein, animals were anaesthetised on a warm table and the peritoneal cavity exposed (laprotomised). After location of the hepatic portal vein (see figure 4), blood was slowly removed using a 26 G hypodermic needle (Becton Dickinson, Dublin) and 2.5 ml syringe. Usually it was possible to re enter the vein, if it had not collapsed, to take a second 2.5 ml blood sample. After sampling the hepatic portal vein, blood could also be withdrawn from the heart by cardiac puncture. Then, whilst still anaesthetised, the animal was sacrificed by cervical dislocation.

2.8.3 PREPARATION OF ISOLATED SMALL INTESTINAL LOOPS

Starved rats were terminally anaesthetised (see section 2.2) on a warm table and laprotomised in order to expose the intestines. The duodenum or ileum regions of the GIT were then identified. Ileal gut loops were characterised by their close proximity to the large intestine and the presence of two or more PPs. Using a piece of string 7 cm in length, the segment of GIT to be ligated was marked. At the distal end of the marked 7 cm section Braided silk suture (Ethicon, U.K) was tied around the gut, such that the intestinal lumen became tightly constricted. Constriction of the surrounding mesentery was avoided if at all possible. The suture was closed tightly, but not to the extent of causing obvious injury to the tissue. The proximal end of the 7 cm segment was ligated in a similar way, but the suture was not tightened at all. At all points between the sutures, innervation, afferent and efferent mesenteric blood and lymphatic vessels remained intact. At a point about 2 cm proximal to the isolated segment, a small incision was made into the intestine. Through this cut a small bore plastic tube was inserted into the intestinal lumen such that one end was inside the isolated gut section. The other end of the tube was connected to a 1.0 ml syringe outside the body cavity of the anaesthetised animal. The proximal suture was closed tightly around the plastic tube and intestine, forming a tight seal. Microspheres and drugs could then be administered into the isolated gut segment, *via* the plastic tube. After administration of the particles into the gut the tube was slowly withdrawn such that the seal around it was maintained and no particles could escape. After removal of the plastic tube, the sutures were knotted tightly and the microsphere containing gut loop was lightly massaged to evenly distribute the particles. The GIT was then placed back into the peritoneal cavity, which was closed using Michel clips (Germany). Tail vein blood samples were withdrawn from the anaesthetised animal at intervals up to 2 hours.

3.0 EFFECT OF VARIABLES ON THE ORAL UPTAKE OF COLLOIDAL PARTICLES FROM THE GASTROINTESTINAL TRACT

3.1 INTRODUCTION

The observation that microspheres can rapidly transfer from the GIT lumen to the general circulation after oral delivery (Alpar *et al.*, 1989, Lewis *et al.*, 1992, Volkheimer, 1993) was re-examined in a series of preliminary experiments. Quantification of the extent of microsphere transfer from the GIT lumen to the vascular compartment was achieved by simply looking at blood samples, from treated animals, under the microscope to visualise the particles. No attempt was made to quantify the extent of microsphere accumulation in tissues such as liver, spleen or gut, although samples were removed for histological studies, the results of which are discussed in a later chapter. In addition to confirming earlier reports concerning the time course of particle transfer from the GIT lumen to circulation after oral administration, the influence of other variables on circulating microsphere numbers such as the tonicity of the suspending vehicle, suspending vehicle volume and microsphere dose were investigated.

In these pilot studies fluorescent carboxylated polystyrene microspheres, of about 0.87 μm diameter were used as a model for other colloidal particles with the potential for drug delivery. The size and chemical nature of these latex particles reflected several important factors regarding their usefulness as a test particle for potential drug delivery systems. Firstly, 0.87 μm diameter particles were used, despite studies by Jani *et al.*, (1990) which demonstrated that the optimal size for microsphere translocation was below this, as this is comparable with the size of drug loaded microspheres produced in other studies at Aston University and elsewhere. Also, individual microspheres of this size are easily discernible in blood or thin sections using light microscopy. Secondly, polystyrene is both non-biodegradable and non-immunogenic and has been used for a wide range of biomedical applications (Arshady, 1993). This aids quantification of microsphere uptake, as polystyrene microspheres persist in tissues and body fluids in which biodegradable microspheres would normally be degraded. The low immunogenicity of latex avoids the complication of enhanced microsphere uptake and accumulation by lymphoid cells and tissues. Carboxylated (negatively charged) polystyrene latex microspheres were used in these studies because particles of this chemical nature were

employed in earlier investigations into the oral uptake of colloids (Alpar *et al* ., 1989).

3.2 MATERIALS AND METHODS

3.2.1 INFLUENCE OF CARRIER MEDIUM TONICITY ON CIRCULATING FLUORESCENT MICROSPHERE NUMBERS AFTER ORAL ADMINISTRATION

Carboxylated fluorescent polystyrene latex microspheres ($0.87 \pm 0.006 \mu\text{m}$ diameter) were administered orally to male Wistar rats in conjunction with either isotonic, hypotonic or hypertonic carrier mediums, in order to assess if the tonicity of the colloidal suspension has any influence on particle uptake. In each case 0.1 ml of stock particles (equivalent to 6.91×10^9 microspheres or 2.5 mg latex) were mixed with 0.4 ml of carrier medium and administered to starved male wistar rats (200 - 300 g) using a gavage needle. All stock microsphere aliquots were extensively washed, to remove surfactant residues, as described in section 2.3. Hypotonic and isotonic solutions comprised of distilled water and 0.9 % w/v sodium chloride solution (Sterile Supply Unit, Wolverhampton) respectively. The hypertonic carrier medium was a 2M Na Cl solution. There were 3 rats in each test group. At various times after dosing (5, 15, 45, 120, 240 minutes) tail vein blood samples were taken and the number of particles in the circulation determined using a Neubaur counting chamber and Zeiss universal microscope fitted with an IV FI epi-fluorescence condenser (section 2.7.1). Two hundred and fifty minutes after dosing, a cardiac puncture was performed under anaesthetic, and the animals were subsequently sacrificed. The GIT, liver, spleen and lungs were then removed from animal carcasses for histological examination (see section 2.7.5).

3.2.2 INFLUENCE OF CARRIER MEDIUM VOLUME ON CIRCULATING FLUORESCENT MICROSPHERE NUMBERS AFTER ORAL ADMINISTRATION

To each of 3 male Wistar strain rats (200 - 300 g) was orally administered 2.5 mg stock (6.91×10^9) carboxylated fluorescent polystyrene latex particles of $0.87 \pm 0.006 \mu\text{m}$ diameter, re-suspended in either 0.1, 0.3, or 0.5 ml of water. All rats were starved overnight prior to oral administration

of the latex beads. After gavage, tail vein samples were obtained at 5, 15, 45, 120 and 240 minutes. Two hundred and fifty minutes after gavage the animals were anaesthetised and a cardiac puncture sample was taken. The rats were then killed by cervical dislocation and the guts, livers and spleens were removed for histological examination (see section 2.7.5). Particle and erythrocyte counts were then performed on samples diluted with heparinised glycerol using a Neubaur counting chamber and fluorescence microscope, as described in section 2.7.1.

3.2.3 INFLUENCE OF THE ADMINISTERED PARTICLE CONCENTRATION ON THE TRANSLOCATION OF PARTICLES FROM THE GIT TO THE BLOOD

To each of 3 male Wistar strain rats was orally administered either 2.5, 7.5 or 12.5 mg of stock $0.87 \pm 0.006 \mu\text{m}$ diameter carboxylated fluorescent polystyrene latex microspheres suspended in water such that the final volume given in each case was equal to 0.5 ml (i.e. 0.3 ml stock particles + 0.2 ml water or 0.5 ml stock particles + 0 ml water). This resulted in doses of 6.91×10^9 , 2.07×10^{10} , and 3.45×10^{10} microspheres. Tail vein samples were obtained at 5, 15, 45, 120 and 240 minutes after dosing. Two hundred and fifty minutes after dosing the animals were anaesthetised and a cardiac puncture sample was withdrawn. The rats were then killed by cervical dislocation. Particle and erythrocyte counts were then performed on samples diluted with heparinised glycerol using a Neubaur counting chamber and fluorescence microscope (section 2.7.1). Tissues were removed from the dead rodents for histological examination (section 2.7.5).

3.3 RESULTS

3.3.1 INFLUENCE OF CARRIER MEDIUM TONICITY ON CIRCULATING FLUORESCENT MICROSPHERE NUMBERS AFTER ORAL ADMINISTRATION

After gavaging 6.91×10^9 carboxylated fluorescent polystyrene microspheres (diameter $0.87 \mu\text{m}$), particles were identified in tail vein blood samples taken from 5 minutes post dosing. The particles were highly distinctive when viewed under the microscope with a fluorescent light source. Their spatial distribution within the haemocytometer was irregular, with the majority of spheres closely associated with what appeared to be

phagocytic cells (see figure 64). The highest microsphere to erythrocyte ratios were observed in blood removed at the 5 and 15 minute time points from rodents gavaged with hypotonic microsphere suspensions. 5 minutes after gavage, circulating levels of microspheres in rats which received particles suspended in water are significantly higher than in the hypertonic ($P \leq 0.005$) or isotonic ($P \leq 0.025$) test groups when compared using a one tailed student t test for unrelated samples with 4 degrees of freedom. At the 15 minute time point the levels of significance are even higher ($P \leq 0.0005$ when hypotonic and isotonic sample groups are compared with the student t test).

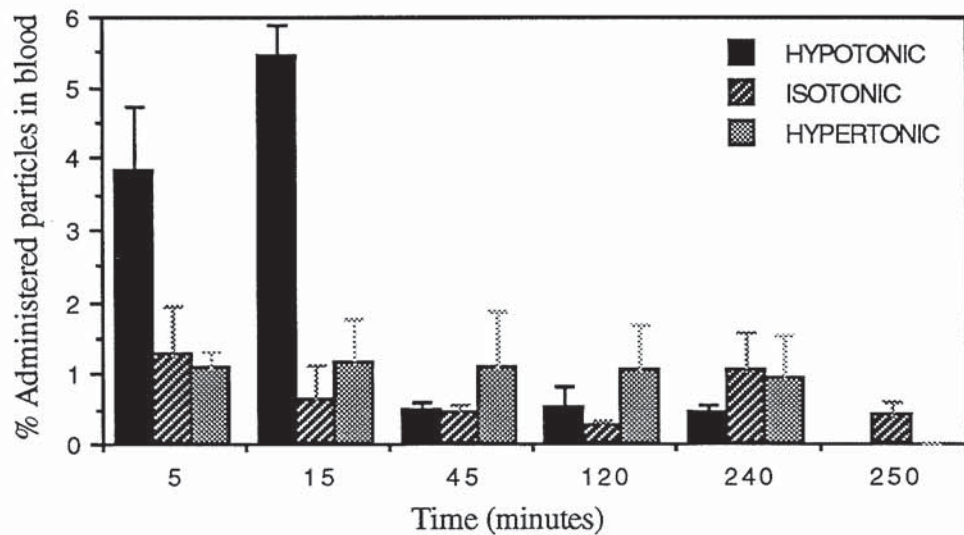


Figure 16. The mean percentage (\pm standard deviation) of an initial dose of 2.5 mg latex (in the form of 6.9×10^9 0.87 μm diameter Fluoresbrite™ carboxylate microspheres) in the blood at various times after gavage. Microspheres were administered in conjunction with either water, 0.9 % w/v Na Cl or 2M Na Cl (n=3).

3.3.2 INFLUENCE OF CARRIER MEDIUM VOLUME ON CIRCULATING FLUORESCENT MICROSPHERE NUMBERS AFTER ORAL ADMINISTRATION

0.87 μm latex microspheres were detected in the systemic circulation 5 minutes after oral administration in different volumes of water (figure 17). The greatest numbers of circulating microspheres were detected within the first 15 minutes of the experiment in animals who had received ~2.5 mg

latex suspended in a total volume of 0.5 ml of water. This is significant to the ($P \leq 0.0005$) level when comparing the 0.5 and 0.3 ml volume groups at the 15 minute time point.

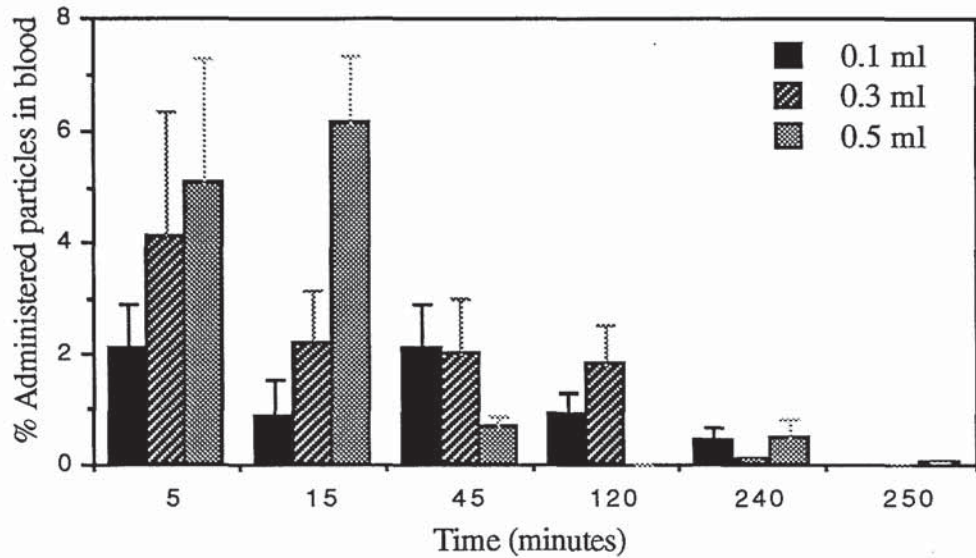


Figure 17. The percentage (mean values \pm standard deviation) of an orally administered dose of 2.5 mg latex (in the form of 6.91×10^9 $0.87 \mu\text{m}$ Fluoresbrite™ carboxylate microspheres) that was present within the vascular compartment at various times after dosing. Microspheres were suspended in either 0.1, 0.3 or 0.5 ml of water prior to administration ($n=3$).

3.3.3 INFLUENCE OF THE ADMINISTERED PARTICLE CONCENTRATION ON THE TRANSLOCATION OF FLUORESCENT MICROSPHERES FROM THE GIT TO BLOOD.

After oral administration of microsphere suspensions containing different concentrations of $0.87 \mu\text{m}$ diameter Fluoresbrite™ particles, blood samples taken from test animals were found to contain fluorescent microparticles. The circulatory profiles appear to show evidence of a relationship between particle dose and subsequent translocation, although significance tests do not support this statement. The uptake profiles from this data are depicted below, both in terms of efficiency of translocation (figure 18) and actual circulating microsphere numbers after oral administration (figure 19).

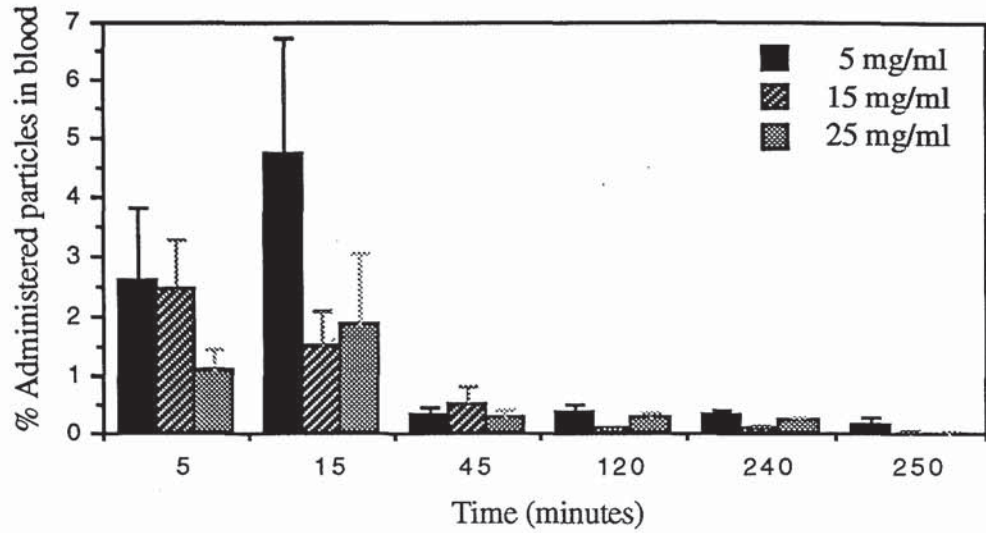


Figure 18. The percentage of 0.87 μm latex microspheres dosed (mean values \pm standard deviation) in the vascular compartment after oral administration over a range of particle concentrations from 1.4×10^{10} to 7.0×10^{10} spheres / ml ($n=3$).

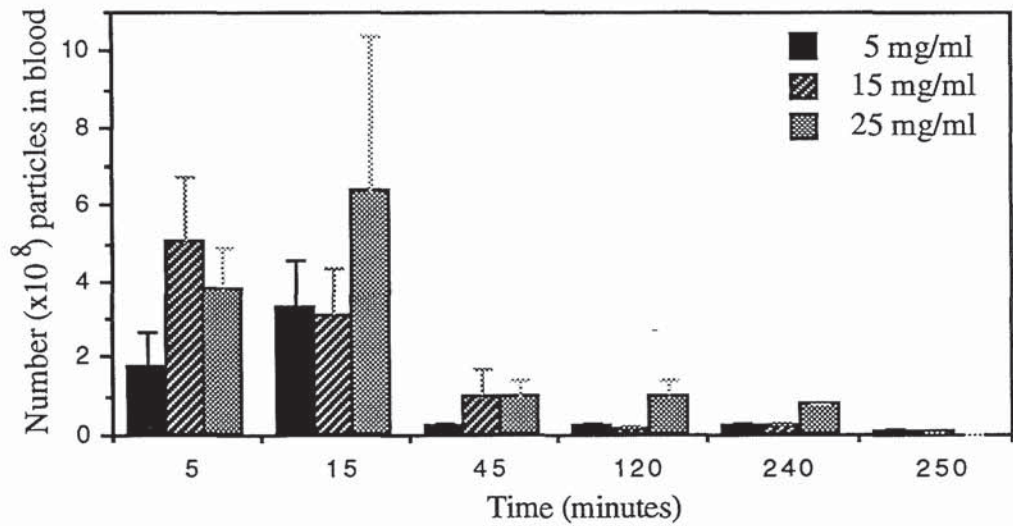


Figure 19. The mean number ($\times 10^8$) of 0.87 μm fluorescent carboxylated polystyrene microspheres in the vascular compartment (\pm standard deviation) after oral gavage using a range of microsphere concentrations, from 1.4×10^{10} (equivalent to 5.0 mg / ml) to 7.0×10^{10} microspheres / ml (equivalent to 25 mg / ml) ($n=3$).

3.4 DISCUSSION

Transfer of labelled particulate matter from GIT lumen to the general circulation in the rat model, occurred almost instantaneously after oral administration of Fluoresbrite™ carboxylate polystyrene latex microspheres of $0.87 \pm 0.006 \mu\text{m}$ in diameter (see figures 16-19). The observed rapidity of test particle translocation shows some similarities with the rate of uptake reported by other workers, both at Aston University and elsewhere. In a pilot study Alpar *et al.*, (1989) detected large numbers (~24 %) of an oral dose of 2.05×10^9 Fluoresbrite™ carboxylate ($1.10 \mu\text{m}$ diameter) polystyrene microspheres within the blood of rats, 10 minutes after oral administration. Lewis *et al.*, (1992) also found high levels ($15.0 \pm 3.7 \%$) of circulating albumin microspheres ($3.1 \pm 1.7 \mu\text{m}$ diameter) as quickly as 5 minutes after gavage (see section 1.2.6.2). In both these studies, microsphere numbers were expressed relative to erythrocyte counts in a semi-quantitative manner. In German studies, oral administration of corn - starch (200 g) to humans resulted in particles appearing within venous blood samples withdrawn from subjects in the first minute of the experiment. Particle numbers peaked after 10 minutes, with a second absorptive peak between 90 and 120 minutes after oral dosing (Volkheimer, 1975). Such findings contradict the majority of reported experimental evidence and scientific opinion. The general consensus is that particulate matter of this nature can only enter the vascular compartment several hours or days after oral administration, if at all (O'Hagan, 1990). LeFevre *et al.*, (1980) failed to confirm previous reports that very large ingested particles (5.7 or $15.8 \mu\text{m}$ diameter) appeared in the blood within 20, 60 or 240 minutes of gavage (although very low numbers of the $5.7 \mu\text{m}$ particle were seen in some blood samples). Semiquantitative analysis of rat tissues after a single oral dose of fluorescent latex microspheres, indicate that 12 to 18 hours are required for particles with diameters of $1.0 \mu\text{m}$ to reach the liver, although no samples were examined before 6 hours (Jani *et al.*, 1992b).

As well as particle size, chemical composition is thought to be an important discriminating factor relating to intestinal uptake. Negatively charged latex microspheres (such as those employed in this experimental section) of 0.1 and $1.1 \mu\text{m}$ diameter were found to be taken up in far lower numbers compared with non-ionic latex beads, after chronic administration over 10 days. Difficulty in distinguishing the Rhodamine fluorescence of the carboxylated particles from the autofluorescence of some of the body tissue

components such as erythrocytes was said to have complicated interpretation of experimental preparations (Jani *et al.*, 1989). However, depleted numbers of absorbed carboxylated compared with neutral microspheres may be related to the fact that the GIT itself has an overall negative charge and as such may be repulsive to anionic entities (Ohyashiki, *et al.*, 1989, Florence *et al.*, 1994). On the other hand, it is possible that negatively charged microsphere species may suffer less mucus associated aggregation, and thus remain as individual particles in the GIT due to electrostatic repulsion. This may aid uptake. Also, the more highly charged a particle is, the greater the extent of opsonisation in the GIT lumen. Opsonised material may have a higher potential for absorption than unopsonised elements (Jani, 1991).

In the opinion of Kreuter (1991), the rapid appearance of microspheres within the circulation as reported by Alpar *et al.*, (1989) and Lewis *et al.*, (1992) could only be accounted for by a paracellular mechanism of absorption (section 1.2.3). The rapid uptake obtained in this study, may be the result of paracellular absorption, although Jenkins *et al.*, (1994) found that particulate absorption is more rapid and complex than assumed previously (see section 1.2.6.1). They detected latex beads in draining mesenteric lymph 5 minutes after administration. Such rapid entry of microspheres into the lymphatic system might conceivably result in transfer of some of the particles into the blood by mechanisms discussed earlier (sections 1.2.6.1 and 1.2.6.2). Nevertheless, in order for large numbers microspheres to reach the general circulation within 5 minutes of oral dosing it seems likely that they must have first directly penetrated the intestinal microcirculation. This hypothesis is supported by the data of Kararli (1989) who showed that the rate of lymph flow is relatively slow (2 ml / minute) whereas the (intestinal) blood flow is about 2000 ml / minute.

The influence of carrier medium tonicity on the circulatory profile of carboxylated latex microspheres after oral administration is shown in figure 16. If isotonic or hypertonic solutions were used to suspend the particles prior to dosing, then low but detectable numbers of fluorescent microspheres were seen within tail vein blood samples taken from 5 minutes after gavage. Administration of particles in conjunction with hypertonic solutions resulted in a reasonably consistent, elevated, level of microspheres within the blood over the 4 hour experimental period. The same is virtually true for isotonic carrier media, although small peaks and troughs in the

estimated blood microsphere level can be seen over the 4 hours. In both cases the percentage of the total number of microspheres given to the animals that could be detected in the blood was substantially lower than that of previous publications from this laboratory (Alpar *et al.*, 1989 and Lewis *et al.*, 1992). Possible explanations for such a discrepancy are discussed in the ensuing text.

Initially, considerable numbers of carboxylated latex particles were detected within the vascular compartment after oral administration of microspheres suspended in 0.4 ml a hypotonic carrier solution (figure 16). At the early time points, blood microsphere levels were significantly ($P \leq 0.025$) higher than those resulting from the other two treatments, suggesting that the tonicity of the carrier medium has an important influence on particle uptake or translocation, at least in the short term.

The sudden introduction of a relatively large volume of hypotonic solution into the duodenum may affect gut physiology in several ways which could impact on microsphere transportation across the intestinal mucosa. Water can move towards both the mucosal and serosal side of the small and large intestines in response to osmotic gradients, until such time that the osmotic pressure of the intestinal contents equals that of the plasma. During net fluid absorption (the mechanics of fluid absorption across the epithelial barrier are described in section 1.1.2.1.3) the epithelial intercellular space is widened to as much as 3 μm between cells lining the upper third to half of the villi (DiBona *et al.*, 1974), although tight junctional integrity is still maintained. The importance, if any, that this intercellular distension and water inflow has on particle transfer is unclear. It may serve to promote entry of absorbed particles into the lamina propria through the basement membrane as extracellular fluid volume increases as a function of water absorption. The blood flow to the small intestine is known to increase substantially after a meal and the same is true after administration of hypotonic solutions, particularly if (as in the case of these studies) the experimental subject has fasted prior to the experiment. If so, this could influence particle dissemination from intestinal sites. Intestinal capillary surface area and / or permeability is thought to increase as a response to removing an absorbed volume from the interstitium (Granger, 1981). This too may be an important influencing factor. In studies by Lewis *et al.*, (1992) Fluoresbrite™ carboxylate particles were found to be taken up more rapidly when suspended in water rather than in an emulsion, consisting of

arachis oil, water, Span 83 and Tween 80 (8:8:1:1 v/v). It was suggested that 'water overload' might increase the number of gaps between epithelial lymphatic cells (Barrowman, 1978). Certainly intestinal and thoracic duct lymph flow increases dramatically (up to 10 fold) to remove absorbed volume from the mucosal interstitium (Granger, 1981). An increase in gastric motility after 'water overload' was also highlighted as a possible influencing factor.

Only speculative suggestions can be put forward to address the reasons why 'water overload' would induce the observed increase in circulating microsphere numbers after oral delivery as seen in this study. However, induction of net luminal to mucosal fluid transfer must in some way increase the GIT's permeability to particle entry, into either the mucosa itself or intestinal vasculature. The time course of particle translocation from the GIT lumen strongly indicates that a proportion of microspheres are capable of rapid penetration of the intestinal mucosa after oral administration, possibly *via* a mechanism similar to that described as persorption (see section 1.2.3).

Hypertonic stimuli were seen to induce a fairly consistent elevation in the level of circulating microspheres over the last three hours of the four hour experimental period when compared to the other treatments (figure 16). This suggests that conditions of hyperosmolarity as well as hyposmolarity may affect intestinal function regarding microsphere translocation. In experiments to investigate enterocyte permeability to proteins such as insulin, hypertonic solutions have been shown to reversibly dilate junctional pathways resulting in increased absorption of the hormone (Madara *et al.*, 1987, Wheeler *et al.*, 1978 and Fitzgerald *et al.*, 1968). The large size of microspheres, in comparison with macromolecules such as insulin, may still preclude them from being absorbed *via* the paracellular route even under conditions of reduced barrier function. However, in addition to a reversal of net fluid absorption seen under hypotonic conditions, hypertonic solutions may place a 'physiological stress' or even temporarily damage the intestinal mucosa, which could manifest itself in elevated levels of particle translocation. This may be one reason for the consistently, although insignificantly, high circulating levels of microspheres throughout the four hours of the experiment, in comparison to the other two treatments.

In its protective role, mucus prevents particle contact with the GIT epithelial layer (section 1.2.1). It may also cause particle aggregation and its influence on microsphere behaviour within the lumen is likely to be a substantial one. Mucus viscosity, and thus its fluid rejecting properties, is highly influenced by the surrounding ionic environment and the presence of surfactants (Alpar *et al.*, 1989). Reductions in mucus viscosity result in increased uptake of high molecular weight proteins and particles into the GIT mucosa (Hemmings, 1980). Hypertonic solutions decrease mucus viscosity and as such, are likely to increase particle presentation to the GIT epithelia. Hypotonicity results in decreased mucus permeability, due to a decrease in counterions to shield negatively charged glycoprotein residues in the mucin network (Gu *et al.*, 1988), thus encouraging mucus-microsphere aggregation. In our studies, experimental evidence for this exists in the form of a statistically insignificant elevation in the number of microspheres within the tail vein blood collected, from the three rats dosed with hypertonic microspheres suspensions, at most of the later time points compared with the hypotonic and isotonic treatments (figure 16). The observed increase in particle numbers, at 45 and 120 minutes after dosing time points, could be indicative of a reduction in the fluid rejecting properties of the mucus layer after extended exposure to the 2M Na Cl solution. It is difficult to define the numerous potential effects of the mucus barrier on microsphere transfer from the GIT lumen to extra-intestinal sites. However, it is likely to be a major factor influencing microsphere exclusion from the GIT mucosa.

In order to compare the relative quantities of latex microspheres absorbed in the different experiments, some pharmacokinetic parameters were calculated. In doing so it is important to bear in mind that in this case such a pharmacokinetic assessment may be of limited usefulness due to lack of confidence in the accuracy of blood levels measured and the lack of any corresponding i.v. data to enable calculation of elimination constants. The extent to which blood sampling at single time points is representative of the true latex plasma profile is also questionable. However, by estimating the area under the blood level curve (AUC) it is possible to gain some idea of the total amount of latex absorbed over the four hour time course in the different experiments. For hypotonic and hypertonic solutions the total area under the blood level curves were found to be approximately equivalent (0.1157 and 0.1015 mg latex hours respectively) with isotonic carrier media resulting in lower number of particles circulating throughout the four hour

time course (0.0701 mg latex hours). Such a finding supports the idea that hypertonic solutions may increase intestinal permeability, for the reasons discussed above, and the concept of 'water overload' under conditions of hypotonicity. Examination of the microsphere uptake verses time profiles reveals that for hypotonic and isotonic dosing regimes the shape is very roughly first order in nature and as such can be tentatively assigned an absorption rate constant (K_a). Zero order absorption is characterised by a constant rate of absorption which is essentially independent of the amount absorbed. K_a was calculated using the method of residuals described in Rowland *et al.*, (1989) and Appendix I. K_a was found to be maximal for hypotonic treatments ($K_a = 0.198 \text{ min}^{-1}$) compared with isotonic ($K_a = 0.07 \text{ min}^{-1}$). Semilogarithmic plots of the data obtained after hypertonic treatments strongly suggested that absorption in this case was not a first order process and as such could not be assigned a rate constant.

The volume of water used to suspend the microspheres prior to oral administration was found to influence microsphere uptake into the vascular compartment (figure 17). Suspension of particles in relatively large volumes of carrier media resulted in a higher percentage of the gavaged particles appearing in the blood at early time points after dosing, compared with lesser volumes of liquid. An estimated 4.5 % of the administered dose of microspheres was detected in tail vein blood from rats given the largest volumes of liquid (0.5 ml water), at 5 minutes after dosing. This compares with an mean uptake of around 2 % for identical rodents gavaged with particles suspended in just 0.1 ml of water, at the same time point. The rate of microsphere absorption was also found to be influenced by the administered particle volume. K_a was estimated at 0.198 min^{-1} for the 0.5 ml dosing regime and 0.154 min^{-1} for the 0.1 ml treatment. The possible influence of osmotic stimuli on particle uptake across the GIT mucosa has been discussed in the previous section of text. The hypothetical effects of microsphere gavage in conjunction with large volumes of hypotonic liquid compared with smaller volumes may be three fold: Firstly, a large volume of microspheres or food bolus in the intestinal lumen causes considerable distension of the gut, which was visible to the naked eye in freshly sacrificed animals. Although the gut is designed for such occurrences, it undoubtedly increases the mucosal surface area available for particle contact / uptake. Stretching of the intestinal wall also stimulates the myenteric reflex (peristaltic waves) and a general increase in intestinal motility. This may be important because in some studies, an increase in intestinal motility

has been shown to enhance particle uptake (Volkheimer *et al.*, 1968, Volkheimer, 1977); Secondly, the sheer physical pressure imposed by a large volume of colloidal particles within the GIT lumen pressing against the epithelial cell barrier, may serve to force particulate matter through zones of enterocyte extrusion, if they are present, and through the basement membrane and into the lamina propria (see section 1.2.3.1). This effect may also serve to force particulate matter into close physical proximity to other sites of particle uptake such as isolated lymphoid follicles or PPs (see sections 1.2.2, 1.2.4 and 1.2.5); Thirdly, enhanced translocation of particles after oral administration of microspheres in conjunction with large volumes of liquid, may result from reduced small intestinal transit times. If so, the time taken for gavaged particles to reach the lower small intestine, and thus the abundant lymphoid follicles therein, will be reduced. This may be an important factor, as PPs and isolated lymphoid follicles have been identified as an important portal for particle entry into the lymphatic system (section 1.2.4). It is debatable if microsphere uptake into the lymph would result in a rapid transfer of large numbers of microspheres into the blood, five or ten minutes after dosing. Experiments by Jani *et al.*, (1992b) indicated that much longer lengths of time were required for lymphatically absorbed microspheres to reach the blood. On the other hand, the rapidity of lymphatic uptake observed by Jenkins *et al.*, (1994) suggest insorption by this route may result in microspheres appearing within the blood stream after relatively short periods of time (~90 minutes). As such, it seems feasible that microspheres from this route of uptake could appear within the blood stream over a very short time scale. Interestingly, calculation of the area under the blood microsphere concentration curve suggests that the volume of water used to suspend the microspheres in before gavage has little difference on the overall quantity of latex absorbed over the four hours. AUC for the animals receiving 0.5 ml volumes of particles = 0.107 mg latex hours. For animals receiving 0.1 ml total volume this figure is 0.122 mg latex hours. However, as mentioned previously, special care must be taken when interpreting these parameters.

Administration of a range of microsphere numbers within a set volume of hypotonic carrier medium appeared to influence the concentration of particles observed in venous blood (figures 18 and 19). At the 5 and 15 minute time points, the highest percentage transfer of administered particles was recorded after gavage of the lowest concentrations of colloid. If the same data is represented in terms of actual microsphere numbers within the

rat vascular compartment at any given time point (figure 19) it seems that the greatest numbers of particles are circulating after oral delivery of the highest relative concentrations. Thus it would appear that an inverse relationship between microsphere concentration and efficiency of transfer may exist at very early time points after dosing. This statistically insignificant trend may give some insight into the actual mechanisms by which particles leave the gut lumen and appear in the general circulation. Over the four hour experimental period, AUC is highest for the rats which received 25 mg / ml latex (0.255 mg latex hours) compared with 0.093 mg latex hours for the 5.0 mg / ml test animals.

If hypothetical, and as yet un-characterised, sites at which particles may penetrate the intestinal barrier into the blood stream are finite in number then considerable competition for each channel may exist. Certainly, K_a values for 25 mg / ml and 5.0 mg / ml treated animals are not dissimilar at 0.276 min^{-1} and 0.221 min^{-1} respectively. If this conceptual model did represent the true situation in the GIT mucosa, then it could account for the observed pattern of microsphere circulation seen in figures 18 and 19. Such a model might also go some way towards explaining the discrepancies between this and earlier studies in which a much higher percentage of particles were seen to be circulating within the vascular compartment shortly after oral delivery (Alpar *et al.*, 1989). This is because in the present study a much larger number of particles (at least 6.91×10^9) were delivered in a maximum volume of 0.5 ml of water. In the previous publication, only 2.05×10^9 microspheres were administered in a 1 ml volume of water. This represents a considerably lower concentration of particles and as such would be expected to demonstrate a higher efficiency of absorption. Smaller volumes were used to suspend the microspheres in the present study. This may also be a factor. However, as in all these preliminary investigations, extreme caution must be taken before formulation of any elaborate conclusions about the nature of this complicated and highly variable phenomenon. Some insight into the mechanisms behind the oral uptake of microspheres is gained by simple examination of blood samples as shown, but the multitude of other variables must not be ignored. Extensive accumulation of particulate matter within hepatic tissue (see section 1.2.6.2) would occur if particles enter the portal vascular compartment. Results from histological examination of liver tissue removed from orally dosed animals (see chapter 5) demonstrates this. The influence of the liver and other MPS compartments on the circulating profile of microsphere particles after oral

administration can not be ignored and it is probable that this factor is responsible for the low numbers of spheres in tail vein blood sampled at the later time points (120 and 240 minutes after dosing).

The simplistic methodology by which the numbers of microspheres were quantified within the blood in this experimental section was found to have several inherent flaws, although overall it gave useful insight into the nature of microsphere translocation from the GIT. The main problem was the huge number of erythrocytes that had to be counted in each blood sample, in order to determine the number of red cells associated with 200 microspheres. This often meant that tens of thousands of erythrocytes had to be counted. In many cases this was not possible, and erythrocyte / microsphere ratios were estimated from smaller population samples which is obviously less satisfactory. One of the other problems arising when counting the Fluoresbrite™ microspheres within diluted blood samples was their distribution relative to erythrocytes. The particles were rarely evenly distributed across the field of view, enabling an accurate determination of microsphere / erythrocyte ratios. More often than not, the fluorescent spheres were intimately associated with large leukocyte cells, presumably phagocytes. In many cases, very large numbers (>35) of FITC labelled beads appeared to be internalised within these cells (see chapter 5). This is an important observation, because internalisation of microspheres within phagocytic cells may result in extended circulatory half lives, due to decreased recognition of the particles within MPS tissues (see section 1.2.6.2). Latex remains unaffected by the normal microbiocidal action of phagocytes, and as such, may persist within these cells until such time that the cell dies or releases the test particle. However, although this observation was obviously an important one in terms of understanding the nature of particulate translocation the un-even spatial distribution of microspheres relative to erythrocytes may skew subsequent estimations of particle numbers within the rat blood compartment.

Having ascertained microsphere to erythrocyte ratios using a haemocytometer, the theoretical number of particles within the entire rat blood system was calculated (see section 2.5.1). The total volume of blood (in ml) in a rat was estimated as a function of body weight ($= 0.0733 \times$ body weight in grams) (Archer, 1965). Normal rat blood has a red cell count of 5.25×10^9 erythrocytes / ml. As the number of erythrocytes associated with 200 microspheres was known, then the number of particles

in each ml of blood, and thus in the whole animal could be calculated. Although this simple equation allowed estimation of particle uptake after examination of dilute blood samples of unknown volume or dilution, the technique probably resulted in an over estimation of the true extent of particle transfer to the vascular compartment after oral delivery. Erythrocyte lysis, during sampling, and afterwards during dilution in heparinised glycerol, is probably the main reason for this. Repeated haemorrhage may also reduce an animal's erythrocyte count. If erythrocyte numbers in the diluted tail vein blood samples are low then un-representative microsphere to erythrocyte ratios will result in high estimations of the efficiency of microsphere translocation. Other discrepancies may also result from inaccurate calculation of the total erythrocyte population in each rat using the method described above. In assuming that an animal's total erythrocyte count is directly related to body weight, one must also recognise that such a value is highly susceptible to biological variation.

Tail vein blood samples of a few hundred μl represent a small fraction of the whole volume of blood in an experimental animal. Haemocytometer erythrocyte and microsphere counts of diluted aliquots from tail vein blood represent a very small sample from the whole population even though very large numbers of aliquots had to be screened in order to obtain a representative mean value. It would have been preferable to have a system in which much larger volumes of blood (2.5 ml+) could be directly analysed for polystyrene microspheres. It is for these reasons, amongst others, that emphasis quickly moved on to the development of other experimental procedures that enabled the accurate detection of microspheres in blood and other animal tissues such as liver, spleen and gut (chapter 4).

Despite the quantification problems encountered during this experimental section, at least similar results were obtained from experiment to experiment where the same dosage formulation was used (compare hypotonic and 5.0 mg / ml results in figures 16 and 18). This observation suggests that although inadequacies exist, this simplistic method of quantification is at least qualitatively if not quantitatively reliable. The findings of this section of experimental work were utilised in these later studies: Oral administration of micro / nanosphere particle suspensions was performed in conjunction with large volumes of hypotonic carrier solution, in order to achieve quantifiable uptake of the particles across the GIT mucosa into the blood and other tissues of test animals.

4.0 KINETIC ASPECTS OF PARTICLE TRANSLOCATION FROM THE GASTROINTESTINAL TRACT

4.1 INTRODUCTION

Having ascertained that under certain conditions microspheres leave the GIT lumen to appear in the vascular compartment of test animals, the extent to which these particles partitioned between this and other body compartments required quantification. Elucidation of the pattern of microsphere traffic between different organs at known times after oral dosing would give valuable insight into the mechanisms behind the observations reported in chapter 3. The feasibility of systemic therapy by oral delivery of drug loaded particles could also be evaluated. A prerequisite in the realisation of such aims was the development of a system for sensitive, accurate and reliable determination of microsphere numbers in biological samples.

Initially, polystyrene microspheres were radiolabelled with ^{125}I in order to monitor their uptake into extra-intestinal sites. However, the stability of the radioisotope-polymer complex was found to be unsatisfactory, especially for use *in vivo*. Emphasis then turned to adopting the methodology developed by Jani *et al.*, (1990) in which the actual polystyrene content of tissues and fluids could be quantified. This technique was found to have considerable advantages over the previous methodologies employed, and was used extensively in the latter half of the project to examine the uptake and distribution of polystyrene test particles in laboratory rodents after oral administration. In these studies rats were dosed orally with either microsphere or nanosphere test particle suspensions (0.97 μm or 0.22 μm diameter respectively) and the resultant concentration of latex determined in eight body compartments as well as small and large intestinal washes, faeces and urine. Microsphere and nanosphere test particles were also characterised with reference to charge, size and hydrophobicity in order that these factors could be related to uptake or kinetic behaviour.

4.2 MATERIALS AND METHODS

4.2.1 CHARACTERISATION OF POLYSTYRENE TEST PARTICLES

4.2.1.1 HYDROPHOBIC INTERACTION CHROMATOGRAPHY (HIC)

HIC analysis of 0.22 μm and 0.97 μm diameter Polybead® microspheres was performed (see section 2.5 for an explanation of HIC). 1.1 μm carboxylated polystyrene latex microspheres were also assayed by HIC, although these particular particles were never used in animal studies.

Four different stationary phases, of different hydrophobicities, were used: Sepharose 4B (Sigma 4B-200), Propyl-agarose (Sigma P-5268), Pentyl-agarose (Sigma P-5393) and Hexyl-agarose (Sigma H-1882). These different stationary phases were washed several times in double distilled water to remove any traces of preservative and then resuspended in 0.6 M NaCl at a pH of 7.4 (adjusted with dilute NaOH). This produced a thick slurry of approximately 70% sepharose / agarose. The stationary phase slurries were then degassed for 15 minutes prior to column packing. Column packing involved layering each stationary phase on top of a glass wool plug inside a glass Pasteur pipette to a height of 30 mm (approximately 1 ml packed gel volume). The columns were then washed with 10 ml of 0.6 M NaCl, pH 7.4, to keep the gels hydrated and to expose the hydrophobic surface. A suspension of sample microspheres was made in 0.6 M NaCl (pH 7.4) and adjusted to an OD of 0.5, at a wavelength of 600 nm using a Phillips UV/Vis Spectrometer PU 8700). 1 ml volumes of this microsphere suspension were loaded onto a set of columns (three replicates *per* gel type), followed by 2 x 1 ml of 0.6M NaCl (pH 7.4) and 2 x 1 ml of 0.1 % Triton X-100. Each 1 ml eluent fraction was collected in a plastic 1 ml cuvette. The OD of each fraction at 600 nm was determined by spectrometry and compared to the OD of the original 1 ml microsphere suspension.

4.2.1.2 ZETA POTENTIAL

The Zeta potential of 0.22 and 0.97 μm diameter Polybeads® was determined by suspending the particles in 10 mM phosphate / citrate buffer of pH 7.07 and injecting the suspension into a Malvern Zetamaster (Malvern

Instruments, U.K). 1.1 μm carboxylated microspheres were also analysed although these particles were never used in animal studies.

4.2.1.3 ELECTRON MICROSCOPY

0.22 μm and 0.97 μm diameter Polybeads were visualised using a scanning electron microscope (see section 2.4.3). Photomicrographs were taken of the particles.

4.2.2 GPC DETERMINED UPTAKE AND DISTRIBUTION OF POLYSTYRENE TEST PARTICLES

4.2.2.1 CALIBRATION OF GPC SYSTEM

EasiCal (Polymer Laboratories Ltd, Shropshire UK 2010-0501) inert PTFE strips coated with polystyrene (~5 mg) were immersed in 50 ml of THF to give a polystyrene concentration of 0.010 % w / v. The kit contained two types of strips (A and B) each representing Mw values of 640, 9375, 66000, 321000, 3066000 and 3250, 28720, 158180, 1028500, 8520000 respectively. After immersion of the strips in THF for at least 30 minutes, 100 μl aliquots were injected into the GPC system to elucidate the retention time for each Mw value (see section 2.7.4.2) Each sample was injected 4 times.

4.2.2.2 DETERMINATION OF MICROSPHERE MOLECULAR WEIGHT AVERAGES

Microsphere molecular weight averages were determined by freeze drying 90 μg of the test particle and dissolving it in 3 ml of THF prior to GPC analysis. The resulting chromatograms were then digitised and the molecular weight averages were calculated using the equations shown in section 2.7.4. The experiment was repeated three times.

4.2.2.3 CALIBRATION AND SENSITIVITY STUDIES

Various concentrations of microspheres were added to either blood (1g), Liver (1g) or dissolved in THF. This enabled calibration for experiments in which organs which had an unknown polystyrene content were to be assayed. It also quantified the efficiency with which polystyrene was

removed from animal tissues using the extraction protocol. 1.02, 4.08, 7.10, 10.20, 13.26 or 16.32 μg of polystyrene microspheres in suspension were treated using one of the following protocols:

- (1) Injected into 1g of liver at the bottom of a conical flask using a syringe and hypodermic needle.
- (2) Mixed with 1g of blood contained within a conical flask.
- (3) Placed at the bottom of a glass test tube.

'Spiked' blood and liver samples were then processed for GPC examination in exactly the same way as 'unknown' tissue samples (see section 2.7.4.3). Microspheres treated according to protocol 3 were simply freeze dried prior to dissolution in 1 ml of THF for GPC analysis. This latter treatment provided a value for 100% efficiency of the tissue extraction process.

4.2.2.4 TISSUE DISTRIBUTION OF 0.22 μm NANOSPHERES AFTER A SINGLE ORAL DOSE

21.7 mg of 220 nm diameter polystyrene microspheres (Park Scientific, Northampton UK 07304) were washed in distilled water inside an eppendorf tube, ultra-centrifuged (MSE, Micro Centaur) and re suspended in 1 ml of distilled water ready for dosing.

All animals used were young male Wistar strain rats (body weights 200 - 250g). Animals were starved overnight before dosing. This involved placing the rats on a grid so that their faeces were not eaten whilst the animals food sources were removed. During this period of starvation, animals were allowed access to a plentiful supply of water. Food was restored 4 hours after oral dosing procedures. Oral administration of the particles was performed using a syringe and gavage needle (stomach tube), a tried and tested method of oral delivery. At selected time points after dosing (15 mins, 45 mins, 240 mins, 24 hours and 4 days) animals were weighed, anaesthetised and a cardiac puncture blood sample removed, usually 2.5 - 7.0 ml of blood. After haemorrhage, whilst still anaesthetised, rats were sacrificed by cervical dislocation. Blood samples were placed in a pre weighed conical flask, weighed and assayed using GPC. Specific organs (liver, spleen, kidney and lung) were then carefully removed from

the animal carcass, placed into pre weighed conical flasks, weighed and then prepared for GPC analysis. Four rats were used for each time point.. A plentiful supply of water was available at all times.

In a second, identical, group of rats (n=4) samples of portal blood were removed, in preference to cardiac punctures, for examination using GPC (see section 2.8.2). In this way a comparison between microsphere numbers in the systemic vascular compartment and the afferent liver supply could be made. These animals were dosed following the same regime as in the previous section of text. 10 minutes before blood sampling, animals were anaesthetised on a warm table and the peritoneal cavity exposed. After location of the hepatic portal vein, blood was slowly removed at the appropriate time point (15 mins, 45 mins, 240 mins, 24 hours and 4 days) using a 25 G hypodermic needle and 2.5 ml syringe. Usually it was possible to re enter the vein, if it had not collapsed, to take a second 2.5 ml blood sample. Then, whilst still anaesthetised, the animal was sacrificed by cervical dislocation. Internal organs and other samples for polystyrene analysis were removed, as before, but following a specific protocol to exclude the risk of contamination. Again, the spleen, liver, lung and kidneys were removed, in that order, and along with the blood sample were placed into separate pre weighed conical flasks, weighed and then treated for polystyrene extraction and GPC analysis. Next, the mesenteric lymph node and surrounding lymphatic and connective tissue was carefully removed from the intact small intestines and was processed for GPC. Small (5 cm) sections of small intestine were then removed and their luminal contents harvested using copious amounts of isotonic saline dispensed from a syringe and gavage needle. This enabled the saline to be forced through into one end of the gut and expelled from the other. Following thorough washing the sections of gut were dissected longitudinally, placed in a small beaker and washed again in an attempt to remove all but the most stubborn microspheres. The two samples, gut wash and gut tissue, were then treated for GPC analysis. The large intestine and its contents were also washed and treated accordingly.

Four animals were used for each time point as before and were treated identically except the one and four day groups who were placed in metabolic cages in order to collect their faeces and urine from the time of dosing. These animals were starved for about 12 hours prior to sacrifice in order to remove the majority of food from the intestines.

4.2.2.5 TISSUE DISTRIBUTION OF 1.0 µm MICROSPHERES AFTER A SINGLE ORAL DOSE

21.7 mg of 0.97 µm diameter polystyrene microspheres (Park Scientific, Northampton UK 07304) were washed in distilled water inside an epindorf tube, ultra-centrifuged (MSE, Micro Centaur) and re suspended in 1 ml of distilled water ready for dosing.

Starved rats were orally dosed as before (section 4.2.2.4). In this case, portal and cardiac blood samples were removed from the same animal (see sections 2.8.1 and 2.8.2). Blood and tissue samples were collected from treated rodents at the same time points: 15 mins, 45 mins, 240 mins, 24 hours and 4 days after gavage. Intestinal tissue and gut wash samples were taken from each animal as before. Four rats were sacrificed at each of the five time points.

4.2.3 PREPARATION AND CHARACTERISATION OF ¹²⁵I LABELLED MICROSPHERES

Polybead[®] microparticles (2.5% solids-latex) (Polysciences, Inc., Northampton, U.K) with a mean batch diameter of 0.82 ± 0.010 µm were radiolabelled using the rationale described in section 2.7.3. The radioactive particle slurry was extensively dialysed for 14 days, during which time the dialysis water was changed up to 20 times a day. Aliquots of dialysate were taken daily for analysis using a LKB WALLAC (Stockholm) 1282 Compugamma universal gamma counter. 14 days after iodination, the activity of dialysate had reached background, the dialysis bag was cut open and the microspheres were collected in a measuring cylinder. 21 ml of particles were collected in total, with a recorded activity of 0.614 MBq *per* ml (determined using the gamma counter). Thus the efficiency of iodination was about 13.5 %.

By comparing the pellet sizes of the original stock solution of microspheres with that of the freshly iodinated particles, after centrifugation, it was found that there were about 1.42×10^{11} radioactive microspheres *per* ml. The iodinated particles were divided into 1 ml aliquots and stored in epindorf tubes at 5 °C. The stability of the radioactive microsphere complex was examined by estimating the amount of free ¹²⁵I associated with the particles. Four 200 µl aliquots of radioactive latex microspheres were dispensed into

separate eppendorf tubes, into each was added 1000 µl of distilled water. The diluted microspheres were WhirliMixed™ (Fisons) for 30 seconds and left for 24 hours. Next day, microsphere aliquots were again WhirliMixed™ (Fisons) for 30 seconds immediately before determination of their radioactivity using a LKB WALLAC (Stockholm) 1282 Compugamma universal gamma counter. The four eppendorf were then centrifuged (MSE, Micro Centaur) for 5 minutes and three 300 µl aliquots of supernatant taken from each tube and counted separately in the universal gamma counter. Any activity in the supernatant samples was thought to represent free ¹²⁵I and was recorded as so. Stored microsphere samples were periodically checked in this way for evidence of un-bound ¹²⁵I.

4.2.4 ORGAN DISTRIBUTION OF RADIOLABELLED 0.82 µm MICROSPHERES IN THE RAT MODEL

Radiolabelled microspheres were prepared as described in sections 2.7.3 and 4.2.3. Rats were divided into groups of 4. Each rat received a dose of 5.67×10^{10} radiolabelled microspheres suspended in 0.4 ml water. The activity of each dose was metered using the Compugamma universal gamma counter. At sampling time points, rats were anaesthetised and a 2 ml cardiac puncture blood sample was taken before sacrifice by cervical dislocation. Samples of blood, liver, spleen, mesentery, mesenteric lymph node, kidney, thyroid and lung were then taken and placed into pre-weighed plastic tubes for analysis using the Compugamma universal gamma counter. The mass of each sample was accurately recorded. The Compugamma universal gamma counter software allowed background activity to be automatically subtracted from each reading. Four animals were sacrificed at each of the following sample times after dosing: 5, 15, 45, 120, 240, 360 minutes and 24 hours.

4.2.5 FLOW CYTOMETRIC ANALYSIS OF BLOOD FROM ANIMALS ORALLY DOSED WITH 0.87 μm CARBOXYLATED MICROSPHERES

Fluoresbrite™ carboxylate polystyrene microspheres (Polysciences, Northampton) with a mean diameter of 0.87 μm were orally administered to four male Wistar rats of 200 g body weight. Each animal received 4.40×10^9 particles (64 μl of stock) in a 1 ml volume of distilled water. A fifth identical rat received 1 ml of distilled water orally as a control. Tail vein samples were taken from all animals at 15, 45, 240 minutes and 24 hours after administration. Blood was 'dripped' directly into eppendorf tubes containing 400 μl of heparinised saline (1000 units / ml) (CP Pharmaceuticals, Wrexham). All the heparinised tubes were carefully weighed before the experiment in order that the exact mass of blood from each tail bleed could be calculated. Having calculated the mass of blood in each tube, it was possible to work out the volume using the specific gravity of rat whole blood. The specific gravity of rat whole blood is 1.056 (Dittmer, 1961). This procedure allowed a known volume of blood to be withdrawn from the animal without clotting. One sample of control blood was 'spiked' with 6.875×10^8 microspheres (10 μl stock) in order to determine assay efficiency. Diluted blood samples were stored in eppendorf tubes at 5°C prior to FACS analysis the following day at Birmingham University Medical School. The exact volume of diluted blood that was FACSed from each sample eppendorf was recorded (usually 10-90 μl). The dead volume of each sample trapped within the FACS plumbing was also accounted for. The FACS machine was extensively purged between each sample. Calibration samples of stock 0.87 μm particles diluted in distilled water were periodically run to identify and correct for signal drift and variations in the fluidics. All samples were vortexed prior to cell sorting.

4.3 RESULTS

4.3.1 CHARACTERISATION OF POLYSTYRENE TEST PARTICLES

4.3.1.1 HYDROPHOBIC INTERACTION CHROMATOGRAPHY (HIC)

The results from HIC analysis of Polybead[®] and Fluoresbrite[™] microsphere systems is represented in figures 20, 21 and 22 below.

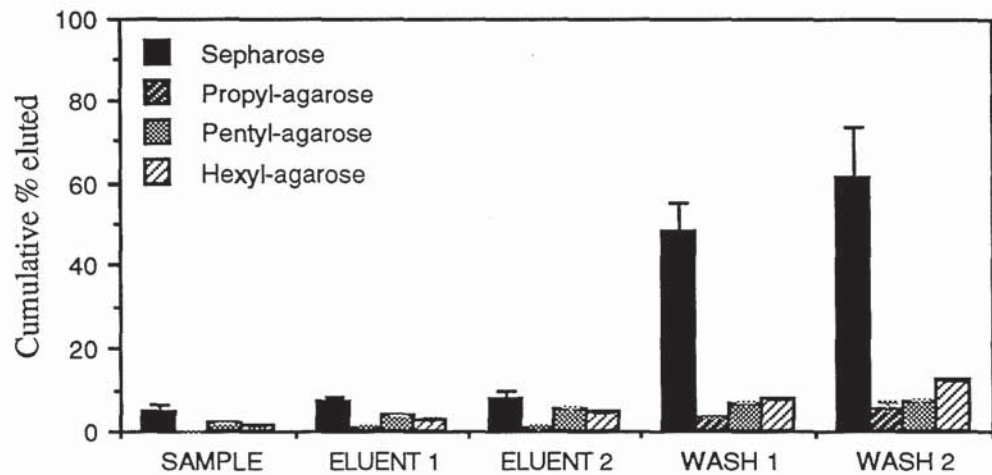


Figure 20. Mean cumulative % eluted (\pm standard deviation) after HIC analysis of 0.22 μm diameter latex Polybeads[®] (n=3).

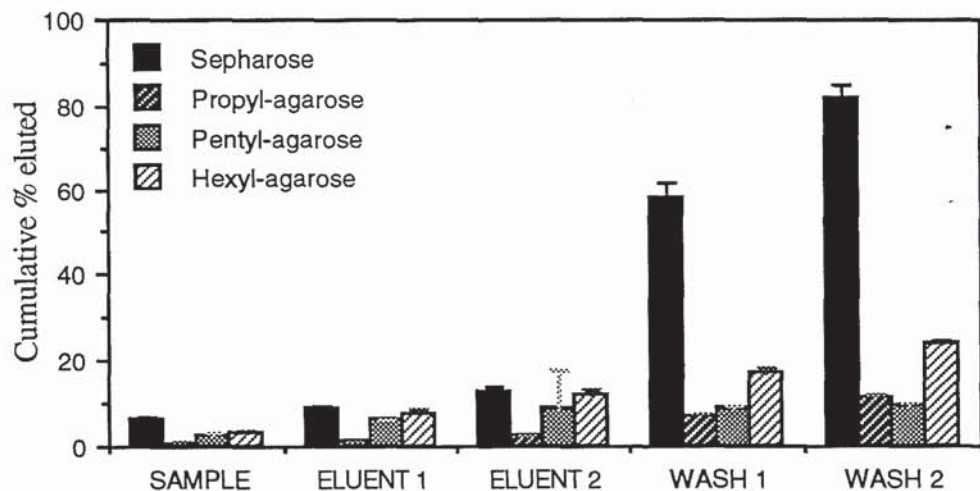


Figure 21. Mean cumulative % eluted (\pm standard deviation) after HIC analysis of 0.97 μm diameter latex Polybeads[®] (n=3).

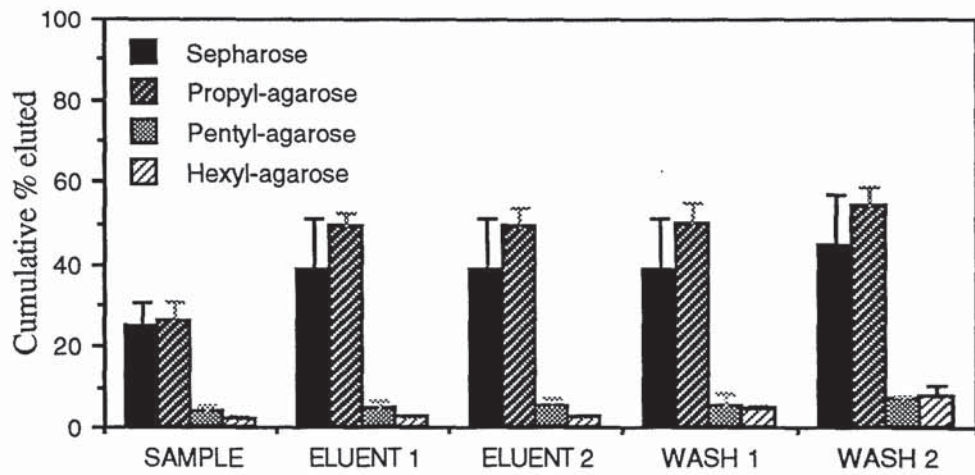


Figure 22. Mean cumulative % eluted (\pm standard deviation) after HIC analysis of 1.10 μm diameter carboxylated latex microspheres (n=3).

4.3.1.2 ZETA POTENTIAL

Microsphere type	Zeta potential	Standard deviation
Polybead 0.22 μm	-51.0 mV	0.9 mV
Polybead 1.0 μm	-52.5 mV	1.2 mV
Carboxyl 1.1 μm	-48.0 mV	1.6 mV

Table 2. Zeta potentials of latex microspheres suspended in 10 mM phos/citrate buffer pH 7.07 (n=5).

4.3.1.3 ELECTRON MICROSCOPY

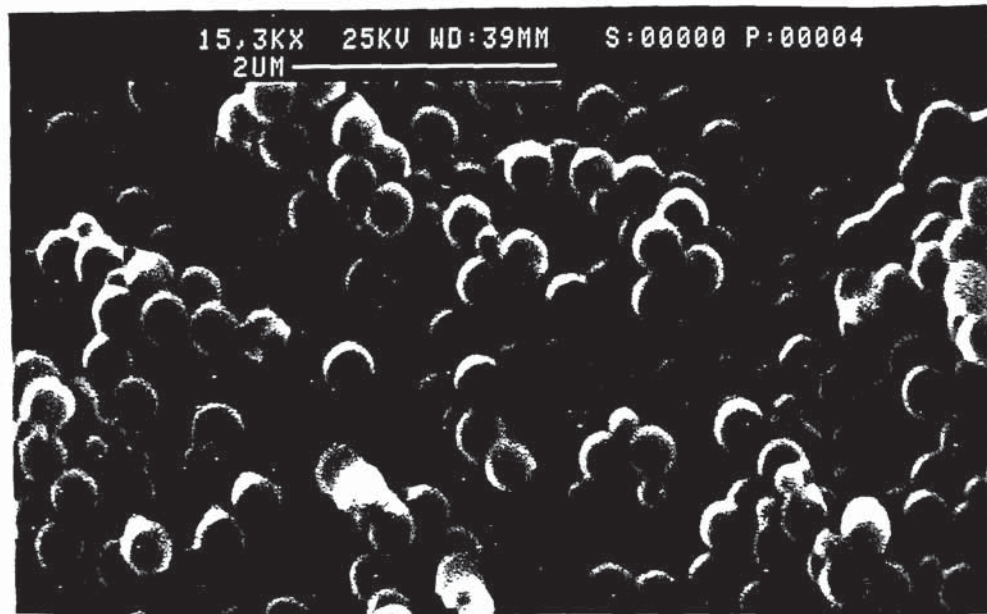


Figure 23. Scanning electron photomicrograph of 0.22 μm Polystyrene microspheres.

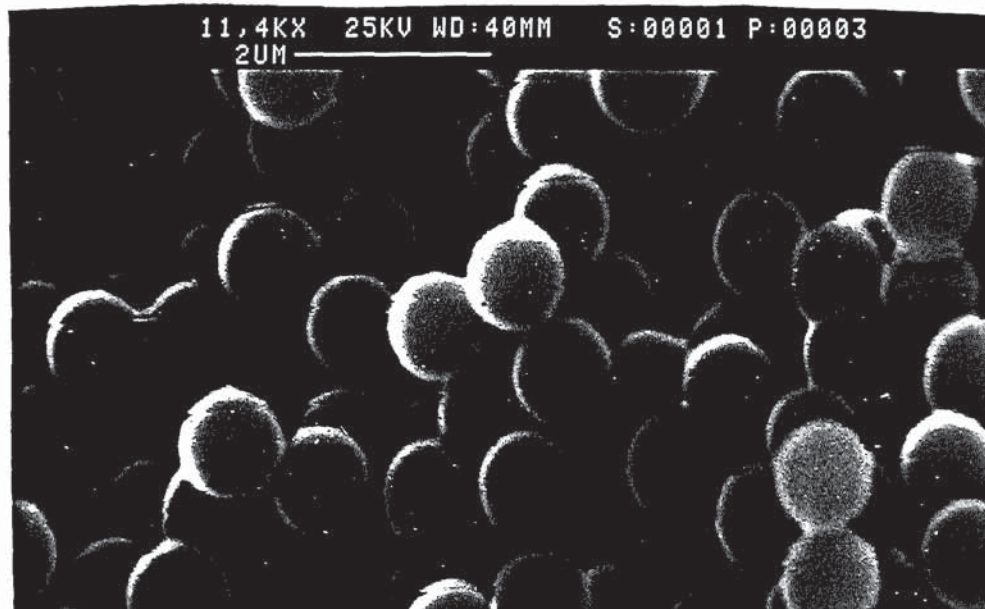


Figure 24. Scanning electron photomicrograph of 0.97 μm Polystyrene microspheres.

4.3.2 GPC DETERMINED UPTAKE AND DISTRIBUTION OF POLYSTYRENE TEST PARTICLES

4.3.2.1 CALIBRATION OF GPC SYSTEM

Injection of four 100 μl aliquots of two narrow MWD standards resulted in chromatograms with a series of sharp peaks, each representing a known molecular weight fraction of polystyrene (figure 25). This enabled calibration of the GPC system with regards to molecular weight (table 3 and figure 26).

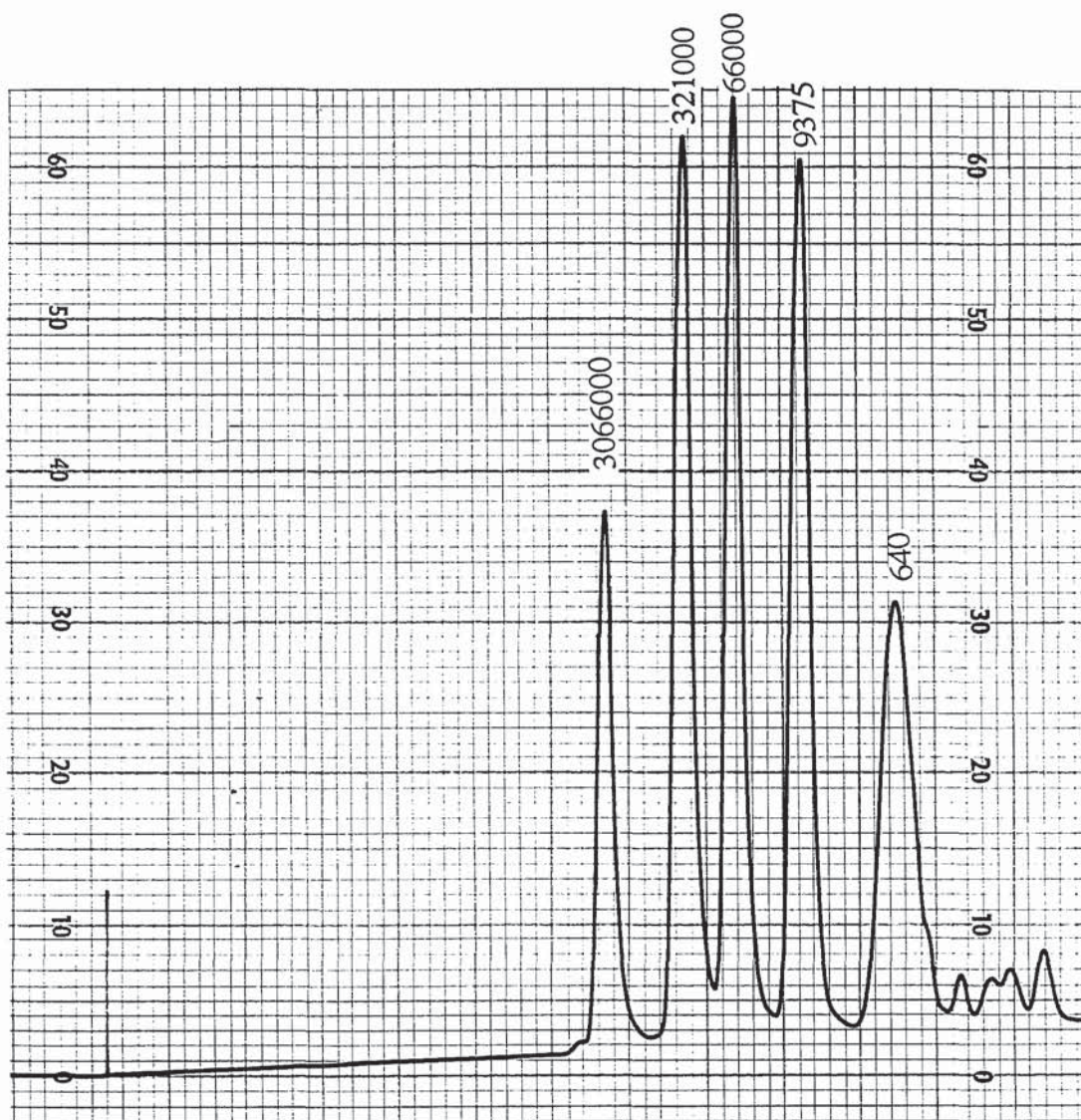


Figure 25. GPC chromatogram produced after injection of EasiCal© polymer calibration mixture 1-5. Peaks represent Mw values of 640, 9375, 66000, 321000 and 3066000.

M _w	Retention time (min)	Standard deviation
8520000	12.31	0.035
3066000	13.19	0.020
1028500	14.21	0.012
321000	15.23	0.016
158180	15.89	0.020
66000	16.54	0.030
28720	17.40	0.012
9375	18.37	0.025
3275	19.41	0.009
640	21.07	0.047

Table 3. Peak retention times of monodisperse polystyrene standards of known molecular weight (EasiCal©) (n=4).

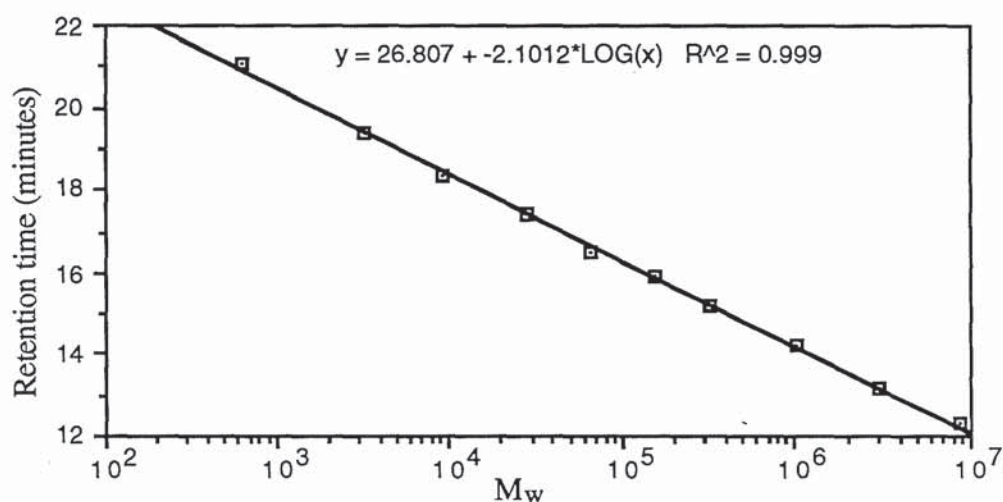


Figure 26. Semi logarithmic plot showing the relationship between molecular weight and retention time of the molecular weight standards after GPC analysis.

4.3.2.2 DETERMINATION OF MICROSPHERE MOLECULAR WEIGHT AVERAGES

GPC analysis of the polystyrene microspheres produced chromatograms (figures 27 and 28) that were digitised (see table 4) in order to calculate the molecular weight averages M_n and M_w .

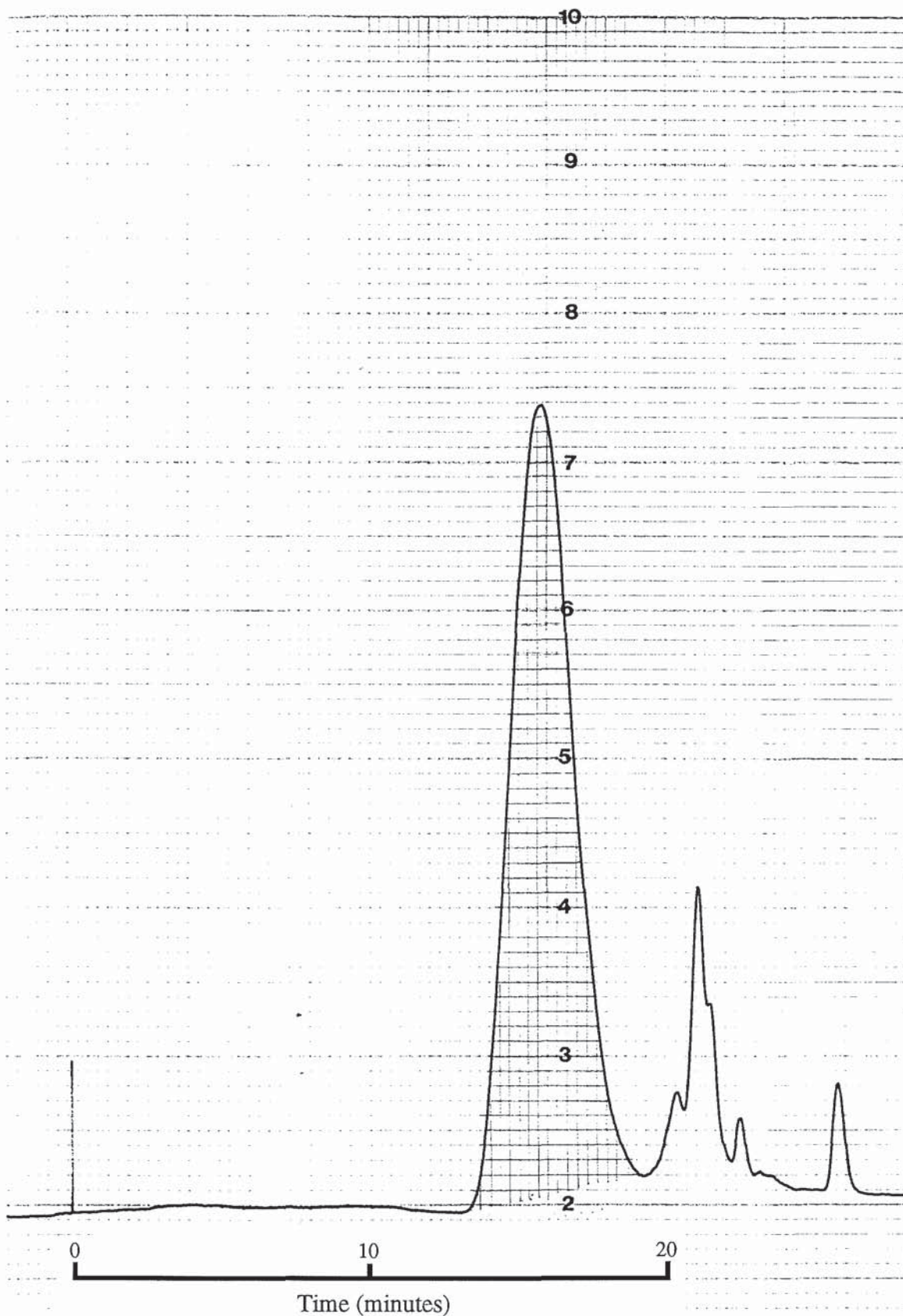


Figure 27. Manually digitised chromatogram produced after GPC analysis of 3 μg of 0.22 μm diameter latex particles in 100 μl of THF.

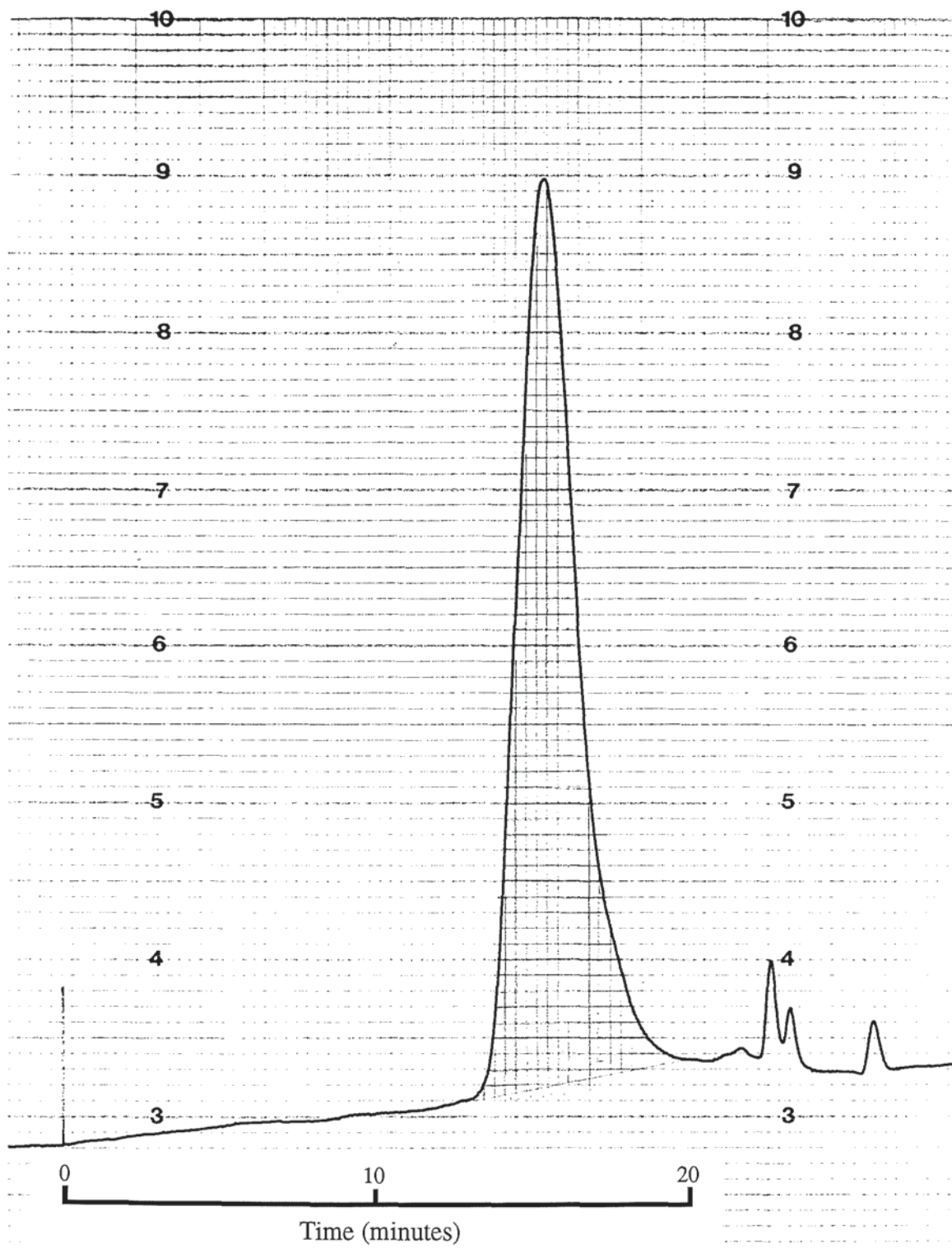


Figure 28. Manually digitised chromatogram produced after GPC analysis of 3 μg of 0.97 μm diameter latex particles in 100 μl of THF.

Calculation of the number-average molecular weight (M_n) is achieved by dividing the total area under the peak, by the sum of the individual digitised areas divided by their corresponding molecular weights.

$$M_n = \frac{\sum h_i}{\sum (h_i / M_i)}$$

Area number	Retention time (min)	Area	M_w
1	13.33	0.5	2593904
2	13.66	2	1806761
3	14.00	9	1244768
4	14.33	21	867032
5	14.66	35	603924
6	15.00	47	416073
7	15.33	58	289812
8	15.66	52	201866
9	16.00	42	139075
10	16.33	29	96872
11	16.66	21	67475
12	17.00	15	46487
13	17.33	11	32380
14	17.66	8	22554
15	18.00	5	15538
16	18.33	3	10823

Table 4. Digitisation of chromatographic data obtained from GPC analysis of 3 μ g of 970 nm latex microspheres.

Thus for 970 nm microspheres:

$$M_n = \frac{360.5}{3.555^{-3}}$$

$$M_n = 101406$$

$$M_w = \frac{\sum (h_i M_i)}{\sum h_i}$$

$$M_w = \frac{115041141}{360.5}$$

$$M_w = 319115.5$$

$$\text{Thus Polydispersity } (M_w/M_n) = 3.1468$$

The mean polydispersity value recorded for the 0.97 μm diameter microspheres after injection of three separate samples was found to be 3.0643 ± 0.0728 . For the smaller 0.22 μm Polybeads[®] polydispersity was calculated to be 2.8795 ± 0.0755 . Comparison of the mean polydispersity values for the 0.97 and 0.22 μm particles using an unpaired student t test suggests that there is a small difference between the two sets of data at the $P \leq 0.10$ level. Therefore, in terms of polydispersity these two batches of microspheres may be regarded as being reasonably similar (see section 2.7.4 for an explanation of polydispersity).

4.3.2.3 CALIBRATION AND SENSITIVITY STUDIES

The detected levels of polystyrene in blood liver and THF spiked with 0.22 μm diameter latex microspheres are shown in figure 29. Recovery and characterisation of polystyrene from tissues spiked with less than 1.0 μg of latex was possible, but highly variable. Hence this figure (1 $\mu\text{g} / \text{g}$) represents the lower limit of sensitivity for the extraction and detection process. The efficiency of polystyrene recovery when tissues were spiked with 10.20 μg latex was estimated to be about 84 % for blood and 79 % for liver. Construction of another calibration curve for the 0.97 μm diameter latex particles was thought to be unnecessary as the polydispersity's of the

Polybeads[®] was found to be so similar. As both sizes of polymeric particle behaved so similarly in organic solvents, we also assumed their percentage recovery from tissues would be of a similar order. Of course, this may not be true *in vivo*, and a good alternative would be to inject particles i.v. prior to GPC analysis of extracted tissues. Construction of a calibration curve along these lines would also take into account the fact that latex extraction from 'spiked' tissues is probably un-representative. The drawback with i.v. administration and subsequent extraction is that it is not clear exactly how much latex will end up in a given organ.

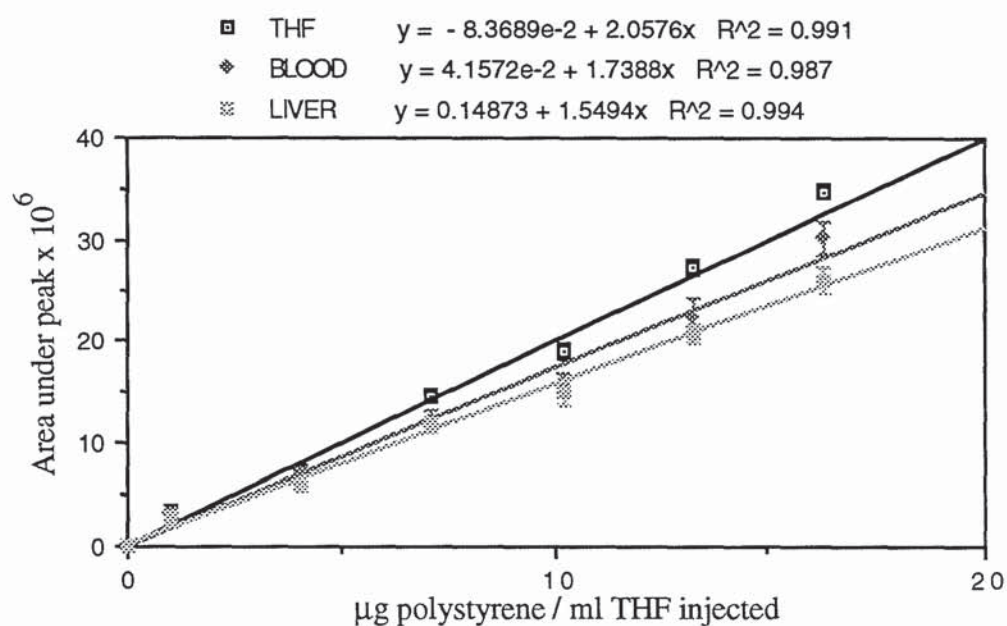


Figure 29. Mean peak integration area (\pm SEM) produced by GPC analysis of 0.22 μm polystyrene latex microsphere spiked samples of blood, liver and THF ($n=7$).

4.3.2.4 TISSUE DISTRIBUTION OF 0.22 μm NANOSPHERES AFTER A SINGLE ORAL DOSE

A typical integrated chromatogram produced by GPC analysis of tissue taken from an animal orally dosed with 0.22 μm latex particles is shown in figure 30. Polystyrene of microsphere origin is represented by a Gaussian peak (retention time \sim 14 minutes) which is eluted shortly before a large peak produced by the action of organic solvents on biological molecules in the sample. Due to size exclusion, the solvent front is eluted last. Figure 31 represents GPC analysis of spleen tissue removed from a control animal which received an oral dose of water and no polystyrene. Quantitation of

the data obtained from nanosphere dosed rats is shown in figures 32 through 39.

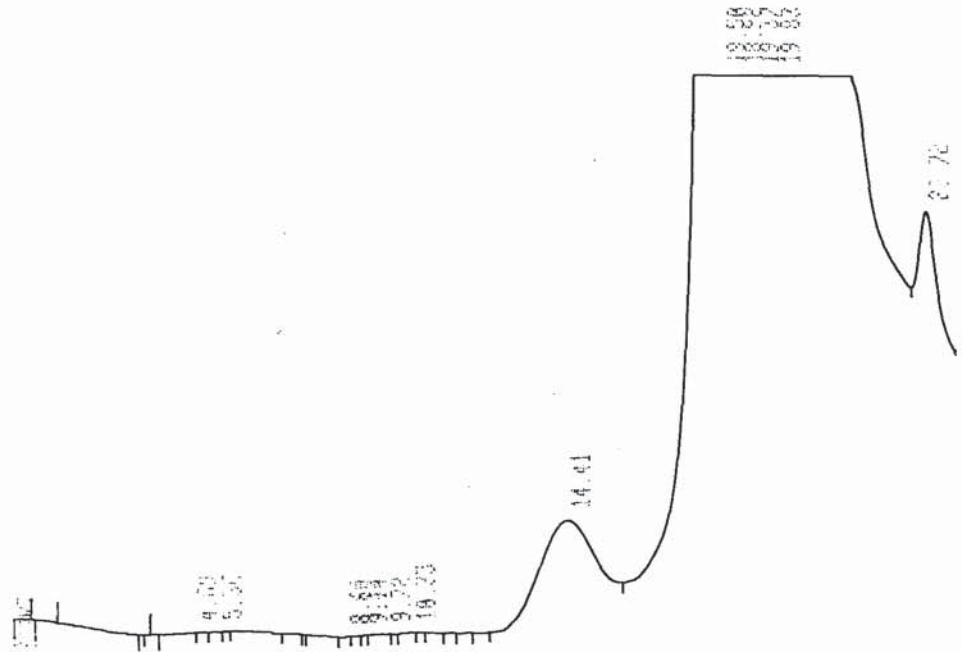


Figure 30. A typical chromatogram produced by GPC analysis of a spleen sample removed from a rat 240 minutes after oral administration of 21.7 mg, 0.22 μm diameter, polystyrene nanospheres.

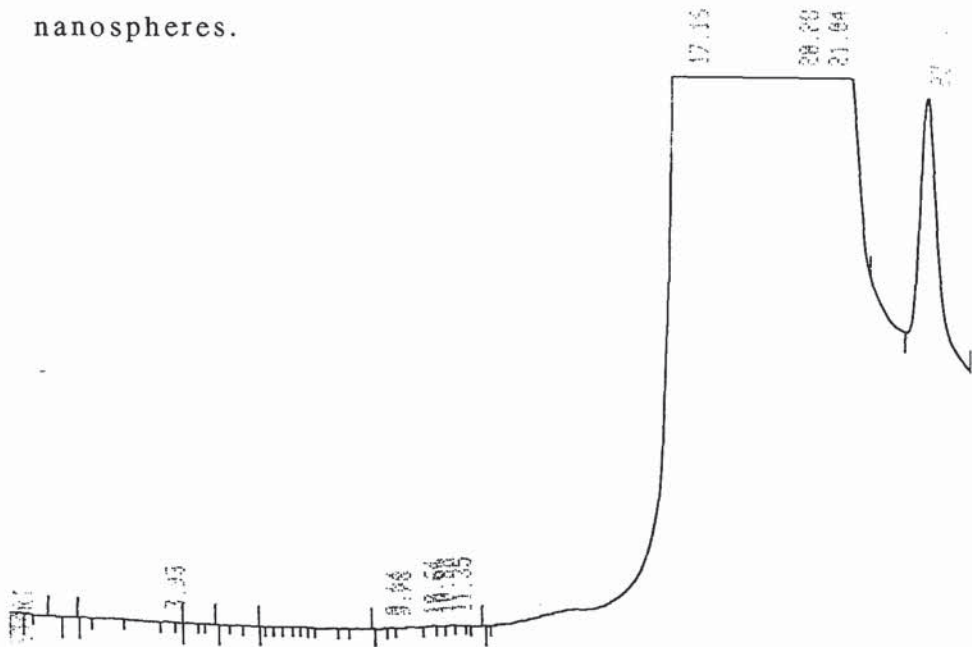


Figure 31. A typical chromatogram produced by GPC analysis of a spleen sample removed from a rat 45 minutes after oral administration of 1 ml of distilled water.

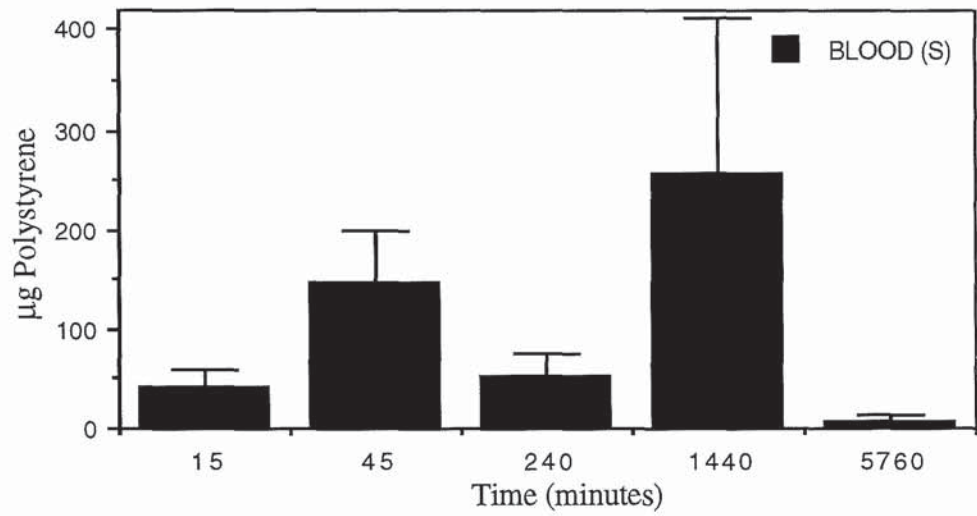


Figure 32. Mean (\pm SEM) mass of latex nanospheres within the entire systemic vascular compartment of rats after oral administration of 21.7 mg 0.22 μm diameter polystyrene nanospheres (n=4).

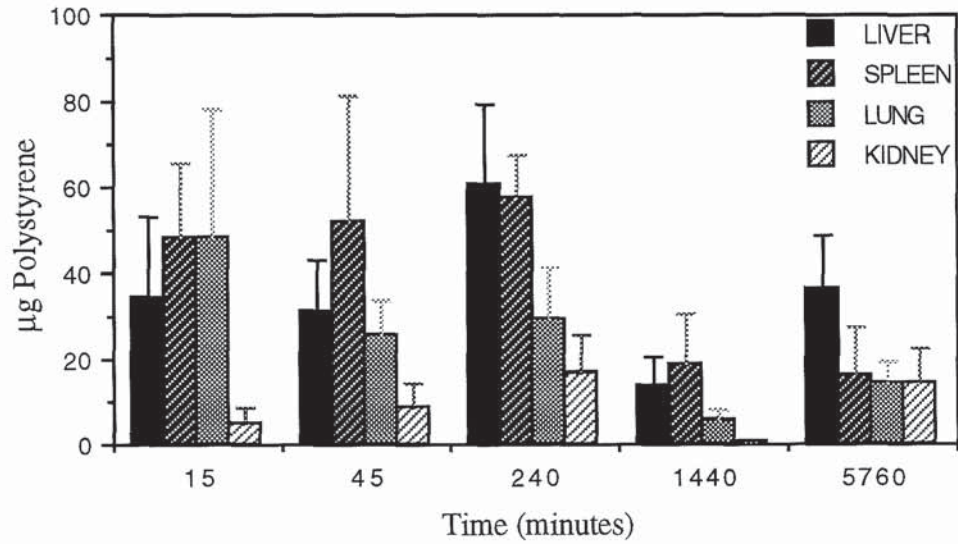


Figure 33. Whole organ accumulation of polystyrene (\pm SEM) after oral administration of 21.7 mg polystyrene nanospheres (diameter 0.22 μm) (n=8).

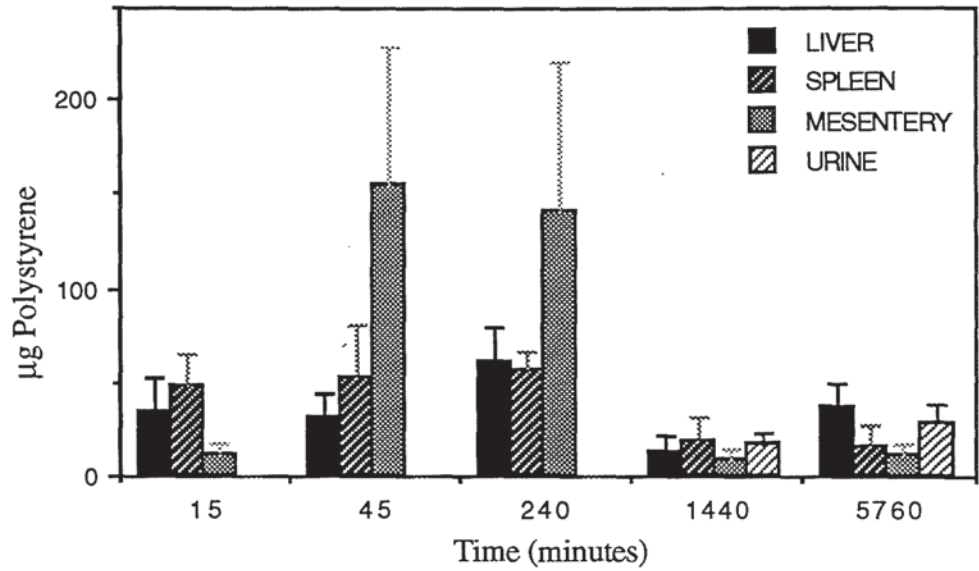


Figure 34. Mean (\pm SEM) urinary excretion ($n=4$) and mesenteric accumulation ($n=4$) in rats after oral administration of 21.7 mg 0.22 μm diameter nanospheres. Whole liver and spleen accumulation data ($n=8$) from figure 33 is also shown for comparison.

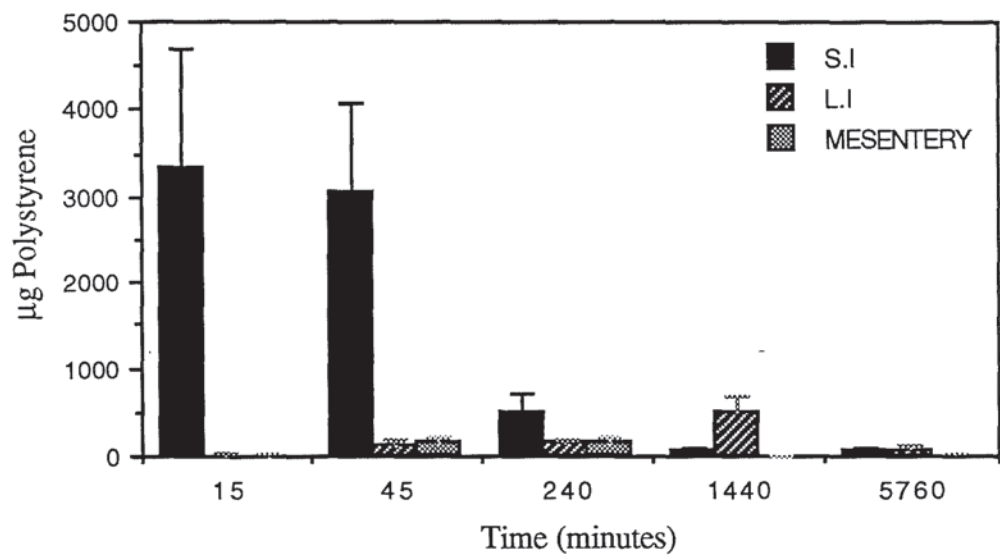


Figure 35. Whole organ accumulation of polystyrene (\pm SEM) in the small and large intestines and mesenteries of rats that received an oral dose of 21.7 mg polystyrene nanospheres (diameter 0.22 μm) ($n=4$).

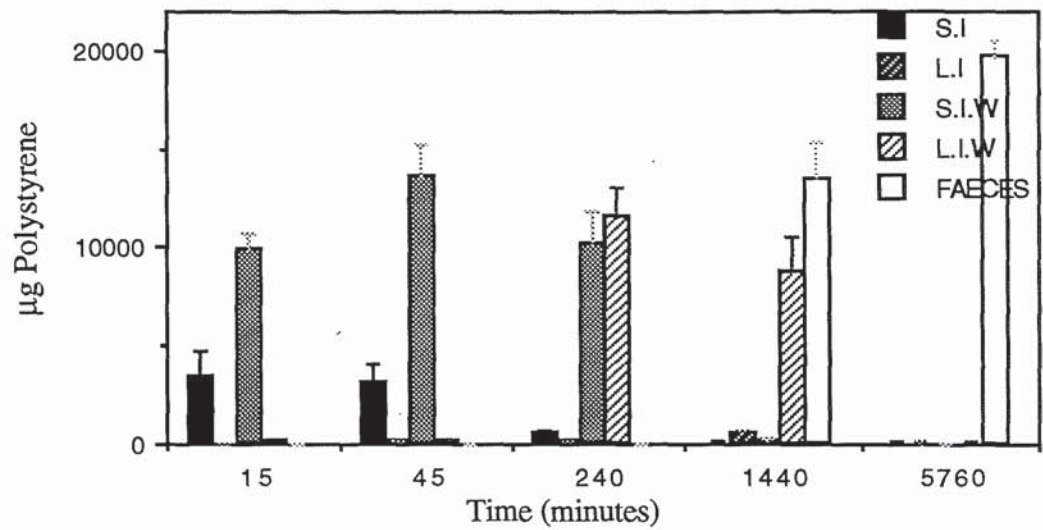


Figure 36. Mean mass of polystyrene (\pm SEM) recovered from whole intestines (SI/LI) complete intestinal washes (SIW/LIW) and faeces of rodents that received 21.7 mg latex nanospheres (0.22 μ m diameter) orally (n=4).

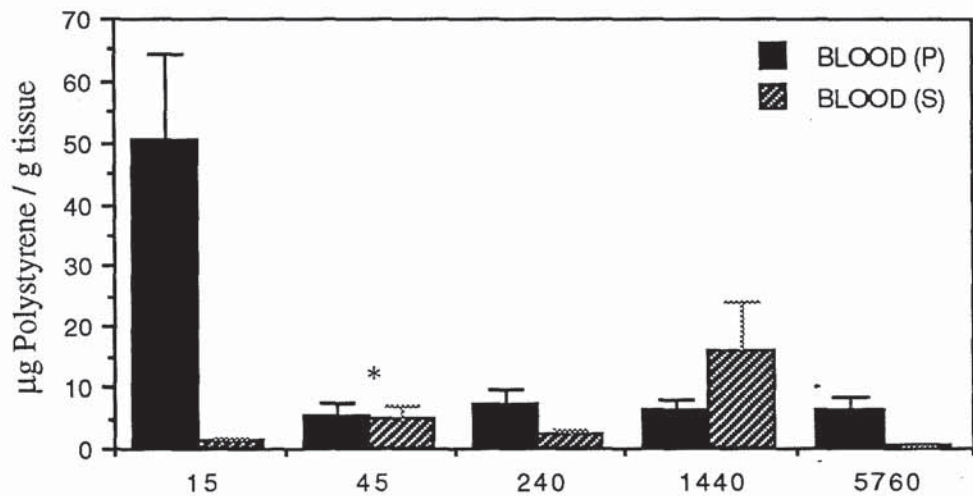


Figure 37. Polystyrene concentration *per gram* (\pm SEM) of portal / systemic blood after oral administration of 21.7 mg polystyrene nanospheres of diameter 0.22 μ m (n=4). No significant difference exists between the two sample sites at 45 minutes (*). At all other time points a significant difference exist between the two sets of data ($P \leq 0.01$ for 2 tail).

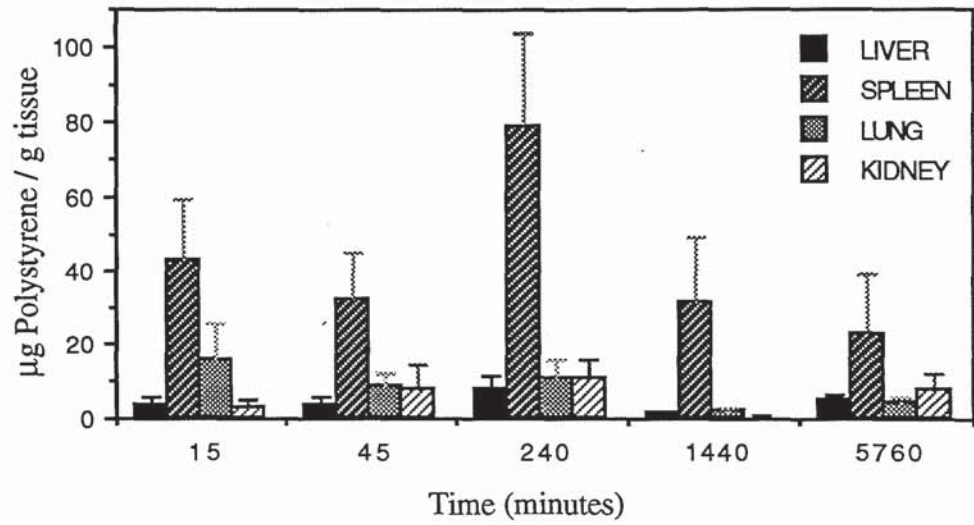


Figure 38. Organ accumulation of polystyrene *per* gram of tissue (\pm SEM) after oral administration of 21.7 mg polystyrene nanospheres of 0.22 μm diameter (n=8).

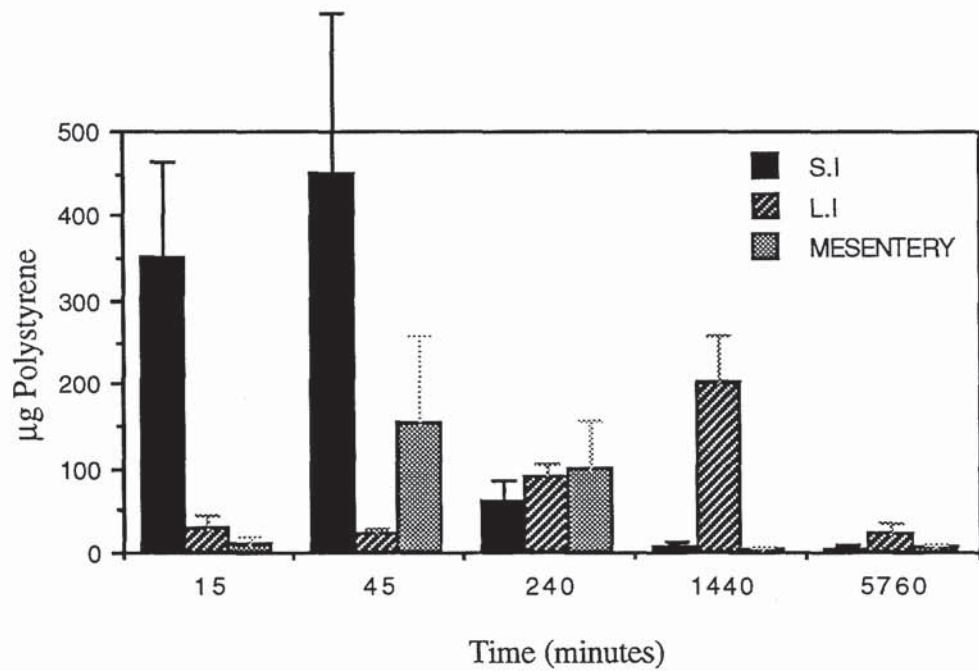


Figure 39. Gut and mesenteric accumulation of polystyrene *per* gram of tissue (\pm SEM) after oral administration of 21.7 mg polystyrene nanospheres of 0.22 μm diameter (n=4).

4.3.2.5 TISSUE DISTRIBUTION OF 0.97 μm MICROSPHERES AFTER A SINGLE ORAL DOSE

The distribution profile obtained after oral administration of 21.7 mg polystyrene latex microspheres ($0.97 \pm 0.010 \mu\text{m}$ diameter) is represented in figures 40 through 47.

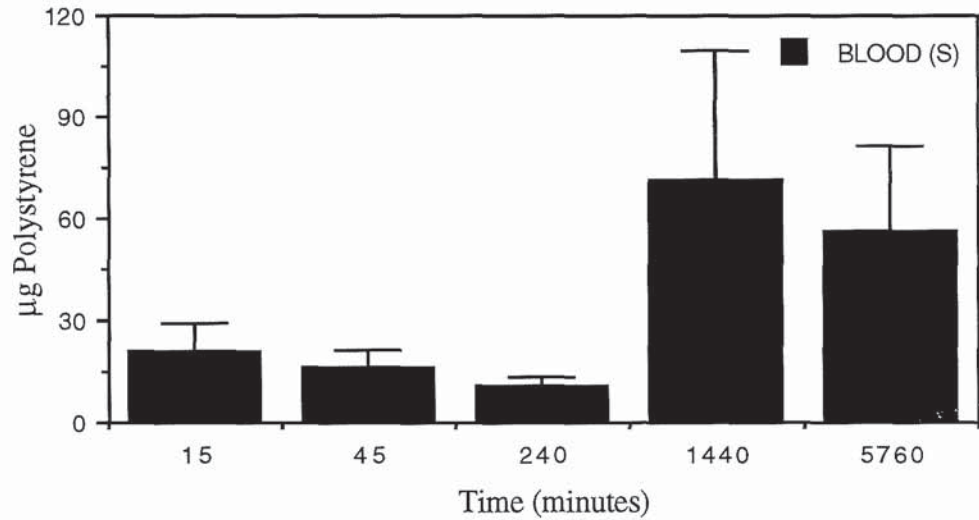


Figure 40. Mean (\pm SEM) mass of latex microspheres within the entire systemic vascular compartment of rats after oral administration of 21.7 mg microspheres (diameter $0.97 \mu\text{m}$) ($n=4$).

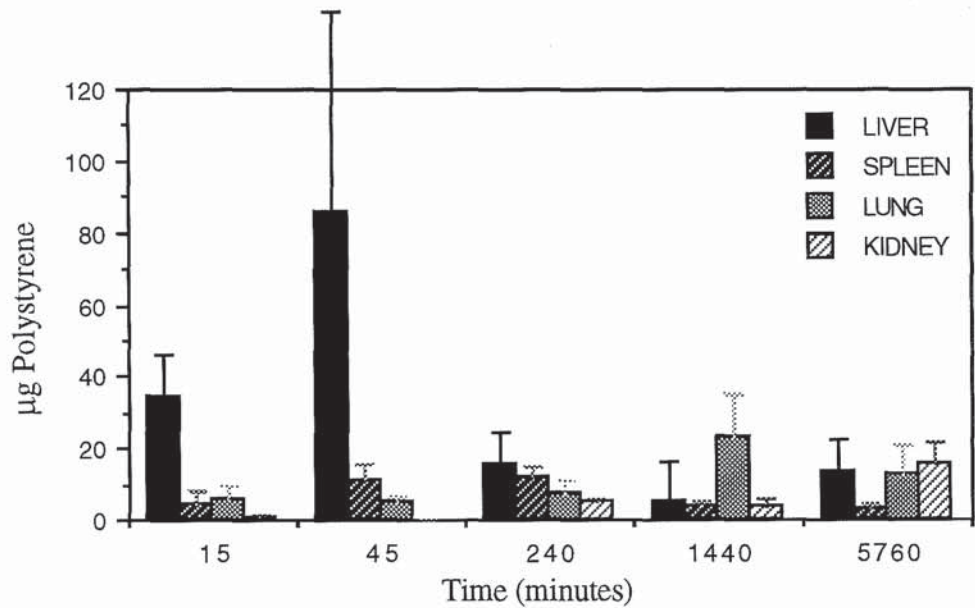


Figure 41. Whole organ accumulation of polystyrene (\pm SEM) after oral administration of 21.7 mg polystyrene microspheres (diameter $0.97 \mu\text{m}$) ($n=4$).

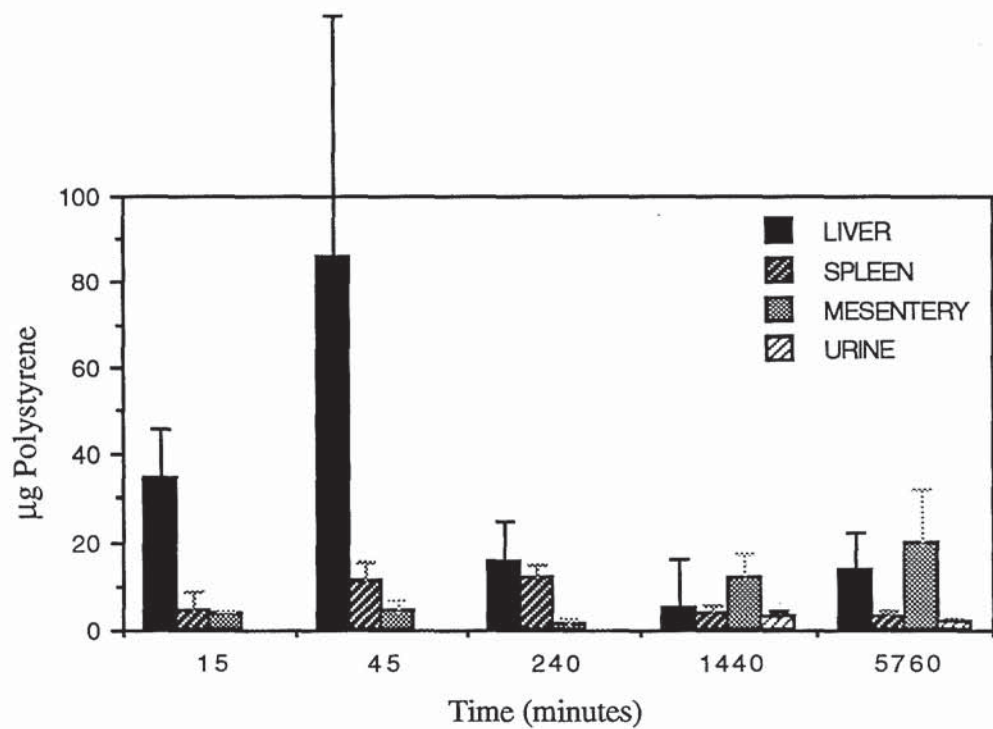


Figure 42. Mean (\pm SEM) urinary excretion (n=4) and mesenteric accumulation (n=4) in rats after oral administration of 21.7 mg 0.97 μ m diameter microspheres. Whole liver and spleen accumulation data (n=4) from figure 41 is also shown for comparison.

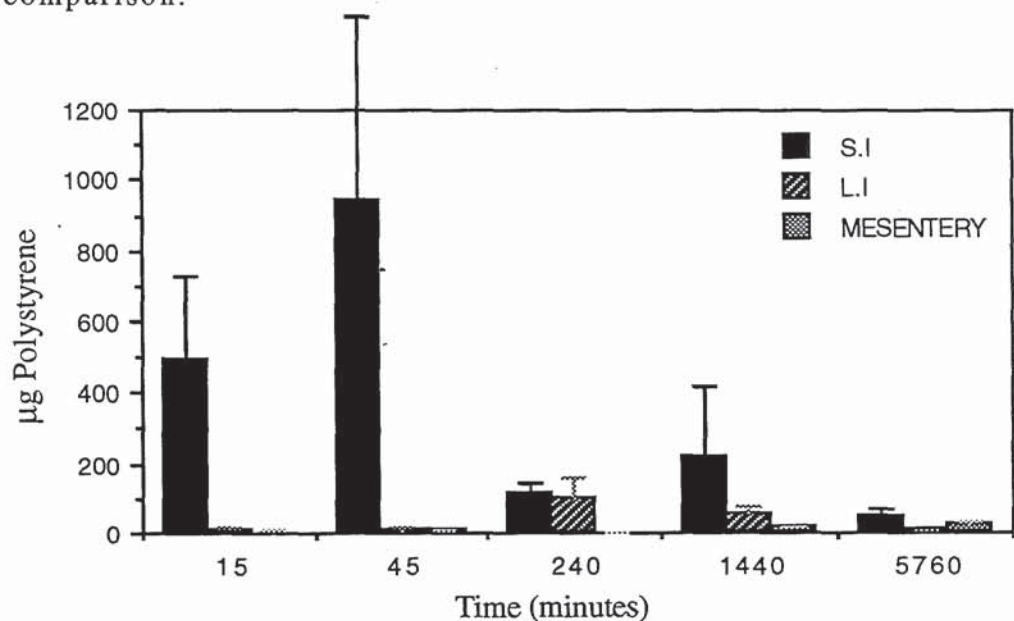


Figure 43. Whole organ accumulation of polystyrene (\pm SEM) in the small and large intestines and mesenteries of rats that received an oral dose of 21.7 mg polystyrene microspheres (diameter 0.97 μ m) (n=4).

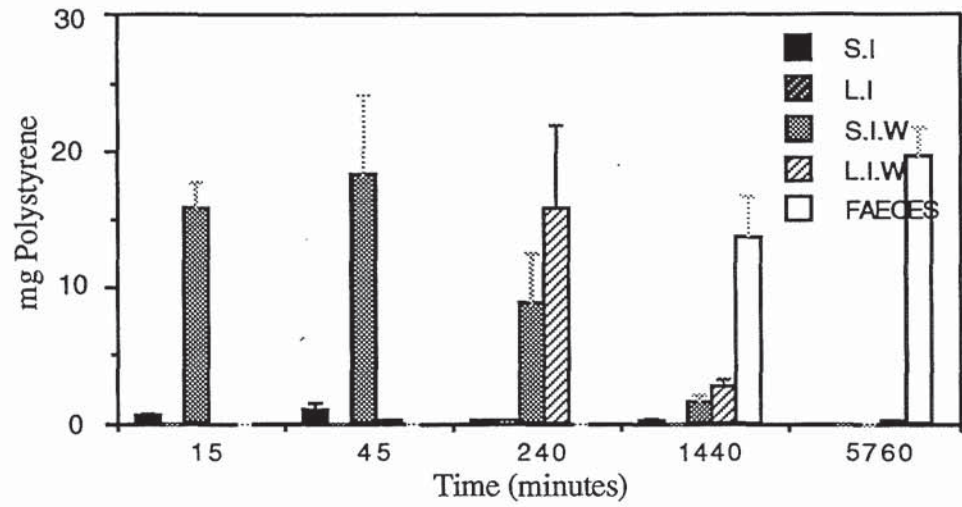


Figure 44. Whole organ accumulation of polystyrene (\pm SEM) in the small and large intestines and mesenteries of rats that received an oral dose of 21.7 mg polystyrene microspheres (diameter 0.97 μ m) (n=4).

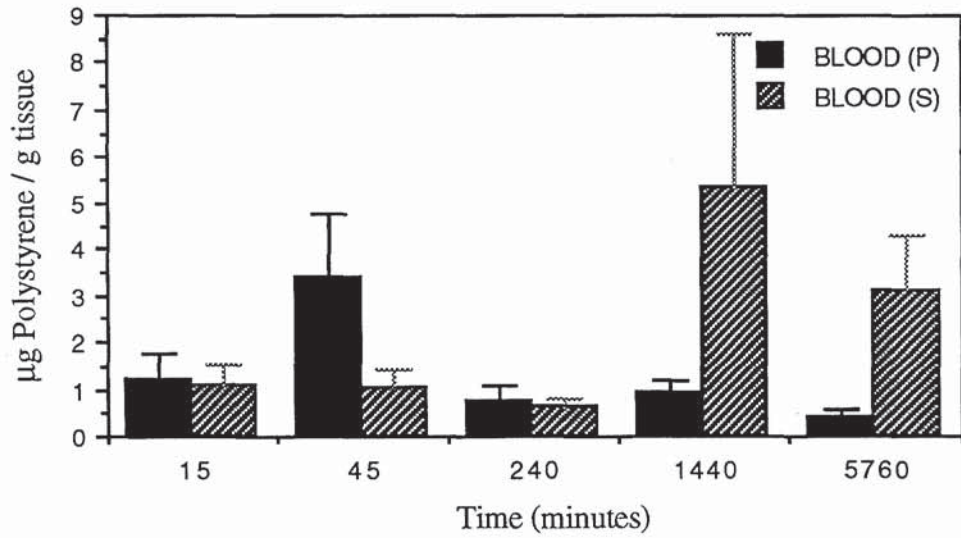


Figure 45. Polystyrene concentration *per gram* (\pm SEM) of portal / systemic blood after oral administration of 21.7 mg polystyrene microspheres (diameter 0.97 μ m) (n=4).

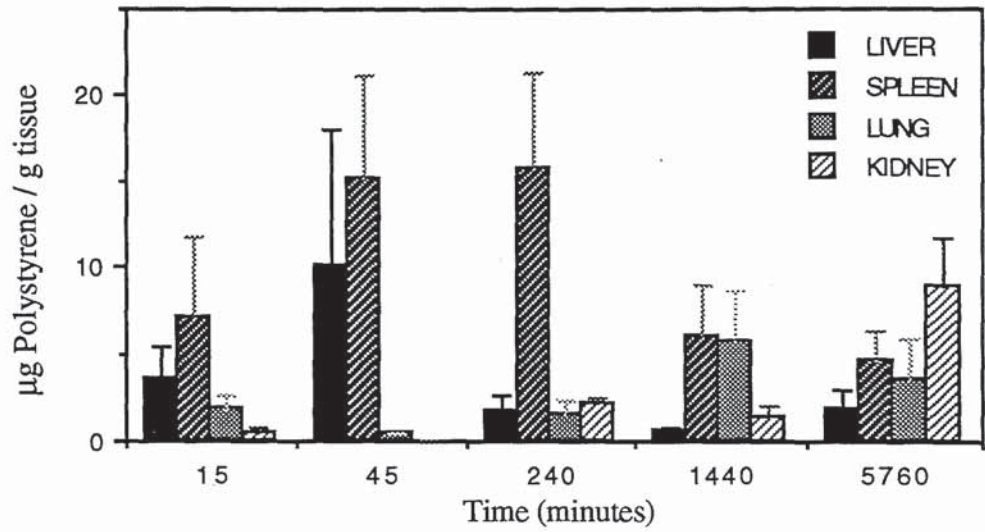


Figure 46. Organ accumulation of polystyrene *per* gram of tissue (\pm SEM) after oral administration of 21.7 mg polystyrene microspheres (diameter 0.97 μ m) (n=4).

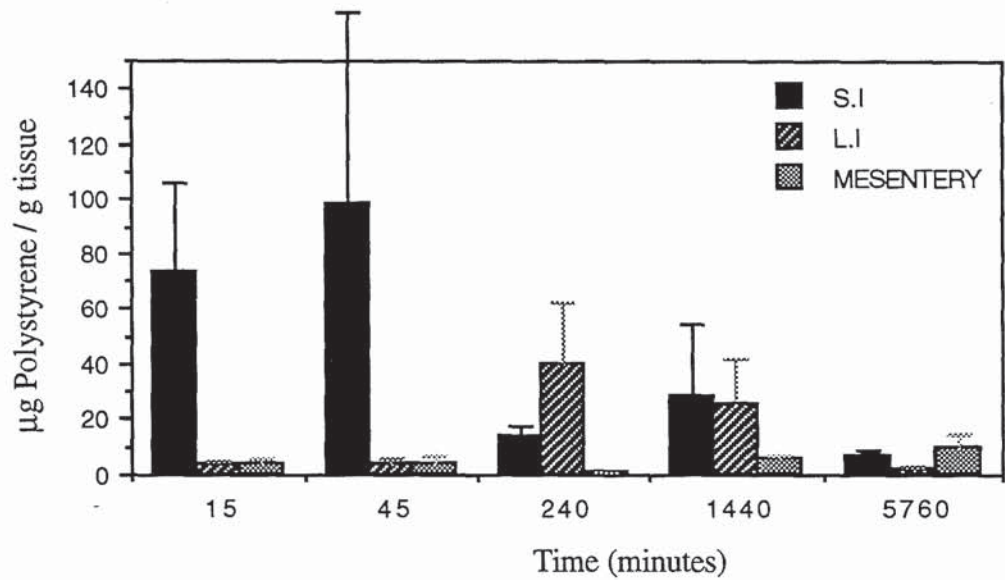


Figure 47. Small / large intestinal and mesenteric accumulation of polystyrene *per* gram of tissue (\pm SEM) after oral administration of 21.7 mg polystyrene microspheres (diameter 0.97 μ m) (n=4).

4.3.3 PREPARATION AND CHARACTERISATION OF ^{125}I LABELLED MICROSPHERES

The average supernatant activity of radioactive microspheres manufactured according to section 4.2.3 was found to be 7.86 ± 1.80 % of the total activity of the suspension after storage for 7 days at 5°C . Free ^{125}I levels, prior to storage i.e. immediately after manufacture of the particles was about 2.16 ± 0.67 % of the total activity.

4.3.4 ORGAN DISTRIBUTION OF RADIOLABELLED $0.82 \mu\text{m}$ MICROSPHERES

The radioactive content of tissues removed from animals which had received an oral dose of ^{125}I -microspheres was found to be considerably higher than background (figure 48 below). The activity of blood and thyroid samples was particularly high at the 24 hour time point (see figure 49). Liver activity was 1.910 ± 0.226 % of the initial dose at 360 minutes and 1.760 ± 0.660 % at 24 hours. Spleen and MLN activity was estimated at 0.900 ± 0.511 % and 0.028 ± 0.011 % at 24 hours respectively.

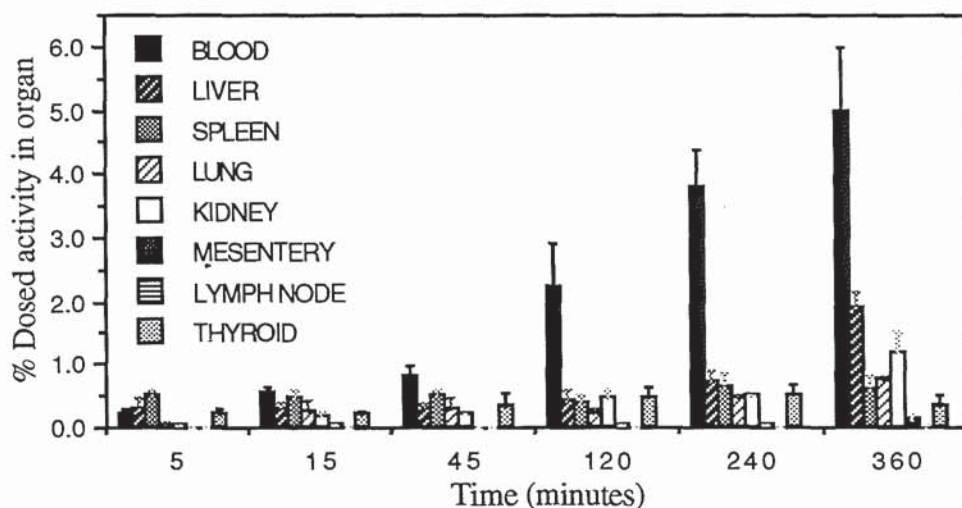


Figure 48. Mean relative activities (\pm SEM) from various tissue samples removed from rats which received 1.42×10^{11} microspheres (with a batch diameter of $0.82 \mu\text{m}$ and an overall activity of 0.614 MBq) by the oral route of administration ($n=4$).

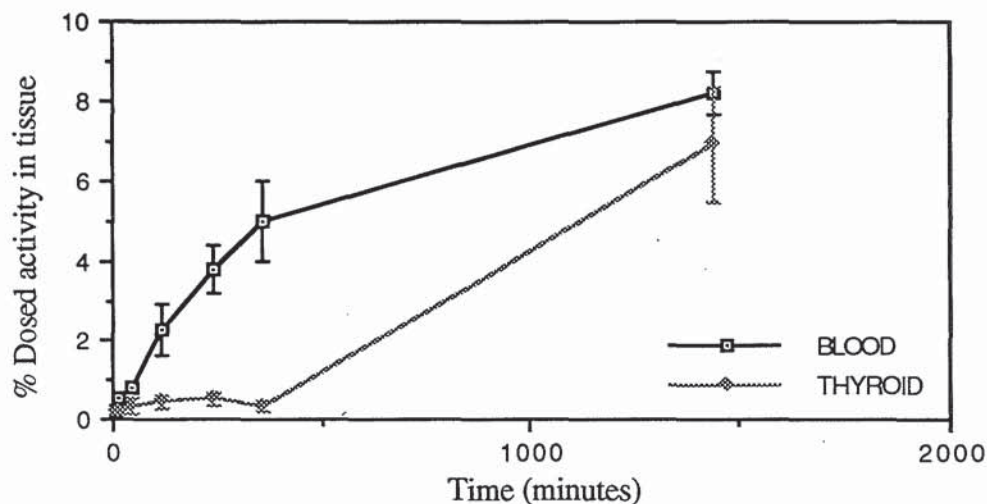


Figure 49. Mean relative activities (\pm SEM) from blood and thyroid samples removed from rats which received 1.42×10^{11} microspheres (with a batch diameter of $0.82 \mu\text{m}$ and an overall activity of 0.614 MBq) by the oral route of administration ($n=4$).

Free iodine is efficiently accumulated within the thyroid glands. Thyroid glands removed from rats 24 hours after oral treatment with radioactive particles were found to be highly radioactive, indicating that the ^{125}I -microsphere complex is unstable *in vivo*. This finding was not entirely surprising as estimated levels of free ^{125}I in the microsphere suspension had increased to about 8 % after a weeks storage at 5°C , indicative of poor label stability (see section 4.2.3).

4.3.5 FLOW CYTOMETRIC ANALYSIS OF BLOOD FROM ANIMALS ORALLY DOSED WITH 0.87 μm CARBOXYLATED MICROSPHERES

The result of FACS analysis of fluorescent microspheres (0.87 μm) suspended in distilled water is shown in figure 50. The uniformity in size and FITC content of the microspheres resulted in a narrow distribution in the resulting FS and FITC values which were used to define an electronic window (z1) in which the microspheres could be counted. Thus when blood samples were counted smaller, larger and / or less fluorescent particulate matter within the suspension would not be counted as microspheres. Within z1 'w1' and a second gate 'w2' were created. w1 represented all microsphere events, while w2 selects multiple microspheres, e.g. doublets, triplet and quadruplet groupings.

As in other studies particles were detected in the vascular compartment at the first sampling time, which was 15 minutes after gavage. Figure 51 shows FACS analysis of blood taken from one of the experimental animals 45 minutes after it received the Fluoresbrite™ particles. Figure 52 shows FACS analysis of blood from the same rat at the 240 minute time point. Analysis of data obtained from all 4 rats is represented in table 5. FACS analysis failed to detect microspheres within blood taken from the 5th control animal which had received water orally. Quantitation of microsphere numbers within 'Spiked' blood samples revealed that the counting procedure had been about 81 % efficient. Uptake values were adjusted accordingly.

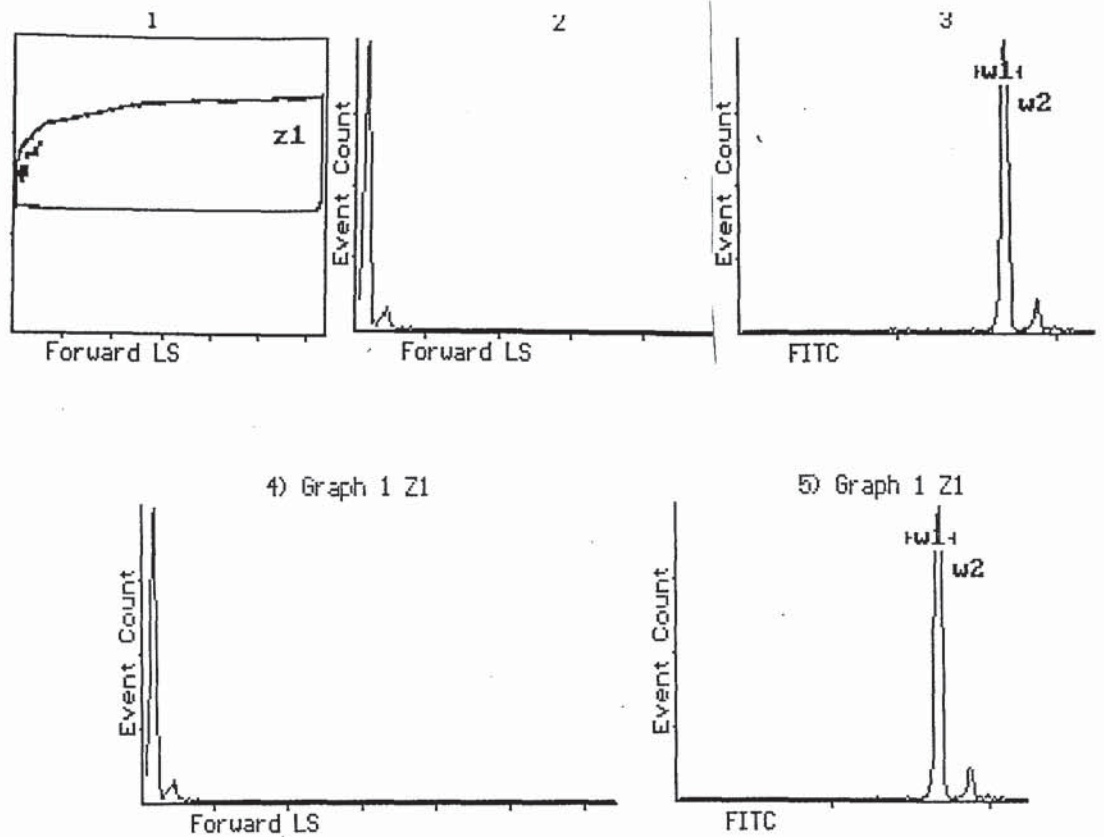


Figure 50. FACS analysis of 0.87 μm diameter Fluoresbrite™ carboxylated polystyrene latex microspheres suspended in distilled water. Running this sample enabled us to instruct the computer to identify microspheres within blood samples by virtue of their high fluorescent activity. Graph 1 shows the electronic window within which microspheres are counted on the basis of their high FITC content (zone 1). The narrow size distribution of the microspheres is obvious in graph 2 representing forward scattering (FS). The fluorescence activity of all particulate matter in the suspension is shown in graph 3. Two peaks are seen, the largest represents single microspheres, whilst the smaller one represents microsphere pairs or doublets. Graphs 4 and 5 show FS and fluorescent activity of zone 1 particulates respectively. Gates w1 and w2 are defined in graph 5.

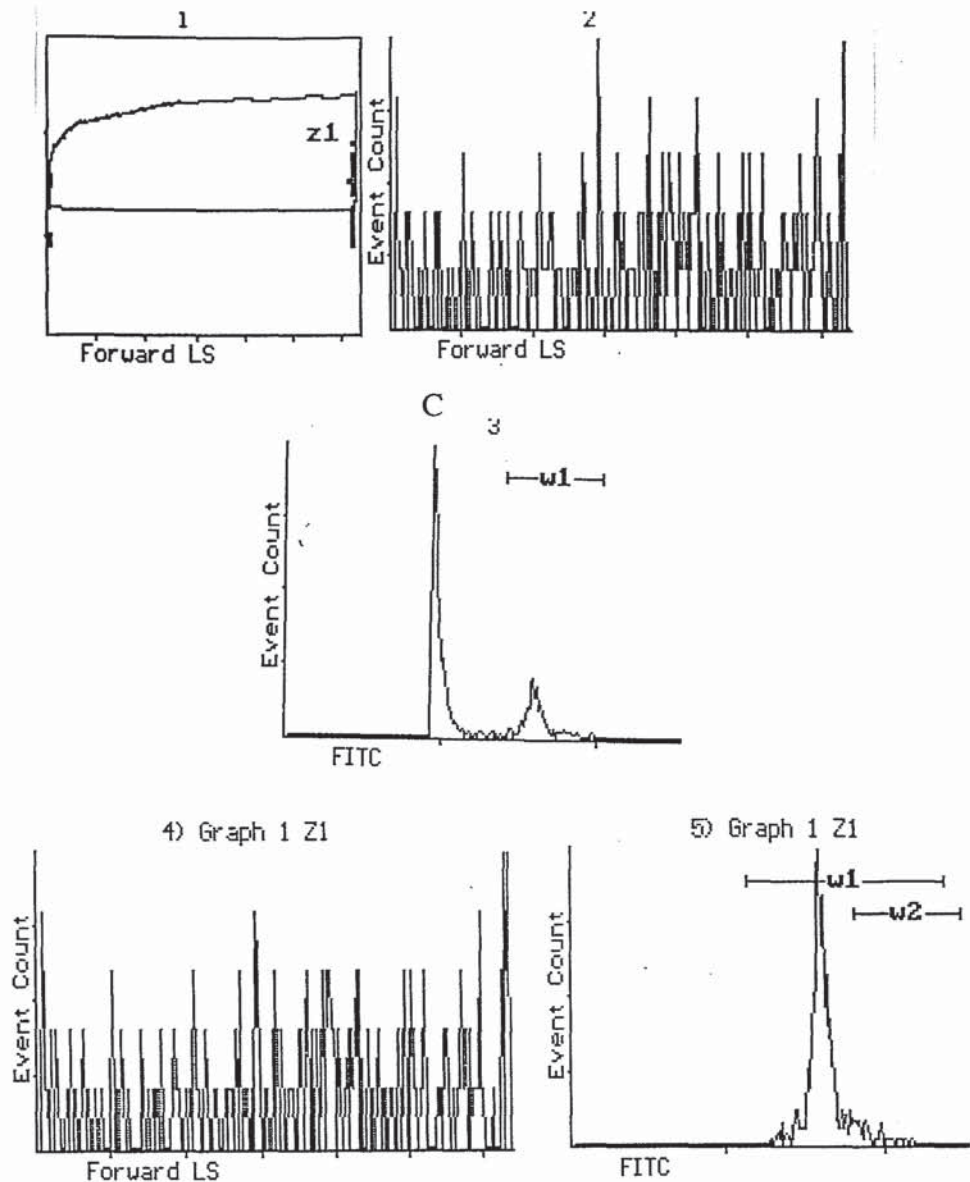


Figure 51. FACS analysis of diluted blood from a rat 45 minutes after oral delivery of 4.40×10^9 $0.87 \mu\text{m}$ diameter Fluoresbrite™ carboxylated polystyrene latex microspheres. The diverse range of particle sizes within the blood sample is obvious in graph 2 representing forward scattering (FS). The fluorescence activity of all particulate matter in the suspension is shown in graph 3. Cells and cell debris (C) exhibit a much lower level of fluorescence than the microspheres (w1), enabling the microspheres to be distinguished from other particulate matter and quantified. Microspheres are counted within gate w1. There is a wide distribution of particle sizes (graph 4) and FITC intensity (graph 5) within gate w1 compared to Figure 50. This suggests that a proportion of microspheres within this blood sample are associated with cells (internally or externally) or cell debris.

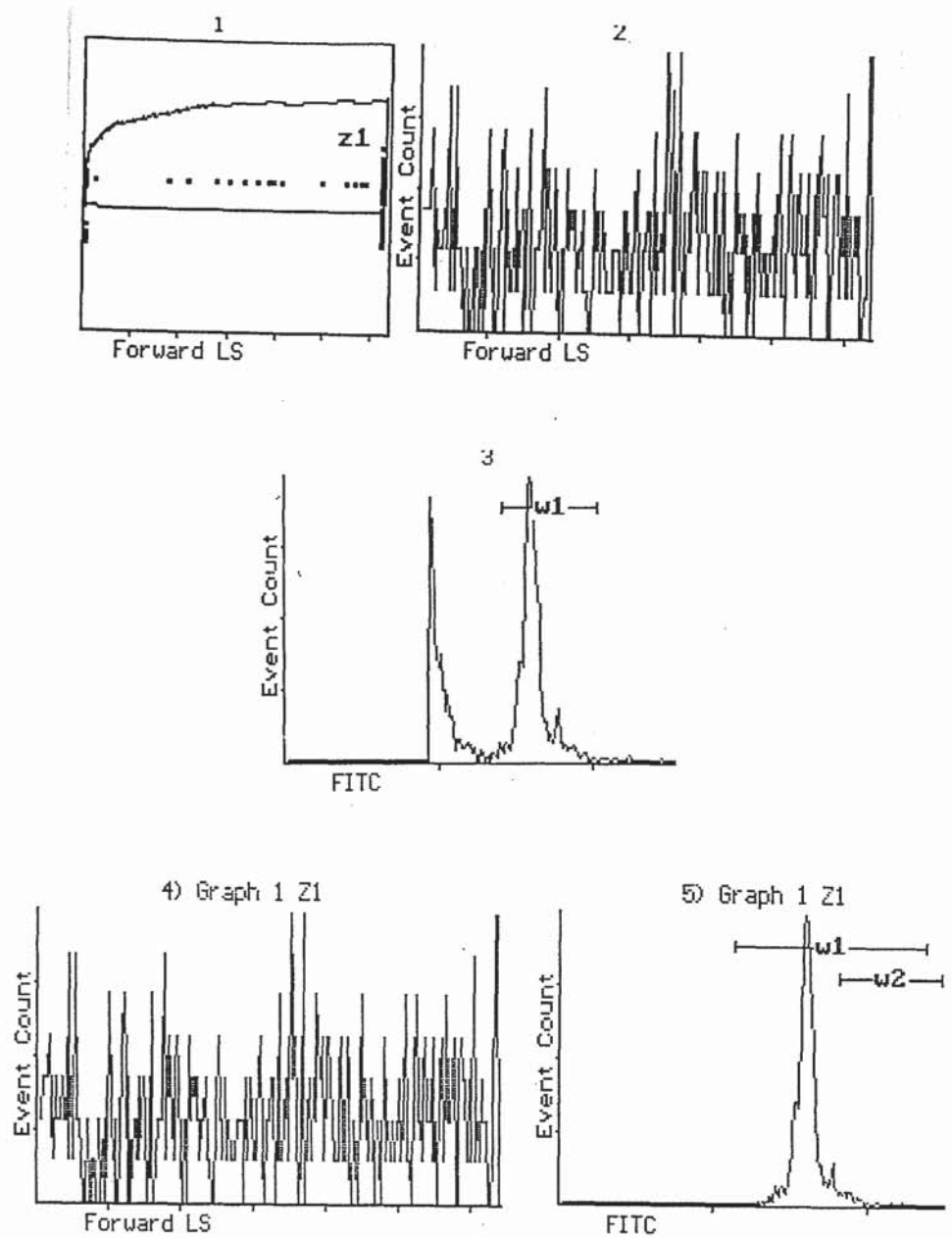


Figure 52. FACS analysis of diluted blood from a rat 4 hours after oral delivery of 4.40×10^9 $0.87 \mu\text{m}$ diameter Fluroesbrite™ carboxylated polystyrene latex microspheres. The high fluorescent intensity of the microspheres compared with other particles present within the blood sample is clear in graphs 3 and 5. Again microsphere numbers are quantified within gate w1. Data represented in graph 5 suggests that large numbers of translocated microspheres within the blood are present in multiple groupings. A secondary (doublet) peak can be clearly seen.

Time after dosing (minutes)	% Dose x 10 ⁻³ in the blood	Standard error of the mean (±)
15	2.777	1.069
45	5.007	2.569
240	15.928	6.354
1440	6.527	2.995

Table 5. FACS determined transfer of 0.87 µm diameter carboxylated Fluoresbrite™ microspheres into the vascular compartment after a single oral dose of 4.40 x 10⁹ particles suspended in 1 ml of water (n=4).

4.4 DISCUSSION

4.4.1 ORGAN DISTRIBUTION OF RADIOLABELLED 0.82 µm MICROSPHERES IN THE RAT MODEL

Body fluids and tissues removed from rats after oral administration of radioactive microspheres were found to contain considerable amounts of ¹²⁵I (figure 48). Gamma ray emission from thyroid glands removed from dosed animals was found to be high at later time points (figure 49) indicating that leaching of the ¹²⁵I label had occurred. Also, the sequential increase in blood activity at time points from dosing was not compatible with earlier uptake profiles. In healthy humans, dietary iodine is almost completely absorbed. In the thyroid, thyroglobulin iodination occurs very rapidly; labelled iodide appears in hormone molecules 1 minute after *in vivo* administration, and by 1 hour 90 - 95 % of iodide is organically bound (Berne *et al* ., 1988). Thus thyroid activity in rats given radioactive latex microspheres probably represents a large percentage of the circulating ¹²⁵I pool. High blood activities at 24 hours after oral administration may be attributed, at least in part, to the formation of ¹²⁵I labelled triiodothyronine and thyroxin hormones. This factor further complicates interpretation of the blood data obtained from microsphere treated rodents.

The poor stability of the ¹²⁵I-particle complex in the body means that it is difficult to draw any meaningful conclusions about the ratio of microsphere distribution amongst the tissue samples assayed, although it is probable that a proportion of the activity detected originated from absorbed test particles.

This is particularly true of the tissue samples removed up to the 6 hour experimental time point. Before the 6 hour time point thyroid gland activity in treated rats was low enough to assume that free ^{125}I represented only a proportion of the radioactive material within assayed tissues.

4.4.2 FLOW CYTOMETRIC ANALYSIS OF BLOOD FROM ANIMALS ORALLY DOSED WITH 0.87 μm CARBOXYLATED MICROSPHERES

FACS analysis of blood from animals given an oral dose of 0.87 μm diameter carboxylated Fluroesbrite™ microspheres, graphically demonstrates that unlikely as it seems, particulate matter may leave the GIT lumen to appear in the blood stream within a few minutes of administration (Figures 50, 51 and 52). However overall, uptake was found to be low. In fact much lower than in the preliminary studies using Fluroesbrite™ particles (chapter 3) in which up to 7 % of the dosed microspheres could be detected in the vascular compartment. Maximal uptake observed in the FACS studies was several hundred fold lower than this value. The shape of the FACS determined circulatory profile of the particles was also slightly different, as a peak in particle numbers within the vascular compartment was detected in blood removed at 4 hours. Reasons for this discrepancy in the observed uptake values when using different experimental methodologies is not obvious. Problems with the direct counting method of particle quantification have been discussed in the previous chapter. Complications also arise with the flow cytometric method for particle assay. From figure 50 it is clear that whilst most of the latex particles are present as a monodispersed suspension in distilled water, this is not the case in blood removed from treated animals (figure 51 and 52). In tail vein blood from dosed animals large numbers of the fluorescent microspheres are present in multiple groupings (see figure 52). One can only speculate, but it seems likely that these multiple groupings represent coalescent microspheres or microspheres within cells, attached to cells or cellular debris. Observations using the light microscope (chapter 3) seem to support this. FACS technology will quantify the number of microsphere events in terms of single or multiple beads. It will not allow accurate determination of the multiple bead population size, although a very rough estimate of this figure may be made manually. As this is the case, it is possible that estimates of the efficiency of microsphere translocation using FACS may not be representative and tend to under estimate the true figure. If so, then one can say with some confidence that the actual number of Fluroesbrite™

carboxylate microspheres that exit the GIT lumen to circulate within the vascular compartment in the rat model is likely to be somewhere in between the values quoted for the FACS and direct counting (chapter 3) methods of quantification.

The observed rapidity of test particle translocation seen in the FACS study again supports the existence of a persorption like mechanism of particle translocation. In his studies, the efficiency of starch granule transportation by persorption was estimated at 0.002 % by Volkheimer (1977). Smith *et al.* (1993) stated that although occasional particles may be transported across GI epithelia by a paracellular route, efficiency of this process is either unknown or low. The results from this experimental section and the previous chapter suggest that while the efficiency of persorption of 0.87 μm carboxylated microspheres is low, it is almost certainly greater than 0.002 %.

4.4.3 CHARACTERISATION OF POLYSTYRENE TEST PARTICLES

The hydrophobicity of the different latex microsphere particles used in animal studies was found to be highly dependent on their chemical composition and to a much lesser extent their size. Polybead[®] microparticulates were found to be considerably more hydrophobic than the carboxylated Fluroesbrite[™] microspheres. This is evident when comparing figures 20 and 21 to figure 22. The carboxylated microspheres are eluted from the sepharose and propyl-agarose columns with considerable ease in comparison to the un-charged Polybead[®] particles which are considerably more hydrophobic and tend to associate with the hydrophobic column packing material. For Polybead[®] particles, a greater percentage of the 0.97 μm particles were eluted or washed off the columns in comparison to the smaller beads. In the case of hexyl-agarose, which is a very hydrophobic column packing gel, the 0.22 μm particles are considerably more resistant to elution or washing than the larger microspheres. Thus the behaviour of the Polybead[®] microparticles during column chromatography indicates that the smaller 0.22 μm nanospheres are more hydrophobic than the larger 0.97 μm microspheres.

The Zeta potential of any spherical colloidal particle is an indication of its effective electrostatic charge and is directly related to the stability of that particle in suspension. Colloidal systems with Zeta potential values less

negative than -14 mV are potentially unstable, tending to aggregate or even precipitate (Riddick, 1968). From table 2 it is evident that in a buffered solution of pH 7.09 all polystyrene microspheres tested had Zeta potentials which were considerably more negative than -14 mV and as such could be regarded as fairly stable suspensions. Both Polybead[®] microparticulates examined had highly similar electrostatic properties. Unexpectedly, the 1.1 μm carboxylated latex microspheres were found to be less electronegative. The presence of carboxyl groupings within the polymer chains would be expected to result in the opposite to the observed reading, i.e. a more electronegative system. The presence of surfactant residues from the manufacturing process may have influenced particle behaviour. An alternative would be to extensively dialyse or wash the beads prior to analysis.

4.4.4 GPC DETERMINED UPTAKE AND DISTRIBUTION OF POLYSTYRENE TEST PARTICLES

Recovery of polystyrene latex from spiked tissues and fluids was always less than 100 % efficient (see figure 29) indicating that considerable scope for loss of latex exists. Filtration of tissue extracts dissolved in THF is probably one stage in the extraction protocol with particular potential for incurring losses. Successful resolution of the polystyrene peak from the peak produced by tissue breakdown products, was heavily reliant on there being complete de-hydration of the tissue samples prior to solvent extraction. On some occasions, the latex peak would be very slightly superimposed on to the tissue breakdown product peak. This factor may be responsible for variation in recovery efficiencies from sample to sample. Recovery of latex from liver was less efficient than blood (figure 29). This finding reflects the higher density of liver compared with blood. The action of organic solvents on liver will produce more breakdown products than in the case of blood. If some of the breakdown products have relatively high molecular weights, then a partial occlusion of the polystyrene peak by the tissue peak may occur. For total occlusion of the polystyrene latex peak to occur, the tissue breakdown product peak would have to contain some extremely high molecular weight compounds whose chemical structure was resistant to the action of chloroform. During our experimental investigations, this was never found to be the case.

Results from the quantitative analysis of body fluids and tissues from rats that received an oral dose of polystyrene latex in the form of 0.22 μm and 0.97 μm diameter microspheres, support previous reports (Alpar *et al.* , 1989, Lewis *et al.* , 1992, Volkheimer, 1977, 1993) that small amounts of particulate matter may transfer rapidly from the gut to extra-intestinal sites, including the blood. Nano / microspheres were present in the general circulation as quickly as 15 minutes after oral administration and could still be detected after 4 days. Nanosphere (0.22 μm) presence in the portal vein appeared to show a rough equivalence with the systemic circulation, except at the 15 minute time point where significantly more polystyrene was detected, suggesting a large influx of microspheres *via* this route. Microsphere (0.97 μm) uptake after oral delivery was much lower than the smaller Polybeads[®], but did display a similar peak in particle numbers within the portal vein shortly (45 minutes) after gavage. Rapid and efficient accumulation of test particles by organs of the MPS was seen prior to 24 hours post dosing although surprisingly, a background level of polystyrene in the blood remained up to 4 days. Amongst the organs of the MPS, the spleen demonstrated an extremely high propensity to accumulate particulates as did the liver and lungs, although to a lesser extent. The concentration of 0.22 μm diameter latex within these four organs became depleted 24 hours after dosing, possibly caused by excretion of the particles *via* bile and urine, although this trend was reversed at 4 days. This observation could be explained by a secondary wave of polystyrene reaching the circulation from the thoracic duct after lymphatic uptake from the GIT. Although there is no solid evidence to support this except that large numbers of nanospheres were extracted from the mesentery and large intestines at later time points. Extra-intestinal accumulation of the 0.97 μm microspheres was less significant, although again MPS organs (liver and spleen) demonstrated a high ability to sequester these particles, particularly within a few hours of dosing. These and other results from the series of experiments are discussed in more detail below.

4.4.4.1 LATEX PARTICLE TRANSFER INTO THE VASCULAR COMPARTMENT AFTER ORAL ADMINISTRATION

Polystyrene nanospheres (0.22 μm diameter) were detected within the vascular compartment from 15 minutes after administration (see figure 32). Such rapid transfer of particulates from gut lumen to the circulation has been reported previously (Arahamian *et al.* , 1987, Lewis *et al.* , 1992, Alpar *et*

al ., 1989, Volkheimer 1977, 1993) although many workers regard this finding with scepticism, even though few have examined blood at short time periods after dosing. Statistical comparison between portal and systemic blood, using the unpaired t test, revealed significant differences between the two sets of data at all but one of the time points examined (45 minutes). For all time points except 24 hours and 45 minutes, the portal blood contained more polystyrene weight for weight of blood. The opposite applied at 24 hours, and no significant differences were observed between the two sample sites at 45 minutes. 15 minutes after dosing, very large numbers of nanospheres (0.22 μm) were detected in the portal blood compartment. Each gram of portal blood at this time point contained about 0.23 % of the administered dose of nanospheres. Thus it seems highly likely from this data that an initial, substantial, influx of particles occurs very shortly after gavage. A large contributory factor to this massive inflow is likely to be that of "physiological stress" placed on the intestinal epithelium by 'water overload' (see chapter 3). This refers to a combination of factors including visible distension of the gut lumen, the opening of macroscopic water channels exposing potential uptake sites, a reduction in the effectiveness of the mucus and unstirred water layers and increase in the rate by which particles pass through defects in the mucosa resulting from the desquamation of epithelial cells at gaps in the tips of villi (Volkheimer, 1968). Aprahamian *et al .*, (1987) obtained similar results after intra-jejunal administration of polyalklycyanoacrylate nanocapsules (0.1 - 0.2 μm diameter) to dogs. Plasma levels of the particles in blood withdrawn from the mesenteric vein, increased from 15 minutes, and peaked after 45 minutes. Mesenteric blood samples withdrawn at 5 minutes were found to contain nanocapsules. At the peak, plasma levels were found to be 3.5 times that of the basal levels recorded at time zero. Normal (basal) plasma levels returned after 105 minutes. Nanocapsules were seen to pass through the epithelium in a paracellular manner and were observed in the vicinity of the basal membrane of enterocytes within 10 minutes of administration (see sections 1.2.3 and 1.2.6.2). The authors said they saw no evidence of intracellular uptake of the nanocapsules by endocytosis (section 1.2.2).

The mechanism by which the nanospheres enter the microcirculation of the intestinal mucosa is poorly understood, although clearly this process must occur in order for such rapid appearance in the portal vein. Passage through the basement membrane might be possible through one of the fenestrations of between 500 and 5000 nm in diameter (Komuro, 1985). Entry into the

lumen of the capillaries could occur, in certain locations and physiological conditions, through channels in endothelial cells formed by fenestral diaphragms of up to 100 nm in size (Aprahamian *et al.*, 1987).

45 minutes after oral administration statistically equivalent numbers of nanospheres (0.22 μm) are present in portal and systemic systems. This observation may reflect the return of intestinal homeostasis after water overload and thus increased resistance to particulate penetration. Marginally elevated particle numbers in the systemic circulation may reflect decreased efficiency in microsphere capture by the MPS, or release of sequestered latex microspheres. After 4 hours polystyrene was still readily detectable in both vascular compartments, but slightly more so in the portal one suggesting continued low level uptake from the gut. At 24 hours after administration elevated particle numbers were detected in the general circulation, possibly caused by the release of harboured nanospheres from sites of accumulation, or alternatively a process of redistribution and elimination. Blood sampled after 4 days also contained low levels of polystyrene, particularly in those samples taken from the hepatic portal vein. The exact reasons for this are unclear but a gradual clearance of insorbed particles from sites within the gut is one explanation.

The presence of large numbers of nanospheres in the circulation at protracted time points after dosing does not equate with the documented efficiency of the MPS at particulate sequestration (see section 1.2.6.2). However, the majority of these studies (Kreuter *et al.* , 1983, 1979, Singer *et al.* , 1969, Yamaoka *et al.* , 1993) have investigated the distribution of particles at time points after i.v. administration. The input of microspheres into the circulation after oral uptake is likely to be different in terms of several variables (see section 1.2.6.2). For example, its likely that after oral administration low numbers of particles may trickle into the blood stream from the thoracic duct, MPS organs or intestinal sites many hours, days or months after dosing. It is also probable that microsphere translocation from gut to circulation results in an increased potential for particle contact with diffuse or aggregated lymphoid tissue compared with simply injecting the colloid as a bolus. This factor may encourage phagocytic uptake of the particles into the circulating blood monocyte or polymorph cell populations. As indicated by earlier experiments, most particles are seen within phagocytes when examining blood samples from orally dosed animals. It is possible that microspheres circulating within blood monocytes may evade

recognition by the MPS, and remain within the circulation for as long as 4 days or more.. A few investigators have examined the blood after oral administration of microspheres. Jani *et al* ., (1990) detected 1.1% of a chronic oral dose consisting of 0.3 μm diameter microspheres, in the blood, two days after the last administration. On average 0.02 % of a chronic oral dose of titanium dioxide particles were recovered from each ml of blood removed from animals 24 hours after last treatment (Jani *et al* ., 1994). Stag (1994) detected 0.82 % of a single oral dose of 0.22 μm latex nanospheres in the blood 24 hours after gavage. Even after i.v. injection, Adlersberg *et al* ., (1969) could detect 1.8 % of a 230 nm nanosphere dose within the blood 6 weeks after dosing.

Heart blood samples from rodents given 0.97 μm diameter Polybeads[®] orally contained significantly less latex at 45 and 1440 minutes after dosing compared to the 0.22 μm diameter Polybeads[®]. The circulatory profile of 0.97 μm microspheres after oral delivery (see figure 40) was also slightly different to that obtained with the nanospheres (0.22 μm). Again a peak in the portal blood polystyrene content was observed shortly after gavage. However most of the latex was detected in blood samples withdrawn from the portal vein at the 45 minute time point. Four hours after dosing microsphere levels in portal and heart blood were similar. At 24 hours and 4 days after gavage, elevated levels of latex was detected within the systemic circulation compared to blood samples from that site that were withdrawn at earlier time points.

Again the rapidity with which the 0.97 μm diameter microspheres appeared in the portal supply suggests that particulate matter of this size may directly penetrate the intestinal microcirculation possibly *via* a paracellular route of absorption. Explanation of how 0.22 μm diameter particles could conceivably enter the intestinal vasculature after oral administration is given in section 1.2.6.2. The feasibility of much larger particles such as those in the micron size range achieving this seems less likely, since the size of the fenestrations in the capillary endothelium would be expected to exclude such objects (see figure 8). The vastly depleted numbers of 0.97 μm particles within the vascular compartments compared to the nanospheres highlights the size dependent nature of this phenomenon, as reported by others (Jani *et al* ., 1990, Eldridge *et al* ., 1989). It may also reflect the fact that HIC measurements revealed the smaller (0.22 μm) nanospheres to be more

Measurement		Uptake ($\mu\text{g/g}$)		P (comparison by two-tailed unpaired t-test)
Tissue	Time (m)	0.22 μm	0.97 μm	
Blood(P)	15	50.3 \pm 41.8	1.2 \pm 1.6	P \leq 0.001
Blood(S)	15	1.4 \pm 1.6	1.1 \pm 1.3	N.S.D
Liver	15	3.8 \pm 6.6	3.6 \pm 5.2	N.S.D
Spleen	15	42.9 \pm 49.8	7.1 \pm 13.8	P \leq 0.001
Lung	15	16.0 \pm 29.3	1.8 \pm 2.4	P \leq 0.020
Kidney	15	3.0 \pm 6.9	0.5 \pm 0.9	N.S.D
Intestine(S)	15	348.8 \pm 351.6	72.8 \pm 100.2	P \leq 0.001
Intestine(L)	15	28.7 \pm 48.3	3.8 \pm 3.4	P \leq 0.001
Mesentery	15	11.0 \pm 19.5	4.3 \pm 5.9	P \leq 0.050
Blood(P)	45	5.1 \pm 6.7	3.3 \pm 4.2	N.S.D
Blood(S)	45	4.9 \pm 6.1	1.1 \pm 1.1	P \leq 0.010
Liver	45	3.6 \pm 5.1	10.1 \pm 23.8	P \leq 0.050
Spleen	45	32.2 \pm 38.5	15.2 \pm 18.1	P \leq 0.020
Lung	45	8.8 \pm 9.6	0.4 \pm 0.3	P \leq 0.001
Kidney	45	7.9 \pm 6.9	0	P \leq 0.100
Intestine(S)	45	447.7 \pm 573.6	98.5 \pm 205.9	P \leq 0.001
Intestine(L)	45	22.4 \pm 22.8	3.9 \pm 5.4	P \leq 0.001
Mesentery	45	154.2 \pm 307	4.2 \pm 8.0	P \leq 0.001
Blood(P)	240	7.1 \pm 7.5	0.8 \pm 0.9	P \leq 0.010
Blood(S)	240	2.1 \pm 3.1	0.6 \pm 0.9	N.S.D
Liver	240	8.0 \pm 11.3	1.7 \pm 2.9	N.S.D
Spleen	240	78.9 \pm 73.6	15.7 \pm 16.6	P \leq 0.001
Lung	240	10.6 \pm 15.1	1.6 \pm 2.0	N.S.D
Kidney	240	10.8 \pm 14.3	2.0 \pm 0.96	P \leq 0.050
Intestine(S)	240	60.0 \pm 74.8	14.0 \pm 11.61	P \leq 0.001
Intestine(L)	240	88.2 \pm 48.6	40.0 \pm 66.2	P \leq 0.001
Mesentery	240	98.3 \pm 173.1	0.9 \pm 0.6	P \leq 0.001

Table 5(a). Mean uptake of polystyrene per gram of tissue (\pm standard deviation) at 15, 45 and 240 minutes after oral administration of either 21.7 mg of 0.22 μm diameter latex nanospheres or 21.7 mg of 0.97 μm diameter latex microspheres. A comparison between uptake of the 0.97 μm particles and the 0.22 μm diameter particles has been performed using a two-tailed unpaired t-test (N.S.D = P $>$ 0.10).

Measurement		Uptake ($\mu\text{g/g}$)		P (comparison by two-tailed unpaired t-test)
Tissue	Time (m)	0.22 μm	0.97 μm	
Blood(P)	1440	5.9 \pm 6.4	0.9 \pm 0.9	N.S.D
Blood(S)	1440	15.9 \pm 24.4	5.3 \pm 9.4	P \leq 0.050
Liver	1440	1.3 \pm 1.5	0.6 \pm 0.6	N.S.D
Spleen	1440	31.7 \pm 52.7	6.0 \pm 9.0	P \leq 0.010
Lung	1440	2.0 \pm 2.5	5.7 \pm 9.0	N.S.D
Kidney	1440	0.3 \pm 0.5	1.3 \pm 1.9	N.S.D
Intestine(S)	1440	7.6 \pm 12.5	28.3 \pm 77.4	P \leq 0.010
Intestine(L)	1440	199.9 \pm 177.0	25.7 \pm 48.0	P \leq 0.001
Mesentery	1440	3.7 \pm 5.4	5.7 \pm 0.9	N.S.D
Blood(P)	5760	5.9 \pm 7.1	0.4 \pm 0.5	P \leq 0.020
Blood(S)	5750	0.2 \pm 0.6	3.1 \pm 3.5	P \leq 0.100
Liver	5760	4.9 \pm 5.4	1.8 \pm 3.4	N.S.D
Spleen	5760	22.7 \pm 49.2	4.5 \pm 5.5	P \leq 0.050
Lung	5760	4.3 \pm 5.1	3.6 \pm 6.6	N.S.D
Kidney	5760	7.8 \pm 13.8	8.9 \pm 8.3	N.S.D
Intestine(S)	5760	4.5 \pm 12.0	6.7 \pm 5.8	N.S.D
Intestine(L)	5760	21.9 \pm 42.0	2.3 \pm 2.4	P \leq 0.001
Mesentery	5760	6.1 \pm 6.6	9.3 \pm 16.7	N.S.D

Table 5(a). Mean uptake of polystyrene per gram of tissue (\pm standard deviation) at 24 and 96 hours after oral administration of either 21.7 mg of 0.22 μm diameter latex nanospheres or 21.7 mg of 0.97 μm diameter latex microspheres. A comparison between uptake of the 0.97 μm particles and the 0.22 μm diameter particles has been performed using a two-tailed unpaired t-test (N.S.D = P $>$ 0.10).

hydrophobic, and as such, better suited to partitioning from the aqueous environment in the GIT lumen into the intestinal epithelium.

The observed pattern of 0.97 μm diameter latex microsphere transfer from the gut to systemic circulation has similarities with that produced by earlier investigations using 0.87 μm diameter Fluoresbrite™ particles (chapter 3) i.e. initially elevated levels which decline over the first 4 hours after oral dosing. The very low numbers, under 0.14 % of the initial dose at early time points, present in the blood compared to earlier studies reinforce suspicions about the quantitative reliability of previous work. However, AUC treatment of the systemic blood uptake profile for 0.97 μm Polybeads® indicate an equivalent of 0.061 mg latex hours was circulating over the first four hours of the experiment. This compares with 0.255 mg latex hours resulting from a single gavage of 0.87 μm Fluoresbrite™ carboxylate microspheres at a concentration of 25 mg / ml. GPC analysis of heart blood taken from rats given 0.22 μm Polybeads® results in an AUC value of 0.384 mg latex hours over the first 240 minutes after gavage. Thus by extrapolating AUC values from data obtained by different methods of quantification a reasonable comparison between the different levels of particulate absorption may be made. While differences in blood microsphere levels exist from one experiment to another, by comparing AUC values its clear that the overall levels of absorption are not vastly dissimilar although they do reflect important differences in test particle size and composition.

High levels of latex were detected in systemic blood 24 and 96 hours after administering the 0.97 μm Polybeads®. As latex levels in the portal supply are depleted then this may represent a polystyrene contribution from the lymphatic compartment. Of course this may also occur at very early time points after oral dosing as demonstrated by Jenkins *et al .*, (1994) (see section 1.2.6.1).

4.4.4.2 LATEX PARTICLE UPTAKE BY THE LIVER AFTER ORAL ADMINISTRATION

It is well documented that the liver is an extremely potent accumulator of microspheres after i.v. injection (Kreuter *et al .*, 1979 and 1983, Singer *et al .*, 1969). For example, Yamaoka *et al .*, (1993) found that 74 % of ¹²⁵I labelled nanospheres (109 nm diameter) had accumulated in that organ 3

hours after i.v. injection. 70 % of the microspheres trapped in the liver were located in the non-parenchymal cells, especially the Kupffer cells (see 1.2.6.2). Studies investigating the oral uptake of microspheres have also highlighted its efficiency at retaining particles. Jani *et al.* , (1990) detected 3.8 % of an oral dose of polystyrene microspheres (100 nm) within the liver two days after the last administration. At Aston University's drug development research group, Stagg (1994) found that about 5 % of a single oral dose of 0.22 μm latex nanospheres, could be detected in the livers of rodents with experimentally induced inflammatory air pouches, 24 hours after gavage. Stagg, (1994) used GPC to quantify nanoparticle translocation from the GIT. Elsewhere, in histological studies, Jani *et al.* , (1992 and 1989) showed unequivocal evidence of microsphere accumulation within hepatic tissue. Microspheres were seen mainly in the Kupffer cells, the endothelial lining and the Space of Disse after oral dosing. Earlier, Saunders *et al.* , (1961) observed 220 nm diameter latex microspheres within hepatic sinusoids 2 hours after oral administration to rats.

Whole livers removed from rats after oral administration of latex Polybeads[®] were found to contain substantial amounts of polystyrene using GPC technology (figures 33 and 41). This was true for both 0.22 μm and 0.97 μm diameter particles. Calculation of polystyrene accumulation *per* gram of liver (figures 38 and 46) and comparison with other internal organs reveals only a modest propensity to accumulate. This highlights its massive size in comparison to other compartments. Polystyrene accumulation in the liver at early time points after oral dosing with 0.22 μm diameter beads is seen to be comparable, although sometimes less than, spleen and lungs (figure 38). This is somewhat surprising as the liver would be the first and largest MPS organ encountered by microspheres in the hepatic vein and might of been expected to accumulate to a greater extent (see section 1.2.6.2). However it is possible that the size and relatively protracted length of time of the initial event may have 'bombarded' the organ with particles, temporally reducing the livers phagocytic capacity. When Singer *et al.* , (1969) injected 230 nm latex particles i.v., the liver accumulation after five minutes was only 29 %. Sixty minutes later this figure was 77 %, indicating that the liver required time to achieve maximal uptake.

At 45 minutes after administration of 0.22 μm diameter test latex, liver uptake is comparable with that at 15. At the 4 hour time point a slight

elevation in liver polystyrene content is seen, the significance of which is unknown, but may reflect a re-distribution of particles amongst the various organs. 24 hours after administration a depletion in liver polystyrene levels is seen, possibly due to excretion of particles through the bile duct. Excretion of polymethyl methacrylate nanoparticles in bile duct cannulated rats was reached a maximum within 1 hour of peroral administration by Nefzger *et al.* , (1984). From one hour after dosing bile excretion of the particles declined in a hyperbolic fashion. Biliary excretion of polystyrene microspheres after oral administration to rats was also found to be rapid (Jani *et al.* , 1995). 9 % of a single oral dose of 50 nm FITC labelled microspheres were detected in draining bile 6 hours after gavage. In our studies, the low levels of polystyrene in the liver at 24 hours compared with the elevated numbers in the blood is difficult to explain without the un-likely conclusion that the liver is failing to accumulate circulating particles. This trend is reversed at 4 days after dosing which may imply that a secondary wave of particles has reached the circulation. Alternatively, entero-hepatic circulation of some particles may occur.

Polystyrene levels within livers removed from rats gavaged with 0.97 μm diameter particles orally were statistically comparable with polystyrene levels in livers removed from rats gavaged with 0.22 μm spheres at all but the 45 minute time point (Table 5a). 45 minutes after gavage of the 0.22 μm particles, $3.63 \pm 1.72 \mu\text{g}$ was detected *per* gram of liver tested. This compares to $10.05 \pm 7.696 \mu\text{g}$ of the 0.97 μm diameter latex particles in each gram of liver at the same time point. This represents a statistical difference ($P \leq 0.05$) when the two sets of data are compared with a two-tailed unpaired t-test. Throughout the 4 day experimental period liver accumulation of 0.97 and 0.22 μm diameter particles is statistically identical when compared using a 2-way analysis of variance test (ANVOA). Thus it appears that although overall uptake of 0.97 μm diameter particles is low, the liver accounts for a much higher fraction of absorbed latex in comparison to the 0.22 μm particles. This could suggest that 0.97 μm particles are better entrapped by hepatic infrastructure in comparison to 0.22 μm test particles. It may also be the case that 0.22 μm sized test particles are more efficiently captured by other MPS compartments, especially the spleen. Experiments in which latex particles are injected as bolus into the blood stream seem to suggest that sub micron sized particles are more effectively trapped by the liver. Mean hepatic accumulation three hours after

i.v. administration of 1.09 and 0.109 μm diameter latex particles was 83.5 % and 74.1 % respectively (Yamaoka *et al.* , 1993).

The lower level of polystyrene detected in livers removed 4 hours after oral administration of 0.97 μm latex particles indicates that elimination of entrapped 0.97 μm particles may be quite rapid. Nefzger *et al.* , (1984) drew a similar conclusion (see text above). At the 1 and 4 day time points whole liver polystyrene content in rats gavaged 0.97 μm diameter particles was of a similar order to that in lung and kidney, although comparison of uptake *per* unit mass suggests the liver does not retain intestinally absorbed particles of this size.

4.4.4.3 LATEX PARTICLE UPTAKE BY THE SPLEEN AFTER ORAL ADMINISTRATION

GPC analysis of tissues removed from rats who received a single oral dose of 0.22 μm diameter latex particles, implicates the spleen as an organ with a high capacity for microsphere accumulation. Nanosphere uptake into the spleen was found to be both rapid, and highly efficient (figure 33). Comparison of polystyrene uptake gram *per* gram of tissue (figure 38) reveals the spleen to be by far the most efficient accumulator of the MPS organs at all the time points examined. At early time points after dosing, 15 minutes to 4 hours, the spleen shows a fairly constant overall level of uptake , although its efficiency appears to increase slightly up to 4 hours. Even at later times, 24 hours and 4 days, the spleen contains considerable, although slightly depleted, amounts of polystyrene.

Spleens removed from rodents gavaged with 0.97 μm diameter latex particles also contained significant amounts of polystyrene (figure 42) In terms of uptake *per* unit mass of tissue, the spleen is the best accumulator of 0.97 μm latex particles after oral administration at all but the last time point investigated (figure 46). These findings are similar to those studies where colloidal particles are injected i.v and the spleen's clearance capacity *per* gram of tissue was found to be greatest (Yamaoka *et al.* , 1993).

Jani *et al.* , (1990) found that about 0.7 % of an oral dose of 100 nm diameter microspheres had accumulated within the spleen two days after the last oral administration. Ebel, (1990) also found considerable numbers of fluorescent latex beads (2.65 μm diameter) within the spleen, 24 hours after

oral administration. In this present study, up to 0.27 % of the oral dose of 0.22 μm nanospheres could be detected *per* gram of spleen tissue. Histological studies by Jani *et al.* , (1992) demonstrated that microspheres accumulated in the trabeculae of the spleen. The sinuses of the spleen are lined by spleen sinus macrophages which would be expected to accumulate latex in a similar way to the Kupffer cells of the liver. In the spleen however, blood flow is impeded by an endothelial border which acts a sieve. Thus, splenic capture is due to mechanical filtration as well as MPS sequestration, and is particularly effective for particles with diameters between 200 and 300 nm (Moghimi *et al.* , 1991) (see section 1.2.6.2).

4.4.4.4 LATEX PARTICLE UPTAKE BY THE LUNG AFTER ORAL ADMINISTRATION

Uptake of 0.22 μm diameter polystyrene by the lung was found to be greatest only 15 minutes after oral administration. At later time points the amount of polystyrene recovered from the lungs was found to be substantially lower. This was true even at the 45 minute time point. Studies on the organ distribution of nanospheres after i.v. injection by Adlersberg *et al.* , (1969) and Singer *et al.* , (1969), using ^{125}I particles of a similar size, showed that 5 minutes after administration, 16 % of the dose was found in the lung. This value fell to 3 %, 30 minutes after injection. The reason for this initial accumulation was thought to be the formation of particle aggregates with the blood contents. This is because individual microspheres in the submicron - size range are not expected to be trapped in lung capillaries. These embolus - like formations were seen to disintegrate after about 15 minutes (Kreuter, 1983). This phenomenon could explain the initially high polystyrene content of the lungs seen at such a short time after oral administration in our study. The amount of polystyrene detected in the lungs at later time points probably represents the microsphere content of the lung's circulating blood. In his studies Adlersberg *et al.* , (1969) noted an increase in lung activity 24 hours after injection of the nanospheres. He attributed this radioactivity to the redistribution and recirculation of phagocytic cells and their particle content. He suggested that the particles also re-entered the circulation by reverse phagocytosis and were picked up by the locally proliferated phagocytic cells in the lungs (Kreuter, 1983). In our investigation, slightly elevated lung polystyrene content was observed 4 days after oral administration of the 0.22 μm particles.

Accumulation of 0.97 μm diameter latex microspheres within lung tissue after oral administration was found to be rather low at the early time points (15, 45 and 240 minutes after gavage) (figure 41). However, by 24 hours post administration, lung accumulation was considerable in comparison to other monitored tissues. At this time point, polystyrene accumulation *per* gram of lung was nearly the same as spleen (figure 46). This elevation in lung levels of latex 24 hours post dosing may reflect redistribution and re-circulation of phagocytic cells and their particle content as visualised by Adlersberg *et al.*, (1969) (see paragraph above).

4.4.4.5 LATEX PARTICLE UPTAKE BY THE KIDNEYS AFTER ORAL ADMINISTRATION

Kidney accumulation of 0.22 μm diameter polystyrene latex nanospheres initially increased with time after oral delivery. At 24 hours after administration very little 0.22 μm latex was detected within the kidneys, although at 4 days the levels had risen again. At all time points significantly less 0.22 μm diameter polystyrene latex was recovered from this organ than the spleen. Surprisingly uptake *per* unit mass was comparable with the liver and lungs throughout the experiment. This could indicate a moderate propensity to accumulate, or simply detection of microspheres within its vasculature or MPS component (see below).

Accumulation of 0.97 μm diameter polystyrene microspheres within the kidneys was low at all but the 4 day time point after oral administration (figures 41 and 46). This result is somewhat un-expected, but not unfounded when considering that low numbers of 0.97 μm particles were observed within the urine of some treated animals. As low numbers of these particles can enter the uriniferous tubules of the kidney then it may be possible some beads become immobilised whilst traversing the filtration barrier of the renal corpuscle, or further downstream. The presence of intraglomerular mesangial macrophages, which are part of the MPS, in the kidney may also account for some degree of particulate sequestration (Roitt *et al.*, 1985).

Latex microspheres were observed within the lumen of glomerular capillaries, after oral dosing, by Saunders *et al.*, (1968) using electron

microscopy. Jani *et al.*, (1990) detected a low number of the very smallest (50 nm) nanospheres in the kidney after chronic oral dosing.

4.4.4.6 LATEX PARTICLE EXCRETION IN THE URINE AFTER ORAL ADMINISTRATION

The presence of polystyrene microspheres in rat urine collected up to 24 hours after their oral administration (figures 34 and 42), suggests that excretion of small numbers of orally absorbed particles occurs by this route. It also provides further evidence that orally absorbed microspheres enter the kidney (see above). After i.v. injection Kreuter *et al.*, (1979) found about 1 % of the poly (methyl methacrylate) nanoparticles had been expelled by this mechanism after 7 days. Nefzger *et al.*, (1984) found 4 - 6% of a peroral dose of nanoparticles within the urine after 8 days. Maximal urinary excretion was observed 2 hours after dosing followed by a hyperbolic decline. Stagg, (1994) found that 0.19 % of a single oral dose of 0.22 μm diameter latex nanospheres had been excreted in the urine within the first 24 hours of administration. Volkheimer, (1993) and Gitzelmann *et al.*, (1993) have demonstrated repeatedly the appearance of starch grains and other relatively large particulates, rapidly, in the urine of patients and animals who received an oral dose of such materials.

The fact that orally absorbed inert microparticulates were excreted within the urine seems, at first, inconsistent with the size constraints imposed by the filtration barrier within the kidney. The renal corpuscle behaves as a filtering device that allows water and ions to pass but retains large objects like cells or large protein molecules. However, the glomerular endothelium contains fenestrae which are larger (about 100 nm) than elsewhere in the body. Glomerular fenestrae generally lack diaphragms, which also increases endothelial permeability, and combined with the very high filtration pressure along the capillary bed will allow small proteins like albumin to enter the filtrate (Bulger, 1988). As such, although 0.97 and 0.22 μm diameter particles are well above the effective pore size of the glomerular filter the fact that a low percentage of the absorbed particles exit the body in this manner may be just as acceptable as the concept of intestinal translocation.

4.4.4.7 LATEX PARTICLE UPTAKE BY THE MESENTERY AFTER ORAL ADMINISTRATION

Substantial numbers of 0.22 μm diameter nanospheres were detected within the mesenteric lymph node and surrounding tissue at 45 minutes and 4 hours after oral administration. Lesser numbers were detected at 15 minutes, 24 hours and 4 days (figure 34).

The presence of microspheres within the lymphatic network of the mesentery would suggest that their uptake from the intestinal lumen had occurred *via* GALT, in particular the PPs (see sections 1.24 and 1.261). Many reports have been published documenting the translocation of inert particulates to the MLN (LeFevre *et al.*, 1989, 1978, Jani *et al.*, 1992, 1990, 1989, Ebel, 1990 and Wells *et al.*, 1987, 1988) and some authors regard transport of particles beyond this tissue as artefact (LeFevre *et al.*, 1989). Jani *et al.*, (1992) observed 500 nm diameter microspheres within the MLN 6 hours after gavage. Sass *et al.*, (1990) observed 500 nm diameter latex beads inside macrophages underneath the dome of lymphatic follicles within 10 minutes of intestinal delivery. In elaborate studies by Jenkins *et al.*, (1993) intraduodenal administration of fluorescent latex beads (0.15 - 10 μm diameter) resulted in a percentage of the particles appearing within draining mesenteric lymph within five minutes of dosing (see section 1.261). Thus, the accumulation of latex within the mesentery after only 15 minutes seen in our experiments is corroborated by other authors. It is also possible that a very small percentage of the polystyrene detected in mesenteric tissue may account for microspheres trapped within the vasculature at the time of dissection. The amount of 0.22 μm nanosphere polystyrene detected within the MLN at the 45 and 240 minute time points is 3 times that of the spleen. This substantial accumulation within the mesentery represents a significant uptake. At later time points the amount of polystyrene extracted from the mesentery is comparable with that in the spleen or liver. The depletion in nanoparticle numbers within the mesentery 24 hours after oral administration could be accounted for by lymphocyte migration to the circulation through the thoracic duct.

Mesenteric accumulation of 0.97 μm microspheres after oral delivery is significantly lower than for 0.22 μm before 24 hours (figure 42). Maximal numbers of 0.97 μm diameter particles were extracted from MLN removed from rats 24 and 96 hours after oral administration. At the 4 day time point

the amount of 0.97 μm latex recovered from the mesentery ($19.71 \pm 12.5 \mu\text{g}$) was greater than any other tissue. The persistence of polystyrene latex within the mesentery may be indicative of lymphatic uptake and nodal retention of particles from the GIT lumen.

4.4.4.8 LATEX PARTICLE UPTAKE BY THE INTESTINES AFTER ORAL ADMINISTRATION

A high concentration of 0.22 μm diameter polystyrene latex nanospheres was detected in the small intestinal mucosa and submucosa at early time points after oral delivery. Gut washes removed the vast majority of adherent microspheres (figure 36), however it seems probable that some particles remained closely associated with the tissue or became embedded within it during the procedure. Still the data obtained suggests that a large number of nanospheres had penetrated the epithelial layer of the small intestine or at least become intimately associated with the organ. Less 0.97 μm latex was detected at 15, 45 and 240 minutes compared with 0.22 μm , although over the 4 day experimental period small intestinal accumulation of both latex particle sizes was statistically comparable (2-way ANOVA).

Polystyrene detected within the intestine is likely to have accumulated within GALT or be trapped within the extensive vascular network after uptake. The highest concentrations of 0.22 μm diameter polystyrene were detected within the small intestine very early after oral administration (15 and 45 minutes). Enterocyte endocytosis (see section 1.2.2) of the 220 nm beads could account for the high levels of latex within the intestinal mucosa at such a short time after dosing. Excretion of these absorbed nanospheres by reverse endocytosis would then account for the decline in absorbed intestinal latex at the 4 hour time point (481 μg after 4 hours, with the levels steadily falling from then on.).

0.22 μm diameter polystyrene recovered from the intestinal washes indicates that very early after oral administration (15 minutes), some of the particles had failed to exit the stomach. At 45 minutes, most particles had entered either the small or large intestine. 4 hours after dosing considerable numbers of 0.22 μm diameter particles were still present within the small intestinal lumen, despite recording poor uptake into the mucosa. Davis *et al* ., (1986) have demonstrated that solutions, pellets and single units have a

small intestinal transit time of approximately 3 hours with a standard deviation of about 1 hour. The pattern of latex nanosphere small intestinal transit appears to be similar. Low levels of polystyrene nanospheres were still persistent in the small intestinal lumen after 24 hours (170 µg) and 4 days (15 µg). This observation may represent polystyrene excreted into the lumen through the bile duct. 0.22 µm diameter polystyrene persistence in the intestinal mucosa at the 1 and 4 day time points was found to be 62 µg and 50 µg respectively. These values for polystyrene could represent microspheres within PPs and GALT. Elimination of these microspheres, and those in the large intestinal mucosa, through lymphatic or vascular pathways may account for the hypothesised 'second wave' of 0.22 µm diameter particle accumulation within the MPS observed at 4 days (figure 33).

In the case of 0.97 µm diameter microspheres, polystyrene levels within the small intestinal mucosa were considerably lower than for the 0.22 µm diameter nanospheres at 15, 45 and 240 minutes (figure 43, 44). This quite probably reflects the obvious differences in size and hydrophobicity of the two test particles. Again, only a proportion (46 % for the 0.22 µm beads) of the 21.7 mg of latex was detected in the washings at the 15 minute time point indicating incomplete gastric emptying.

Small numbers of nanospheres and microspheres were detected in the large intestinal gut washes only 15 minutes after dosing. This is indication of the rapidity with which the particles negotiate the alimentary canal. It also suggests that the time taken for orally delivered particles to come into close contact with the large numbers of PPs and other potential uptake sites in the lower small, and large intestines is relatively short after gavage in conjunction with large volumes of liquid.

Four hours after administration of 0.22 µm microspheres, 160 µg of polystyrene was recovered from the tissues comprising the large intestines. These are the caecum, colon, appendix and visible aggregates of lymphoid tissue. The amount of 0.22 µm diameter latex recovered from these tissues at 24 hours had increased to an average of 488 µg. Over 11 mg of 0.22 µm polystyrene nanospheres was present in the large intestinal lumen at this point in time, consistent with the findings of Davis, (1989) stating that a controlled-release dosage form is likely to spend most of its time within the large intestine. Four days after administration, 67 µg of polystyrene latex

was recovered from the large intestine itself with about 50 µg still left in the lumen. Hillery *et al.*, (1994) has identified the large intestines as an important site of microsphere translocation from the lumen. In their studies, 3.0% of the oral dose of 50 nm microspheres were detected in the lymphatic regions of the large intestine. 2.1% was detected in the non-lymphatic area, even though its mass is much greater. In GPC studies by Jani *et al.*, (1990) 3.4 % of a chronic oral dose of 100 nm nanospheres was detected within the small intestines and mesenteric lymph node two days after cessation. In the same study, the large intestines had accumulated about 16 % of the dose. In our studies, about 2.2 % of the oral dose of 220 nm particles was detected within the large intestinal mucosa 24 hours after administration. Small intestinal and MLN uptake of the 0.22 µm particles was about 0.3 % at that time point.

Large intestinal accumulation of the 0.97 µm diameter microspheres was much lower than the 0.22 µm particles at all time points examined ($P \leq 0.001$). Maximal uptake into the large intestinal mucosa occurred at the 4 hour time point and accounted for only 101.6 ± 55.9 µg of the 21.7 mg dose. 51.7 ± 25.2 µg was recovered from large intestinal material removed 24 hours after dosing. 6.0 ± 2.8 µg of 0.97 µm latex remained at 4 days.

The pattern of 0.97 µm diameter transit along the alimentary canal was found to be slightly different to that of the smaller beads. A larger percentage of 0.97 µm particles were detected within the large intestinal lumen at the four hour time point in comparison to the 0.22 µm beads (72 compared to just 53 % for the 0.22 µm particles). At 24 hours, considerably fewer of the 0.97 µm particles were detected within the large intestinal lumen, suggesting that many had been excreted within the faeces. At the same time point, large intestinal washings were found to contain large numbers of 0.22 µm latex particles. Such findings suggest that the large intestinal residence time for the 0.97 µm diameter polystyrene test particles may be shorter than for the 0.22 µm diameter Polybeads[®]. It could be that the 0.97 µm beads may have a greater degree of association with the large intestinal gut contents and developing faeces. Conversely, it may be that the more hydrophobic 0.22 µm latex beads tend to associate with the intestinal mucosa to a greater extent.

4.4.4.9 LATEX PARTICLE EXCRETION IN THE FAECES AFTER ORAL ADMINISTRATION

GPC examination of faeces collected 24 hours and 4 days after oral administration of 21.7 mg polystyrene nanospheres (0.22 μm diameter) indicated that over 91 % of the particles were excreted in this way. 61.7% of the dose was found in faeces excreted before 24 hours after administration. An average of 1.83 % of the oral dose remained in monitored tissues at 4 days. This leaves an average discrepancy of about 7 % or 1.5 mg. Reasons for this error might include inter - animal variation, incomplete collection of all the faeces, small variations in the administered dose and the possible uptake of latex into un-metered tissues.

Examination of faeces collected from rodents given a single oral dose of 21.7 mg of 0.97 μm diameter polystyrene latex microspheres revealed that on average 90 % of the microspheres had been eliminated in this way. About 63 % of the dose was eliminated in the faeces before the 24 hour time point. An average of 1.57 % of the initial dose was detected in tissues and washes at the 4 day time point. This leaves an average discrepancy of about 8.5 % or 1.8 mg of latex to be accounted for.

4.4.5 CONCLUSION

In conclusion, the data obtained in this experimental chapter suggests that while absorption of inert particulate matter from the GIT lumen is quantifiable it is low and tends to be highly variable. In line with similar studies, translocation was found to be highly dependent on particle size. An AUC value for the transfer of 0.97 μm diameter latex microspheres into extra-intestinal sites was estimated at 12.983 mg latex hours over the 4 day experimental period compared to 34.871 mg latex hours for 0.22 μm particles. With data represented graphically (see figure 53 below) its clear that while a considerable proportion of the initial dose may be detected within monitored tissues at the 15 and 45 minute time points, much lower levels remain within these body compartments at later times. This indicates that while this work has identified an initial rapid absorption of material, particularly into the intestinal mucosa and vascular compartments, the majority of these absorbed particles are eliminated rather rapidly. However, it seems that absorbed particulates that are not rapidly eliminated in the first few hours after oral delivery, tend to persist

within both intestinal and non intestinal sites for at least four days and probably longer. Such findings mirror those of Le Ray *et al.*, (1994), although a direct comparison may be inappropriate due to the obvious differences in particle type, and means of detection. In their study, 2.4 % of recoverable radioactivity was detectable in extra-intestinal tissues one hour after oral administration of ^{14}C labelled PLA nanoparticles with milk. At 4 hours this had fell to around 1.6 %, declining to 1.4 % and 0.8 % at 24 and 48 hours respectively.

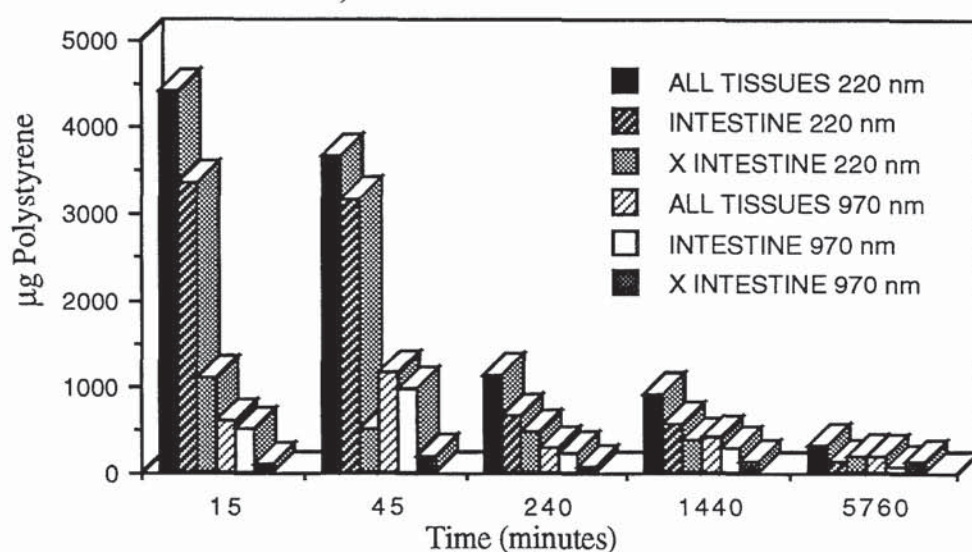


Figure 53. Cumulative uptake of polystyrene particles into extra-intestinal (X INTESTINAL) and intestinal tissues at time points after oral delivery of 21.7 mg 0.97 μm or 0.22 μm diameter latex particles in the rat model.

The data compiled for this experimental chapter strongly supports previous findings (Jani *et al.*, 1990) regarding the size dependent nature of particulate translocation into extra-intestinal sites. Statistically more ($F \leq 0.05$ using 2-way ANOVA) 0.22 μm particles entered extra-intestinal tissues during the 4 days after administration than 0.97 μm diameter microspheres. Chronic oral administration (12.5 mg / kg) for 10 days, resulted in 5.84 and 2.69 % of the 100 and 200 nm latex test particles being absorbed into extra-intestinal organs (Jani *et al.*, 1990). In the same study, 0.78 % of the 1.0 μm diameter test microspheres were recovered from these tissues. In our studies, 24 hours after single gavage of 0.22 μm latex microspheres, about 1.78 % of the 21.7 mg dose was recovered from extra-intestinal tissues. 0.61 % of the 1.0 μm diameter polystyrene microspheres were detected in

these tissues at the 24 hour time point. Such comparisons indicate that lower, although comparable, amounts of particulate matter are present in these tissues 24 hours after a single administration compared with 24 hours after a consecutive 10 day administration. Of course, the levels of latex recovered from extra-intestinal tissues at early (15, 45 and 240 minutes) time points after a single oral administration are much higher (5.0 %, 2.2 % and 2.1 % respectively). As such, it is not clear if repeated administration enhances GIT absorption and extra-intestinal accumulation of particulate matter, or if the rate of particle elimination from extra-intestinal tissues is lower than the rate of particle deposition during the multiple absorptive events induced by chronic administrations. Our findings indicate that while the majority of absorbed particles are rapidly eliminated from extra-intestinal sites after a single oral dosing, a percentage (about 1 % for the 0.22 μm microspheres) persists for at least four days and probably longer. Thus, if multiple doses are administered there may be 'build up' of these un-eliminated microspheres within systemic compartments.

5.0 MECHANISMS OF ABSORPTION OF PARTICULATE MATTER FROM THE GIT

5.1 INTRODUCTION

Clearly the gastrointestinal mucosa is an imperfect barrier to a very small fraction of insoluble particulates that negotiate the alimentary canal (chapters 3 and 4). Several postulated absorption models have been described in the literature (reviewed in chapter 1). Some relate observations to known physiological processes, while others rely on as yet less accepted theories and concepts of particulate translocation. A major goal of this research undertaking was to gain some more insight into the actual mechanics behind this interesting phenomenon. Of course, many parts of the jig-saw are already in place courtesy of other researchers (Saunders *et al.*, 1961, Jani *et al.*, 1989, Volkheimer, 1968, Aprahamian *et al.*, 1987, LeFevre *et al.*, 1978a, Pappo *et al.*, 1991, Jepson *et al.*, 1994, Sass *et al.*, 1990, Jenkins *et al.*, 1994 and Wells *et al.*, 1987). However, as our results both reinforce the findings of some previous publications, yet suggest that less well understood processes may be involved, there appears to be gaps which require definition if not clarification. The construction of any elaborate, all encompassing, model which exactly describes the real time events behind microsphere translocation from the GIT lumen is probably inappropriate after three years work. However, by using histological methods to visualise the spatial distribution of labelled material within the intestinal lamina propria of treated animals and the parallel use of metabolic inhibitors which can blockade certain uptake pathways, some relevant information has been obtained.

5.2 MATERIALS AND METHODS

5.2.1 HISTOLOGICAL STUDIES INVESTIGATING MICROSPHERE UPTAKE AND TRANSLOCATION FROM THE GIT AFTER ORAL ADMINISTRATION

Tissue biopsies were processed for histological examination as described in section 2.7.5. Tissues were taken from a variety of sacrificed rats that were treated orally with FITC labelled Fluoresbrite™ carboxylate microspheres of 0.87 μm diameter. Treated animals included those used in chapter 3, section 4.25 and a group of four rodents treated as described below:

Each of the four rats was received a single oral dose of 2.5 mg (~0.1 ml stock) 0.87 μm Fluoresbrite™ carboxylate microspheres using a gavage needle and syringe. At 5, 15, 45 and 60 minutes after administration one of the group of four was removed and sacrificed by cervical dislocation. The animal was then dissected and tissue samples (liver, spleen, mesentery and GIT) removed for histological treatment as described (see section 2.7.5). Histological sections were examined using fluorescence microscopy (section 2.4.1) and if necessary, photographed as described in section 2.4.2.

5.2.2 INVESTIGATIONS INTO THE TRANSLOCATION OF 220 nm DIAMETER MICROSPHERES FROM ILEAL AND DUODENAL GUT LOOPS IN THE PRESENCE AND ABSENCE OF CYTOCHALASIN B

In one group of eight rats, isolated duodenal loops were prepared as described in section 2.8.3. 1 ml of water containing 21.7 mg of 220 nm diameter Polybead® nanospheres was then introduced into the isolated gut segment as described in section 2.8.3. Of the 8 rats in the experimental group, 4 were given the particles in conjunction with cytochalasin B (Sigma, Poole, U.K). In the latter case cytochalasin B was mixed into the nanosphere suspension, prior to administration and vortexed, at a concentration of 21 μM . At several time points after administration (15, 45, 90 and 120 minutes) tail vein blood samples were removed from the anaesthetised animals and placed into pre-weighed glass conical flasks. Approximately 1 -2 ml of blood was removed at each time point. After the two hour time point all anaesthetised rats were sacrificed. Blood samples were taken for polystyrene content analysis using GPC (see section 2.7.4).

In a second group of eight rats isolated ileal loops were prepared as described in section 2.8.3. Again 1 ml of water containing 21.7 mg of 220 nm diameter Polybead[®] nanospheres was then introduced into the isolated gut segment as described in section 2.8.3. Four rats in the group were given particles mixed with cytochalasin B as before (concentration 21 μ M). 15, 45, 90 and 120 minutes after introduction of the nanospheres, in the presence and absence of cytochalasin B, tail vein blood was sampled from the halothane anaesthetised animals. Just after the two hour time point the animals were sacrificed and dissected. Liver and spleen samples were taken from each of the rats and placed into a pre-weighed glass conical flask, together. The mesentery and mesenteric lymph node was also excised and placed into a pre-weighed glass conical flask. After these tissues had been removed, the entire particle containing isolated gut section was excised. The two Peyer's patches which were present in the particle exposed segment of GIT were carefully micro-dissected away from the rest of the intestine. These two pieces of lymphoid tissue were then extensively washed in isotonic saline to remove adherent polystyrene particles. This involved placing the PPs into a 30 ml universal tube containing isotonic saline, and gently shaking for 30 seconds. The patches were then removed and exhaustively washed with a strong jet of saline dispensed from a syringe with hypodermic needle attached. The luminal side of the lymphoid follicle received particular attention. Once washed, patch tissue was placed into a pre-weighed conical flask. In addition to patch tissue from the particle exposed intestinal segment, a similarly sized piece of non patch tissue was removed. The non patch piece of intestine was washed and treated in the same way as the lymphoid follicles before being placed into another pre-weighed glass conical flask. For these intestinal tissue samples, the dry weight of each tissue was recorded after freeze drying. Otherwise, all blood samples and tissues were then taken for GPC analysis as described in section 2.7.4.

5.3 RESULTS

5.3.1 HISTOLOGICAL EVIDENCE OF MICROSPHERE UPTAKE AND TRANSLOCATION FROM THE GIT AFTER ORAL ADMINISTRATION

The results from histological examination of tissues from animals treated orally with FITC labelled carboxylated polystyrene microspheres are represented as a series of photomicrographs (figures 54 to 64). These data are discussed in depth in section 5.4.

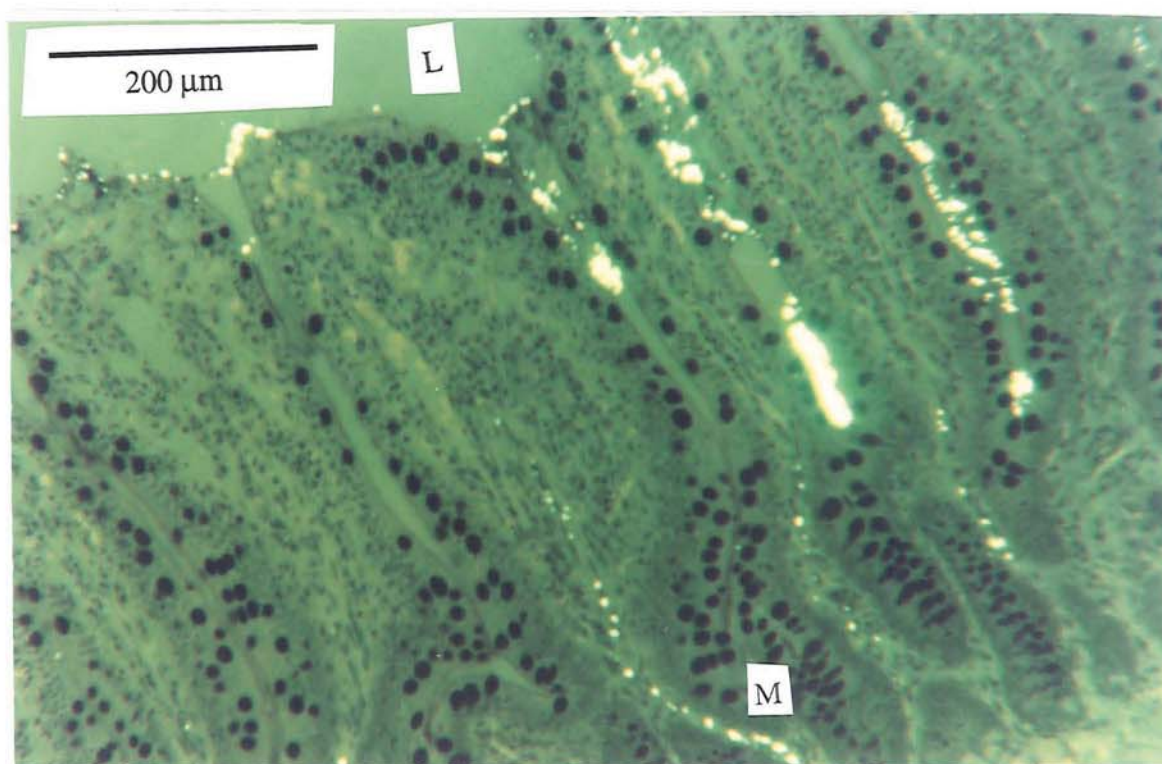


Figure 54. Plastic embedded jejunal / duodenal biopsy taken 15 minutes after oral administration of 2.5 mg 0.87 μm Fluoresbrite™ carboxylate microspheres. The majority of test particles are associated with mucus within the intestinal lumen (L). A proportion of the microsphere (M) dose appears to have entered the intestinal mucosa. These particles are arranged linearly within the villus, suggesting they may be contained within vascular or lymphatic vessels (x100 Total magnification; Longitudinal section; UV light source; Bar=200 μm).

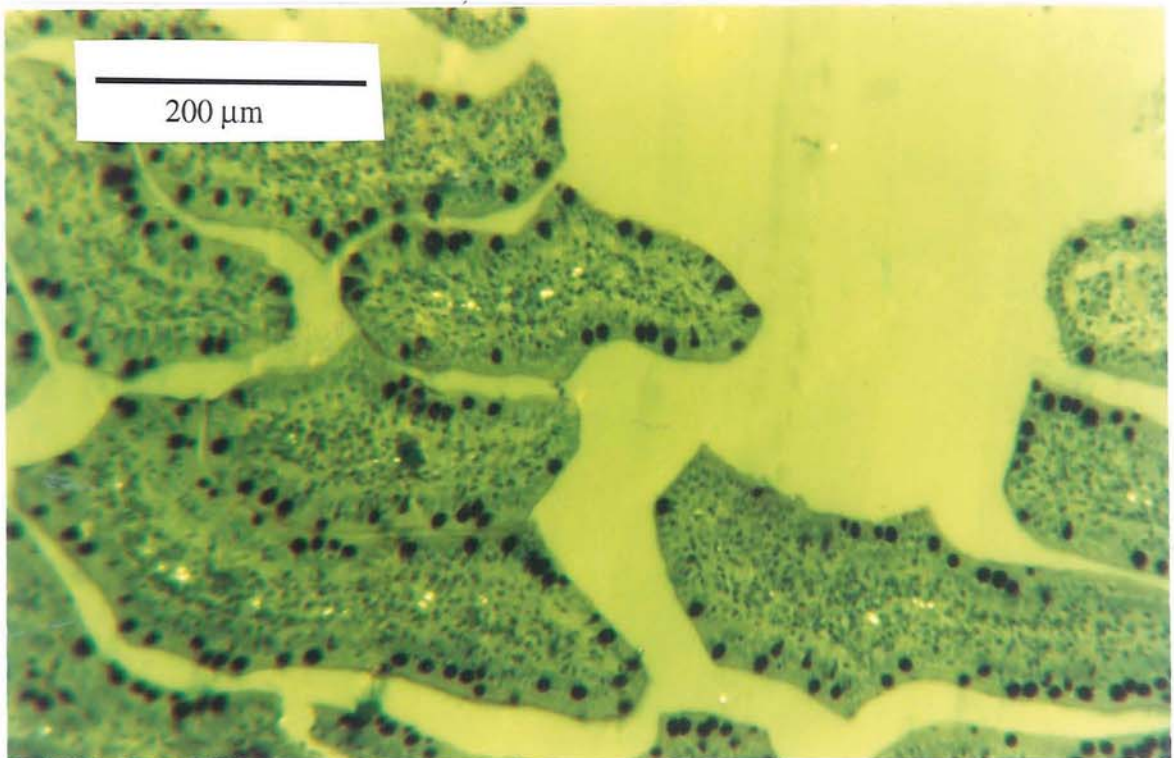


Figure 55. Plastic embedded jejunal / duodenal biopsy taken 15 minutes after oral administration of 2.5 mg 0.87 μm Fluoresbrite™ carboxylate microspheres. As in figure 54, the spatial distribution of microspheres within the intestinal mucosa does not follow a random pattern, but suggests that particles are conveyed from uptake sites at the villus tips within defined anatomical structures (x100 Total magnification; Transverse section; UV light source; Bar=200 μm).

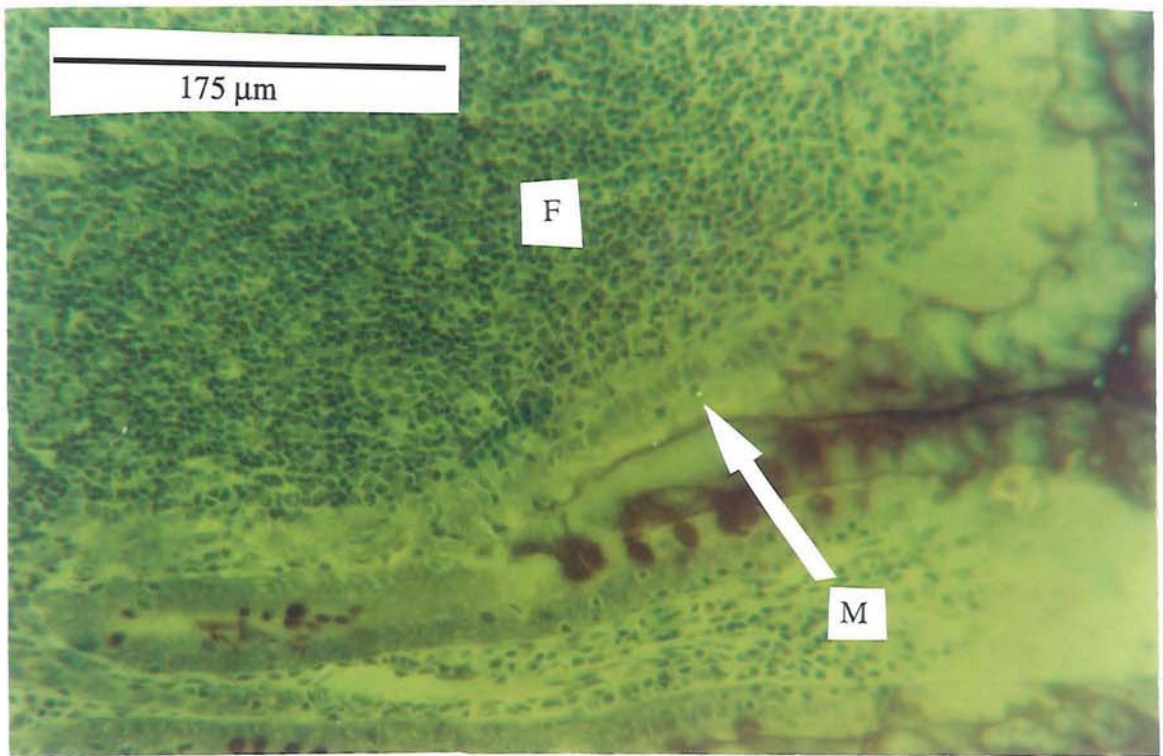


Figure 56. Plastic embedded ileal biopsy taken 45 minutes after oral administration of 2.5 mg 0.87 μm Fluoresbrite™ carboxylate microspheres. Microspheres (M) are visualised in the process of absorption into a lymphatic follicle (F). (x160 Total magnification; UV light source; Bar=175 μm).

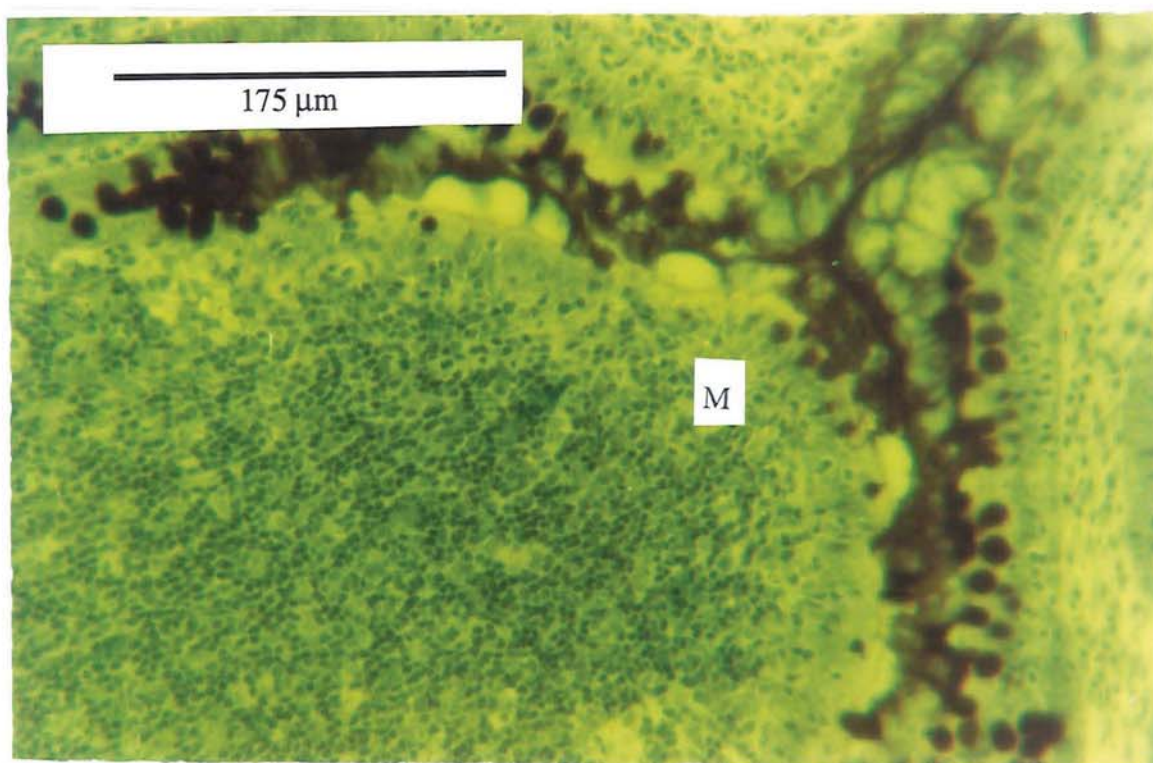


Figure 57. Plastic embedded ileal biopsy taken 45 minutes after oral administration of 2.5 mg 0.87 μm Fluoresbrite™ carboxylate microspheres. Similar photomicrograph to figure 55, only microspheres (M) are located below the follicle associated epithelium (x160 Total magnification; UV light source; Bar=175 μm).

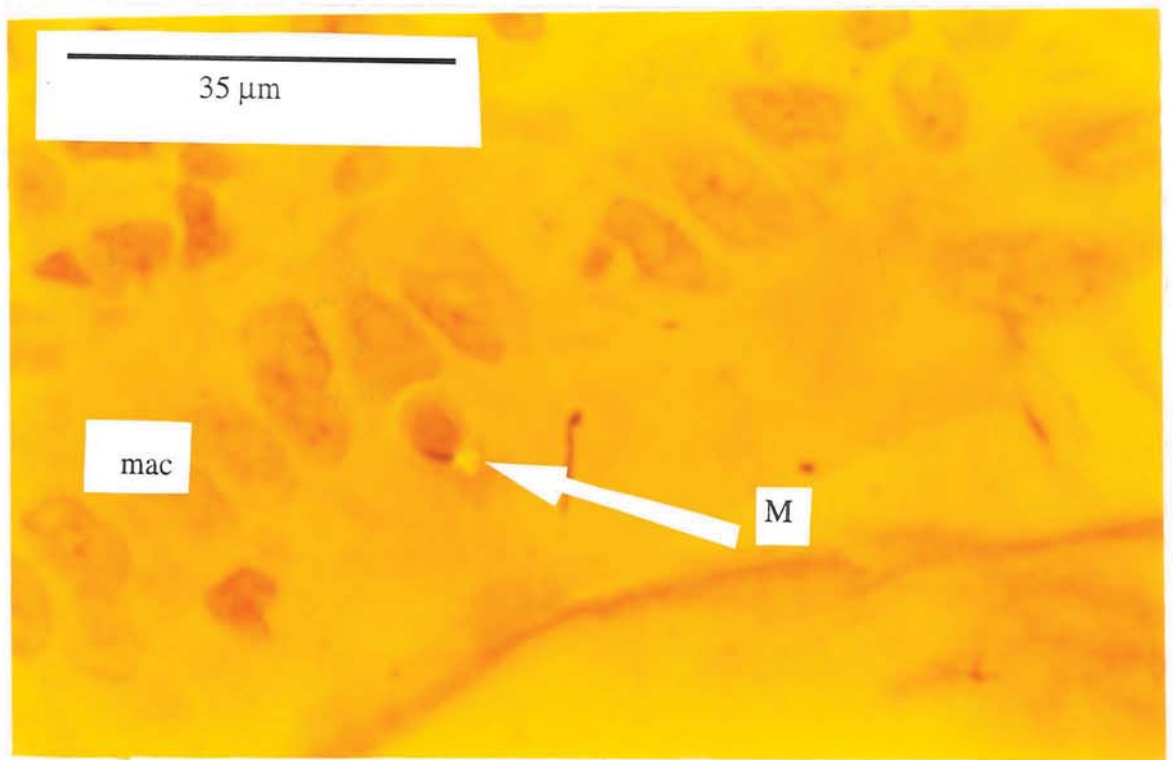


Figure 58. Plastic embedded ileal biopsy taken 45 minutes after oral administration of 2.5 mg 0.87 μm Fluoresbrite™ carboxylate microspheres. This is the same section as shown in figure 56 under higher magnification. Microspheres (M) appear to be in very close association with sub epithelial macrophages (mac) which infiltrate M-cell basolateral membranes (x1000 Total magnification; UV and transmitting light source; Bar=35 μm).

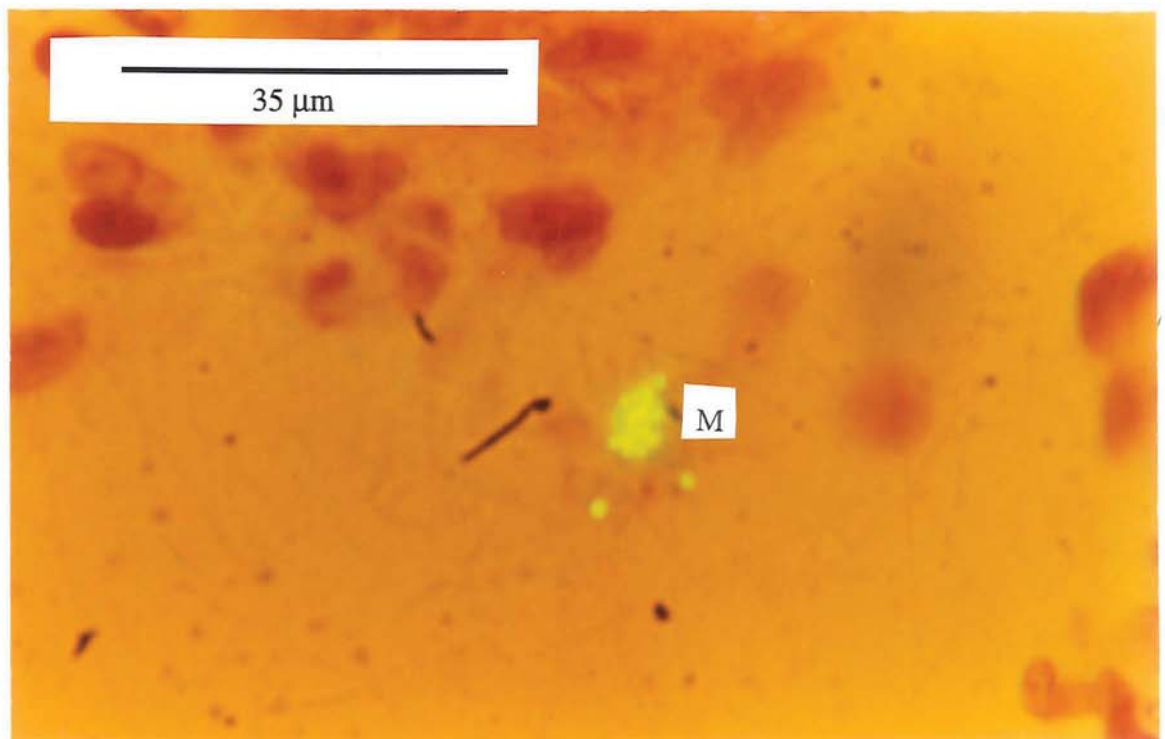


Figure 59. Plastic embedded ileal biopsy taken 240 minutes after oral administration of 2.5 mg 0.87 μm Fluoresbrite™ carboxylate microspheres. Microspheres (M) were frequently visualised deep within the follicle dome of Peyer's patches, often in multiple groupings (x1000 Total magnification; UV and transmitting light source; Bar=35 μm).

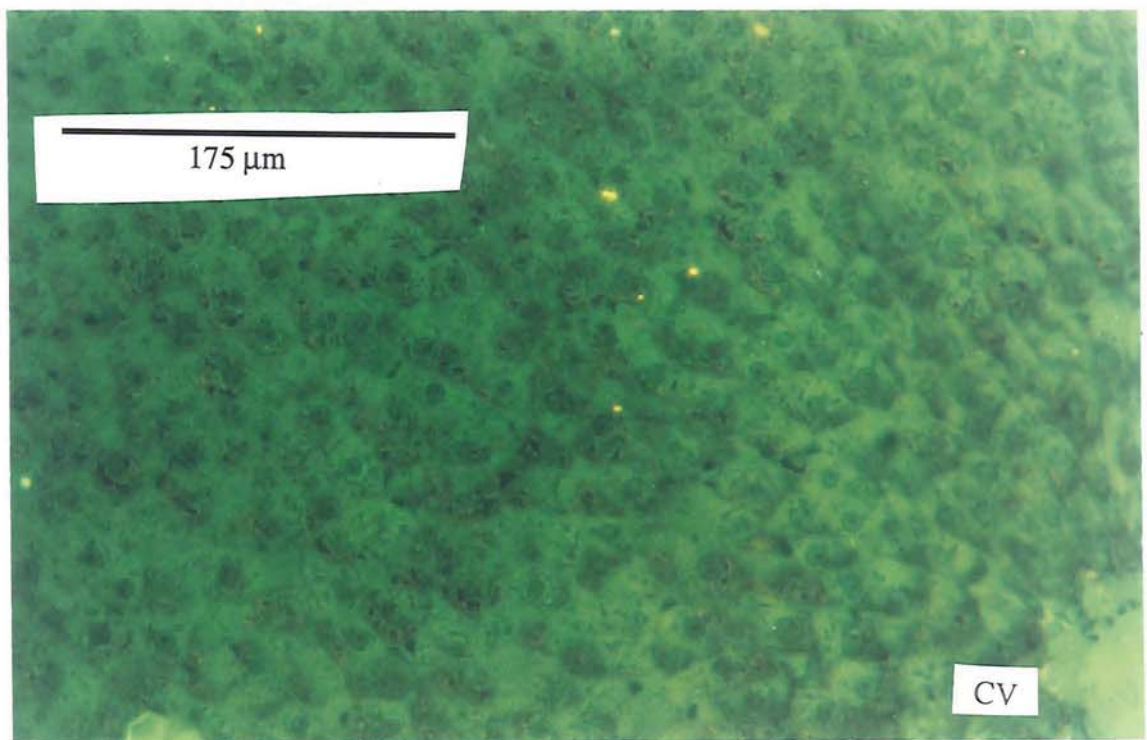


Figure 60. Plastic embedded liver biopsy taken 240 minutes after oral administration of 2.5 mg 0.87 μm Fluoresbrite™ carboxylate microspheres. Microspheres appear to be randomly scattered throughout the hepatic tissue, possibly sequestered within Kupffer cells. A central vein (CV) can be seen in the bottom right hand corner of the photomicrograph (x160 Total magnification; UV light source; Bar=175 μm).

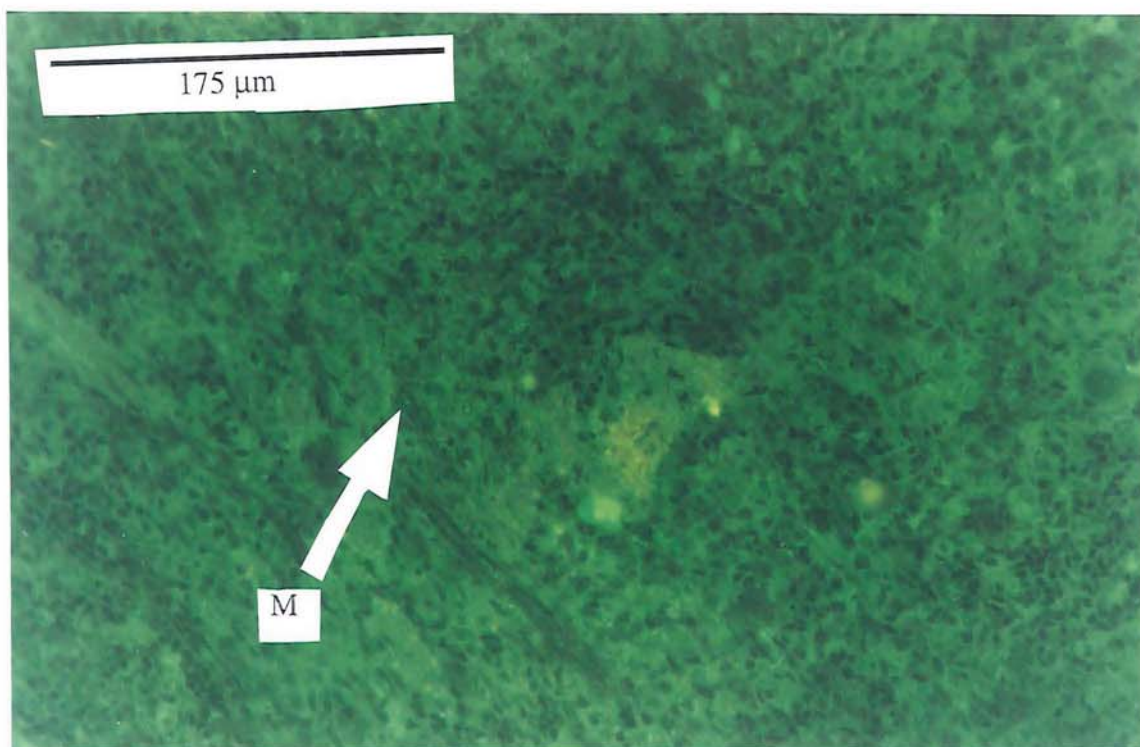


Figure 61. Plastic embedded spleen biopsy taken 240 minutes after oral administration of 2.5 mg 0.87 μm Fluoresbrite™ carboxylate microspheres. Entrapped microsphere(s) are denoted (M) (x160 Total magnification UV light source; Bar=175 μm).

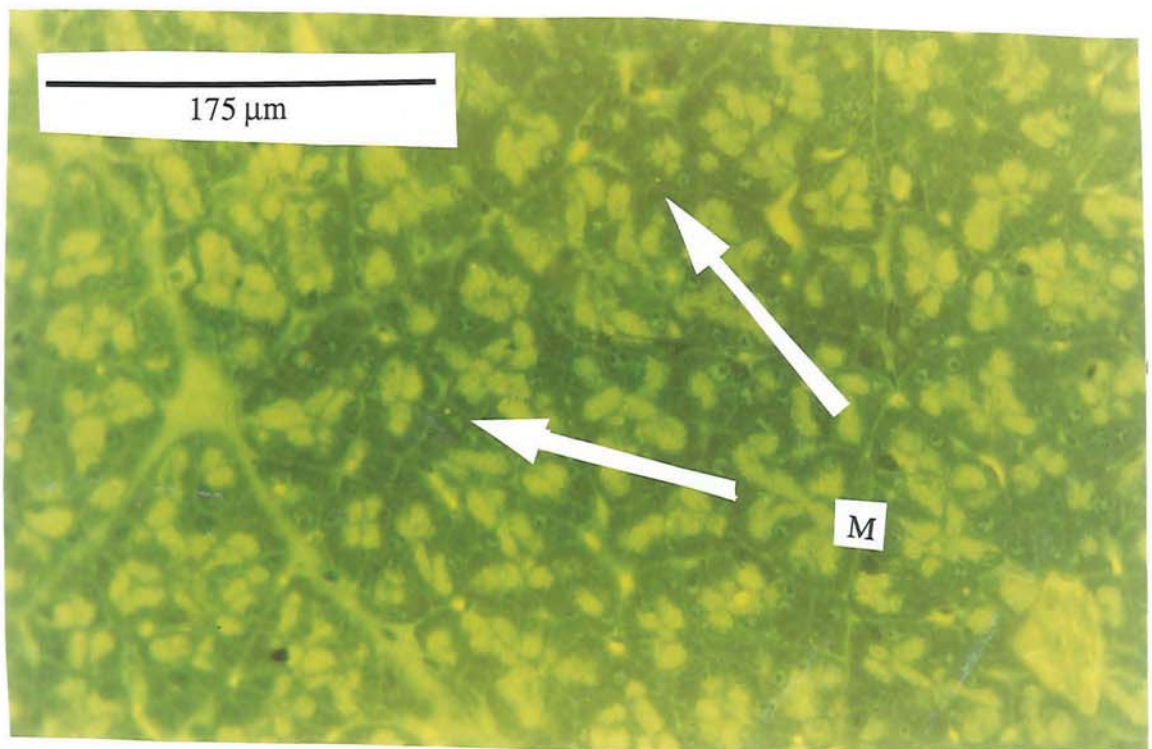


Figure 62. Plastic embedded Mesenteric lymph node biopsy taken 240 minutes after oral administration of 2.5 mg 0.87 μm Fluoresbrite™ carboxylate microspheres. Entrapped microspheres are denoted (M) (x160 Total magnification; UV light source; Bar=175 μm).

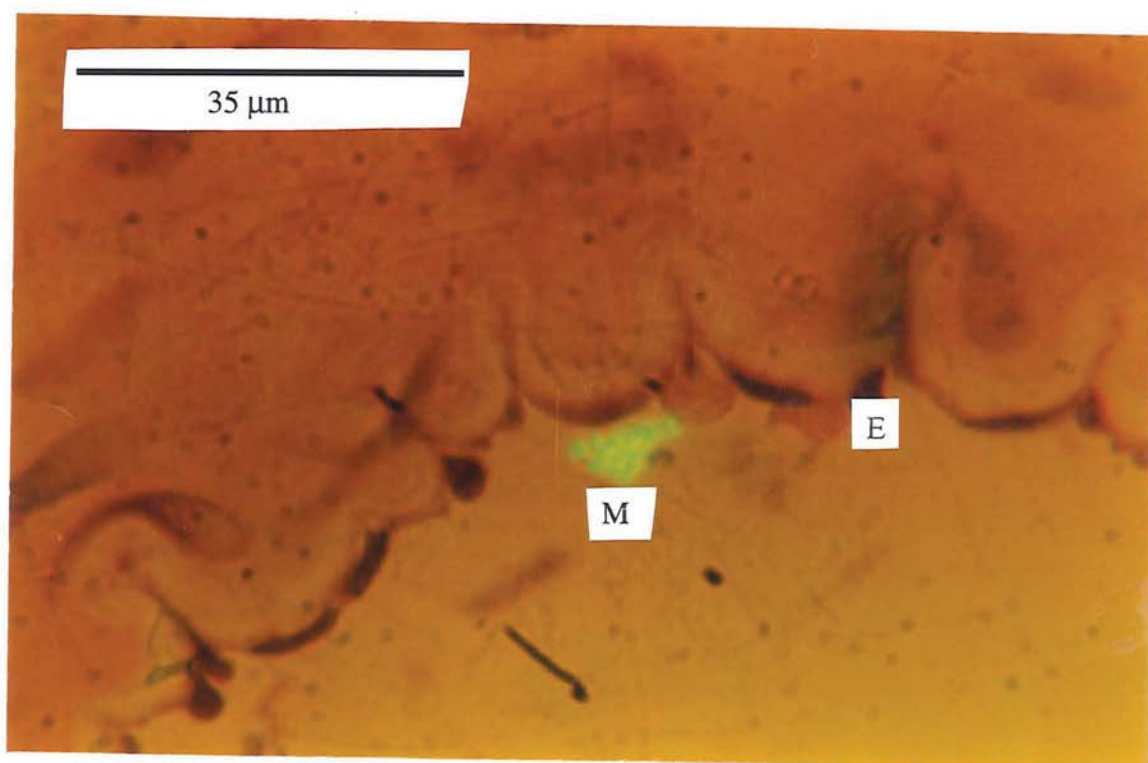


Figure 63. Plastic embedded section of a mesenteric blood vessel taken 240 minutes after oral administration of 2.5 mg 0.87 µm Fluoresbrite™ carboxylate microspheres. Within the arteriole (identified by its internal elastic lamina) microspheres (M) appear internalised within a phagocytic cell. Erythrocytes (E) are also present. (x1000 Total magnification; UV and transmitting light sources; Bar=35 µm).

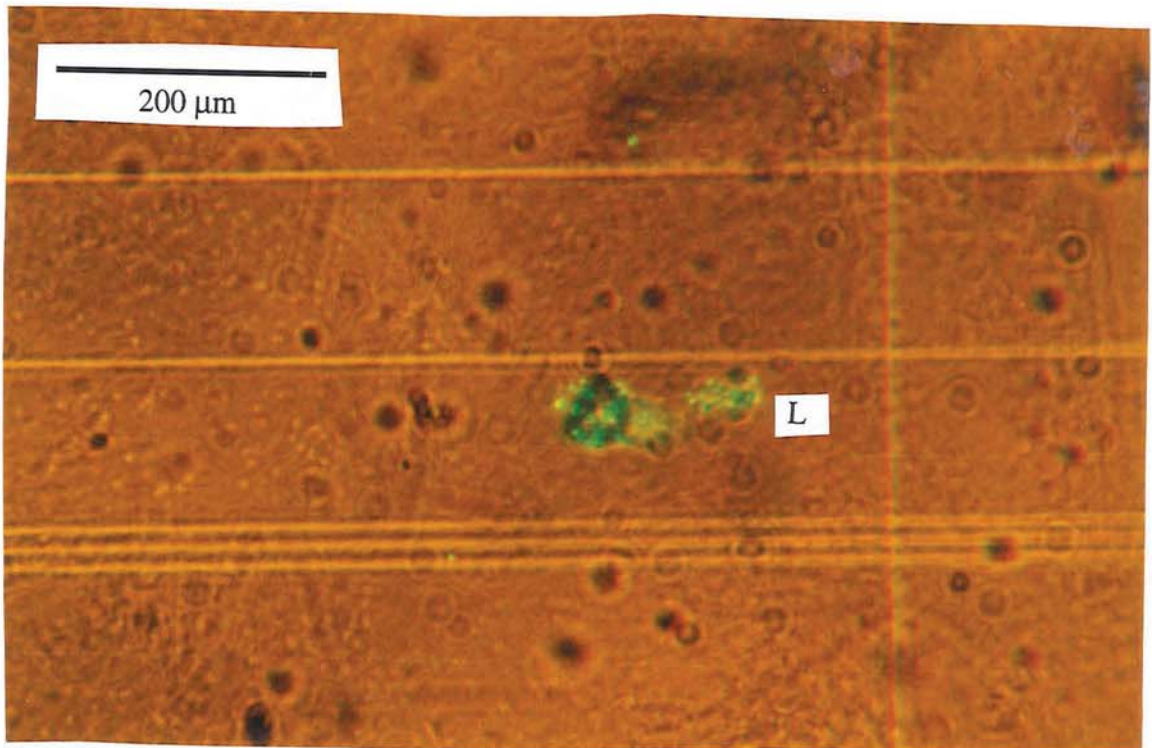


Figure 64. Photomicrograph of blood, diluted with heparinised glycerol, taken 15 minutes after oral administration of 2.5 mg 0.87 μm Fluoresbrite™ carboxylate microspheres. Amongst the erythrocytes, there a microsphere containing leukocyte (L) ($\times 100$ Total magnification; UV and transmitting light sources; Bar=200 μm).

5.3.2 THE TRANSLOCATION OF 220 nm DIAMETER MICROSPHERES FROM ILEAL AND DUODENAL GUT LOOPS IN THE PRESENCE AND ABSENCE OF CYTOCHALASIN B

Estimated blood polystyrene content from treated animals is shown in figures 65 and 66. GPC analysis revealed that higher concentrations of latex were present in blood samples from rodents which received nanospheres in conjunction with water only as opposed to aqueous solutions of the metabolic inhibitor cytochalasin B. Interestingly, higher latex transfer was observed from duodenal rather than ileal gut loops. Uptake of latex into aggregate and non aggregate lymphoid intestinal tissue is shown in figure 67.

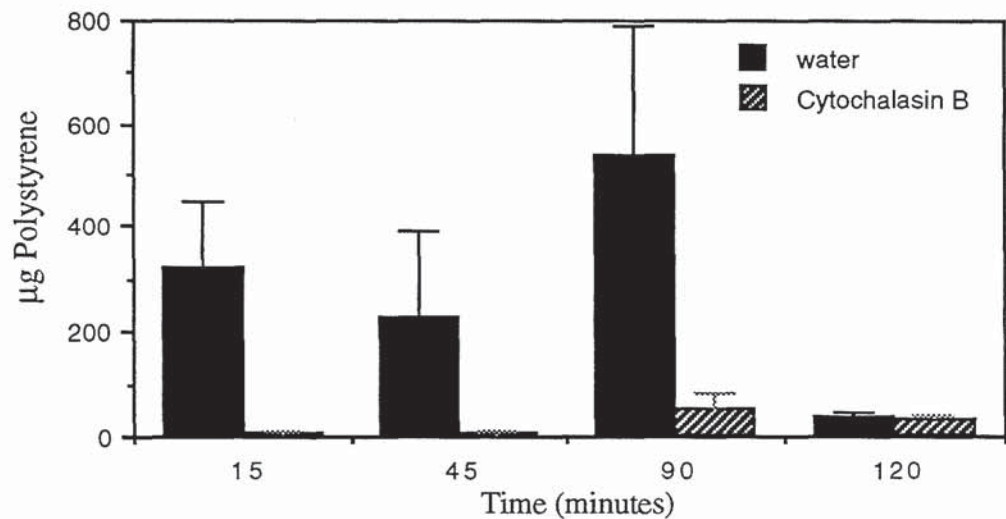


Figure 65. Mean latex nanosphere concentration (\pm SEM) within the vascular compartment of rats at time points after introduction of 21.7 mg of the particles into isolated duodenal loops in the presence and absence of cytochalasin B (n=4).

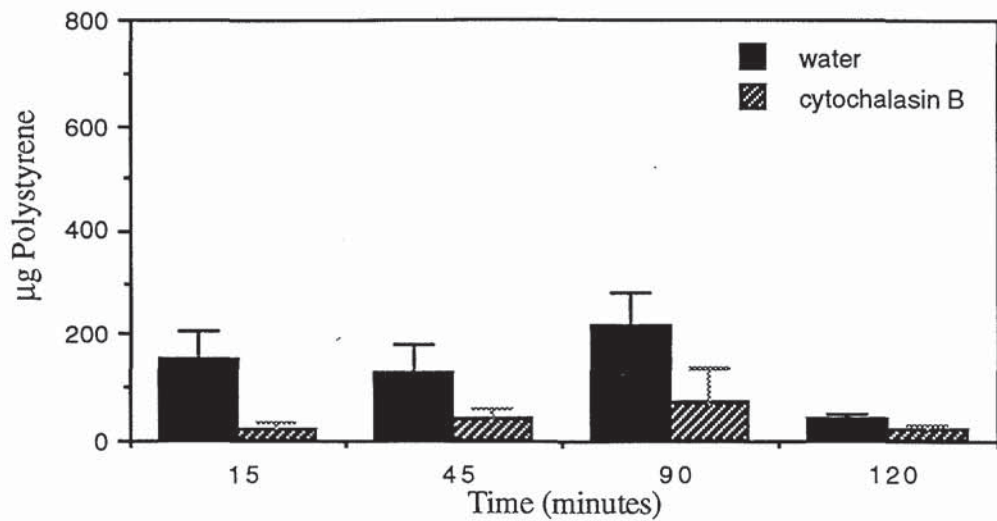


Figure 66. Mean latex nanosphere concentration (\pm SEM) within the vascular compartment of rats at time points after introduction of 21.7 mg of the particles into isolated ileal loops in the presence and absence of cytochalasin B (n=4).

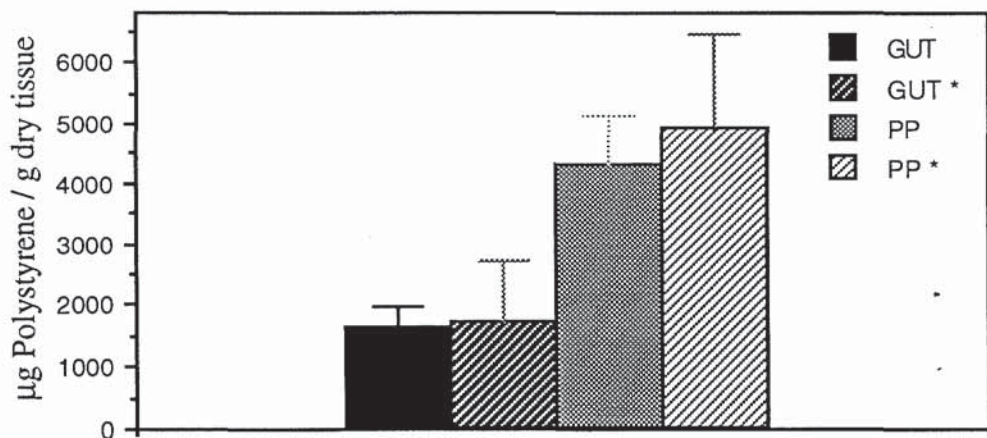


Figure 67. Mean polystyrene accumulation (\pm SEM) *per* gram of dry Peyer's patch tissue or Peyer's patch absent tissue excised from ileal loops after 2 hours incubation of 21.7 mg of 0.22 μ m diameter latex nanospheres, in the presence (*) and absence of cytochalasin B at a concentration of 21 μ M (n=4).

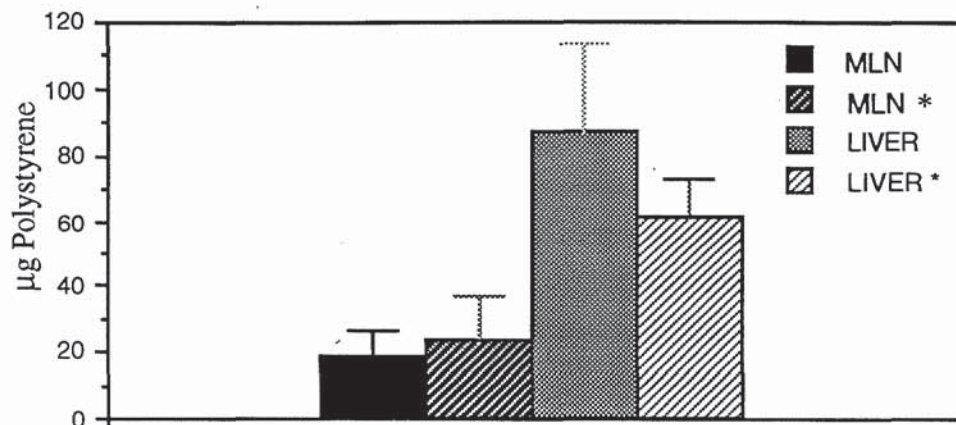


Figure 68. Mean polystyrene content (\pm SEM) of combined spleens and livers and MLN removed from rats 120 minutes after introduction of 21.7 mg of latex nanospheres (0.22 μ m diameter) into isolated ileal loops in the presence (*) and absence of Cytochalasin B at a concentration of 21 μ M (n=4).

5.4 DISCUSSION

5.4.1 HISTOLOGICAL EVIDENCE OF MICROSPHERE UPTAKE AND TRANSLOCATION FROM THE GIT AFTER ORAL ADMINISTRATION

Fluoresbrite™ carboxylate microspheres were able to penetrate the GIT mucosa and accumulate within extra-intestinal sites after oral delivery, as evidenced by histological sections represented in figures 54 to 64. Particles were observed within the intestinal villi shortly (15 minutes) after oral administration (figures 54 and 55). The spatial distribution of the microspheres within the mucosa strongly suggests they are confined to either vascular or lymphatic vessels. The lacteal occupies a central position in the lamina propria of intestinal villi. Arterioles, veins and capillaries tend to occupy a more peripheral position. With light microscopy, the villus lacteal cannot be distinguished with certainty from adjacent blood vessels. Electron microscopy is required to be absolutely certain of the distinction of a lymphatic channel from a blood channel (Dobbins, 1971). Thus it is not certain from light microscopical evidence (figures 54 and 55) if the Fluoresbrite™ particles are conveyed from uptake sites by lymphatic or vascular pathways. Transportation of the microspheres within the blood

stream would be more conducive to acceptance of a persorption type uptake mechanism. It would also help to explain how microspheres are able to enter the general circulation at such short time interval after dosing (see chapters 3 and 4). Close scrutiny of the photomicrographs in question does not enable one to ascertain the morphological nature of particle 'conduits' within the villi. Sections cut longitudinally to the villi (figure 54) suggest the fluorescent particles are nearly always confined to a central position within the villi, and as such are probably contained within large central lymphatic vessels. If true, such an occurrence might also allow rapid translocation of test particles to the blood stream. Conditions of 'water overload' (Eyles *et al.*, 1995) may reduce the time taken for lymphatically absorbed microparticulates to reach the blood stream. Lymph flow in the nonabsorbing small intestine ranges from between 0.02 and 0.08 ml / minute / 100g. During water absorption, lymph flow values above 0.20 ml / minute / 100g are not uncommon (Granger, 1981). As other researchers (Jenkins *et al.*, 1994) have recently ascertained that lymphatic absorption of microparticulates from the small intestine can be rapid, administration of microspheres in conjunction with large volumes of hypotonic media ('water overload') may serve to promote microparticle translocation into these body compartments. If fluorescent microspheres in this size range (0.87 μm diameter) can penetrate the non-aggregate intestinal lymphatics so rapidly after oral delivery, as indicated by these histological studies, it challenges the currently accepted models of particle absorption which highlight the PPs as the primary site for microparticle insorption.

Visual examination of figure 55, which represents a transverse section of intestinal villi, reveals that most of the fluorescent microspheres are fairly widely distributed within these structures when viewed from this perspective. The more scattered appearance of particles within transverse slices may be representative of a hematogenous mode of transportation from uptake zones (see above). As with lymph, blood flow also increases dramatically during water absorption. Physiologists also think that intestinal capillary surface area and / or capillary permeability increase(s) during fluid absorption (Granger, 1981). Such events might render capillary vasculature more permeable to microparticulate invasion after oral delivery.

It is well documented that inert particulate matter can accumulate within the aggregates of lymphatic tissue in the small intestine known as the Peyer's

patches. Our findings support this (figures 56, 57, 58 and 59). Fluoresbrite™ particles can be seen in very close proximity to FAE, undergoing a process most likely to be that of endocytosis (figure 56). This is clearer at higher magnification (figure 58). Three microspheres can be visualised, inside what is likely to be an M-cell within the FAE. Sub-epithelial macrophages are abundant, with a few lymphocytes resident within M cell basolateral pocket subdomains. Figure 57 shows a microsphere(s) located deeper underneath the FAE. In other samples, microspheres were observed deep within patch tissue, often in multiple groupings (figure 59). The histological data represented in figures 56-59 further corroborates the now well accepted pattern of particle uptake through aggregate lymphoid follicles in the small intestine (see section 1.2.4). The time course of microsphere uptake from the intestinal lumen *via* this pathway is known to be rapid (Jenkins *et al.*, 1994, Sass *et al.*, 1990). This was found to be true in the intact animal as well, with particles visualised beneath FAE in sections taken from rodents sacrificed only 45 minutes after administration. The time taken for these insorbed particles to reach the general circulation, if indeed they do at all, is less clearly defined (see section 1.2.6). Although in recent studies (Jenkins *et al.*, 1994) particles were detected in draining mesenteric lymph from 5 minutes after duodenal administration.

In addition to identifying labelled particulate matter within intestinal mucosal sites, Fluoresbrite™ particles were visualised within various extra-intestinal locations after oral treatment. Microspheres are clearly evident in thin sections of liver tissue taken from animals sacrificed at various times after dosing (figure 60). The particles appear to be randomly scattered across the field of view. In reality, the particles are probably engulfed within Kupffer cells which sit astride hepatic sinusoids in an ideal position to sequester passing microspheres (see section 1.2.6.2). The observed accumulation of Fluoresbrite™ latex microspheres within hepatic tissue, supports findings from previous histological investigations by other workers in which orally administered particles were seen within this organ (Saunders *et al.*, 1961, Volkheimer, 1975, Jani *et al.*, 1989, 1992a, 1992b). Fluoresbrite™ latex microspheres were seen in histological sections of liver removed from rats only 5 minutes after gavage, corroborating both our earlier statements regarding the rapidity of microsphere transfer from the intestinal lumen to the general circulation (chapter 3) and previous publications from this laboratory (Alpar *et al.*, 1989). Thin sections of spleen tissue removed

from treated animals (figure 61) also showed evidence of microsphere sequestration after oral administration. As indicated earlier (section 1.2.6.2) the spleen is known to be a very effective accumulator of blood borne colloidal particles due to a combination of mechanical filtration and MPS activity.

Microspheres were found within mesenteric lymphoid tissue after oral delivery (figure 62). Histological investigations by a number of other investigators showed similar results (Jani *et al.*, 1989, 1992a, 1992b, Joel *et al.*, 1978, LeFevre *et al.*, 1977, 1978a, 1978b, 1980, 1985a, 1985b, 1986). The mesenteric lymph node is known to act as a depot for intestinally absorbed particles and antigens (section 1.2.6.1). The presence of Fluoresbrite™ microspheres within this tissue after oral delivery, is therefore, another good indicator that inert particulates may penetrate the GIT mucosa. Moreover, accumulation of particles within the MLN compartment is probably indicative of a lymphatic absorption pathway.

Fluoresbrite™ microspheres were seen within the actual vasculature of mesenteric tissue samples from treated rodents (figure 63). Thus in histological sections from the same tissue, oral test particles were observed within both vascular and lymphatic compartments. Such findings typify the complex nature of this phenomenon and further reinforce the thesis that a combination of absorption pathways are probably involved: Lymphatically absorbed microspheres could enter the vascular compartment *via* the thoracic duct to appear within the mesenteric vasculature (section 1.2.6.1). Alternatively, particles could enter the intestinal microcirculation directly (section 1.2.6.2).

The Fluoresbrite™ microspheres visualised in the photomicrograph (figure 63) appear to be contained within a phagocyte. Such findings concur with concomitant studies (chapter 3) in which Fluoresbrite™ particles were visualised within blood samples largely in association with this type of circulating cell (figure 64). The high frequency with which orally administered microspheres were observed in close association with members of the phagocyte population suggests that this particular type of leukocyte plays a central role in either the process of particle uptake from the gut lumen, or the process by which intestinally absorbed particles become disseminated within the vascular and lymphatic compartments. If either, or both, of the above are true, it may help explain why the drug cytochalasin B

has such a dramatic influence on microparticle uptake / translocation (see below).

5.4.2 THE TRANSLOCATION OF 220 nm DIAMETER MICROSPHERES FROM ILEAL AND DUODENAL GUT LOOPS IN THE PRESENCE AND ABSENCE OF CYTOCHALASIN B

Polystyrene transfer from duodenal segments inoculated with 220 nm diameter latex nanospheres suspended in water was found to be significantly higher than the levels of transfer recorded from duodenal loops inoculated with nanosphere suspensions mixed with cytochalasin B ($P \leq 0.05$ at 15 minutes). Mean transfer of 220 nm latex nanospheres from ileal loops to the general circulation was found to be (insignificantly) lower in comparison to the proximal small intestinal segments. In both cases, non cytochalasin B exposed nanospheres could be detected within blood samples removed shortly (15 minutes) after administration. Particle translocation to the blood was lower if cytochalasin B was introduced into the artificial gut segments (figures 65 and 66). Such findings suggest that nanosphere translocation from ileal gut segments to the circulation is of a lower order than from duodenal segments under these identical, although, artificial conditions. At early time points, a higher percentage of the 21.7 mg latex dose was transferred to the general circulation from isolated duodenal segments compared with previous studies where nanospheres were simply gavaged (chapter 4). Percentage transfer from ileal loops was of a similar order to that observed after single dose experiments (chapter 4). In either case, duodenal or ileal, the levels of latex detected in blood samples taken at the 120 minute time point were depleted compared to 15, 45 and 90 minute time points.

Latex nanosphere uptake in conscious rodents after gavage (chapter 4) is likely to differ from latex absorption from artificially prepared gut loops, for a number of reasons: In intact, conscious rodents incomplete gastric emptying of the nanospheres will delay the transit of a fraction of the particles along the alimentary canal. This will not be the case with gut loops, as there will be an instantaneous and direct input of the entire 21.7 mg of latex into the appropriate section of the GIT. Having isolated specific segments of intestine, particles therein will be artificially contained, unable to travel onwards. The action of peristaltic movements on these trapped particles may act to enhance their absorption (Volkheimer, 1975). The

effect of anaesthesia and the act of operating on the rat may also affect absorption parameters. Certainly some degree of physiological stress will be endured by the intestinal mucosa. Surgical actions may produce an inflammatory response, such as polymorphonuclear granulocytes flooding into the region. The influence of mucus on nanosphere translocation from *in situ* closed loops may differ considerably from its influence in intact whole animal experiments. Such factors have important implications and make any comparison between particulate absorption from the whole animal intestine and *in situ* models complicated. There are however, clear advantages in using *in situ* models when studying nanosphere absorption kinetics *in vivo*. With the *in situ* model, a known amount of particles may be introduced directly into a predetermined region of the GIT. Other agents may be introduced into closed loops at defined concentrations. Most importantly, all parts of the intestinal mucosa which comprise the closed loop system should in theory have an equal opportunity for microparticulate absorption from the lumen. As this is the case, a statistical comparison may be made between different discernible anatomical structures within the artificial gut loop system.

The inclusion of cytochalasin B with the latex suspensions prior to administration produced pronounced changes in both the levels and pattern of latex circulation throughout the 2 hour period. Nanosphere translocation from isolated duodenal loops was practically abolished during the first 90 minute period, although only the 15 minute values are statistically different. Mean transfer from ileal segments was considerably diminished in the presence of cytochalasin B at these time periods.

Cytochalasin B is a compound derived from *Helminthosporium dematidoideum* which can elicit a number of interesting cytological effects. *In vitro* cytochalasin B has been shown to reversibly inhibit the phagocytic ability of cultured macrophages when the drug is present at concentrations above 2×10^{-6} M. Transport of hexose sugars by macrophages is also inhibited by cytochalasin B, but at much lower concentration of the drug (2×10^{-7} M). The effects of glucose deprivation for 2 hours on cultured macrophage morphology and phagocytic activity was found to be negligible. This is because, inhibition of phagocytosis was found to be caused by disruption and / or disorganisation of oriented bundles of subplasmalemmal microfilaments by cytochalasin B, rather than inhibition of hexose transport. Disruption of microfilamentous structure interferes

with plasma membrane translocation, an integral process required for endocytosis and cell motility (Axline *et al.*, 1974).

Cytochalasin B was also used to influence the transmucosal passage of liposomally-entrapped drugs in the rat small intestine (Kimura *et al.*, 1984). Mucosal to serosal clearance of Liposomally entrapped FITC-D was inhibited by cytochalasin B (4.1×10^{-5} M) when FITC-D was entrapped within Egg PC liposomes, but not other liposome preparations. The authors stated that this abolishment of FITC-D transmucosal transport was due to the fact that egg PC liposome preparations are absorbed *via* endocytosis, while other liposomes rely on fusion with luminal epithelial cell membranes.

The observed reduction in latex levels within blood taken at early time points from animals exposed to cytochalasin, indicate that particulate transfer from GIT lumen to the vascular compartment may involve processes which are affected by this compound (figures 65 and 66). Earlier experiments where small intestinal tissue was removed shortly after gavage, of 220 nm nanospheres, suggested that large amounts of latex had reversibly partitioned into the mucosa to such an extent that they could not be removed by simple but vigorous washing procedures (section 4.4). Non-specific endocytosis of the nanospheres into epithelial or M-cells throughout the intestine could account for such an occurrence. Such an absorption pathway may well be influenced by metabolic inhibitors such as cytochalasin B. If the action of cytochalasin B completely blockades this route of absorption then one interpretation of the obtained data would be that uptake and / or translocation of particulate matter from the GIT lumen is predominately an active process which may be completely inhibited by this agent (cytochalasin B).

As mentioned previously, non cytochalasin B exposed nanosphere transfer from ileal segments was diminished, although in-significantly, in comparison to the duodenal closed loops. As the ileum contains a higher density of lymphoid tissue available for particulate insorption, including PPs, one might expect greater polymer uptake and transfer from distal regions of GIT. However, it could be for this very reason that mean polystyrene transfer from ileal loops was lower. One could speculate that particulate uptake from the distal regions of the small intestine is likely to involve these aggregate lymphoid follicles, and as such, result in some

degree of microparticle sequestration within the GALT. This could result in a slower transfer of the nanospheres into the vascular compartment because microparticulates may be harboured within patch tissues after intestinal absorption.(see section 1.2.6.1). Following this line of thinking, uptake of particulates from the proximal regions of the GIT would be expected to result in a predominately hematogenous transfer away from the intestines due to a much lower density of lymphatic tissue. The problem with this explanation is that cytochalasin B inhibition of nanosphere translocation from ileal loops to the vascular compartments of rats, was not as pronounced as in the case of duodenal loops. This factor strongly indicates that active processes, which are susceptible to cytochalasin B, are essential during translocation of inert particulate matter from both the proximal and distal regions of the GIT to the vascular compartment. An alternative to the above hypothesis would be to say that this particular inhibitor may not influence uptake of nanospheres into intestinal mucosal regions, but instead, severely disrupt the transfer of absorbed material into the blood stream. In this case, particulates enter the intestinal mucosa by mechanisms unaffected by the action of cytochalasin B, but require cytochalasin B sensitive entities to negotiate passage into the vascular compartment. Wells *et al.*, (1988) found that microspheres were transported from PP deficient jejunal loops to the MLN of experimental animals (dogs). In an earlier report, Wells *et al.*, (1987) identified that it was specifically the macrophage population of phagocytes which were responsible for this activity. Our experimental studies took place over a much shorter time scale than that of Wells *et al.*, (1987 and 1988) and examined blood samples rather than MLN digests. However, it does provide further evidence, albeit circumstantial, that inert particles may be absorbed into the intestinal mucosa at regions otherwise devoid of aggregated lymphatic tissue. These findings also indicate that cytochalasin B sensitive entities may play a central role in the transportation of microparticulates from the GIT to the vascular compartment. This also ties in with the experimental evidence accumulated in the previous experimental chapters, which implicates the phagocyte as a key player in the process of nano / microsphere uptake and translocation from the GIT (see figures 63, 64 above).

Analysis of polystyrene levels within washed intestinal tissues from rats with artificial ileal closed loops inoculated with latex nanospheres in the absence of cytochalasin B, suggests that at the two hour time point latex absorption into both patch and non patch tissue was substantial (figure 67).

Statistically, much more latex was detected *per* gram of PP tissue compared with non patch ileal samples ($P \leq 0.025$). Approximately 7 % of the 21.7 mg polystyrene inoculum was estimated to be absorbed within each gram of patch free ileal tissue. At the same time point an average of 18 % of the 21.7 mg latex nanosphere dose was detected *per* gram of dry PP tissue excised. Such high levels of particle absorption would probably not be reciprocated in whole animal studies. Indeed, when 21.7 mg of latex nanospheres were administered as a gavaged bolus a maximum of 2.1 % of the dose could be detected *per* gram of small intestinal tissue. This was at the 45 minute time point (section 4.3.2.4). In this study, the relatively high levels of latex detected within normal intestinal tissue, re-emphasise the likelihood that particulate absorption may occur at sites which are anatomically remote from PPs. The absence of PPs within these regions does not mean that active uptake of particulate matter from the intestinal lumen may not occur. The presence of SLFs (see section 1.2.5) throughout the gut may well account for a significant absorption of polymeric material into the intestinal mucosa. It is also possible although less likely, that some of the absorbed microparticulates may have been taken up by ordinary enterocytes by a process of endocytosis (see section 1.2.2). Statistically high levels of latex uptake into PP tissue corresponds with the documented efficiency of these structures for particulate accumulation (LeFevre *et al.*, 1978, Jani *et al.*, 1989, Pappo *et al.*, 1989, Jepson *et al.*, 1992, Sass *et al.*, 1990 and Jenkins *et al.*, 1994) (section 1.2.4). A polystyrene nanosphere filled artificial intestinal loop, of the kind used in this used in this experimental investigation, probably represents a near optimal environment for PP mediated particulate uptake from the gut lumen. As such, hypothesised absorption mechanisms may become saturated and it is possible that the figure of 18 % accumulation per gram of PP may be around the upper limit of absorption efficiency under these experimental conditions. In the studies of Hillery *et al.*, (1994) 10 % of the administered dose of 50 nm nanospheres was detected within intestinal tissue after chronic oral delivery. Of this 10 %, 60 % of the latex was recovered from small intestinal PPs from treated rodents.

On average, the mass of latex recovered from excised PP tissue was found to be statistically unaffected by the presence or absence of cytochalasin B (figure 67). In terms of its effects on polystyrene uptake, plain gut tissue was found to be similarly unresponsive to the pharmacological actions of cytochalasin B. Comparisons between PP and plain gut absorption of the

polymeric particles in the presence and absence of cytochalasin B may also be made. It is reasonably clear however, that cytochalasin B has little effect on the natural absorptive capacity of either tissue type in this model.

In light of the guts apparent insensitivity to cytochalasin B in relation to latex nanosphere insorption, one might conclude that the absorption of particulate matter into the gastrointestinal mucosa (pathway A in figure 69) is unaffected by this compound. If this were true, it would mean that microparticle uptake from the gut lumen occurs without the need for enterocyte or M-cell endocytosis. As mentioned previously, endocytosis is disrupted by the action, disorganisation of subplasmalemmal microfilaments, of cytochalasin B. If cytochalasin B were to completely blockade the process of particle endocytosis some other mechanism of particle absorption (see sections 1.2.1 to 1.2.5) would have to account for the observed transfer of latex into the gastrointestinal mucosa. The paracellular route is one contender. Histological data from Fluoresbrite™ dosed animals strongly supports the existence of such a pathway (see figure 54). If microspheres did enter the mucosa *via* this mechanism, it would still not explain why a far greater percentage of dosed nanospheres accumulated within PP as opposed to plain gut tissue (figure 67). If persorption did account for the mucosal absorption of latex shown in figure 67, then one might expect a more even distribution of polymer between the two tissue types. This would seem logical unless the PPs are inherently more penetrable to microspheres than non-patch intestinal mucosa, irrespective of uptake mechanism. In this case, other factors like reduced M-cell mucus covering, a more leaky basement membrane and a sparser glycocalyx may facilitate increased particle penetration of the FAE by non-endocytotic mechanisms and could account for the observed distribution.

Microspheres may have entered PP and non-PP tissue to an equal degree by cytochalasin B insensitive processes, but become retained to a much greater extent within patch tissue. This might be because PPs contain a far higher ratio of lymphoid cells than plain gut tissue, and are to all intents and purposes antigen sampling, processing, storage and distribution depots for the GIT. Whilst other regions of small intestinal mucosa also contain innumerable lymphoid cells, their primary function concerned with the absorption and distribution of the molecular products of digestion, solutes and water. As such, we might speculate that absorbed microspheres would be retained to a lesser extent in non-patch compared to PP tissue on a weight

per weight basis. It is also feasible is that intestinally absorbed microspheres circulating within the lymphatics or blood become accumulated within the PPs to a greater degree than non-lymphoid gut tissue on their journey around the body.

If we summarise nanosphere absorption from the GIT as follows:

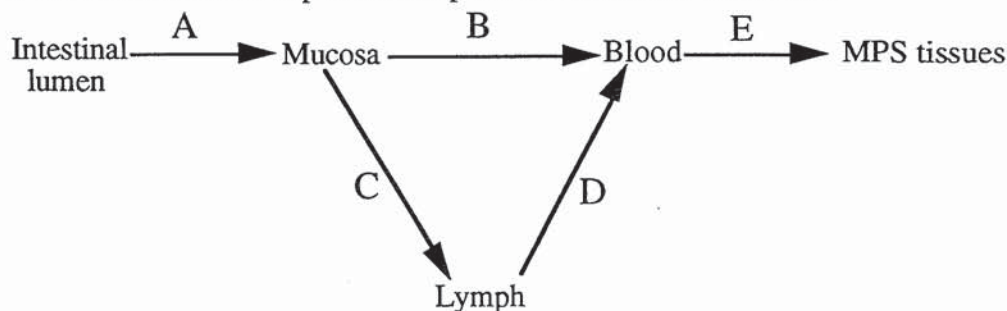


Figure 69. Schematic representation of particle translocation after intestinal absorption.

We have already established that cytochalasin B probably has little effect on the process of nanoparticle absorption into the mucosa itself (process A, figure 69). Polystyrene content analysis of pooled livers and spleens and MLN tissue removed from rats 120 minutes after nanosphere introduction (figure 68) showed that low, but detectable amounts of latex had reached extra-intestinal sites at this point in the experiment. Latex levels within pooled livers and spleens taken from non cytochalasin B treated rats were comparable with the amounts of polystyrene extracted from these tissues after a single oral dose (section 4.3.2.4). Pooled liver and spleens removed from individual cytochalasin B treated rodents contained depleted amounts of latex. Such a finding is consistent with the lower levels of latex circulating at time points after nanosphere introduction into the ileal loops in conjunction with the metabolic inhibitor, and indicates that the presence of cytochalasin B may dictate the accessibility of the vascular compartment for intestinally absorbed microparticles (pathway B, figure 69). The exact reason for this effect is unclear and any discussion must be limited to speculation. It is however, apparent that the ability to disseminate intestinally absorbed microparticles *via* the lymphatics is heavily reliant on the migrating macrophage (MAC-1⁺) population of cells within the lamina propria and GALT, and that this process can be rapid. These factors are documented elsewhere (Jenkins *et al.*, 1994, Wells *et al.*, 1987, 1988). If one of the actions of cytochalasin B was to debilitate these phagocytic cells, then the ability to transport intestinally absorbed microspheres from lymphatic compartments within the GIT through the thoracic duct and beyond (pathway C and D, figure 69) might be compromised. This might explain the depletion in microsphere numbers detected within the blood during cytochalasin B exposure. This observation is an important one, and

enables us to draw two very tentative conclusions about the nature of microsphere translocation: Firstly, in this model the transfer of particulates from the GIT lumen to the blood stream probably occurs primarily through lymphatic pathways which contain cytochalasin B sensitive elements such as migrating macrophage (MAC-1⁺) cells. Secondly, uptake and transfer from the gut lumen to the blood is rapid and does not require the presence of lymphoid aggregates because polystyrene nanospheres entered the blood stream after introduction to duodenal loops which do not contain PP. Thus it may be that nanosphere uptake from *in situ* loops occurs via lacteals, as evidenced by histological data, followed by macrophage mediated transportation of particles to the blood stream through the thoracic duct.

A variation on the above model might help explain why latex levels within PP and non-PP intestinal tissue (figure 67) were not dramatically influenced by the drug. If Cytochalasin B slightly reduced microsphere absorption from the intestinal lumen and at the same time inhibited particle migration from the sites of intestinal uptake, then the latex levels within intestinal biopsies from control and treated rodents might indeed be similar.

It can not be ruled out that hematogenous routes of microsphere dissemination from uptake sites in the GIT require phagocyte assistance, and as such be influenced by cytochalasin B. The exact morphology and tissular distribution of this hypothetical population of cells still remains undefined. Damage *et al.*, (1994) found that when Rhodamine B loaded poly [D, L-lactide / glycolide] microspheres (1-5 μm) were introduced into the ileal lumen of rats, the concentration of Rhodamine in the mesenteric vein increased from 10 minutes after administration, reaching a maximal level 4 hours later. There was no evidence of microsphere uptake at any location other than the PPs. The absorption efficiency was estimated to be about 12.7 % of the administered dose. In such an absorption pathway, its possible that cytochalasin B might influence the transfer of microparticles from the PPs directly into the vascular compartment. This would explain both the rapid appearance and disappearance of microspheres in the blood in the presence and absence of cytochalasin B, and the fact that gut accumulation patterns of latex were unaffected by the drug.

In addition to localised effects on the gastrointestinal mucosa and GALT, its possible that cytochalasin B may be able to induce a biological response at anatomically remote locations. If the drug were absorbed across the

intestinal epithelium and into the vasculature the liver could receive a considerable dose of the drug *via* the hepatic portal vein. This might result in an aberration of the liver's normal MPS functionality if hepatic Kupffer cells were exposed to a high enough concentration of the compound. The depleted latex levels in livers and spleens from the cytochalasin B exposed animals suggests there might indeed be some inhibition of Kupffer cell functioning (figure 68). In which case we might conclude that pathway E, see figure 69, representing the sequestration of latex colloids from the blood into MPS compartments is also influenced by the pharmacological actions of cytochalasin B.

Statistically equivocal amounts of polystyrene was recovered from MLN removed from treated and non cytochalasin B treated animals at the two hour time point. Thus, cytochalasin B treatment resulted in lower latex levels in blood and liver, but not MLN and intestines. Such observations could point to a hypothetical situation where nanosphere uptake from the lumen into the intestinal mucosa is not affected by cytochalasin B, but the drug's action is detrimental to nanosphere accumulation in and translocation beyond the MLN. The migration of nanosphere loaded macrophages from gut uptake sites into the lymph nodes could be disrupted by the actions of cytochalasin B (pathway C, figure 69). The presence of polystyrene within the MLN indicates that this effect is a partial one, possibly because some microspheres are carried 'free' in the afferent lymph. Microsphere transportation from the MLN into the circulation through the thoracic duct could also be disrupted by cytochalasin B (pathway D, figure 69). If both of the above were true, then one might expect a depletion of latex within the MLN of Cytochalasin B treated rodents compared with control rats. In the case of cytochalasin B treated rats, much lower levels of latex were detected in the blood and livers compared with the control group. Thus MLN latex levels in control rodents would probably be much higher if nanosphere translocation *via* the thoracic duct was impeded, as might be the case in the cytochalasin B treated group.

Having ascertained that cytochalasin B was ineffectual in altering the pattern of microsphere absorption into the different types of ileal tissue, and that there was little evidence of its effect on latex levels within blood samples taken at the two hour time point, it seems prudent to examine the possibility that the drug became pharmacologically ineffective at some point before the end of the 2 hour experimental period. cytochalasin B's documented use

previously has mainly been restricted to *in vitro* investigations (Axline *et al.*, 1974 and Odeyale *et al.*, 1990) or everted sac procedures (Kimura *et al.*, 1984) where its concentration, and thus its potency, may be carefully monitored. We used the drug at a high concentration, well in excess of that required for phagocyte inhibition *in vitro*, in anticipation of these possible limitations. Even so, it is theoretically possible, if not probable, that cytochalasin B could elicit a maximal response at 90 minutes and no response at 120 minutes if it has a very short half life *in vivo*. The drug's half life *in vitro* is well over 120 minutes, although this is unlikely to be the case inside the gut lumen due to breakdown, elimination or dilution of drug molecules.

Whilst it is possible that cytochalasin B became ineffective at some point before the two hour time point, other factors indicate that this may not be the case: Depleted polystyrene microsphere levels in the blood, in comparison to control animals, show strong evidence that cytochalasin B is exerting an effect over the first 90 minutes of the experiment (figures 65 and 66). We could speculate that cytochalasin B would have to have very peculiar pharmacokinetics to show a maximal response from 0 to 90 minutes followed by a complete shutdown in activity between 90 and 120 minutes. Why blood latex levels in control animals declined to a level comparable with the cytochalasin B treated rodents at 120 minutes remains uncertain. However, for the aforementioned reason it seems possible that this represents a genuine decline in the extent of nanosphere translocation from the artificial gut loops for both experimental groups. It may be related to the repeated haemorrhagic acts performed prior to that time point in the experimental investigation. If this were true, then it is clear that reduced blood and lymphatic pressures are detrimental to the transfer of microparticles from the intestinal lumen to vascular compartments. It is also possible that hypothesised absorption pathways and / or uptake sites effectively become saturated after an as yet undefined period of test particle exposure resulting in reduced microsphere throughput into the blood. Livers removed from cytochalasin B exposed animals at the two hour time point contained less latex than hepatic tissue removed from control rats. As mentioned previously, this may be due to the metabolic inhibitor's influence on the hepatic Kupffer cell population. If this second hypothesis is true then it is a further indicator that cytochalasin B retains its potency up to the two hour time point.

Future experimental endeavours to validate these preliminary findings regarding the nature of latex nanosphere translocation from *in situ* gut loops in the presence and absence of cytochalasin B are essential. It is of paramount importance to confirm that cytochalasin B retains its pharmacological potency throughout the two hour experimental period. This could be achieved by inoculating intestinal loops with Fluoresbrite™ microspheres in the presence and absence of the metabolic inhibitor. At various time points after inoculation, aliquots of microspheres could be removed from the artificial gut loops and fed to cultured macrophages *in vitro* (e.g. J774 or RAW cell lines). The phagocytic index of each microsphere aliquot could be determined using fluorescence microscopy. This would give a good indication of the potency of cytochalasin B within the gut loops at each of the time points. It would also be useful to determine the minimal concentration of drug which is required to observe an effect. Conversely, the influence of increasing the concentration of cytochalasin B on microparticle translocation could be investigated, i.e. a dose responsive study covering a wide range of concentrations.

As we have determined that cytochalasin B modifies the uptake pattern of microspheres into the liver and spleens of test rodents and the end of the experimental period, it would be interesting to determine the latex concentration within these tissues at earlier time points. It would also be highly informative to determine the pattern of microsphere accumulation within PP and non-PP sections of gut at other time points besides the two hour one.

5.4.3 CONCLUSION

In summary, histological examination of tissues taken from animals given a single oral dose of Fluoresbrite™ microspheres (0.87 µm diameter) indicate that such entities may penetrate the GIT mucosa to appear in diverse body compartments, spatially distinct from the intestines. Labelled material was also visualised within intestinal tissue. Absorbed particles were seen in villus structures within what could be either vascular or lymphatic vessels. Microspheres were also detected inside and beneath the FAE within PP tissue.

Data from *in situ* closed gut loop investigations indicate that the translocation of 220 nm diameter latex nanospheres from these loops to the

vascular compartment may be inhibited, at least partially by the action of cytochalasin B. At the two hour time point, uptake of latex nanospheres into PP and PP absent intestinal strips was statistically different in the absence of cytochalasin B. The pattern of latex distribution in PP absent and present intestinal samples removed two hours after the introduction of nanosphere suspensions containing cytochalasin B was similar to that obtained without the drug, although there is some doubt regarding the pharmacological activity of cytochalasin B at this time point. If cytochalasin B retained its activity throughout the experimental period, it appears that the uptake and distribution of latex particles into the gastrointestinal mucosa was not influenced by the presence of cytochalasin B. If this is true, either cytochalasin B has no effect on M-cell and / or ordinary enterocyte endocytosis, or this process is not required for microparticle penetration of the epithelium. Livers and spleens removed from cytochalasin B exposed rodents contained depleted levels of latex. This could reflect the reduced GIT / blood transfer of particles in the presence of the drug. It could also indicate that the drug itself may inhibit the phagocytic activity of MPS compartments leading to a reduced accumulation of colloid. Tentative conclusions from this study indicate that cytochalasin B sensitive entities are required for the transfer of orally administered particles from the GIT lumen to the general circulation. The exact identity of such entities remains elusive, although the migrating macrophage (MAC-1⁺) cells within the GALT may be involved. If this is the case then it suggests that the rapid appearance of microspheres within the blood stream after intra-intestinal administration into artificial gut loops is primarily the result of a lymphatic dissemination of particles after absorption. The extent to which these early observations using *in situ* closed loops mirror the actual physiological processes within the intact gastrointestinal mucosa will only become evident after further investigation. The level of latex translocation into extra-intestinal sites from the ligated sections of GIT, was however, roughly equivocal with that obtained when the microspheres were administered to conscious rodents as gavaged bolus. It is of up-most importance, at some time in the future, to confirm that cytochalasin B retains its pharmacological potency throughout the two hour experimental period using this model.

6.0 UPTAKE AND DISTRIBUTION OF MICROENCAPSULATED INTERFERON AFTER ORAL DELIVERY

6.1 INTRODUCTION

As initial studies demonstrated that inert microparticles were detectable in diverse body compartments after oral administration, a logical progression in any investigation would be to examine the possibility of delivering small amounts of therapeutically important agents by this route. To achieve such an aim, the scientifically informative, but pharmaceutically useless latex microsphere systems were abandoned in favour of a biodegradable one with drug carrying potential. Radiolabelled interferon- γ (IFN- γ) was encapsulated within Poly-L-Lactide microspheres and administered orally to test animals as before. The radioactive content of various tissues was then assayed, in order to assess the body distribution of interferon. Interferons (IFNs) are a complex group of proteins and glycoproteins able to express antiviral, immunomodulatory, and differentiation activities. Human IFN- γ is produced by T lymphocytes in response to specific antigens to which they are sensitised, or to mitogens. IFN- γ is a glycoprotein consisting of 166 amino acids and carbohydrates, resulting in a molecular weight of 17 kDa. It is basic, with an isoelectric point at about pH 8.7, acid-labile and is denatured at 56°C. The binding of IFN- γ to receptors induces biological responses *via* intracellular signalling and interaction with IFN responsive genes. One such response is the production of enzymes which are destructive to viral mRNA. IFN also induces several modifications in the cell membrane leading to decreased virus penetration, maturation and release (Bocci, 1992).

Poly-L-Lactide particles have been employed previously to deliver vaccines orally (Eldridge *et al.*, 1990, Almeida, 1993). Our interest lies in the development of technologies capable of delivering systemically active agents, such as IFN- γ , by the oral route. Poly-L-Lactide microspheres are just one of the many polymeric microsphere systems which may realise this aim. Their biodegradability means they are eroded *in vivo* and release their encapsulated payload. Although such characteristics enable drug delivery, they complicate the interpretation of tracer distribution data because gamma ray emission from assayed tissues could originate from encapsulated drug, free drug or drug molecule fragments. To help validate our experimental data from interferon loaded microsphere dosed rats, we administered free

IFN- γ in conjunction with empty microspheres to a second group of rodents. We also investigated the profile of IFN- γ release from PLA microspheres *in vitro*.

6.2 MATERIALS AND METHODS

(3-[125 I] iodotyrosyl) γ -interferon (IM 202) was purchased from Amersham International plc, Bucks UK. 125 I-IFN- γ was encapsulated within Poly-L-Lactide microspheres using the double emulsion method (Conway *et al.*, 1994) by Miss Barbara Conway at the Department of Pharmaceutical and Biological Sciences, Aston University. Poly-L-lactide with a molecular weight of 2000 (Resomer L104) was purchased from Boehringer Ingelheim, Bereich Germany. After preparation, microspheres were freeze-dried and stored in a desiccator at 5°C prior to use in animal studies. The size distribution of the microsphere preparation was determined using a Malvern Mastersizer / E (Malvern Instruments, UK).

The animal model was identical to that used in previous chapters (see section 2.1). Prior to oral dosing procedures, rodents were starved overnight as before. At the start of the experimental period, each rat received 10 mg of Poly-L-lactide microspheres which contained trace amounts of (3-[125 I] iodotyrosyl) γ -interferon. The radioactivity of each 10 mg microsphere batch was recorded as the initial dose activity (see section 4.2.4). Microspheres were suspended in 1 ml of water, and vortexed, before gavage. At various time points after gavage, 15 minutes, 4 hours, 24 hours and 4 days, three animals were anaesthetised (see section 2.2) and blood was sampled from portal and cardiac sites as described previously (See sections 2.8.2, 2.8.1). All animals were sacrificed immediately after haemorrhage whilst under terminal anaesthesia. Liver, spleen, lung, kidney, mesentery and thyroid were then removed. The small intestines were also excised. The contents of the small intestinal lumen was harvested with copious amounts of isotonic saline as described in section 4.2.2.4. The large intestine was treated similarly. The washed small intestine was cut longitudinally and further washed. The PPs were located and micro-dissected as before (see section 5.2.2). All pieces of gut tissue and all gut wash samples were saved and collected for 125 I content analysis as described (see section 4.2.4). For gut washes, the exact volume of the entire sample was recorded. Usually, only two or three aliquots (5 ml) of this liquid was assayed. All tissue samples were weighed before 125 I

content analysis. In the case of gut tissue samples, dry weights of each tissue sample (upper small intestine, lower small intestine, small intestinal Peyer's patches and large intestine) were obtained. Rodents in the 1 and 4 day groups were placed in metabolic cages after dosing. The urine and faeces from these rats was collected and quantitatively analysed for ^{125}I content.

In a second (control) group of six rats, free (3- ^{125}I iodotyrosyl) γ -interferon was given orally with a suspension of empty Poly-L-Lactide microspheres prepared using the double emulsion method. The amount of free interferon in each dose was identical to that which the microencapsulated interferon dosed rats received. Each rat received 10 mg of empty microspheres which was suspended in 1 ml of water containing the drug. The suspension was vortexed prior to gavage. At 15 and 240 minutes after gavage, animals were anaesthetised and blood samples were taken as described above. Three rats were sacrificed at each time point. Again, all tissue samples were weighed prior to ^{125}I content analysis.

6.3 RESULTS

The (3- ^{125}I iodotyrosyl) γ -interferon containing Poly-L-Lactide microspheres were found to have a mean diameter of 0.79 μm (standard deviation 0.48 μm). Microsphere loading of interferon was low (~0.01 % w/w). Thus each 10 mg batch of microspheres contained about 1 μg of IFN- γ . The mean activity of each 10 mg microsphere batch prior to gavage was about 1700 Bq. (3- ^{125}I iodotyrosyl) γ -interferon release from PLA microspheres into 20 mM phosphate buffer solution is shown in table 6.

Gamma ray emission from body fluids and tissues removed from rodents which had received encapsulated radioactive drug orally, suggested that a percentage of the ^{125}I label had been absorbed from the GIT lumen into diverse extra intestinal locations. This was found to be the case as quickly as 15 minutes after dosing (see table 7). The GIT transit pattern, intestinal and extraintestinal organ distribution and GALT / non GALT compartment accumulation of the drug is represented as a series of tables and histograms below (tables 7 and 9, figures 70-76). Distribution data from rats which were given free drug orally, is represented in tables 8 and 10, and figure 70.

Time (hours)	Mean release (%)	Standard deviation (\pm)
0.25	3.66	0.96
0.75	4.05	0.63
1	5.04	0.46
2	5.38	0.52
3	6.44	1.11

Table 6. Release of trace loaded ^{125}I -IFN- γ from $0.79 \pm 0.48 \mu\text{m}$ diameter PLA microspheres into 20 mM phosphate buffer pH 7.5 (n=3).

Organ	% Accumulation ¹²⁵ I-IFN in tissue	Standard deviation (±)
Blood (P)	1.307	0.361
Blood (S)	8.406	0.226
Liver	1.919	0.086
Spleen	0.211	0.048
Lung	0.883	0.077
Kidney	1.278	0.058
Upper S.I	1.989	0.789
Lower S.I	1.228	0.603
P.Ps	0.101	0.065
L.I	0.433	0.088
S.I.W	21.61	19.70
L.I.W	0.353	0.220
Mesentery	0.503	0.191
Thyroid	0.021	0.029

Table 7. Body distribution, represented as a percentage of the initial dose within each organ (whole) or site, of ¹²⁵I 15 minutes after oral administration of trace amounts of ¹²⁵I-IFN- γ encapsulated within Poly-L-Lactide microspheres with a mean diameter of $0.79 \pm 0.48 \mu\text{m}$ (n=3).

Organ	% Accumulation ¹²⁵ I-IFN in tissue	Standard deviation (±)
Blood (P)	0.381	0.077
Blood (S)	3.319	0.469
Liver	1.064	0.102
Spleen	0.062	0.033
Lung	0.437	0.052
Kidney	0.521	0.084
Thyroid	0.278	0.144

Table 8. Body distribution, represented as a percentage of the initial dose within each organ (whole), of ¹²⁵I 15 minutes after oral administration of trace amounts of free ¹²⁵I-IFN- γ in conjunction with empty Poly-L-Lactide microspheres with a mean diameter of $0.79 \pm 0.48 \mu\text{m}$ (n=3).

Organ	% Accumulation ¹²⁵ I-IFN in tissue	Standard deviation (±)
Blood (P)	1.507	1.303
Blood (S)	5.796	0.666
Liver	1.138	0.029
Spleen	0.142	0.029
Lung	0.912	0.492
Kidney	1.388	0.754
Upper S.I	0.463	0.085
Lower S.I	0.510	0.104
P.Ps	0.070	0.013
L.I	0.428	0.119
S.I.W	8.953	3.256
L.I.W	3.461	2.263
Mesentery	0.688	0.459
Thyroid	1.523	2.015

Table 9. Body distribution, represented as a percentage of the initial dose within each organ (whole) or site, of ¹²⁵I 240 minutes after oral administration of trace amounts of ¹²⁵I-IFN- γ encapsulated within Poly-L-Lactide microspheres with a mean diameter of $0.79 \pm 0.48 \mu\text{m}$ (n=3).

Organ	% Accumulation ¹²⁵ I-IFN in tissue	Standard deviation (±)
Blood (P)	1.014	0.342
Blood (S)	9.232	1.113
Liver	3.060	0.502
Spleen	0.248	0.088
Lung	1.114	0.124
Kidney	1.163	0.097
Thyroid	11.41	2.956

Table 10. Body distribution, represented as a percentage of the initial dose within each organ (whole), of ¹²⁵I 240 minutes after oral administration of trace amounts of free ¹²⁵I-IFN- γ in conjunction with empty Poly-L-Lactide microspheres with a mean diameter of $0.79 \pm 0.48 \mu\text{m}$ (n=3).

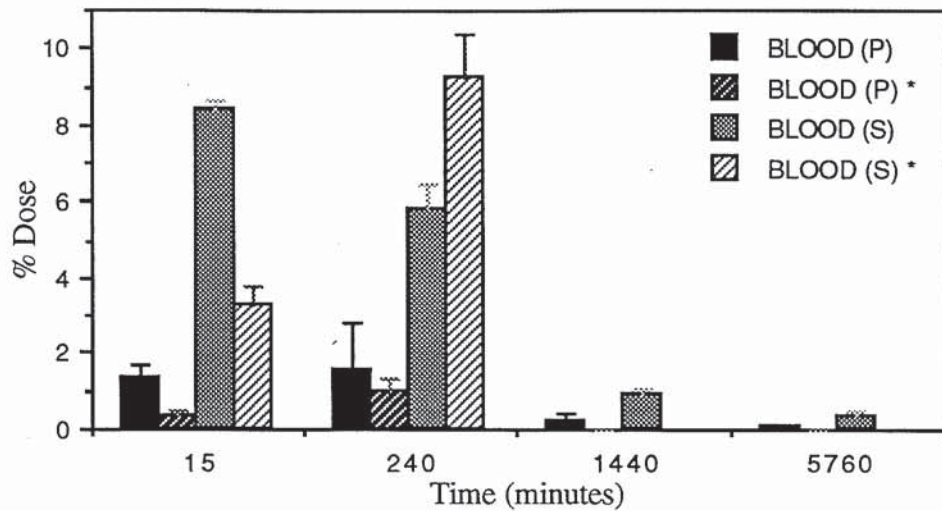


Figure 70. Mean (\pm standard deviation) ^{125}I concentration within the portal (P) and systemic (S) vascular compartments at monitored time points after oral administration of microencapsulated ^{125}I -IFN- γ or free ^{125}I -IFN- γ in conjunction with empty Poly-L-Lactide microspheres (*) (n=3).

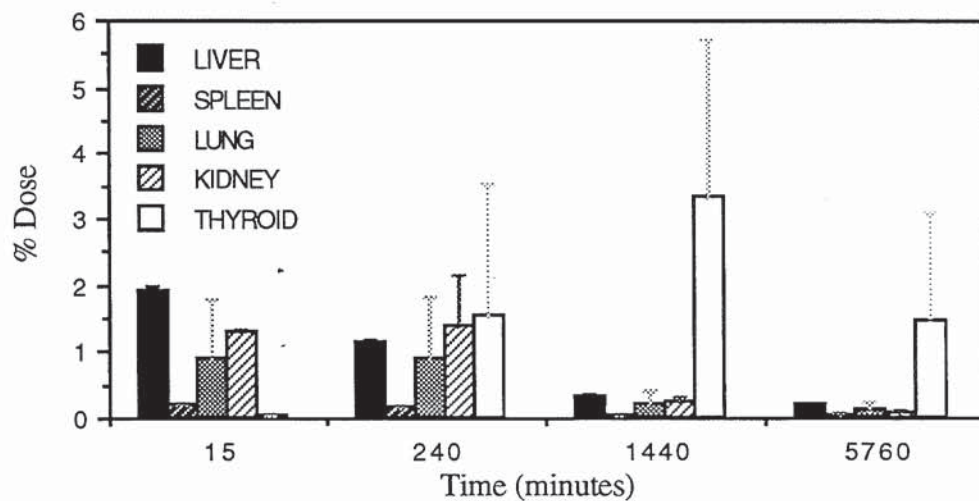


Figure 71. Whole organ distribution of ^{125}I at various time points after oral administration of Poly-L-Lactide microsphere encapsulated ^{125}I -IFN- γ . Uptake is represented as a mean percentage (\pm standard deviation) of the initial oral dose (n=3).

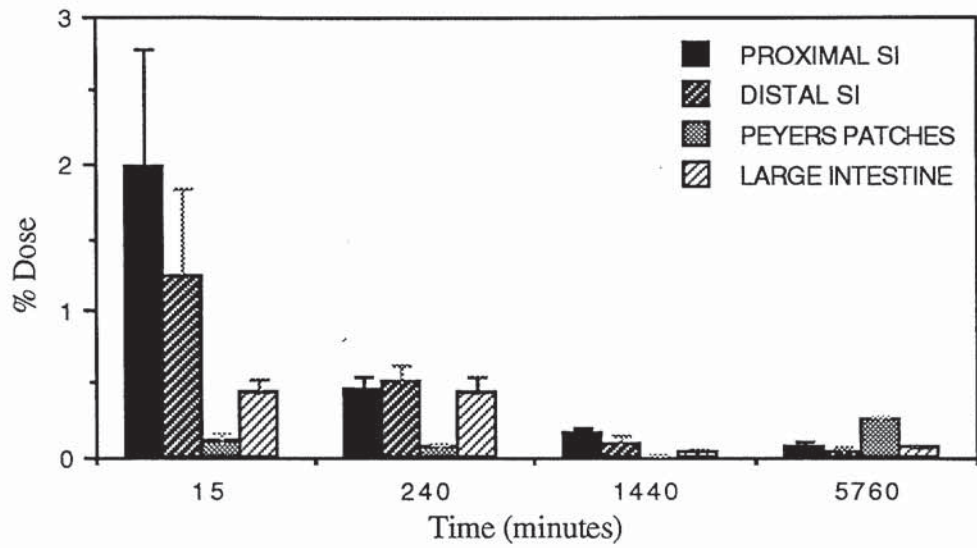


Figure 72. Intestinal accumulation of ¹²⁵I at various time points after oral administration of Poly-L-Lactide microsphere encapsulated ¹²⁵I-IFN- γ . Uptake is represented as a mean percentage (\pm standard deviation) of the initial oral dose (n=3).

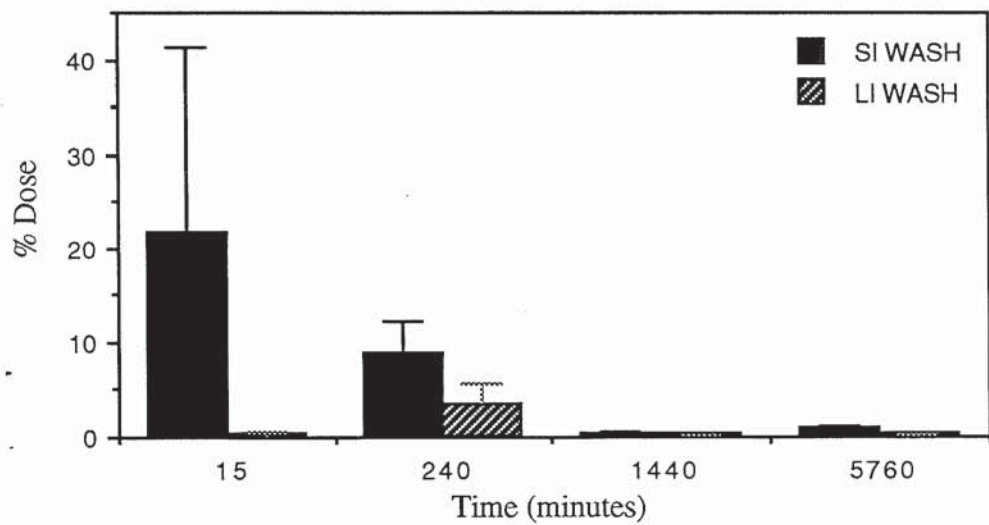


Figure 73. ¹²⁵I levels within gut washes taken throughout the experimental period after oral administration of microsphere encapsulated ¹²⁵I-IFN- γ . Values are represented as a mean percentage (\pm standard deviation) of the administered ¹²⁵I-IFN- γ dose (n=3).

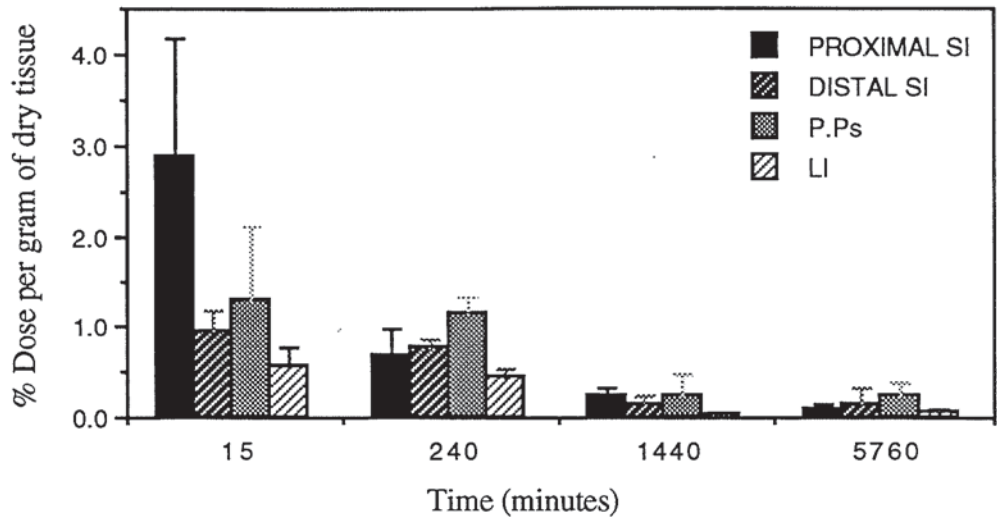


Figure 74. Mean percentage accumulation (\pm standard deviation) of ^{125}I per gram of dry intestine after oral delivery of microencapsulated ^{125}I -IFN- γ (n=3).

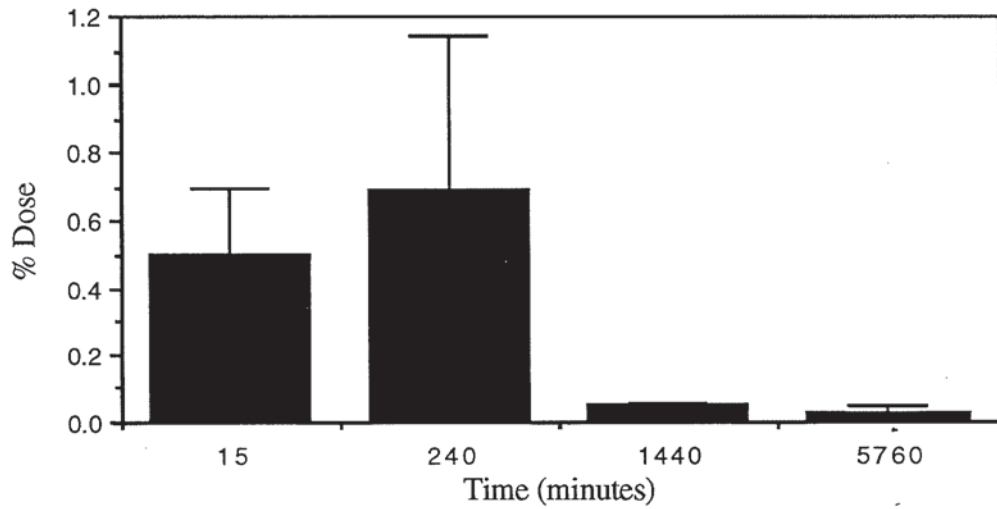


Figure 75. Mean uptake (\pm standard deviation) of ^{125}I into mesenteric tissue at time points after oral delivery of microencapsulated ^{125}I -IFN- γ (n=3).

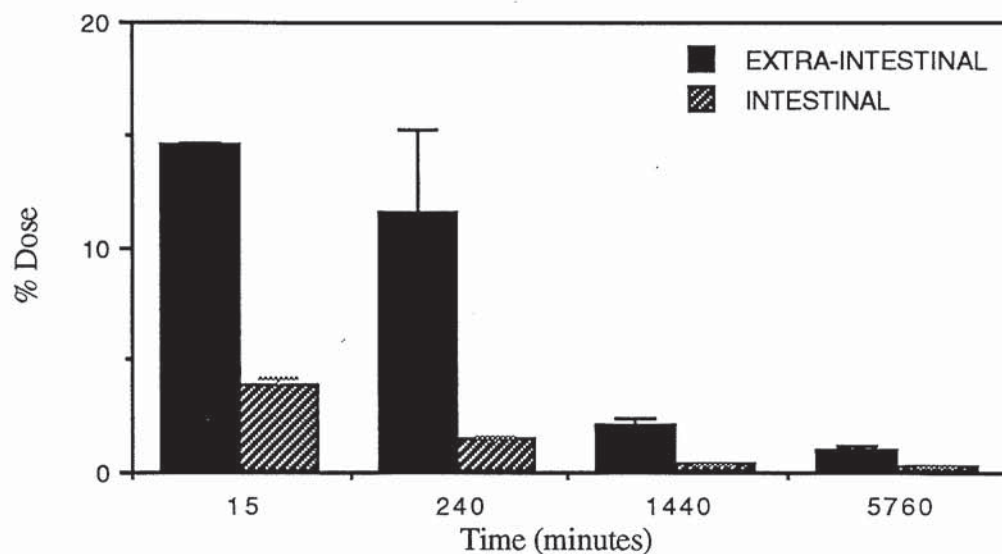


Figure 76. Cumulative uptake of ^{125}I into all monitored tissues, both intestinal and extra-intestinal after oral administration of microencapsulated ^{125}I -IFN- γ (n=3).

24 hours after oral administration of the microencapsulated radiolabelled drug (IFN), the mean percentage of gavaged activity that was detected in the urine was 56.08 ± 12.65 . Faeces collected up to 24 hours after dosing contained 5.51 ± 0.94 percent of the administered activity. Urine collected from the time of treatment to 4 days after administration, contained 39.62 ± 39.81 percent of the administered ^{125}I . Faeces collected over the four day experimental period were found to contain a total of 13.15 ± 5.07 percent of the gavaged radioactive dose.

6.4 DISCUSSION

6.4.1 CHARACTERISATION OF IFN- γ LOADED PLA MICROSPHERES

Only trace amounts (~ 0.01 % w/w) of IFN- γ were encapsulated using the double emulsion method. This was in part deliberate, for two main reasons: Firstly we anticipated that as each particle contained only a small amount of protein, drug release after gavage would occur gradually over a prolonged period of time. Higher IFN encapsulation efficiencies might result in a 'burst' effect, causing the premature release of free drug shortly after

gavage. It was hoped that trace loaded microspheres would not display this characteristic, enabling us to determine the bio-distribution of encapsulated IFN- γ rather than free ^{125}I or free drug. The results from *in vitro* experiments in which PLA microspheres were incubated in phosphate buffer (table 6) go some way to confirming this. Although $3.66 \pm 0.96 \%$ of the IFN- γ loading was released into the buffer within 15 minutes of incubation, only $6.44 \pm 1.11 \%$ was released after 3 hours of incubation. Secondly, the specific activity of IFN- γ measured in antiviral units is about 1×10^7 Units / mg protein or higher. Addition of a 100 Units of IFN- γ per ml of culture fluid increases the tumoricidal activity of mouse peritoneal macrophages against B16-F10 melanoma from 0 to 12 % (Eppstein *et al.*, 1985). In other words, IFN levels as low as 10^{-13} M can still be effective, a fact that emphasises the potency of this natural compound (Bocci, 1992). As such, all but very low loadings of IFN- γ would be theoretically capable of initiating a biological response *in vivo*, and as each 10 mg of microspheres contained the equivalent of about 1 μg or 10000 U of interferon, this loading was deemed acceptable. Higher loadings of IFN- γ are achievable using the double emulsion method if desired.

6.4.2 *IN VIVO* DISTRIBUTION AFTER ORAL ADMINISTRATION OF MICROENCAPSULATED AND FREE IFN- γ

Radiolabel was rapidly transferred from GIT lumen to extra-intestinal sites after oral delivery within biodegradable microspheres (see tables 7 and 9 and figures 70 to 76). In this study we are trying to elucidate the biological distribution of a labelled drug encapsulated within a polymeric carrier system after oral delivery. As such, it is essential to consider the chemical status of the radiolabel before participation in any discussion concerning the bio-availability of the drug. It is not acceptable to assume that the presence of ^{125}I within tissue samples directly equates with the presence of biologically active drug. When free IFN- γ was administered to test animals a quite different distribution of radioactivity was recorded at the 15 and 240 minute time points in comparison to those rodents which received encapsulated drug (see tables 8 and 9 and figure 70). The importance of this finding is discussed in more depth in the ensuing text.

We have established that a fraction of polystyrene microspheres become widely distributed throughout the body of test animals, almost

instantaneously after gavage (chapter 4). This is particularly true if the particles are administered in conjunction with large volumes of water (chapter 3). It seems probable therefore that similarly sized Poly-L-Lactide microspheres may behave in a similar manner providing they are still intact. Other factors such as hydrophobicity and charge will of course influence particle uptake into the mucosa. Poly-L-Lactide microspheres are less hydrophobic than latex and as such are less favourably absorbed into PPs (Eldridge *et al.*, 1990, Jepson *et al.*, 1994).

If intact Poly-L-Lactide microspheres did rapidly penetrate the vascular compartment, it could account for the ^{125}I distribution represented in table 6. Alternatively, microsphere integrity could be rapidly disrupted within the GIT lumen or extraintestinal sites which would result in the release of a large percentage of encapsulated radiolabelled drug at these locations (Poly-L-Lactide microspheres biodegrade *in vivo* into lactic acid *via* hydrolysis of ester linkages). This seems unlikely at early time points (15 minutes) after administration in light of other studies. Miller *et al.*, (1977) found that the half life of Poly (DL-lactide) *in vivo* was about 6 months. Eldridge *et al.*, (1989) found that intact DL-PLG microspheres containing fluorochrome coumarin-6 were observable in histological sections of MLN and PP excised 35 days after oral administration of the particles. After exposure to artificial blood, stomach and intestinal environments, Le Ray *et al.*, (1994) found that minimal amounts of the ^{14}C polymer backbone were released from radiolabelled Poly(D, L-lactide) nanoparticles. The *in vitro* stability data of Le Ray *et al.*, (1994) showed a release of 0.12 and 0.21 % of radioactivity at 1 and 4 hours respectively, in an artificial intestinal medium (USP XXII). We would expect the stability of our Poly-L-Lactide microspheres in artificial gut media to be of a similar order, if not greater because Poly(D, L-lactide) degrades much faster than Poly-L-Lactide. However, we did find evidence to suggest that actual drug release from our Poly-L-Lactide particles, albeit a very small percentage of the total loading, occurs quite quickly *in vitro* (table 6).

In the absence of an appropriate pharmaceutical preparation containing absorption-promoting adjuvants, the systemic bioavailability of IFN- α and IFN- β from the gut or rectum has been reported as nil (Bocci, 1992). If absorption enhancers are used then small amounts (< 1 %) of biologically active IFN can be detected in the blood with anti-viral assays for a few hours after administration (Bocci *et al.*, 1986). Very serious obstacles to

IFN absorption are presented by the intestinal mucus layer, bile salts, potent proteolytic enzymes (Wills *et al.*, 1984) and the epithelial barrier itself. IFN- γ is denatured at pHs below 4 and above 9. Thus, the stomach environment is particularly destructive to IFN- γ due to its low pH, between 5.0 and 3.3 in the rat (Kararli, 1989), and pepsin digestion. The higher pH within the small intestine, between 6.5 and 7.1 in the rat (Kararli, 1989), is probably less conducive to IFN- γ denaturation and it is possible that some intact cationic protein may partition into the anionic mucosa by endocytosis (section 1.2.2), or other absorption mechanisms described in chapter 1, if it can first penetrate the mucus layer (section 1.2.1). In order to be absorbed intact into the small intestinal mucosa, IFN- γ would also have to evade proteolysis by the endopeptidases, exopeptidases and carboxypeptidases present therein.

The preliminary results from our study indicate that microencapsulation of IFN- γ may serve to dramatically enhance the bioavailability of this compound after oral administration (see table 7). There may be several reasons for this absorption enhancement, although increased protection of the sensitive drug molecule from the harsh GIT environment, particularly the stomach, is likely to be of greatest importance. Poly-L-Lactide microencapsulation may also influence the post uptake distribution kinetics of the drug within the blood and other body compartments. We also envisage that by encapsulating IFN- γ the severity of un-wanted 'flu-like' symptoms and granulocytopenia sometimes associated with its use *in vivo* might be reduced (Bocci, 1992). This was found to be the case when IFN- γ was incorporated into starch microparticles (Degling *et al.*, 1993).

Kurzrock *et al.*, (1985) reported the pharmacokinetics, single dose tolerance and biological activity of recombinant human IFN- γ describing a very short half-life after i.v. administration (25-35 minutes). The half lives of the cytokine after intramuscular (i.m.) injection was longer, between 227 and 462 minutes. In the plasma, IFN molecules do not usually bind to carriers, such as albumin, but tend to undergo transendothelial passage in the liver, spleen, renal glomeruli, intestinal villi, lymph node HEV's and bone marrow. There are a number of proteases in body fluids which can hydrolyse IFN, but these are usually kept in check by an excess of protease inhibitors. In some microenvironments such as the spleen, where the concentration of macrophages releasing hydrolytic enzymes is high, there is often rapid breakdown of circulating IFN due to an imbalance in the

protease / inhibitor ratio. IFN breakdown may also occur at the cell surface by proteases bound to the cell membrane. Most importantly, intracellular catabolism of IFN may occur after internalisation of ligand-receptors. Although some receptors are coupled to transduction mechanisms which result in a biological response (see section 6.1), many simply lead to lysosomal digestion. The liver is rich in both receptor types. Hence, a considerable amount of IFN can be removed from the circulation, by organs like the liver, without triggering any biological effect (Bocci, 1992).

Substantial amounts (up to 8 % of the administered dose) of radioactivity were detected in blood samples withdrawn from cardiac and portal sites at the 15 minutes time point (table 7). This represents a hypothetical concentration of approximately 50 antiviral units of interferon *per* ml of blood, if the drug were 'free' in the circulation. Substantially lower (about 3 %) activities were recorded in systemic and portal blood samples withdrawn from rodents which received free drug in combination with empty particles (see table 8). 15 minutes after oral administration of encapsulated drug liver, lung and kidney activities are high (table 7), although in contrast to the latex studies, spleen accumulation of microspheres / radiolabelled drug is low. This could reflect a reduction in splenic capture efficiency, related to particle size, charge or deformability (see section 1.2.6.2). In rats which received free radiolabelled drug, gamma ray emission from livers, spleens, lungs and kidneys removed at the 15 minutes time point was of a significantly lower order than those tissues from the IFN loaded microsphere test group (see table 8).

IFN sensitive tumours are effectively inhibited when local IFN concentrations reach levels as high as 25000 units / g tissue (Bocci, 1992). Clearly, the amount of IFN delivered to tissues and fluids after oral administration inside microspheres is below the level required for direct tumoricidal action. In addition to anti-viral activity IFN is also useful for the treatment of some haematological malignancies, bacterial and parasitic infections (Baron *et al.*, 1991, Zhaong *et al.*, 1989, Kagaya *et al.*, 1989 and Badaro *et al.*, 1990). Thus, whilst it will not be possible to deliver tumoricidal amounts of IFN by the oral route, or the parenteral route for that matter (Bocci, 1992), it may be possible to initiate other beneficial responses. It is known, for example, that physiological doses of IFN in the range of 1 to 2 units of IFN *per* kilogram body weight initiate therapeutic effects (Bocci, 1992). Indeed when human recombinant IFN- α (3.2×10^6

units) was administered buccally, a small percentage was quickly absorbed *via* the oropharyngeal mucosa and could be detected by an antiviral bioassay in the blood (up to 20 units / ml of blood) of rats with an oesophageal fistula (Paulesu *et al.*, 1988). According to our calculations, the efficiency of gastrointestinal absorption following oral administration of encapsulated IFN- γ ($\sim 0.1 \times 10^6$ units) is much greater than this, and would therefore be capable of initiating a similar biological response. By increasing the microsphere loading of drug prior to administration, it may be possible to deliver even greater amounts of protein to the circulation and other body compartments by the oral route.

Whilst the radioactive content of blood and tissue samples removed from rats which received encapsulated IFN orally are higher than blood and tissues removed from the control group at 15 minutes, the thyroid activities are significantly lower ($P \leq 0.05$). Mean thyroid accumulation at 15 minutes was 0.021 ± 0.029 % of the administered dose in those glands removed from rats which were given encapsulated drug. In control rats, this figure was 0.278 ± 0.144 %. Such findings seem to reinforce the thesis that it is intact, drug loaded microspheres which penetrate systemic compartments rapidly after oral delivery, rather than free ^{125}I -IFN, ^{125}I -IFN fragments or free ^{125}I . As such, it seems reasonable to suggest that at the 15 minute time point most of the radioactivity detected in extra-intestinal organs originates from drug loaded microspheres therein. It is particularly informative to compare thyroid activities in both experimental groups at the 4 hour time point (see table 9 and 10). Whilst there is an unacceptable elevation in the amount of radioactive material within thyroid glands removed from both experimental groups, compared with the 15 minute samples, the percentage of gavaged activity within the thyroids from control rats is 11.414 ± 2.956 % compared with only 1.523 ± 2.015 % for the rats which received IFN encapsulated within Poly-L-Lactide microspheres. For the latter group of animals, the elevation in thyroid activity between the 15 minute and 4 hour time point is indicative of ^{125}I -IFN release and breakdown. This means that we cannot say with any certainty that the radioactive emissions from organs and tissues removed at the 4 hour, 24 hour and 4 day time points originates from intact ^{125}I -IFN or microspheres containing ^{125}I -IFN within these biological samples. It is telling, however, the un-mistakable difference between the mean thyroid activities of the two experimental groups at the 240 minute time point ($P \leq 0.01$). It appears that by microencapsulating the ^{125}I -IFN prior to oral administration the release of free ^{125}I *in vivo* is

dramatically reduced, at least at the 15 and 240 minute time points, highlighting two important characteristics of polymeric microsphere delivery systems: The ability to control the release of their drug payload whilst protecting it from destructive elements *in vivo*.

The presence of some free ^{125}I within the animal is to be expected when using a labile drug and biodegradable delivery system. Both are susceptible to breakdown and we could say that ^{125}I is produced as a result of successful delivery. However, it is possible, if not probable that some free ^{125}I within the GIT lumen was absorbed. Such an occurrence would not allow us to attribute ^{125}I activity directly to ^{125}I -IFN presence. It would also prevent us from drawing any conclusions about the nature of Poly-L-Lactide microsphere translocation from the GIT. At present we can only speculate about the stability of the microspheres within the gut lumen, although with current knowledge regarding their *in vitro* status we would not expect any significant drug release ($3.66 \pm 0.96\%$) within 15 minutes of administration. As such we may conclude that data obtained from animals sacrificed at the 15 minute time level is reliable and demonstrates a successful oral delivery of a protein drug. Data obtained from animals sacrificed 15 minutes after oral administration of free ^{125}I -IFN supports this.

With the exception of increased thyroid activity, the organ distribution of radioactivity 4 hours after the oral administration of encapsulated IFN (table 9) is not dissimilar to that at 15 minutes. If anything, the activities of most of the monitored MPS organs fell slightly between 15 and 240 minutes. This is not true for those rats which received free ^{125}I -IFN (table 10). In the control group, the radioactive content of MPS organs at 4 hours was much higher than either group at both the 15 minute or 4 hour time points. Whilst high thyroid activity at the 4 hour time point prevents any elaboration regarding the bio-distribution of orally administered Poly-L-Lactide microsphere encapsulated IFN, the significantly lower ($P \leq 0.005$) activities of the livers compared with the control group suggests two things: Firstly, while some free ^{125}I is present at 4 hours, there is very little in comparison with the control group and that most of the gamma ray emissions from monitored organs probably originates from ^{125}I -IFN loaded microspheres therein. Secondly that microencapsulation of ^{125}I -IFN prior to oral administration probably influences both absorption and / or pharmacokinetic parameters at least up to the 4 hour time point.

As with the MPS tissues, the radioactivity of blood from control rats was significantly higher at 240 minutes than 15. For rats gavaged with microencapsulated drug (figure 70), systemic blood activity was significantly lower ($P \leq 0.005$), but portal blood activity was insignificantly higher at 240 minutes compared with 15. At 240 minutes there was no significant difference between the mean activity of portal blood sampled from the control or microencapsulated drug groups. Conversely, there was a significant difference between the mean activity of cardiac blood sampled from the control and microencapsulated drug groups at 240 minutes ($P \leq 0.05$ for 2 tail). Meaningful interpretation of the complex pattern of radioactivity within the different vascular compartments of control and microsphere encapsulated drug treated rats at 4 hours is not straight forward. Radioactivity within portal and cardiac blood samples represents either circulating or absorbed ^{125}I or ^{125}I -IFN originating from the intestinal lumen in those control animals which received free ^{125}I -IFN orally. For those rats which were given microencapsulated drug the situation is less clear cut. As discussed previously, blood iodemia in these rats at 15 minutes almost certainly represents circulating microspheres, containing radioactive drug, which were absorbed from the intestinal lumen at some point after gavage. This is unlikely to be true at the 4 hour time point, where blood activity could be representative of ^{125}I , ^{125}I -IFN, encapsulated ^{125}I -IFN, ^{125}I -IFN released from microspheres harboured within tissues, re-circulating microspheres containing ^{125}I -IFN, recently absorbed microspheres containing ^{125}I -IFN, or a multitude of other possibilities. At the 240 minute time point its probable that some free ^{125}I is present within the GIT lumen after release, and breakdown, of ^{125}I -IFN from degraded microspheres. Absorption of ^{125}I from the gut lumen could explain why portal blood activities in control and microencapsulated drug treated rats are so similar at 240 minutes.

It is of particular significance that systemic blood levels of radioactivity in control rats, increased from a level statistically lower ($P \leq 0.0005$) than the encapsulated drug dosed rats at 15 minutes, to a level which was statistically higher at 4 hours ($P \leq 0.025$). After directly delivering an un-protected labile compound into the destructive environment of the GIT for 4 hours one would expect some degree of drug breakdown, for aforementioned reasons, followed by considerable absorption of free radiolabel into systemic compartments such as the liver and blood. Our findings seem to

support this hypothesis, but crucially, rats given microencapsulated drug demonstrated a dramatically different distribution of radioactivity at 4 hours. Whilst there is some evidence of free ^{125}I release from IFN loaded microspheres *in vivo* after 4 hours, it seems probable that much of the drug is still retained within particles, either within the GIT lumen, intestinal mucosa or extra-intestinal tissues. Such findings further reinforce our proposal that by including a drug within microparticulate carriers, prior to oral delivery, its absorptive and post uptake kinetics may be altered.

In a recent publication, Le Ray *et al.*, (1994) demonstrated the rapid oral uptake of biodegradable nanoparticles into diverse tissue locations using the mouse model. 0.062 % and 0.138 % of recovered radioactivity was detected within blood and liver compartments, one hour after co-administration of [^{14}C]poly(DL-lactide-co-glycolide) nanoparticles with condensed milk. Overall, between 1.9 and 2.3 % of the nanoparticle dose was transferred into non-intestinal tissues within an hour of oral dosing. ^{14}C persisted within these tissues for at least 48 hours after administration. Following our investigations, we estimate a similar level of absorption for a microencapsulated radiolabelled drug (^{125}I -IFN), although we found considerably more radioactivity in the blood stream of treated rodents. Several reasons might explain this. Detection of ^{125}I in tissue samples is much easier and more sensitive than ^{14}C which requires extensive tissue solubilisation, and is prone to quenching. As such, percentage uptake values for ^{14}C might, in reality, be higher. Conversely, for reasons mentioned above, small amounts of free ^{125}I or ^{125}I -IFN may have been absorbed across the GIT mucosa resulting in un-realistically high recordings. In the study of Le Ray *et al.*, (1994) ^{14}C was incorporated into the polymer backbone, resulting in a more stable radiolabelled particle, so this may have been less of a problem. Lastly, different animal models were employed in the two studies.

The urinary and faecal data indicate that the majority of gavaged radioactivity was excreted within the first 24 hours in the urine (56.08 ± 12.65 %). Faeces collected up to this time point was far less active (5.51 ± 0.94). Even the faeces collected over the 4 day experimental period contained as little as 13.15 ± 5.07 % of the gavaged radiation, indicating that the majority of administered radiolabel was absorbed in one form or another. It is possible that a large percentage of the urinary activity is attributable to intact ^{125}I -IFN, as it is a small enough protein to enter the

ultrafiltrate. The glomerular filter itself is negatively charged, which aids the filtration of cationic proteins such as IFN- γ . In terms of the glomerular sieving coefficient, which ranges from one for small peptides to almost zero for albumin, IFN- γ has a value of 0.8. This compares with a glomerular sieving coefficient of 0.5 for the more anionic IFN- α . Filtered cationic proteins are extensively absorbed by proximal tubular cells *via* an adsorptive endocytic process. Thus kidney is known to act a major detoxifying organ for IFN and other hormone like proteins, and prevents their retention and potential toxicity (Bocci, 1992). The fact that cationic IFN- γ molecules are extensively re-absorbed in the proximal tubules may account for some of the radioactivity of kidneys removed after oral administration of both free and encapsulated IFN- γ (figure 71).

Despite elevated thyroid radioactivity at the 24 and 96 hour time points, blood iodemia remains low (Figure 71). Such a profile contrasts the results from our previous investigations using radiolabelled polystyrene microspheres in which the level of blood and tissue radioactivity rose almost exponentially at the 24 hour time point (section 4.3.4). This may indicate that the majority of free ^{125}I produced by catabolism of ^{125}I -IFN is sequestered within the thyroid gland or rapidly excreted within the urine. If so, then the radioactivity's of fluids and tissues at the later time points may truly be representative of encapsulated or free ^{125}I -IFN.

Transit of the encapsulated radioactive drug along the GIT is represented in figure 73. As expected, a lot of the radioactivity was recovered from the small intestinal washes at the 15 minute time point ($23 \pm 20\%$) with the remainder either absorbed or still resident in the stomach. Four hours after administration, the majority of radioactivity was absorbed into the intestinal mucosa and beyond. Only $12.4 \pm 5.519\%$ was recoverable from the entire GIT lumen, indicating a massive uptake of labelled material had occurred. This factor might infer that most of the Poly-L-Lactide carriers had broken down within either the stomach or intestinal lumen. As mentioned previously, such an occurrence might result in the absorption of free ^{125}I from the lumen. Very low amounts of radiation were detected in intestinal washings at the 1 and 4 day time points.

Radiation absorption into the various regions of the alimentary canal was not uniform at the different time points (figures 72 and 74). 15 minutes after gavage, high activities were detected in both the proximal and distal

small intestine, although accumulation *per* unit mass was much higher in the proximal segments (figure 74). This mirrors findings made using polystyrene test microspheres, which demonstrated a propensity to partition into the small intestinal mucosa very quickly after gavage (see section 4.4). Uptake of radiolabel into PPs was high (1.3 ± 0.8 % *per* gram of dry patch tissue) relative to other GIT regions. The presence of some ^{125}I within large intestinal biopsies removed at the 15 minute time point seems at first sight surprising. It may be caused by circulating drug loaded microspheres becoming entrapped within the large intestinal vasculature and / or the extensive lymphatic network within this organ. In the small intestine, free IFN may accumulate within the lamina propria due to the high permeability of the villi microvasculature (Bocci, 1992).

At time points beyond 15 minutes, the levels of radiolabel within intestinal tissue declined steadily. A proportion of activity remained in these tissues up to 4 days after gavage (figure 73). At the 4, 24 hour and 4 day time points, the highest activity *per* unit mass of gut was detected in PP tissue (figure 74). This may be indicative of microparticle retention within this compartment. Mesenteric ^{125}I levels were highest at the 4 hour time point, with a subsequent decline in activity thereafter (figure 74). Unfortunately, the high levels of free ^{125}I in the body of test animals at this time point does not allow us to directly attribute this activity to absorbed microspheres / drug. However, previous studies (Jani *et al.*, 1989, Jenkins *et al.*, 1994) indicate that PP insorbed microparticles would be routed through the mesentery on their way to the thoracic duct. If there is a significant delivery of IFN to the lymphatics after oral delivery of a microencapsulated form of the drug, it may have important therapeutic implications. This is because if IFN is to be used as an immunoenhancer, it should act selectively on lymphoid cells, sparing the parenchymal cells. Concentrations of lymphoid cells are from 15 - 1000 fold greater in lymph and lymph nodes than in plasma and an increased concentration of IFN in the lymph pool should augment the immune response with minimal toxicity (Bocci, 1992).

6.4.3 CONCLUSION

In summary, oral administration of encapsulated radiolabelled IFN- γ resulted in the transfer of labelled material to the blood and other extra-intestinal sites. Compared to published values, and our control experiments, a promising elevation in the potential bioavailability of orally

administered IFN- γ was observed. Inherent stability problems with the radiolabelled drug and carrier system do not allow much further elaboration with regards to uptake values or organ distributions. It does appear however that the effect of microencapsulating labile molecules, combined with 'water overload', may potentate their rapid absorption into the gastrointestinal mucosa early after oral delivery. The results from this preliminary study also tentatively suggest that microencapsulation of drug molecules may also influence post-uptake pharmacokinetic parameters.

7.0 CONCLUDING REMARKS

The goal of developing workable strategies to deliver labile and / or other therapeutic molecules that do not normally penetrate the gastrointestinal epithelia, provides ample impetus for research into the area of particulate absorption. Microspheres are just one of the drug carriers under investigation. In order to deliver therapeutic compounds in this way, other considerations besides the intrinsically low permeability of the gastrointestinal mucosa to drug carrying vehicles have to be addressed. These include the pharmacological requirements of any drug that is to be orally administered within particulate carrier systems. It is also important to attain adequate bioavailability of drug after intestinal absorption. Development of any system which proved to satisfy both delivery and pharmacological parameters could expect to afford substantial financial rewards in light of consumer preference for non-parenteral modes of drug administration.

During the course of this investigation, we have found evidence to suggest that the GIT is far from an impenetrable barrier with regards to sub-micron sized polymeric particles. Of course, this was already established by other workers (Alpar *et al.*, 1989, Saunders *et al.*, 1968, Volkheimer 1968, Aprahamian *et al.*, 1987, Joel *et al.*, 1978, Jani *et al.*, 1989, Sass *et al.*, 1990 and Wells *et al.*, 1987) although there is considerable divergence of opinions regarding quantitation and time course of particle translocation. This is reflected in the scientific community as a whole, where the consensus is that previous publications are a result of misconception of a physiological quirk. Despite this, several recent studies (Jani *et al.*, 1994, Jenkins *et al.*, 1994, Hillery *et al.*, 1994, Jepson *et al.*, 1994 and Le Ray *et al.*, 1994) have added weight to the increasing body of evidence which points towards the probable existence of an exploitable opportunity for the oral delivery of vaccines, peptidergic molecules or highly potent insoluble drugs. As a spin off, these studies also provide increased knowledge about gastrointestinal physiology and function. They also raise some important discussion points regarding the possible toxicological consequences of non selective absorption of particulate matter from the GIT. It seems likely therefore, that this contentious area of scientific research will continue to attract the attentions of industry and academia, for the reasons aforementioned, for some time to come.

In contrast to the majority of currently published literature regarding this subject, our experimental findings indicate that orally administered microspheres may enter the general circulation within a matter of minutes of gavage. Early studies using Fluoresbrite™ carboxylate microspheres were prone to quantitative error, although they indicated that increased microsphere numbers were transferred from the GIT lumen to the blood stream if the microspheres were gavaged in conjunction with large volumes of hypotonic liquid. The increased permeability / surface area of intestinal vasculature which accompanies water inflow, is one explanation for this observation. Blood and lymph flow also increase dramatically during water absorption. It may also be that some kind of physiological stress is placed on the intestinal mucosa under such conditions, resulting in decreased epithelial barrier function and increased particle penetration. This might be related to an increase in intestinal motility, known to enhance particle uptake (Volkheimer *et al.*, 1968, Volkheimer 1977). Any large volume of food or microspheres in the intestinal lumen will cause considerable distension of the gut, which may increase the mucosal surface area available for particle contact.

When flow cytometric assays were employed to quantify the numbers of microspheres within blood samples from treated animals, they suggested that the overall level of microsphere translocation was much lower than was recorded using direct counting methods. FACS did however, solidly support the previous observations that the time taken for microsphere exit from the intestinal lumen, and entry into the vascular compartment was a matter of minutes rather than hours after gavage.

Quantitative analysis, using GPC, of body fluids and tissues removed from animals treated orally with polystyrene microsphere systems reinforce earlier findings regarding the rapidity of particle relocation. Only 15 minutes after oral delivery of 0.22 μm diameter latex microspheres, about 5 % of the administered dose was recovered from non-intestinal tissues and fluids. Surprisingly, this value fell to about 2.2 % 30 minutes later, but from then on declined only gradually such that 1.0 % was still detectable at the 4 day time point. The distribution of 0.22 μm diameter latex particles amongst the various body compartments removed for GPC analysis followed a general trend in which tissues defined as belonging to the MPS showed the greatest propensity to accumulate the microspheres. This was particularly true of the spleen. Considerably lower numbers of 0.97 μm

diameter latex microspheres were detectable within extra-intestinal tissue locations after oral delivery, although about 0.6 % remained there at 4 days. Such findings corroborate other studies in which the extent of particle translocation was found to be highly dependent on microsphere size. Our HIC experiments indicated that the larger test particles were significantly less hydrophobic than the smaller 0.22 μm microspheres. This must be an important contributing factor related to partitioning of the microspheres into the hydrophobic gastrointestinal mucosa. As size and surface properties of microparticle preparations are so influential in dictating the accessibility of systemic compartments after oral administration, successful exploitation of these preliminary findings will be heavily reliant upon the ability to custom make materials which satisfy these parameters. Besides hydrophobicity and size, chemical nature and carrier shape may also influence gastrointestinal absorption and dissemination.

Histological treatment of tissues removed from animals dosed orally with Fluoresbrite™ microspheres enabled us to visualise the spatial distribution of the particles within relevant anatomical locations. Having visualised the microspheres within the blood of test animals after oral administration, it did not come as a surprise that the particles were detectable within their livers, spleens, lymph nodes and vasculature. The particles were also observed within the intestinal mucosa, presumably immediately after absorption. This was true for both GALT and non-GALT regions of the GIT, conducive to the acceptance that more than one mechanism of particle absorption may operate. This factor, combined with the observed rapidity of test particle appearance within the blood stream after oral delivery, points to the existence of a persorption (Volkheimer, 1968) type model to explain some microsphere absorption from the GIT. Fluoresbrite™ microspheres were also visualised within PPs. The physiology behind this method of particle uptake from the GIT lumen has been well documented previously, although the time course by which particles absorbed by this route could enter the blood stream could be as much as several hours (Jani *et al.*, 1992b), or a few minutes (Jenkins *et al.*, 1994).

Introduction of 0.22 μm diameter latex microspheres into *in situ* closed gut loops resulted in the transfer of some polystyrene to the circulation within a few minutes. This was true for both ileal or duodenal artificial loops, although particle transfer from the proximal segments appeared to be greater. Addition of cytochalasin B to the microsphere suspension prior to

inoculation of the particles served to dramatically reduce the levels of polystyrene that were detectable, using GPC technology, within blood samples removed at early time points in the experiment. The mass of polystyrene latex recovered from washed ileal tissues removed at the end of the experiment was substantial. Statistically, much more latex was detected *per* gram of PP tissue compared with non patch intestine ($P \leq 0.025$). About 7 % of the 21.7 mg polystyrene inoculum was absorbed within each gram of dry patch free mucosa. 18 % of the dose was recovered from each gram of dry patch tissue. Perhaps surprisingly, the mean mass of latex recoverable from both patch and non-patch tissue was statistically unaffected by the presence or absence of cytochalasin B, indicating that microparticle absorption into the intestinal mucosa is unaffected by this drug. Pooled livers and spleens removed from drug treated rodents contained less latex than tissues removed from control rats at the 2 hour time point. The observed reduction in latex transfer into the vascular compartment, but not the intestinal mucosa after cytochalasin B treatment, lead us to the tentative conclusion that the drug influences the accessibility of the blood rather than directly blockading microparticle uptake from the intestinal lumen. Its thought that the ability to disseminate intestinally absorbed microparticles *via* the lymphatics is heavily reliant on (MAC-1+) migrating macrophages within the lamina propria and GALT (Jenkins *et al.*, 1994). We think that if cytochalasin B can debilitate these cells, then the ability to transport intestinally absorbed microspheres from lymphatic compartments within the GIT, and GALT, through the thoracic duct, might be compromised. If this is the case, then it indicates that microsphere translocation to the blood stream from *in situ* closed gut loops occurs primarily through lymphatic pathways and can be rapid. The fact that cytochalasin B was ineffectual at altering the pattern of microsphere absorption into the gut leads us to believe that either M-cell and ordinary enterocyte endocytosis was not inhibited by the drug, or that other mechanisms must account for the observed uptake. Thus in the *in situ* closed gut model, and indeed in the intact animal, its possible that some microparticles may be passively absorbed into the intestinal mucosa. Further experimental endeavours to consolidate these preliminary findings are required.

Microencapsulation of a radiolabelled cytokine (IFN- γ) within biodegradable microspheres and subsequent oral administration to test animals, resulted in about 8.4 % of the radiolabel being transferred to the

general circulation within 15 minutes of gavage. This is hypothetically equivalent to about 840 antiviral units of drug within the blood stream, and as such represents a promising increase in bioavailability of this molecule after oral dosing compared to published, and our, values for non encapsulated IFN- γ . The chemical status of the ^{125}I -IFN- γ complex within the animal was unknown. The levels of thyroid activity at the 15 minute time point were significantly low, in comparison to rats given unencapsulated ^{125}I -IFN- γ , indicating minimal encapsulated radiolabelled drug breakdown ($P \leq 0.05$). The radioactivity of MPS tissues removed from rats 15 minutes after the oral administration of free ^{125}I -IFN- γ was statistically lower than those rodents treated with the microsphere encapsulated drug ($P \leq 0.025$ for the liver). The process of microencapsulation of the sensitive drug molecule must have dramatically enhanced its likelihood of survival within the harsh environment of the GIT. In common with latex particles, evidence suggests that biodegradable PLA microspheres are absorbed into the gut and blood within minutes of gavage. As with the inert polystyrene particles, the mechanics behind PLA microsphere entry into intestinal and systemic tissue compartments so quickly after delivery is likely to complex, although similar in nature. It could be the result of a persorption like mechanism, or one similar to that responsible for the rapid translocation of latex particles from the *in situ* closed gut loop model (see above). The presence of free ^{125}I , within animals that received microsphere encapsulated ^{125}I -IFN- γ , at the later time points means that interpretations concerning these experimental samples must be limited to speculation. It seems possible however, that microencapsulation of a hypothetical drug which has a wide therapeutic window and is effective at low concentrations, would allow it to be used as an oral therapy. Administration of drug loaded microsphere suspensions, of the appropriate size and physico-chemical nature, in conjunction with large volumes of liquid, or suitable absorption-promoting adjuvants might facilitate further increases in bioavailability.

8.0 REFERENCES

- Aldersberg, L.**, Singer, J.M. and Ende, E. (1969) Redistribution and elimination of intravenously injected latex particles in mice. *Journal of Reticuloendothelial Society* 6, 536-560.
- Almeida, A.J.** (1993) Particulate carriers as immunological adjuvants. *PhD Thesis*, Aston University, Birmingham
- Alpar, H.O.**, Field, W.N., Hyde, R. and Lewis, D.A. (1989) The transport of microspheres from the GIT to inflammatory air pouches in the rat. *Journal of Pharmacy and Pharmacology* 41, 194-196.
- Aprahamian, M.**, Michel, C., Humbert, W., Devissaguet, J.P., and Dange, C. (1987) Transmucosal passage of polyalkylcyanoacrylate nanocapsules as a new drug carrier. *Biology of the Cell* 61, 69-76.
- Archer, R.K.** (1965) Haematological techniques for use on animals. Blackwell, Oxford.
- Arshady, R.** (1993) Microspheres for biomedical applications: preparation of reactive and labelled microspheres. *Biomaterials* 14, 5-15.
- Axline, S.G.** and Raven, E.P. (1974). Inhibition of phagocytosis and plasma membrane mobility of the cultivated macrophage by cytochalasin B. *Journal of Cell Biology* 62, 647-651.
- Badaro, R.**, Falcoff, E., Badaro, F.S., Carvalho, E.M., Pedral-Sampaio, D., Barral, A., Carvalho, J.S., Barral-Netto, M., Brandely, M., Silva, L., Bina, J.C., Texeria, R., Falcoff, R., Rocha, H., Ho, J.L. and Johnson, W.D. (1990) Treatment of visceral leishmaniasis with pentavalent antimony and interferon gamma. *New England Journal of Medicine* 322, 16-21.
- Baker, G.** and Jones, L.H.P. (1961) Opal in the animal body. *Nature* 189, 682-683.
- Balfour, W.E.** and Comline, R.S. (1959) The specificity of intestinal absorption of large molecules by the new-born calf. *Journal of Physiology* (London) 148, 77-78.
- Barbour, W. McA.** and Hopwood, D. (1983) Uptake of cationized ferritin by colonic epithelium. *Journal of Pathology* 139, 167-178.
- Barnett, R.J.** (1959) The demonstration with the electron microscope of the end products of the histochemical reactions in relation to the fine structure of cells. *Experimental Cell Research*, Supplement 7, 65-89.
- Baron, S.**, Tying, S.K., Fleishmann, E.R., Coppenhaver, D.H., Nissel, D.W., Klimpel, G.R., Stanton, G.J and Hughes, T.K. (1991) The Interferons. Mechanisms of action and clinical applications. *Journal of the American Medical Association* 266, 1375-1383.
- Barrowman, J.A.** (1978) Physiology of the G.I lymphatic system. Cambridge University Press, Cambridge.
- Bearer, E.L.** and Orci, L. (1985). Endothelial fenestral diaphragms. *Journal of Cell Biology* 100, 418-428.

- Berne, R.M.** and Levy, M.N. (Editors) (1988) *Physiology*. Mosby-Year Book Inc, St. Louis
- Bocci, V.**, Corradeschi, F., Naldini, A. and Lencioni, E. (1986) Enteric absorption of human interferons α and β in the rat. *International Journal of Pharmaceutics* 34, 111-114.
- Bocci, V.** (1992) Physiochemical and Biologic Properties of Interferons and Their Potential Uses in Drug Delivery Systems. *Critical Reviews in Therapeutic Drug Carrier Systems* 9, 91-133.
- Brown, A.L.** (1962) Microvilli of the human jejunal epithelial cell. *Journal of Cell Biology* 12, 623-627.
- Bulger, R.E.** (1988) The urinary system, Chapter 26 in *Cell and Tissue Biology, a textbook of histology VI*. (Weiss, L. Editor) Urban & Schwarzenberg. Munich.
- Bye, W.A.**, Allan, C.H. and Trier, J.S. (1984) Structure, distribution, and origin of M cells in Peyer's patches of mouse ileum. *Gastroenterology* 86, 789 - 801.
- Carr, K.E.** and Toner, P.G. (1984) Morphology of the intestinal mucosa. *Pharmacology of the intestinal Permeation I*. Springer-Verlag, Berlin.
- Charman, W.N.A.** and Stella, V.J. (1986) Effects of lipid class and lipids vehicle volume on the intestinal lymphatic transport of DDT. *International Journal of Pharmaceutics* 33, 165-172.
- Conway, B.R.**, Alpar, H.O. and Lewis, D.A. (1994) Studies on the optimisation of loading and release kinetics of interferon-gamma from polylactide microspheres. *Proceedings of the 21st International Symposium on Controlled Release of Bioactive Materials, Nice, France*. 284-285.
- Couvreur, P.** (1988) Polyalkcyanoacrylates as colloidal drug carriers. *Critical Reviews in Therapeutic Drug Carrier Systems* 5, 1-20.
- Damage, C.**, Aprahamian, M., Balboni, G., Hoeltzel, A., Andrieu, V. and Devissaguet, J.P. (1987). Polyalkcyanoacrylate nanocapsules increase the intestinal absorption of a lipophilic drug. *International Journal of Pharmaceutics* 36, 121-125.
- Damgé, C.**, Michel, C., Aprahamian, M. and Couvreur, P. (1988) New approach for oral administration of insulin with polyalkcyanoarylate nanocapsules as drug carrier. *Diabetes* 37, 246-251.
- Damgé, C.**, Michel, C., Aprahamian, M. and Couvreur, P. and Devissaguet, J.P. (1990) Nanocapsules as carriers for oral peptide delivery. *Journal of Controlled Release* 13, 233-239.
- Damgé, C.**, Aprahamian, M., Koenig, M., Hoeltzel, A., Balboni, G., Marchais, H. and Benoit, J.P. (1994) Intestinal absorption of polymeric microspheres in the rat. *Proceedings of the 21st International Symposium on Controlled Release of Bioactive Materials, Nice, France*, 577-578.

- Davis, S.S., Hardy, J.G. and Fara, J.W.** (1986) The transit of pharmaceutical dosage forms through the small intestine. *Gut* 27, 886-892
- Davis, S.S.** (1989) Assessment of gastrointestinal transit and drug absorption in Novel Drug Delivery and Its Therapeutic Application (Prescott, L.F. and Nimmo, W.S. Editors) John Wiley & Sons Ltd, 89-101.
- Davis, S.S., Illum, L., Moghimi, S.M., Davis, M.C., Porter, C.J., Muir, I.S., Brindley, A., Christy, N.M., Norman, M.E., Williams, P. and Dunn, S.E.** (1993) Microspheres for targeting drugs to specific body sites. *Journal of Controlled Release* 24, 157-163.
- Dedek, W., Grahl, R., Mothes, B., Uhlemann, J., Schwarz, H., Reuter, H., Sabrowski, E. and Mohring, M.** (1983) Persorption of ³⁵S labelled cation exchangers in mammals. *Archives of Experimental Veterinary Medicine* 37, 741-750.
- Degling, L., Stjarnkvist, P. and Sjöholm, I.** (1993) Interferon-gamma in starch microparticles: nitric oxide-generating activity *in vitro* and antileishmanial effect in mice. *Pharmaceutical Research* 10, 783-790.
- Diamond, J.M.** (1966) A rapid method for determining voltage-concentration relations across membranes. *Journal of Physiology* 183, 83-100.
- DiBona, D.R., Chen, L.C., and Sharp, G.W.** (1974) A study of intercellular spaces in the rabbit jejunum during acute volume expansion and after treatment cholera toxin. *Journal of Clinical Investigation* 53, 1300-1307.
- Dittmer, D.S.** (Editor) and Altman, P.L. (1961) Blood and other body fluids. Federation of American Societies for Experimental Biology, Washington DC.
- Dobbins, W.O.** (1971) Intestinal mucosa lacteal in transport of macromolecules and chylomicrons, *The American Journal of Clinical Nutrition* 24, 77-90.
- Ebel, J.D.** (1990) A method for quantifying particle absorption from the small intestine of the mouse. *Pharmaceutical Research* 8, 848-851.
- Eldridge, J.H., Meulbroek, J.A., Stass, J.K., Tice, T.R. and Gilley, R.M.** (1989) Vaccine-containing biodegradable microspheres specifically enter the gut-associated lymphoid tissue following oral administration and induce a disseminated mucosal immune response. *Advances in Experimental Medicine and Biology* 251, 191-202.
- Eldridge, J.H., Hammond, C.J., Meulbroek, J.A., Staas, J.K., Gilley, R.M. and Tice, T.R.** (1990) Controlled vaccine release in the gut associated lymphoid tissue. I. Orally administered biodegradable microspheres target the Peyer's patches. *Journal of Controlled Release* 11, 205-214.
- Eldridge, J.H., E Staas, J.K., Chen, D., Marx, P.A., Tice, T.R. and Gilley, R.M.** (1993) New advances in vaccine delivery systems. *Seminars in Hematology* 30, 16-25.

- Eppstein, D.A.,** Marsh, Y.V., van der Pass, M.A., Felgner, P.L., and Schreiber, A.B. (1985) Biological activity of liposome-encapsulated murine interferon- γ is mediated by a cell membrane receptor. *Proceedings of the National Academy of Science, USA* 82, 3688-3692.
- Eyles, J.E.,** Alpar, H.O., Field, W.N., Lewis, D.A. and Keswick, M. (1995) The transfer of polystyrene microspheres from the gastrointestinal tract to the circulation after oral administration in the rat. *Journal of Pharmacy and Pharmacology* 47, 561-565.
- Fitzgerald, J.F.,** Kottmeier, P.K., Adamsons, R.J., Butt, K.M., Hochman, R.A, and Dennis, C. (1968) Effect of hypertonic solutions on intestinal mucosal integrity. *Surgical Forum* 19, 297-299.
- Florence, A.T.,** and Jani P.U. (1993) Particulate Delivery: The Challenge of the Oral Route, Chapter 4 in *Pharmaceutical Particulate Carriers (Drugs and the Pharmaceutical Sciences Series Volume 61)* (Rolland, A. Editor) Marcel Dekker, New York.
- Gerhart, E.H.,** Liukkonen, R.J., Carlson, R.M., Stokes, G.N., Lukasewycz, M., Oyler, A.R. (1981) Histological effects and bioaccumulation potential of coal particulate-bound phenanthrene in the feathered minnow. *Environmental Pollution* 25: 165-180.
- Glitzelmann, R.,** Spycher, M.A. (1993) Oral cornstarch therapy: is persorption harmless?. *European Journal of Pediatrics* 152, 592-594.
- Granger, D.N.** (1981) Intestinal microcirculation and transmucosal fluid transport. *American Journal of Physiology* 240, G343-349.
- Greenwood, F.C.,** Hunter, W.M. and Glover, J.S. (1963) The preparation of ^{131}I -Labelled human growth hormone of high specific radioactivity. *Biochemical Journal* 89, 114-123.
- Gu, J.M.,** Robinson, J.R. and Leung, S.H. (1988) Binding of acrylic polymers to mucin / epithelial surfaces: structure - property relationships. *Critical Reviews in Therapeutic Drug Carrier Systems* 5, 21-67.
- Gullikson, G.W.,** Cline, W.S., Lorenzsonn, V., Benz, L., Olsen., W.A. and Bass, P (1977) Effects of anionic surfactants on hamster small intestinal membrane structure and function: relationship to surface activity. *Gastroenterology* 73, 501-511.
- Hemmings, W.A.** (1980) Distributed digestion. *Medical Hypotheses* 6, 1209-1213.
- Herbst** (1844) Das lymphgefäßsystem und seine Verrichtungeng. Vandenhoeck and Ruprecht, Gottingen S. 333-337.
- Hillery, A.M.,** Jani, P.U. and Florence, A.T. (1994) Comparative, quantitative study of lymphoid and non-lymphoid uptake of 60 nm polystyrene particles. *Journal of Drug Targeting* 2, 151-156.
- Hillery, A.M.,** Toth, I. and Florence, A.T. (1995) Co-Polymerised peptide particles (CPP): a novel co-polymeric nanoparticulate delivery system for the oral absorption of peptides. *Proceedings of the British Pharmaceutical Conference, Warwick* 41.

- Hopfer U.** (1977) Isolated membrane vesicles as tools for analysis of epithelial transport. *American Journal of Physiology* 233, E445-E449.
- Hussain, N., Jani, P.U. and Florence, A.T.** (1994) Intestinal uptake of lectin-conjugated microspheres. *Proceedings of the 21st International Symposium on Controlled Release of Bioactive Materials, Nice, France.* 29-30.
- Illum, L., Davis, S.S., Wilson C.G., Thomas N.W., Frier M. and Hardy. J.G** (1982). Blood clearance and organ deposition of intravenously administered colloidal particles. The effects of particle size, nature and shape. *International Journal of Pharmaceutics* 12, 135-146.
- Illum, L. and Davis, S.S.** (1984) The organ uptake of intravenously administered colloidal particles can be altered using a non-ionic surfactant (Ploxadmer 338). *Federation of European Biochemical Sciences* 167, 79-82.
- Illum, L., Davis, S.S., Muller, R.H., Mak, E. and West, P.** (1987a) The organ distribution and circulation time of intravenously injected colloidal carriers sterically stabilised with a blockcopolymer - poloxamine 908. *Life Sciences* 40, 367-374.
- Illum, L. and Davis, S.S.** (1987b) Targeting of colloidal particles to the bone marrow. *Life Sciences* 40, 1553-1560.
- Jacobsson, H., Viland, H. and Blomgren, H.** (1993) Route of administration may determine the biological effects of RU 41, 740 (Biostim). Trapping of ^{99m}Tc-labelled human albumin colloids in mice. *International Journal of Immunopharmacology* 15, 353-360.
- Jani, P.U., Halbert, G.W., Langridge, J. and Florence, A.T** (1989) The uptake and translocation of latex nanospheres and microspheres after oral administration to rats. *Journal of Pharmacy and Pharmacology* 41, 809-812.
- Jani, P.U., Halbert, G.W., Langridge, J. and Florence, A.T.**(1990) Nanoparticle uptake by the rat G.I mucosa: quantitation and particle size dependency. *Journal of Pharmacy and Pharmacology* 42, 821-826.
- Jani, P.U.** (1991) Uptake and translocation of microspheres from the rats gastrointestinal tract. *PhD Thesis, University of London, London*
- Jani, P.U., Florence, A.T. and McCarthy, D.E.**(1992a) Further histological evidence of the gastrointestinal absorption of polystyrene microspheres in the rat. *International Journal of Pharmaceutics* 84, 245-252.
- Jani, P.U., McCarthy, D.E. and Florence, A.T.** (1992b) Nanosphere and microsphere uptake via Peyer's patches: observation of the rate of uptake in the rat after a single oral dose. *International Journal of Pharmaceutics* 86, 239-246.
- Jani, P.U., McCarthy, D.E. and Florence, A.T.** (1994) Titanium dioxide (rutile) particle uptake from the rat GI tract and translocation to systemic organs after oral administration. *International Journal of Pharmaceutics* 105, 157-168.

- Jani, P.U., Yamashita, F., Nomura, T., Florence, A.T. and Hashida, M.** (1995) Biliary excretion of polystyrene microspheres after oral and parenteral administration to rats. *Proceedings of the 22nd International Symposium on Controlled Release of Bioactive Materials, Seattle, USA* 198-199.
- Jenkins, P.G., Howard, K.A., Blackhall, N.W., Thomas, N.W., Davis, S.S. and O'Hagan, D.T.** (1994) Microparticulate absorption from the rat intestine. *Journal of Controlled Release* 29, 339-350.
- Jepson, M.A., Mason, C.M., Bennet, M.K., Simmons, N.L. and Hirst B.H.** (1992) Co-expression of vimentin and cytokeratins in M cells of rabbit intestinal lymphoid FAE. *Histochemical Journal* 24, 33-39.
- Jepson, M.A., Simmons, N.L., Savidge, T.C., James, P.S. and Hirst B.H.** (1993) Selective binding and transcytosis of latex microspheres by rabbit intestinal M cells. *Cell and Tissue Research* 271, 399-405.
- Jepson, M.A., Simmons, N.L., O'Hagan, D.T. and Hirst, B.H.** (1994) Comparison of Poly (DL-Lactide-co-Glycolide) and Polystyrene Microsphere Targeting to Intestinal M cells. *Journal of Drug Targeting* 1, 245-249.
- Jeurissen, S.H.M., Kraal, G. and Sminia, T.** (1987) The role of Peyer's patches in intestinal humoral immune responses is limited to memory formation. *Advances in Experimental Medicine and Biology* 216A, 257-265.
- Joel, D.D., Laissue, J.A. and LeFevre, M.E.** (1978) Distribution and fate of ingested carbon particles in mice. *Journal of Reticuloendothelial Society* 24, 477-487.
- Jones, A.L. and Spring-Mills, E.** (1988) The liver and gallbladder, Chapter 22 in *Cell and Tissue Biology, a textbook of histology VI*. (Weiss, L. Editor) Urban & Schwarzenberg. Munich.
- Kagaya, K., Wantanabe, K. and Fukazawa, Y.** (1989) Capacity of recombinant gamma interferon to activate macrophages for Salmonella-killing activity. *Infection and Immunity* 57, 609-615.
- Kararli, T.T.** (1989) Gastrointestinal absorption of drugs. *Critical Reviews in Therapeutic Drug Carrier Systems* 6, 39-86.
- Kimura, T., Higaki, K. and Sezaki, H.** (1984) Transmucosal passage of liposomally entrapped drugs in rat small intestine. *Pharmaceutical Research* 1, 221-224.
- Komuro, T.** (1985) Fenestration of the basal lamina of intestinal villi of the rat. Scanning and transmission electron microscopy, *Cell and Tissue Research* 239, 183-188.
- Kreuter, J., Tauber, U. and Illi, V.** (1979) Distribution and elimination of poly(methyl-2-¹⁴C-methacrylate) nanoparticle radioactivity after injection in rats and mice. *Journal of Pharmaceutical Sciences* 68, 1443-1447.

- Kreuter J.** (1983) Evaluation of nanoparticles as drug delivery systems II: Comparison of the body distribution of nanoparticles with the body distribution of microspheres (diameter > 1 μm), liposomes, and emulsions. *Pharmaceutica Acta Helvetica* 58 (8), 217-226.
- Kreuter, J., Muller, U. and Munz, K.** (1989) Quantitative and microautoradiographic study on mouse intestinal distribution of polycyanoacrylate nanoparticles. *Journal of Pharmaceutics* 55, 39-45.
- Kreuter, J.** (1991) Peroral administration of nanoparticles. *Advanced Drug Delivery Reviews* 7, 71-86.
- Kreuter, J., Scherer, D., Mooren, F.C., Kinne, R.K.H.** (1992) Uptake of nanoparticles by porcine and rabbit intestinal wall *in vitro*. *Proceedings of the 19th International Symposium on Controlled Release of Bioactive Materials, Orlando, U.S.A.* 34-35.
- Kukan, M., Bezek, S., Koprda, V., Labsky, J., Kalal, J., Bauerova, K. and Trnovec, T.** (1989) Fate of ^{14}C -terpolymer (methylmethacrylate- ^{14}C , 2-hydroxyethylmethacrylate, butylacrylate) nanoparticles after peroral administration to rats, *Pharmazie* 44, 399-340.
- Kurzrock, R., Rosenblum, M.G., Sherwin, S.A., Rios, A., Talpaz, M., Quesada, J.R. and Gutterman, J.U.** (1985) Pharmacokinetics, single-dose tolerance, and biological activity of recombinant gamma-interferon in cancer patients. *Cancer Research* 45, 2866-2872.
- Laissue, J.A., Chappuis, B.B., Muller, C., Reubi, J.C. and Gebbers, J.A.** (1993) The intestinal immune system and its relation to disease. *Digest of Disease* 11, 298-312.
- Lee, J.S.** (1971) Contraction of villi and fluid transport in the dog jejunal mucosa *in vitro*. *American Journal of Physiology* 221, 488 - 495.
- Leeson, T.S., Leeson, C.R. and Papara, A.A.** (1988). Text / atlas of histology. W.B Saunders. Philadelphia.
- LeFevre, M.E., Joel, D.D., Laissue, J.A., El-Aasser, M.S. and Vanderhoff, J.W.** (1977) Stability of ^{125}I label after intra gastric or intra venous administration of radioiodinated latexes to mice. *Journal of Reticuloendothelial Society* 22, 189-198.
- LeFevre, M.E., Olivo, R., Vanderhoff, J.W. and Joel, D.D.** (1978a) Accumulation of latex in Peyer's patches and its subsequent appearance in villi and mesenteric lymph nodes (40336). *Proceedings of the Society for Experimental Biology and Medicine* 159, 298-302.
- LeFevre, M.E., Vanderhoff, J.W., Laissue, J.A. and Joel, D.D.** (1978b) Accumulation of 2- μm latex particles in mouse Peyer's patches during chronic latex feeding. *Experientia* : 34, 120-122.
- LeFevre, M.E., Hancock, D.C and Joel, D.D.** (1980) Intestinal barrier to large particulates in mice. *Journal of Toxicology and Environmental Health* 6, 691-704.
- LeFevre, M.E., and Joel, D.D** (1984) Peyer's patch epithelium: an imperfect barrier. *Intestinal toxicology* (Scholler, C.M. Editor) Raven Press, New York, 45-56.

- LeFevre, M.E., Warren, J.B. and Joel, D.D (1985a)** Particles and macrophages in murine Peyer's patches. *Experimental Cell Biology* 53, 121-129.
- LeFevre, M.E., Joel, D.D. and Schidlovsky (1985b)** Retention of ingested latex particles in Peyer's patches of germfree and conventional mice. *Proceedings of the Society for Experimental Biology and Medicine* 179, 522-528.
- LeFevre, M.E., and Joel, D.D (1986)** Distribution of label after intragastric administration of ⁷Be-labelled carbon to weaning and aged mice (42318). *Proceedings of the Society for Experimental Biology and Medicine* 182, 112-119.
- LeFevre, M.E., Brocco, A.M. and Joel, D.D (1989)** Intestinal uptake of fluorescent microspheres in young and aged mice (4825). *Proceedings of the Society for Experimental Biology and Medicine* 190, 23-27.
- Le Ray, A.M., Vert, M., Gautier, J.C. and Benoit, J.P (1994)** Fate of [¹⁴C] poly(DL-lactide-co-glycolide) nanoparticles after intravenous and oral administration to mice. *International Journal of Pharmaceutics* 106, 201-211.
- Le Ray, A.M., Vert, M., Gautier, J.C. and Benoit, J.P (1994)** End-chain radiolabeling and *in vitro* stability studies of radiolabeled poly(hydroxy acid) nanoparticles. *Journal of Pharmaceutical Sciences* 83, 845-851.
- Leu, D., Manthey, B., Kreuter, J., Speiser P. and DeLuca, P.P. (1984)** Distribution and elimination of coated polymethyl (2-¹⁴C)methacrylate nanoparticles after intravenous injection in rats. *Journal of Pharmaceutical Sciences* 73, 1433-1437.
- Lewis, D.A., Field, W.N., Hays, K. and Alpar, H.O. (1992)** The use of albumin microspheres in the treatment of carrageenan-induced inflammation in the rat. *Journal of Pharmacy and Pharmacology* 44, 271-274.
- Loeschke, K., Bentzel, C.J. and Csaky, T.Z. (1970).** Asymmetry of osmotic flow in frog intestine. *American Journal of Physiology* 218, 1723-1729.
- Lowden, S. and Heath, T. (1992)** Lymph pathways associated with Peyer's patches in sheep. *Journal of Anatomy* 181, 209-219.
- Ma, T.Y., Hollander, D., Krugliak, P and Katz, K. (1990)** PEG, a hydrophilic molecular probe for measuring intestinal permeability. *Gastroenterology* 98, 39-46.
- Madara, J.L and Trier, J.S (1987)** Functional morphology of the mucosa of the small intestine, Chapter 44 in *Physiology of the gastrointestinal tract*, second edition (Johnson, L.R. Editor) Raven Press, New York
- Madara, J.L. (1990).** Maintenance of the macromolecular barrier at cell extrusion sites in intestinal epithelium: physiological rearrangement of tight junctions. *The Journal of Membrane Biology* 2, 177-184.

- Madara, J.L.**, Nash, S., Moore, R. and Atisook, K. (1990). Structure of the intestinal epithelial barrier. *Monographs in Pathology* 31, 306-324.
- Maincent, P.**, Le Verge, R., Sado, P., Couvreur, P. and Devissaguet, J.P. (1986) Disposition kinetics and oral bioavailability of vincamine-loaded polyalkylcyanoacrylate nanoparticles. *Journal of Pharmaceutical Science* 75, 955-958.
- Matsumo, K.**, Schaffner, T., Gerber, H.A., Ruchti, C., Hess, M.W., and Cottier, H. (1983) Uptake by enterocytes and subsequent translocation to internal organs of Percoll microspheres administered per os to sucking mice. *Journal of Reticuloendothelial Society* 33, 263-273.
- McClugage, S.G.** and Low, F.N (1984) Microdissection by ultrasonication: Porosity of the intestinal epithelial basal lamina. *American Journal of Anatomy* 171, 207-216.
- McClugage, S.G.**, Low, F.N. and Zimny, M.L. (1986) Porosity of the basement membrane overlaying Peyer's patches in rats and monkeys. *Gastroenterology* 91, 1128-1133.
- Mestecky, J.** and McGhee, J.R. (1992) Prospects for human mucosal vaccines. *Advances in Experimental Medicine and Biology* 327, 13 - 23.
- Miller, R.A.**, Brady, J.M. and Cutright, D.E. (1977) Degradation rates of oral resorbable implants (polylactates and polyglycolates): Rate modification with changes in PLA / PGA copolymer ratios. *Journal of Biomedical Materials Research* 11, 711-719.
- Moghimi, S.M.**, Porter, C.J.H., Muir, I.S., Illum, L. and Davis, S.S. (1991) Non-phagocytic uptake of intravenously injected microspheres in rat spleen: Influence of particle size and hydrophilic coating. *Biochemical and Biophysical Research Communications* 177, 861-866.
- Morishita, I.**, Morishita, M., Takayama, K., Machida, Y. and Nagai, T. (1992) Novel oral microspheres of insulin with protease inhibitor protecting from enzyme degradation. *International journal of Pharmaceutics* 78, 1-7.
- Nefzger, M.**, Kreuter, J., Voges, R., Liehl, E. and Cook, R. (1984) Distribution and elimination of poly (methyl methacrylate) nanoparticles after peroral administration to rats. *Journal of Pharmaceutical Science* 73, 1309-1311.
- Neutra, M.R.** (1988) The Gastrointestinal Tract, Chapter 21 in *Cell and Tissue Biology, a textbook of histology VI*. (Weiss, L. Editor) Urban & Schwarzenberg. Munich.
- Nottle, M.C.** (1977) Plant particles in kidneys and mesenteric lymph nodes of sheep. *Austrian Veterinary Journal* 53, 404-405.
- Odeyale, C.O.** and Hook, G.R. (1990). Computer image analysis method for rapid quantitation of macrophage phagocytosis. *Journal of Leukocyte Biology* 48, 403-411.
- O'Hagan, D.T.**, Palin, K.J., and Davis, S.S. (1987) Intestinal absorption of macromolecules and the immunological response. *Critical Reviews in Therapeutic Drug Carrier Systems* 4, 197-220.

- O'Hagan, D.T.,** Palin, K., Davis, S.S., Artursson, P. and Sjöholm, I. (1989). Microparticles as potentially orally active immunological adjuvants. *Vaccine* 7, 421-424.
- O'Hagan, D.T.** (1990). Intestinal translocation of particulates - implications for drug and antigen delivery. *Advanced Drug Delivery Reviews* 5, 265-285.
- O'Hagan, D.T.,** McGee, J.P., Holmgren, J., Mowat, M.C., Donachie, A.M., Mills, K.H.G., Gaisford, W., Rahman, D. and Challacombe, S.J. (1993) Biodegradable microparticles for oral immunization. *Vaccine* 11, 149-154.
- Ohyashiki, T.,** Taka, M. and Mori, T. (1989) Changes in the membrane surface charge density and / or Membrane potential of the porcine intestinal brush-border membrane vesicles induced by treatment with neuraminidase. *Journal of Biochemistry* 106, 584-588.
- Oppenheim, R.C.,** Stewart, N.F., Gordon, L. and Patel, H.M. (1982) The production and evaluation of orally administered insulin nanoparticles. *Drug Development and Industrial Pharmacy* 8, 531-546.
- Oss, V.** (1978). Phagocytosis as a surface phenomenon. *Annual Review of Microbiology* 32, 19-39.
- Owen, R.L.** and Jones, A.L. (1974) Epithelial cell specialization within human Peyer's patches: an ultrastructural study of intestinal lymphoid follicles. *Gastroenterology* 64, 189-203.
- Owen, R.L.** (1977) Sequential uptake of horseradish peroxidase by lymphoid follicle epithelium of Peyer's patches in the normal unobstructed mouse intestine. *Gastroenterology* 72, 440-451.
- Owen, R.L.,** Allen, C.L. and Stevens, D.P. (1981) Phagocytosis of *Giardia muris* by macrophages in Peyer's patch epithelium in mice. *Infection and Immunity* 33, 591-601.
- Owen, R.L.** and Heyworth, M.F. (1985) Lymphocyte migration from Peyer's patches by diapedesis through M cells into the intestinal lumen. *Advances in Experimental Medical Biology* 186, 647-654.
- Pang K.,** Bresson, J.L. and Walker, W.A. (1983) Development of the gastrointestinal mucosal barrier - evidence for structural differences in microvillus membranes from new-born and adult rabbits. *Biochimica et Biophysica Acta* 727, 201-208.
- Pappo, J.** and Ermak, T.H. (1989) Uptake and translocation of fluorescent latex particles by rabbit Peyer's patches FAE: a quantitative model for M cell uptake. *Clinical Experimental Immunology* 76, 144-148.
- Pappo, J.,** Steger, H.J. and Owen, R.L. (1988) Differential adherence of epithelium overlaying GALT. *Laboratory Investigation* 58, 692-697.
- Pappo, J.,** Ermak, T.H. and Steger, H.J. (1991) Monoclonal antibody directed targeting of fluorescent polystyrene microspheres to M cells. *Immunology* 3, 277-280.

- Paulesu, L.,** Corradeschi, F. Nicoletti, C. and Bocci, V. (1988) Oral administration of human recombinant interferon- α 2 in rats. *International Journal of Pharmaceutics* 46, 199-202.
- Polyscience Inc.** (1987). Polybead[®] Microparticulates, Technical information sheet. from: Polyscience Ltd, 24 Low farm place, Mountain Park, Northampton, UK
- Poole, T.** and Robinson, R. (1987) The UFAW handbook on the care & management of laboratory animals. Longman Scientific & Technical, Essex UK
- Pratten, M.K.** and Lloyd J.B. (1984) Phagocytic uptake of latex beads by rat peritoneal macrophages: Comparison of morphological and radiochemical assay methods. *Bioscience Reports* 4, 497-504.
- Riddick, T.M.** (1968) Control of colloid stability through zeta potential. Volume 1. Livingston, New York
- Ritschel, W.A.** (1991) Targeting in the gastrointestinal tract: New approaches. *Methods and Findings in Experimental and Clinical Pharmacology* 13, 313-336.
- Roitt, I.,** Brostoff, J. and Male, D. (1989). Immunology. Gower medical publishing. London.
- Rowland, M.** and Tucker, G.T (1989) Pharmacokinetics: theory and methodology. Pergamon, Oxford
- Saba, T.M.** (1970) Physiology and physiopathology of the reticuloendothelial system. *Archives of Internal Medicine* 126, 1031-1052.
- Sanders, E.** and Ashworth, C.T (1961) A study of particulate intestinal absorption and hepatocellular uptake. *Experimental Cell Research* 22, 137-145.
- Santiago, N.,** Milstein, S., Rivera, T., Garcia, E., Zaidi, T., Hong, H. and Bucher, D. (1993) Oral immunization of rats with proteinoid microspheres encapsulating influenza virus antigens. *Pharmaceutical Research* 10, 1243-1247.
- Sarubbi, D.,** Varino, B., Haas, S., Maher, J., Falzarano, L., Burnett, B., Fuller, G., Santiago, N., Milstein S. and Baughman, R.A. (1994) Oral delivery of calcitonin in rats and primates using proteinoid microspheres. *Proceedings of the 21st International Symposium on Controlled Release of Bioactive Materials, Nice, France.* 288-289.
- Sass, W.,** Dreyer, H.P. and Seifert, J. (1990). Rapid insorption of small particles in the gut. *American Journal of Gastroenterology* 3, 255-260.
- Saunders, J.,** Davis, S.S., Wilson, C.G. and Smith, A. (1991). Effect of uptake of albumin microspheres on cellular activity of mouse peritoneal macrophages. *International Journal of Pharmaceutics* 68, 265-270.
- Scherer, D.** Mooren, F.C., Kinne, R.K.H. and Kreuter, J. (1993) *In Vitro* permeability of PBCA nanoparticles through Porcine small intestine. *Journal of Drug Targeting* 1, 21-27.

Schneider, H.J., Dedek, W., Grahl, R., Mothes, B., Uhlemann, J., Schwarz, H., Schwachulla, G., Reuter, H. and Mohring, M. (1983) Studies on persorption of large particles from radio-labelled cation exchangers. *Urologia Internationalis* 38, 116-120.

Seymour, L., Schacht, E. and Duncan, R. (1991). The effect of size of polystyrene particles on their retention within the rat peritoneal compartment, and on their interaction with rat macrophages *in vitro*. *Cell Biology International Reports* 1, 38-45.

Silverstein, S.C., Michl, J. and Sung, S.S. (1978) Transport of macromolecules by cellular systems. Dahlem Konferenzen, Berlin. 245-264.

Sims, B. (1974). A simple method of preparing 1-2 μm sections using glycol methacrylate. *Journal of Microscopy* 101, 223-227.

Singer, J.M., Aldersberg, L., Hoenig, E.M., Ende, E. and Tchorsch, Y. (1969). Radiolabeled latex particles in the investigation of phagocytosis *in vivo*. *Journal of Reticuloendothelial Society* 6, 561-589.

Sjoholm, T. and Eldman P. (1979) Acrylic microspheres *in vivo*. I. Distribution and elimination of polyacrylamide microparticles after intravenous and intraperitoneal injection in mouse and rat. *Journal of Pharmacology and Experimental Therapy* 211, 655-662.

Smith, P.L., Wall, D.A. and Wilson, G. (1994) Drug carriers for the oral administration and transport of peptide drugs across the G.I epithelium, Chapter 5 in *Pharmaceutical Particulate Carriers (Drugs and the Pharmaceutical Sciences Series Volume 61)* (Rolland, A. Editor) Marcel Dekker, New York.

Stag, D.J. (1994) The targeting of corticosteroids to inflamed tissues. *PhD Thesis*, Aston University, Birmingham

Steege, H.H., Lewerenz, H.J., Phillip, B. and George, J. (1980) Studies on the characterisation of cellulose powder especially as related to physiological aspects. *International Dissolving Pulps Conference, G.D.R* (conference paper). 5, 169-176.

Tygat, G.N., Rubin, C.E. and Saunders, D.R. (1971) Synthesis and transport of lipoprotein particles by intestinal absorptive cells in man. *Journal of Clinical Investigation* 50, 2065-2078.

Udall, J.N., Pang, K., Fritze, I., Kleinman, R. and Walker, W. (1981b) Development of gastrointestinal mucosal barrier. I. The effect of age on intestinal permeability to macromolecules. *Pediatric Research* 15, 241-244.

Volkheimer, G. and Schulz, F.H. (1968) The phenomenon of persorption. *Digestion* 1, 213-218.

Volkheimer, G., Schulz, F.H., Hofmann, I., Pieser, J., Rack, O., Reichelt, G., Rothenbaecher, W., Schemelich, G., Schurig, B., Teicher, G. and Weiss G. (1968) The effect of drugs on the rate of persorption. *Pharmacology* 1, 8-14.

Volkheimer, G., Schulz, F.H and John, H. (1969) Persorbed food particles in the blood of new-borns. *Gynaecologia* 168, 86-92.

Volkheimer, G. (1972) Persorption. Georg Thieme Verlag Stuttgart.

Volkheimer, G. (1975) Hematogenous dissemination of ingested polyvinyl chloride particles. *Annals of the New York Academy of Science* 246, 164-171.

Volkheimer, G. (1977) Persorption of particles, physiology and pharmacology, *Advances in Pharmacology and Chemotherapy* 14, 163-187.

Volkheimer, G. (1993) The phenomenon of persorption, its history and facts, *Gastroenterologie* 87, 217-221.

Walker, W.A. (1987) Role of the mucosal barrier in antigen handling in the gut, in Food Allergy and Intolerance (Brostoff, J. and Challacombe, S.J. Editors) Balliere Tindall, London, 209-222.

Weiss, L. (1988). Cell and tissue biology, a textbook of histology. VI. (Weiss, L. Editor) Urban & Schwarzenberg. Munich.

Wells, C.L., Maddaus, M.A., Erlandsen, S.L. and Simmons, R.L. (1988) Evidence for the phagocytic transport of intestinal particles in dogs and rats. *Infection and Immunity* 56, 278-282.

Wells, C.L., Maddaus, M.A., and Simmons, R.L (1988) Proposed mechanisms for the translocation of intestinal bacteria. *Infectious Disease* 10, 958-979.

Wells, C.L., Maddaus, M.A. and Simmons, R.L. (1987) Role of the macrophage in the translocation of intestinal bacteria. *Archives of Surgery* 122, 48-53.

Wheeler, P.G., Menzies, I.S. and Creamer, B. (1978) Effect of hyperosmolar stimuli and coeliac disease on the permeability of human gastrointestinal tract. *Clinical Science and Molecular Medicine* 54, 495-501.

Wills, R.J., Spiegel, H.E. and Soike, K.F. (1984) Pharmacokinetics of recombinant alpha A interferon following IV infusion and bolus IM, and PO administration to African green monkeys. *Journal of Interferon Research* 4, 399-409.

Woodley, J. Liposomes for oral administration of drugs. *Critical Reviews in Therapeutic Drug Carrier Systems* 2, 1-18.

Yamamoto, T. (1982) Ultrastructural basis of intestinal absorption. *Archives of Histology (Japan)* 45, 1-22.

Yamaoka, T., Tabata, Y. and Ikada, Y. (1993) Blood clearance and organ distribution of intravenously administered polystyrene microspheres of different sizes. *Journal of Bioactive and Compatible Polymers* 8, 220-235.

Yau, W.W., Kirkland, J.J. and Bly, D.D. (1979) *Modern Size-Exclusion Liquid Chromatography. Practice of Gel Permeation and Gel Filtration Chromatography*, John Wiley and Sons, New York

Zhong, G., Peterson, E.M., Czarniecki, C.W., Schreiber, R.D. and De La Maza, L.M. (1989) Role of endogenous gamma interferon in host defence against *Chlamydia trachomatis* infections. *Infection and Immunity* 57, 152-157.

APPENDIX I

ESTIMATION OF THE ABSORPTION RATE CONSTANT K_a FROM BLOOD MICROSPHERE DATA

The method of residuals described by Rowland *et al.*, (1989) was used in chapter 3 to give a very rough indication whether or not microsphere absorption could be described as a first-order process or not and if so, to assign an absorption rate constant.

Using this method, a line of best fit was extrapolated through the points on the blood microsphere vs time graph (figure 77). The observed blood microsphere concentration was then subtracted from the corresponding extrapolated value at each time point. These residual values were then plotted against time on a semilogarithmic graph (figure 78). If the residual plot is a straight line, then absorption is probably a first order process. The absorption half-life ($t_{1/2}$), which is the time taken for the residual value to diminish by one-half, can then be converted into an absorption rate constant K_a by dividing 0.693 by the absorption half life.

In order to demonstrate this, we can look at the observed blood microsphere level at time points after oral administration of 7.5 mg Fluoresbrite™ microspheres in 0.5 ml of water. Data is first plotted on a semilogarithmic graph (figure 78, below). The observed blood microsphere levels are then subtracted from the corresponding extrapolated value at each time point and re-plotted on the same axis (figure 78). If absorption obeyed first-order principles, as in this example, then a straight line results. The absorption half life ($t_{1/2}$) can be estimated from the time taken for the residual value to fall by one-half, which in this case is approximately 52 minutes. Thus after oral administration of 7.5 mg Fluoresbrite™ microspheres in 0.5 ml of water, K_a was equal to approximately 0.013 min^{-1} . However, as mentioned in chapter 3, it is very important to bear in mind that such pharmacokinetic assessments are of very limited usefulness when examining microsphere translocation data.

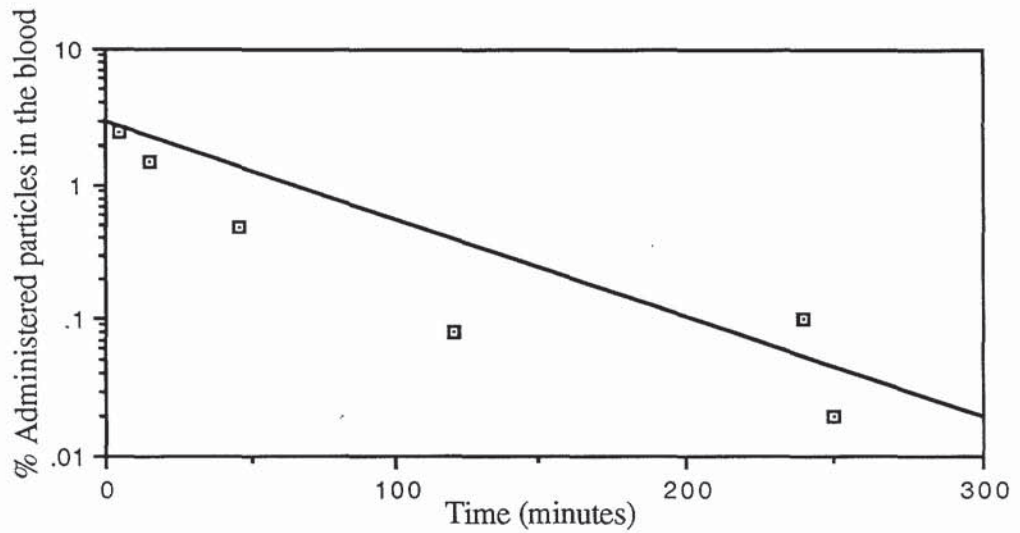


Figure 77. Semilogarithmic plot of blood microsphere uptake at time points after oral administration of 7.5 mg Fluoresbrite™ microspheres in 0.5 ml of water (n=3).

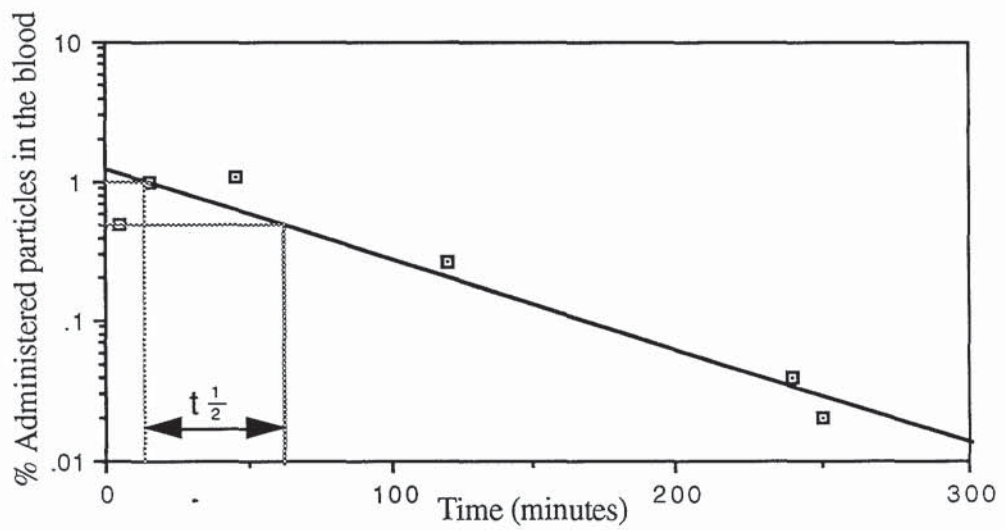


Figure 78. Semilogarithmic plot of residual values after oral administration of 7.5 mg Fluoresbrite™ microspheres in 0.5 ml of water ($t_{\frac{1}{2}}$ represents the absorption half life)(n=3).

APPENDIX II

PHYSIOLOGICAL DATA FOR THE RAT

Weight of organs in percent of body weight:

Blood	7.00
Brain	0.99
GIT	7.46
Heart	0.59
Kidney	0.75
Liver	3.30
Lung	1.13
Thyroid	0.01

Data from Poole *et al.*, (1987)